



Guidelines

for
Design
of
Wind Turbines



A publication from
DNV/Risø

Second Edition

Guidelines for Design of Wind Turbines
2nd Edition

© Det Norske Veritas, Copenhagen (Wind.Turbine.Certification@dnv.com) and Wind Energy Department, Risø National Laboratory (Certification@risoe.dk) 2002.

All rights reserved. No part of this publication may be reproduced, stored in a retrieval system, or transmitted, in any form or by any means, electronic, mechanical, photocopying, recording and/or otherwise without the prior written permission of the publishers.

This book may not be lent, resold, hired out or otherwise disposed of by way of trade in any form of binding or cover other than that in which it is published, without the prior consent of the publishers.

The front-page picture is from Microsoft Clipart Gallery ver. 2.0.

Printed by Jydsk Centraltrykkeri, Denmark 2002

ISBN 87-550-2870-5

Preface

The guidelines for design of wind turbines have been developed with an aim to compile into one book much of the knowledge about design and construction of wind turbines that has been gained over the past few years. This applies to knowledge achieved from research projects as well as to knowledge resulting from practical design experience. In addition, the various rules and methods required for type approval within the major markets for the wind turbine industry form a basis for the guidelines, with emphasis on the international standards for wind turbines given by the International Electrotechnical Commission, IEC.

The objective is to provide guidelines, which can be used for design of different types of wind turbines in the future. The guidelines provide recommendations and guidance for design together with application-oriented solutions to commonly encountered design problems.

The guidelines can be used by wind turbine manufacturers, certifying authorities, and wind turbine owners. The guidelines will also be useful as an introduction and tutorial for new technical personnel and as a reference for experienced engineers.

The guidelines are available as a printed book in a handy format as well as electronically in pdf format on a CD-ROM.

The development of the guidelines is the result of a joint effort between Det Norske Veritas and Risø National Laboratory. The development has been funded by Danish Energy Agency, Det Norske Veritas and Risø National Laboratory.

These guidelines for design of wind turbines have been thoroughly reviewed by internal and external experts. However, no warranty, expressed or implied, is made by Det Norske Veritas and Risø National Laboratory, as to the accuracy or functionality of the guidelines, and no responsibility is assumed in connection therewith.

Contents

1. WIND TURBINE CONCEPTS	1	2.5.1	Transportation, installation and commissioning	28	
1.1	INTRODUCTION.....	1	2.5.2	Normal operation.....	29
1.2	CONCEPTUAL ASPECTS.....	1	2.5.3	Service, maintenance and repair ..	29
1.2.1	Vertical axis turbines.....	2	2.6	CODES AND STANDARDS	30
1.2.2	Horizontal axis turbines.....	2	REFERENCES	30	
1.2.3	Number of rotor blades.....	3			
1.2.4	Power control aspects	3			
1.3	ECONOMICAL ASPECTS.....	5	3. EXTERNAL CONDITIONS.....	32	
1.4	POWER PRODUCTION	5	3.1	WIND CONDITIONS	32
1.4.1	Power curve.....	6	3.1.1	10-minute mean wind speed	32
1.4.2	Annual energy production	7	3.1.2	Standard deviation of wind speed	34
1.5	CONFIGURATIONS AND SIZES	7	3.1.3	Turbulence intensity	36
1.6	FUTURE CONCEPTS	8	3.1.4	Lateral and vertical turbulence ..	37
REFERENCES	9	3.1.5	Stochastic turbulence models	37	
		3.1.6	Wind shear.....	40	
2. SAFETY AND RELIABILITY.....	10	3.1.7	Wind direction.....	42	
2.1	SAFETY PHILOSOPHY	10	3.1.8	Transient wind conditions	43
2.2	SYSTEM SAFETY AND OPERATIONAL RELIABILITY	11	3.1.9	Extreme winds – gusts.....	43
2.2.1	Control system.....	12	3.1.10	Site assessment	46
2.2.2	Protection system.....	13	3.2	OTHER EXTERNAL CONDITIONS	48
2.2.3	Brake system	14	3.2.1	Temperatures	48
2.2.4	Failure mode and effects analysis	15	3.2.2	Density of air	49
2.2.5	Fault tree analysis	16	3.2.3	Humidity.....	50
2.3	STRUCTURAL SAFETY.....	18	3.2.4	Radiation and ultraviolet light	50
2.3.1	Limit states	18	3.2.5	Ice	50
2.3.2	Failure probability and other measures of structural reliability.	18	3.2.6	Rain, snow and hail	50
2.3.3	Structural reliability methods	19	3.2.7	Atmospheric corrosion and abrasion.....	51
2.3.4	Code format, characteristic values, and partial safety factors.	19	3.2.8	Earthquake.....	51
2.3.5	Code calibration.....	20	3.2.9	Lightning	53
2.3.6	Example – axially loaded steel tower.....	22	REFERENCES	53	
2.3.7	Example – fatigue of FRP blade root in bending	24			
2.3.8	Tests and calculations for verification.....	26	4. LOADS.....	55	
2.3.9	Inspection and inspection intervals	26	4.1	LOAD CASES.....	55
2.4	MECHANICAL SAFETY	27	4.1.1	Design situations	55
2.5	LABOUR SAFETY	28	4.1.2	Wind events.....	55
			4.1.3	Design load cases	55
			4.2	LOAD TYPES	58
			4.2.1	Inertia and gravity loads	58
			4.2.2	Aerodynamic loads.....	59
			4.2.3	Functional loads.....	60

4.2.4	Other loads.....	60	5.2.5	Materials.....	118
4.3	AEROELASTIC LOAD CALCULATIONS	60	5.2.6	Standards	119
4.3.1	Model elements.....	61	REFERENCES		119
4.3.2	Aeroelastic models for load prediction.....	70	6. NACELLE		120
4.3.3	Aerodynamic data assessment	70	6.1	MAIN SHAFT.....	120
4.3.4	Special considerations	72	6.1.1	Determination of design loads..	120
4.4	LOAD ANALYSIS AND SYNTHESIS ...	76	6.1.2	Strength analysis.....	120
4.4.1	Fatigue loads.....	76	6.1.3	Fatigue strength	121
4.4.2	Ultimate loads.....	82	6.1.4	Ultimate strength	125
4.5	SIMPLIFIED LOAD CALCULATIONS ..	86	6.1.5	Main shaft-gear connection	126
4.5.1	Parametrised empirical models...	86	6.1.6	Materials	126
4.5.2	The simple load basis	86	6.1.7	Standards	127
4.5.3	Quasi-static method	87	6.2	MAIN BEARING	127
4.5.4	Peak factor approach for extreme loads.....	88	6.2.1	Determination of design loads..	129
4.5.5	Parametrised load spectra	89	6.2.2	Selection of bearing types.....	130
4.6	SITE-SPECIFIC DESIGN LOADS	92	6.2.3	Operational and environmental conditions.....	130
4.7	LOADS FROM OTHER SOURCES THAN WIND.....	93	6.2.4	Seals, lubrication and temperatures.....	130
4.7.1	Wave loads	93	6.2.5	Rating life calculations	132
4.7.2	Current loads	99	6.2.6	Connection to main shaft.....	133
4.7.3	Ice loads.....	99	6.2.7	Bearing housing.....	133
4.7.4	Earthquake loads.....	99	6.2.8	Connection to machine frame...	133
4.8	LOAD COMBINATION	99	6.2.9	Standards	133
REFERENCES		101	6.3	MAIN GEAR	133
5. ROTOR.....		104	6.3.1	Gear types.....	134
5.1	BLADES	104	6.3.2	Loads and capacity	137
5.1.1	Blade geometry.....	104	6.3.3	Codes and standards	141
5.1.2	Design loads	105	6.3.4	Lubrication	141
5.1.3	Blade materials	105	6.3.5	Materials and testing.....	142
5.1.4	Manufacturing techniques	108	6.4	COUPLINGS	145
5.1.5	Quality assurance for blade design and manufacture	109	6.4.1	Flange couplings.....	145
5.1.6	Strength analyses	110	6.4.2	Shrink fit couplings	146
5.1.7	Tip deflections	113	6.4.3	Key connections	146
5.1.8	Lightning protection	113	6.4.4	Torsionally elastic couplings...	146
5.1.9	Blade testing.....	114	6.4.5	Tooth couplings.....	146
5.1.10	Maintenance	116	6.5	MECHANICAL BRAKE	146
5.2	HUB	116	6.5.1	Types of brakes.....	146
5.2.1	Determination of design loads ..	117	6.5.2	Brake discs and brake pads.....	148
5.2.2	Strength Analysis.....	117	6.5.3	Brake torque sequence.....	148
5.2.3	Analysis of bolt connections.....	118	6.6	HYDRAULIC SYSTEMS	149
5.2.4	Hub enclosure.....	118	6.6.1	Arrangement.....	149
			6.6.2	Accumulators.....	149
			6.6.3	Valves.....	149

6.6.4	Application in protection systems	150	7.4.7	Stability analysis.....	177
6.6.5	Additional provisions	151	7.4.8	Flange connections	178
6.6.6	Codes and standards	151	7.4.9	Corrosion protection.....	179
6.7	GENERATOR	151	7.4.10	Tolerances and specifications... ..	179
6.7.1	Types of generators	151	7.5	ACCESS AND WORKING ENVIRONMENT	180
6.7.2	Climate aspects	153	7.6	EXAMPLE OF TOWER LOAD CALCULATION	180
6.7.3	Safety aspects	153	7.6.1	Loads and responses	180
6.7.4	Cooling and degree of sealing ..	155	7.6.2	Occurrence of extreme loads during normal power production.....	181
6.7.5	Vibrations	155	7.6.3	Extreme loads – parked turbine	182
6.7.6	Overspeed	155	7.6.4	Fatigue loading	183
6.7.7	Overloading	155	REFERENCES		186
6.7.8	Materials	156			
6.7.9	Generator braking	156			
6.7.10	Lifetime	157			
6.7.11	Testing of generators	157			
6.8	MACHINE SUPPORT FRAME.....	157	8. FOUNDATIONS.....		187
6.9	NACELLE ENCLOSURE	158	8.1	SOIL INVESTIGATIONS	187
6.10	YAW SYSTEM	158	8.1.1	General	187
6.10.1	Determination of design loads ..	160	8.1.2	Recommendations for gravity based foundations	188
6.10.2	Yaw drive	161	8.1.3	Recommendations for pile foundations	189
6.10.3	Yaw ring	162	8.2	GRAVITY-BASED FOUNDATIONS... ..	189
6.10.4	Yaw brake.....	162	8.2.1	Bearing capacity formulas	190
6.10.5	Yaw bearing.....	163	8.3	PILE-SUPPORTED FOUNDATIONS... ..	193
6.10.6	Yaw error and control.....	166	8.3.1	Pile groups	194
6.10.7	Cable twist.....	166	8.3.2	Axial pile resistance.....	195
6.10.8	Special design considerations... ..	166	8.3.3	Laterally loaded piles.....	197
REFERENCES		167	8.3.4	Soil resistance for embedded pile caps.....	200
			8.4	FOUNDATION STIFFNESS.....	201
7. TOWER.....		169	8.5	PROPERTIES OF REINFORCED CONCRETE	206
7.1	LOAD CASES.....	170	8.5.1	Fatigue	206
7.2	DESIGN LOADS	170	8.5.2	Crack-width	207
7.3	GENERAL VERIFICATIONS FOR TOWERS.....	171	8.5.3	Execution.....	208
7.3.1	Dynamic response and resonance	171	8.6	SELECTED FOUNDATION STRUCTURE CONCEPTS FOR OFFSHORE APPLICATIONS	208
7.3.2	Critical blade deflection analysis	172	8.6.1	Introduction to concepts	208
7.4	TUBULAR TOWERS	173	8.6.2	Monopile	209
7.4.1	Loads and responses	173	8.6.3	Tripod	215
7.4.2	Extreme loads	174	REFERENCES		221
7.4.3	Fatigue loads.....	174			
7.4.4	Vortex induced vibrations.....	174			
7.4.5	Welded joints.....	175			
7.4.6	Stress concentrations near hatches and doors.....	176			

9. ELECTRICAL SYSTEM.....	223	A.7	MINIMUM DEPTH OF THREADED HOLES.....	244	
9.1	ELECTRICAL COMPONENTS.....	223	A.8	BOLT FORCE ANALYSIS	245
9.1.1	Generators.....	223	A.8.1	Stiffness of bolts	245
9.1.2	Softstarter	225	A.8.2	Stiffness of the mating parts	246
9.1.3	Capacitor bank.....	225	A.8.3	Force triangle.....	246
9.1.4	Frequency converter	226	A.9	CONNECTIONS SUBJECTED TO SHEAR	247
9.2	WIND TURBINE CONFIGURATIONS	227	A.10	BOLTS SUBJECTED TO TENSILE LOAD	248
9.3	POWER QUALITY AND GRID CONNECTION	229	A.11	BOLTS SUBJECTED TO TENSILE LOAD AND SHEAR.....	249
9.4	ELECTRICAL SAFETY	230	A.12	EXECUTION OF BOLT CONNECTIONS	249
9.5	WIND FARM INTEGRATION	231	A.13	CODES AND STANDARDS.....	249
REFERENCES	232	REFERENCES	249
10. MANUALS	233	B. RULES OF THUMB.....	250		
10.1	USER MANUAL	233	B.1	LOADS.....	250
10.2	SERVICE AND MAINTENANCE MANUAL	233	B.1.1	Rotor loads.....	250
10.3	INSTALLATION MANUAL.....	233	B.1.2	Fatigue loads.....	250
REFERENCE	233	B.2	ROTOR	250
 			B.3	NACELLE.....	251
11. TESTS AND MEASUREMENTS..	234	C. FATIGUE CALCULATIONS	252		
11.1	POWER PERFORMANCE MEASUREMENTS.....	234	C.1	STRESS RANGES.....	252
11.2	LOAD MEASUREMENTS.....	236	C.2	FRACTURE MECHANICS	252
11.3	TEST OF CONTROL AND PROTECTION SYSTEM.....	237	C.3	S-N CURVES	253
11.4	POWER QUALITY MEASUREMENT	237	C.4	THE PALMGREN-MINER RULE	254
11.5	BLADE TESTING.....	237	C.5	FATIGUE IN WELDED STRUCTURES	255
11.6	NOISE MEASUREMENTS	237	C.6	CHARACTERISTIC S-N CURVES FOR STRUCTURAL STEEL.....	256
REFERENCES	237	C.7	CHARACTERISTIC S-N CURVES FOR FORGED OR ROLLED STEEL	256
 			C.8	S-N CURVES FOR COMPOSITES	257
A. BOLT CONNECTIONS.....	239	C.9	OTHER TYPES OF FATIGUE ASSESSMENT	258	
A.1	BOLT STANDARDIZATION	239	REFERENCES	258
A.2	STRENGTH.....	239			
A.3	IMPACT STRENGTH	239			
A.4	SURFACE TREATMENT	239			
A.5	S-N CURVES.....	240			
A.5.1	S-N curves in structural steel codes.....	241			
A.5.2	Allowable surface pressure.....	242			
A.6	PRETENSION	242			
A.6.1	Safety against loosening	244			

D. FEM CALCULATIONS..... 260

D.1	TYPES OF ANALYSIS	260
D.2	MODELLING	261
D.2.1	Model.....	261
D.2.2	Elements	262
D.2.3	Boundary conditions.....	264
D.2.4	Loads	265
D.3	DOCUMENTATION	265
D.3.1	Model.....	265
D.3.2	Results	267

E. MATERIAL PROPERTIES 268

E.1	STEEL.....	268
E.1.1	Structural steel.....	268
E.1.2	Alloy steel.....	269
E.2	CAST IRON.....	269
E.3	FIBRE REINFORCED PLASTICS	269
E.3.1	Glass fibre reinforced plastics ..	269
E.4	CONCRETE	270
E.4.1	Mechanical properties.....	270
	REFERENCES	270

F. TERMS AND DEFINITIONS 271

	REFERENCES	276
--	------------------	-----

G. TABLES AND CONVERSIONS... 277

G.1	ENGLISH/METRIC CONVERSION	277
G.2	AIR DENSITY VS. TEMPERATURE ..	277
G.3	AIR DENSITY VS. HEIGHT.....	277
G.4	RAYLEIGH WIND DISTRIBUTION....	277

1. Wind Turbine Concepts

1.1 Introduction

Wind-powered ships, grain mills, water pumps, and threshing machines all exemplify that extraction of power from wind is an ancient endeavour. With the evolution of mechanical insight and technology, the last decades of the 20th century, in particular, saw the development of machines which efficiently extract power from wind. "Wind turbines" is now being used as a generic term for machines with rotating blades that convert the kinetic energy of wind into useful power.

In the 20th century, early wind turbine designs were driven by three basic philosophies for handling loads: (1) withstanding loads, (2) shedding or avoiding loads, and (3) managing loads mechanically, electrically, or both. In the midst of this evolution, many wind turbine designs saw the light of day, including horizontal axis and vertical axis turbines. Turbines that spin about horizontal and vertical axes, respectively, and are equipped with one, two, three or multiple blades.

Modern turbines evolved from the early designs and can be classified as two or three-bladed turbines with horizontal axes and upwind rotors. Today, the choice between two or three-bladed wind turbines is merely a matter of a trade-off between aerodynamic efficiency, complexity, cost, noise and aesthetics.

Additional key turbine design considerations include wind climate, rotor type, generator type, load and noise minimisation, and control approach. Moreover, current trends, driven by the operating regime and the market environment, involve development of low-cost, megawatt-scale turbines and lightweight turbine concepts. Whereas

turbines operating at constant rotor speed have been dominating up to now, turbines with variable rotor speed are becoming increasingly more common in an attempt to optimise the energy capture, lower the loads, obtain better power quality, and enable more advanced power control aspects.

1.2 Conceptual aspects

Some early wind turbine designs include multiple-bladed concepts. These turbines are all characterised by rotors with high solidity, i.e. the exposed area of the blades is relatively large compared to the swept area of the rotor.



Figure 1-1. Multiple-bladed wind turbines of various designs.

A disadvantage of such a high-solidity rotor is the excessive forces that it will attract during extreme wind speeds such as in hurricanes. To limit this undesirable effect of extreme winds and to increase efficiency, modern wind turbines are built with fewer, longer, and more slender blades, i.e. with a

much smaller solidity. To compensate for the slenderness of the blades, modern turbines operate at high tip speeds.

1.2.1 Vertical axis turbines

Vertical axis wind turbines (VAWTs), such as the one shown in Figure 1-2 with C-shaped blades, are among the types of turbine that have seen the light of day in the past century.



Figure 1-2. Eole C, a 4200 kW vertical axis Darrieus wind turbine with 100 m rotor diameter at Cap Chat, Québec, Canada. The machine, which is the world's largest wind turbine, is no longer operational. From www.windpower.org (2000), © Danish Wind Turbine Manufacturers Association.

Classical water wheels allow the water to arrive tangentially to the water wheel at a right angle to the rotational axis of the wheel. Vertical axis wind turbines are designed to act correspondingly towards air. Though, such a design would, in principle, work with a horizontal axis as well, it would require a more complex design, which would hardly be able to beat the efficiency of a propeller-type turbine. The major advantages of a vertical axis wind turbine, as

the one illustrated in Figure 1-2, are that the generator and gearbox are placed on the ground and are thus easily accessible, and that no yaw mechanism is needed. Among the disadvantages are an overall much lower level of efficiency, the fact that the turbine needs total dismantling just to replace the main bearing, and that the rotor is placed relatively close to the ground where there is not much wind.

1.2.2 Horizontal axis turbines

Horizontal axis wind turbines (HAWTs), such as the ones shown in Figure 1-3, constitute the most common type of wind turbine in use today. In fact all grid-connected commercial wind turbines are today designed with propeller-type rotors mounted on a horizontal axis on top of a vertical tower. In contrast to the mode of operation of the vertical axis turbines, the horizontal axis turbines need to be aligned with the direction of the wind, thereby allowing the wind to flow parallel to the axis of rotation.



Figure 1-3. Three-bladed upwind turbines being tested at Risø, August 1986.

Insofar as concerns horizontal axis wind turbines, a distinction is made between upwind and downwind rotors. Upwind rotors face the wind in front of the vertical tower and have the advantage of somewhat avoiding the wind shade effect from the presence of the tower. Upwind rotors need a yaw mechanism to keep the rotor axis

aligned with the direction of the wind. Downwind rotors are placed on the lee side of the tower. A great disadvantage in this design is the fluctuations in the wind power due to the rotor passing through the wind shade of the tower which gives rise to more fatigue loads. Theoretically, downwind rotors can be built without a yaw mechanism, provided that the rotor and nacelle can be designed in such a way that the nacelle will follow the wind passively. This may, however, induce gyroscopic loads and hamper the possibility of unwinding the cables when the rotor has been yawing passively in the same direction for a long time, thereby causing the power cables to twist. As regards large wind turbines, it is rather difficult to use slip rings or mechanical collectors to circumvent this problem. Whereas, upwind rotors need to be rather inflexible to keep the rotor blades clear of the tower, downwind rotors can be made more flexible. The latter implies possible savings with respect to weight and may contribute to reducing the loads on the tower. The vast majority of wind turbines in operation today have upwind rotors.

1.2.3 Number of rotor blades

The three-bladed concept is the most common concept for modern wind turbines. A turbine with an upwind rotor, an asynchronous generator and an active yaw system is usually referred to as the Danish concept. This is a concept, which tends to be a standard against which other concepts are evaluated.

Relative to the three-bladed concept, the two and one-bladed concepts have the advantage of representing a possible saving in relation to the cost and weight of the rotor. However, their use of fewer rotor blades implies that a higher rotational speed or a larger chord is needed to yield the same energy output as a three-bladed turbine of a similar size. The use of one or two blades will also result in

more fluctuating loads because of the variation of the inertia, depending on the blades being in horizontal or vertical position and on the variation of wind speed when the blade is pointing upward and downward. Therefore, the two and one-bladed concepts usually have so-called teetering hubs, implying that they have the rotor hinged to the main shaft. This design allows the rotor to teeter in order to eliminate some of the unbalanced loads. One-bladed wind turbines are less widespread than two-bladed turbines. This is due to the fact that they, in addition to a higher rotational speed, more noise and visual intrusion problems, need a counterweight to balance the rotor blade.

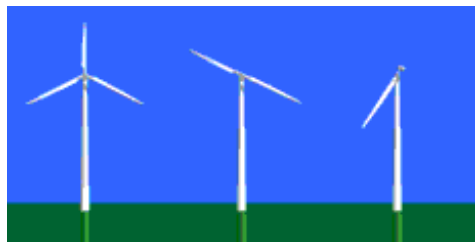


Figure 1-4. Three, two and one-bladed wind turbine concepts. From www.windpower.org (2000), © Danish Wind Turbine Manufacturers Association.

1.2.4 Power control aspects

Wind turbines are designed to produce electricity as cheap as possible. For this purpose, wind turbines are in general designed to yield a maximum power output at wind speeds around 15 m/s. It would not pay to design turbines to maximise their power output at stronger winds, because such strong winds are usually too rare. However, in case of stronger winds, it is necessary to waste part of the excess energy to avoid damage on the wind turbine. Thus, the wind turbine needs some sort of power control. The power control is divided into two regimes with different concepts:

- power optimisation for low wind speeds
- power limitation for high wind speeds

These regimes are separated by the wind speed at which the maximum power output is achieved, typically about 15 m/sec.

Basically, there are three approaches to power control:

- stall control
- pitch control
- active stall control

Stall-controlled wind turbines have their rotor blades bolted to the hub at a fixed angle. The stall phenomenon is used to limit the power output when the wind speed becomes too high. This is achieved by designing the geometry of the rotor blade in such a way that flow separation is created on the downwind side of the blade when the wind speed exceeds some chosen critical value. Stall control of wind turbines requires correct trimming of the rotor blades and correct setting of the blade angle relative to the rotor plane. Some drawbacks of this method are: lower efficiency at low wind speeds, no assisted start and variations in the maximum steady state power due to variation in the air density and grid frequencies.

Pitch-controlled wind turbines have blades that can be pitched out of the wind to an angle where the blade chord is parallel to the wind direction. The power output is monitored and whenever it becomes too high, the blades will be pitched slightly out of the wind to reduce the produced power. The blades will be pitched back again once the wind speed drops. Pitch control of wind turbines requires a design that ensures that the blades are pitched at the exact angle required in order to optimise the power output at all wind speeds. Nowadays, pitch control of wind turbines is only used in conjunction with variable rotor speed. An advantage of this type of control is that it has a good power control, i.e. that the mean value of the power output is kept close to the

rated power of the generator at high wind speeds. Disadvantages encompass extra complexity due to the pitch mechanism and high power fluctuations at high wind speeds.

Active stall-controlled turbines resemble pitch-controlled turbines by having pitchable blades. At low wind speeds, active stall turbines will operate like pitch-controlled turbines. At high wind speeds, they will pitch the blades in the opposite direction of what a pitch-controlled turbine would do and force the blades into stall. This enables a rather accurate control of the power output, and makes it possible to run the turbine at the rated power at all high wind speeds. This control type has the advantage of having the ability to compensate for the variations in the air density.

Figure 1-5 shows iso-power curves for a wind turbine as a function of the blade angle and the mean wind speed. The ranges for pitch control and active stall control are separated at a blade angle of 0° with the rotor plane. At low wind speeds, the optimal operation of the wind turbine is achieved at a blade angle close to 0° . At higher wind speeds, the turbine will overproduce if the blade angle is not adjusted accordingly. With pitch control, the blade is pitched positively with its leading edge being turned towards the wind. With active stall control, the blade is pitched negatively with its trailing edge turned towards the wind. The power control and, in particular, the power limitation at higher wind speeds are indicated in an idealised manner for both control approaches by the dashed curves in Figure 1-5. The dashed curves illustrate how the transition between operation with 0° blade angle at low wind speeds and power-limiting operation along an iso-power curve at high wind speeds can be achieved for a three-bladed rotor at a rated power of 400 kW. In this example, the rated power is reached at a wind speed of about 12 m/sec.

1.3 Economical aspects

The ideal wind turbine design is not dictated by technology alone, but by a combination of technology and economy. Wind turbine manufacturers wish to optimise their machines, so that they deliver electricity at the lowest possible cost per unit of energy. In this context, it is not necessarily optimal to maximise the annual energy production, if that would require a very expensive wind turbine. Since the energy input (the wind) is free, the optimal turbine design is one with low production costs per produced kWh.

The choice of rotor size and generator size depends heavily on the distribution of the wind speed and the wind energy potential at a prospective location. A large rotor fitted with a small generator will produce electricity during many hours of the year, but it will only capture a small part of the wind energy potential. A large generator will be very efficient at high wind speeds, but inefficient at low wind speeds. Sometimes it will be beneficial to fit a wind turbine with two generators with different rated powers.

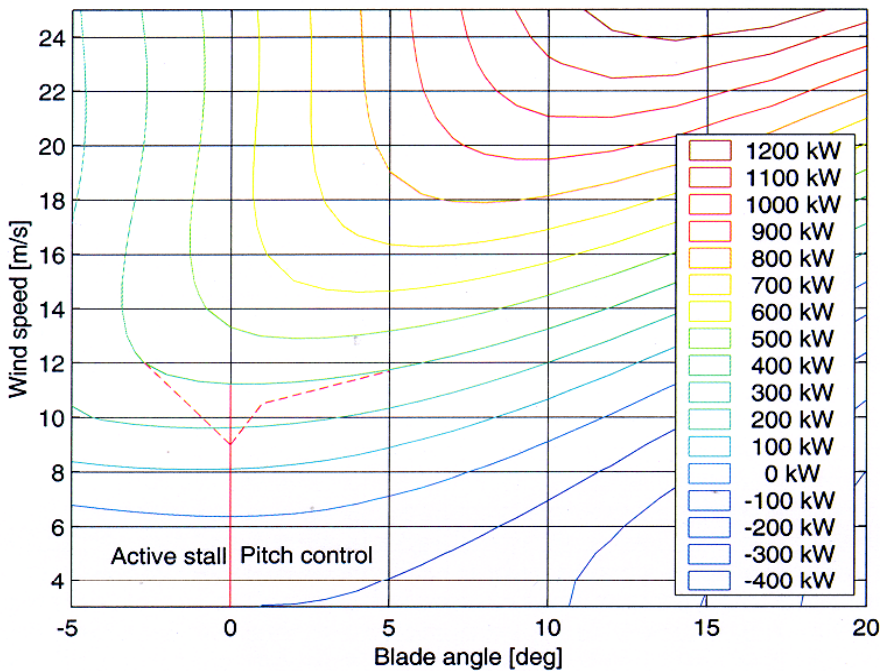


Figure 1-5. Iso-power curves for a wind turbine at 26.88 rpm vs. blade angle and mean wind speed

1.4 Power production

A study of different Danish wind turbine designs shows that the specific power performance in terms of produced energy per m^2 rotor area per year ($kWh/m^2/year$) is

almost independent of the rotor size. See Petersen, 1998.

Hence, the main consideration in the evaluation of the cost of the turbine is the specific rotor power (kW/m^2) and the specific cost ($cost/m^2$ rotor) together with

expected service life and cost and availability. An availability factor, i.e. the amount of time that the turbine is producing energy, or is ready for production, of 98 % is common for commercial turbines.

Thus the primary factor affecting the power performance is the rotor size. Secondary factors are the control principle such as stall- or pitch control and single- dual- or variable speed.

1.4.1 Power curve

The power being produced by any type of wind turbine can be expressed as

$$P = \frac{1}{2} \cdot \rho \cdot V^3 \cdot A \cdot C_p$$

- P output power
- ρ air density
- V free wind speed
- A rotor area
- C_p efficiency factor

The power coefficient C_p is a product of the mechanical efficiency η_m , the electrical efficiency η_e , and of the aerodynamic efficiency. All three factors are dependent on the wind speed and the produced power, respectively. The mechanical efficiency η_m is mainly determined by losses in the gearbox and is typically 0.95 to 0.97 at full load. The electrical efficiency covers losses in the generator and electrical circuits. At full load $\eta_e = 0.97 - 0.98$ is common for configurations with an induction generator. It can be shown that the maximum possible value of the aerodynamic efficiency is $16/27 = 0.59$, which is achieved when the turbine reduces the wind speed to one-third of the free wind speed (Betz' law).

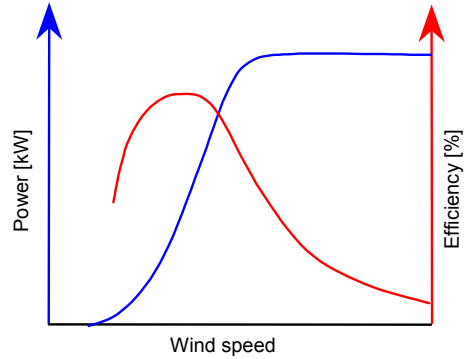


Figure 1-6. Power- and efficiency curve

The produced power varies with the wind speed as can be seen from the blue graph in Figure 1-6. The form of the graph varies slightly from different concepts. Assuming constant efficiency (e.g. constant tip speed ratio) the graph basically consists of a third degree polynomial up to the rated wind speed at which the nominal power is reached. At this point the power regulation sets in, either by the blades stalling or by pitching the blades to attain an approximately constant power. The power curve and the power efficiency curve are often presented in the same graph, with the power and the efficiency scales on each side of the graph as shown in Figure 1-6.

Figure 1-7 illustrates the controlled power curve of a wind turbine, in the case of 1) stall controlled, fixed speed configuration, and 2) pitch controlled, variable speed configuration.

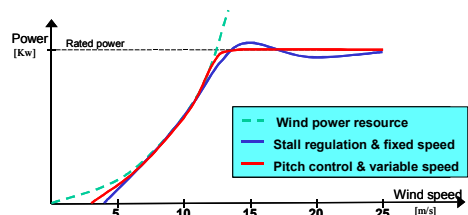


Figure 1-7. Examples of power curves for two types of wind turbines.

The efficiency factor C_p typically reaches a maximum at a wind speed of 7-9 m/sec and, normally, it does not exceed 50%. The electric power typically reaches the rated power of the turbine at a wind speed of 14-16 m/sec.

In the Danish approval scheme as well as in the IEC wind turbine classification system, the power curve is required to be determined from measurements.

1.4.2 Annual energy production

The wind speed distribution is often represented by a Weibull distribution. The density function of the Weibull probability can be expressed as shown in Figure 1-8.

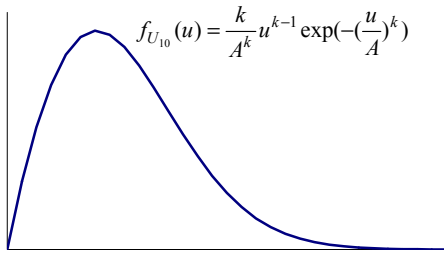


Figure 1-8. Weibull density function.

Hence, for a specific site the wind climate can be described in terms of the parameters A and k , and from these the average wind speed V_{ave} , as defined in IEC 61400-1, can be calculated

$$V_{ave} = \begin{cases} A\Gamma(1 + 1/k) \\ A\sqrt{\pi}/2, & \text{if } k = 2 \end{cases}$$

in which Γ is the gamma function.

In the Danish standard it is common to describe the wind climate in terms of the roughness class, and an explicit correlation exists between the roughness class and the average wind speed.

For a particular wind turbine, the power production is defined by the power curve as described above. By combining the power curve with the wind distribution the actual energy production is yielded, often expressed in terms of the annual energy production E_{year} .

$$E_{year} = N_0 \int_{V_{start}}^{V_{stop}} P(u)f(u) du$$

- $P(u)$ power curve function
- $f(u)$ wind distribution function
- V_{start} cut-in wind speed
- V_{stop} cut-out wind speed
- $N_0 = 8765$ hours/year

Dividing E_{year} by the rotor area yields the specific power performance, which is another common way to express the turbine efficiency.

Yet another way of expressing the efficiency of a particular turbine is given by using the capacity factor, which is defined as the ratio of actual average power to the rated power measured over a period of time (average kW/rated kW). The total energy that would be produced by a wind turbine during a one-year period, assuming a certain distribution of wind speed probability density and assuming 100 per cent availability, is referred to as the potential annual energy output.

1.5 Configurations and sizes

Wind turbines are erected as stand-alone turbines, in clusters of multiple turbines, or – on a larger scale – in park configurations. Before the 1980's, wind energy development focused on the individual wind turbine. By the late 1980's, this perspective began to change as attention shifted to collective generation of electric power from

an array of wind turbines located in the vicinity of each other and commonly referred to as wind parks or wind farms. In the early 1980's, the typical size of a wind turbine was about 55 kW in terms of rated power, whereas turbine sizes today have exceeded 2 MW. Table 1-1 gives examples of typical combinations of rotor diameter and rated power for a number of different tower heights.

Tower height (m)	Rotor diameter (m)	Rated power (kW)
22	21	55
31	30	225
35	35	450
35-40	41-44	500
44	43	600
50	48	750
50	54	1000
60	58	1500
64-80	72-76	2000
85	115	5000



Figure 1-9. Vindeby Offshore Wind Farm. From www.windpower.org (1997) © Bonus.

While wind energy is already economic in terms of good onshore locations, it is currently about to cross the economic frontier set by shorelines: offshore wind energy is becoming competitive with other power-generating technologies. Offshore wind energy is a promising application of wind power, in particular, in countries with

high population density and thus with difficulties in finding suitable sites on land. Construction costs are much higher at sea, but energy production is also much higher. Currently, wind energy from turbines erected on fixed foundations in up to 15 m water depth is considered economically feasible. Figure 1-9 shows an example of an early offshore wind farm.

1.6 Future concepts



Figure 1-10. A conception of a flexible wind turbine. During stand-still, the blades deflect as a rush in the wind.

Until now the development of large wind turbines has mainly been prompted by upscaling the dominating concepts described in this section. Still, new concepts for wind turbine designs and components are being developed in an attempt to anticipate the demands for the continuing growth of wind turbines.

One proposal for a future concept is characterised by more flexible wind turbine concepts. One element in this is an expected increase in the structural flexibility of wind turbines. Figure 1-10 exemplifies how the latter can be conceived. Another element is an expected increase in the flexibility of the drive train, e.g. in terms of gearless designs with variable rotational speeds, and a more

extensive use of power electronics can also be expected.

Also, more flexible control systems can be foreseen as an increasing number of computers and sensors are incorporated to allow for adaptive operation. In this context, it is possible that a shift may take place from focusing on wind turbine control to focusing on wind farm control. A development which will inevitably, put other requirements on the individual wind turbine in addition to the ones we are experiencing today.

REFERENCES

Danish Energy Agency, *Technical Criteria for the Danish Approval Scheme for Wind Turbines*, 2000.

IEC 61400-12 *Wind turbine generator systems, part 12: Wind turbine power performance testing*, 1st edition, 1999.

IEC WT0, *IEC System for Conformity Testing and Certification of Wind turbines, Rules and Procedures*, International Electrotechnical Commission, 1st edition, 2001-04.

Petersen, H., *Comparison of wind turbines based on power curve analysis*, Helge Petersen Consult, Darup Associates Ltd., 1998.

2. Safety and Reliability

2.1 Safety philosophy

A wind turbine should be designed, dimensioned and manufactured in such a way that it, if correctly used and maintained over its anticipated service life, can withstand the assumed loads within the prescribed level of safety and possess a sufficient degree of durability and robustness. Calculation, or a combination of calculation and testing, can be used to demonstrate that the structural elements of a wind turbine meet the prescribed level of safety.

The prescribed level of safety for a structural element can be expressed in terms of a requirement for the probability of failure and be determined on the basis of so-called risk acceptance criteria. It depends on the type and consequence of failure. The type of failure can be characterised by the degree of ductility and the amount of reserve capacity or structural redundancy. The consequence of failure can be characterised in terms of the fatalities and societal consequences involved. The more severe the consequence is, and the more limited the reserve capacity is, the smaller is the acceptable failure probability. The prescribed safety is standardised in terms of safety classes as described in more detail in Section 2.3. A distinction is made between low, normal and high safety class. The higher the safety class is, the heavier is the requirement for the level of safety, i.e. the smaller is the acceptable failure probability.

A wind turbine is equipped with a control and protection system, which defines an envelope of possible design situations that the wind turbine will experience. To keep the wind turbine within this envelope, it is part of the safety philosophy that the protection system shall possess a sufficiently

high level of reliability to render the joint probability negligible that a failure should occur during an extreme event and that the protection system should be unable to fulfil its task. Usually, non-redundant structural parts of the protection system are therefore designed to high safety class.

The prescribed level of safety or the choice of safety class may differ for different parts of the wind turbine. The rotor is usually designed to at least normal safety class. Other structural parts such as tower and foundation are usually assigned to safety classes according to the possible consequences of a failure. Since failure of the foundation will have consequences for the tower and the rotor, while failure of the rotor or the tower may not necessarily have consequences for the foundation, an attractive approach to the choice of safety classes for various structural parts could be to attempt a so-called fail-grace sequence, i.e. a sequence of failures in which the foundation will be the last structural part to fail. This sequence is based on a feasibility study of the consequences of failure for the wind turbine structure and its foundation only. However, usually the rotor is designed to normal or high safety class, which is not necessarily in accordance with the above fail-grace philosophy. Requirements for designing a wind turbine rotor to normal or high safety class derive from the hazards that the rotor poses on its surroundings, when the turbine runs away, or when the rotor fails. In such events, parts of the rotor may be shed in distances up to one kilometre or even farther away from the turbine location.

It should be noted that the level of safety is usually the result of a trade-off with economy. In DS472, emphasis is placed on safety. However, in terms of offshore turbines it is inevitable that economical aspects will become more predominant than

they are onshore, and that more emphasis will eventually be placed on financial factors when it comes to safety issues and determination of acceptable safety levels.

Limit state design is used to achieve the prescribed level of safety. It is common to verify the safety of a wind turbine with respect to the following limit states:

- ultimate limit state
- serviceability limit state
- accidental limit state

For this purpose, design loads are derived from multiplying characteristic loads by one or more partial safety factors, and design capacities are derived from dividing characteristic capacities by one or several other partial safety factors. Partial safety factors are applied to loads and material strengths to account for uncertainties in the characteristic values. Verification of the structural safety is achieved by ensuring that the design load, or the combination of a set of design loads, does not exceed the design capacity. In case a combination of loads is used, it should be noted that it is common always to combine one extreme load with one or several “normal” loads. Two or several extreme loads are usually not combined, unless they have some correlation.

Characteristic loads and characteristic capacities constitute important parameters in the design process. Characteristic loads for assessment of the ultimate limit state are usually determined as load values with a 50-year recurrence period, and they are therefore often interpreted as the 98% quantile in the distribution of the annual maximum load. This choice does not necessarily imply that a design lifetime of exactly 50 years is considered. It is more a matter of tradition and convenience. Nor should it be taken as a 50-year guarantee within which failures will not occur. For assessment of fatigue, a design lifetime is needed, and in this context it is common to

consider a 20-year design lifetime for wind turbines. Characteristic capacities are usually chosen as low quantiles in the associated capacity distributions. The partial safety factors that are applied in the design account for the possible more unfavourable realisation of the loads and capacities than those assumed by the choice of characteristic values. Note in this context that some of the partial safety factors, which are specified in standards, are not safety factors in the true sense, but rather reduction factors which account for degradation effects, scale effects, temperature effects, etc. and which happen to appear in the design expressions in exactly the same manner as true partial safety factors.

With structural safety being a major goal of the design, it is important to make sure that the characteristic values of load and material quantities, which have been assumed for the design, are achieved in practice. Non-destructive testing of completed structural parts plays a role in this context, and control of workmanship another. Material certificates also come in handy in this context. In general, one may say that inspection is an important part of the safety philosophy. Not least, as it will allow for verification of assumptions made during the design and for taking remedial actions if averse conditions are detected during the service life of the wind turbine.

For details about structural safety and limit state design, reference is made to Section 2.3. For details about combinations of design situations and external conditions, as well as a definition of load cases, reference is made to Chapter 4.

2.2 System safety and operational reliability

A wind turbine is to be equipped with control and protection systems which are

meant to govern the safe operation of the wind turbine and to protect the wind turbine from ill conditions. Some components will act in both the control and the protection function, but distinction is made in that the control system monitors and regulates the essential operating parameters to keep the turbine within defined operating range whereas the protection system ensures that the turbine is kept within the design limits. The protection system must take precedence over the control system.

2.2.1 Control system

Controls are used for the following functions:

- to enable automatic operation
- to keep the turbine in alignment with the wind
- to engage and disengage the generator
- to govern the rotor speed
- to protect the turbine from overspeed or damage caused by very strong winds
- to sense malfunctions and warn operators of the need for maintenance or repair

The control system is meant to control the operation of the wind turbine by active or passive means and to keep operating parameters within their normal limits. Passive controls use their own sensing and are exercised by use of natural forces, e.g. centrifugal stalling or centrifugal feathering. Active controls use electrical, mechanical, hydraulic or pneumatic means and require transducers to sense the variables that will determine the control action needed. Typical variables and features to be monitored in this respect include:

- rotor speed
- wind speed
- vibration
- external temperature
- generator temperature

- voltage and frequency at mains connection
- connection of the electrical load
- power output
- cable twist
- yaw error
- brake wear

The control system is meant to keep the wind turbine within its normal operating range. As a minimum, the normal operating range should be characterised by the following properties and requirements:

- a maximum 10-minute mean wind speed at hub height, V_{\max} , i.e. the stop wind speed below which the wind turbine may be in operation
- a maximum long-term mean nominal power P_{nom} , interpreted as the highest power on the power curve of the wind turbine in the wind speed interval $[V_{\min}; V_{\max}]$, where V_{\min} denotes the start wind speed for the turbine
- a maximum nominal power P_{\max} , which on average over 10 minutes may not be exceeded for a wind speed at hub height of $V_{10\text{min, hub}} < V_{\max}$
- a maximum operating frequency of rotation $n_{r, \max}$ for the wind turbine
- a maximum transient frequency of rotation n_{\max} for the wind turbine
- a wind speed below which the wind turbine may be stopped

The wind turbine is kept within its normal operating range by means of the control system, which activates and/or deactivates the necessary controls, e.g.:

- yaw (alignment with the wind)
- blade angle regulation
- activation of the brake system
- power network connection
- power limitation
- shutdown at loss of electrical network or electrical load

In addition, it must be possible to stop the wind turbine, e.g. for the purpose of inspection and repairs, or in case of emergencies. Monitoring of the control system and its functions must be adapted to the actual design of the wind turbine. Design of a wind turbine control system requires a background in servo theory, i.e. theory dealing with control of continuous systems.

The control system is of particular importance in areas where weak grids are encountered. Weak grids can, for example, be found in sparsely populated areas where the capacity of the grids can often be a limiting factor for the exploitation of the wind resource in question. Two problems are identified in this context:

- increase of the steady-state voltage level of the grid above the limit where power consumption is low and wind power input is high
- voltage fluctuations above the flicker limit may result from fluctuating wind power input caused by fluctuating wind and wind turbine cut-ins.

The solution to the above problems is to use a so-called power control as part of the control system. The power control concept implies buffering the wind turbine power in periods where the voltage limits may be violated and releasing it when the voltage is lower. This method is combined with a smoothening of the power output, such that fluctuations are removed, in particular those that would exceed the flicker limit.

2.2.2 Protection system

The protection system is sometimes referred to as the safety system. Mechanical, electrical and aerodynamic protection systems are available. The protection system is to be activated when, as a result of control system failure or of the effects of some other failure event, the wind turbine is not kept within its normal operation range. The protection system shall then bring the wind

turbine to a safe condition and maintain the turbine in this condition. It is usually required that the protection system shall be capable of bringing the rotor to rest or to an idling state from any operating condition. In the IEC standard an additional requirement is that means shall be provided for bringing the rotor to a complete stop from a hazardous idling state in any wind speed less than the annual extreme wind speed. The activation levels for the protection system have to be set in such a way that design limits are not exceeded.

Situations which call for activation of the protection system include, but are not necessarily limited to:

- overspeed
- generator overload or fault
- excessive vibration
- failure to shut down following network loss, disconnection from the network, or loss of electrical load
- abnormal cable twist owing to nacelle rotation by yawing

The protection system should therefore as a minimum cover monitoring of the following:

- rotational speed or rotational frequency
- overload of a generator or other energy conversion system/load
- extreme vibrations in the nacelle
- safety-related functioning of the control system

As overspeed is by far the most critical error, rotational speed monitors form a crucial element of the protection system.

A protection system consists of:

- a registering unit
- an activating unit
- a brake unit

The protection system shall include one or more systems (mechanical, electrical or aerodynamic) capable of bringing the rotor to rest or to an idling state. In the Danish

standard at least two brake systems must be included, and at least one of these must have an aerodynamically operated brake unit. See Section 2.3.3.

To ensure immediate machine shutdown in case of personal risk, an emergency stop button, which will overrule both the control and normal protection system, shall be provided at all work places.

In addition to what is stated above, the protection system is, as a minimum, to be subjected to the following requirements:

- the protection system must take precedence over the control system
- the protection system must be fail-safe in the event that the power supply fails
- structural components in mechanisms of the protection system shall be designed to high safety class
- the protection system must be able to register a fault and to bring the wind turbine to a standstill or to controlled freewheeling in all situations in which the rotor speed is less than n_{max} .
- the protection system must be tolerant towards a single fault in a sensor, in the electronic and electrical as well as the hydraulic systems or in active mechanical devices, i.e. an undetected fault in the system must not prevent the system from detecting a fault condition and carrying out its function
- the reliability of the protection system must ensure that situations caused by failures in the protection system, whereby the extreme operating range is exceeded, can be neglected

The reliability of the protection system may be ensured by means of either (1) the entire protection system being of a fail-safe design, or (2) redundancy of the parts of the protection system where it cannot be made fail-safe, or (3) frequent inspections of the functioning of the protection system, in

which risk assessment is used to determine the interval between inspections.

Fail-safe is a design philosophy, which through redundancy or adequacy of design in the structure, ensures that in the event of a failure of a component or power source, the wind turbine will remain in a non-hazardous condition.

2.2.3 Brake system

The brake system is the active part of the protection system. Examples of brake systems are:

- mechanical brake
- aerodynamic brake
- generator brake

An aerodynamic brake system usually consists of turning the blade tip or, as commonly seen on active stall- and pitch-controlled turbines, of turning the entire blade 90° about the longitudinal axis of the blade. This results in aerodynamic forces that counteract the rotor torque. Also, spoilers and parachutes have been used as aerodynamic brakes.



Figure 2-1. Tip brake, from www.windpower.org (2000), © Danish Wind Turbine Manufacturers' Association.

The reliability of a brake system is of the utmost importance to ensure that the system will serve its purpose adequately. In this respect, it is important to be aware of possible dependencies between different brakes or different brake components. For example, if all three blades are equipped with tip brakes, some dependency between the three tip brakes can be expected, cf. the common cause failures that can be foreseen for these brakes. This will influence the overall reliability against failure of the system of the three tip brakes and needs to

be taken into account if the failure probability exceeds 0.0002 per year.

Brakes or components of brake systems will be subject to wear. Thus, current monitoring and maintenance are required.

IEC61400-1 requires that the protection system shall include one or more systems, i.e. mechanical, electrical, or aerodynamic brakes, capable of bringing the rotor to rest or to an idling state from any operating condition. At least one of these systems shall act on the low-speed shaft or on the rotor of the wind turbine. The idea behind this is to have a brake system which ensures that a fault will not lead to a complete failure of the wind turbine.

DS472 is more strict by requiring at least two fail-safe brake systems. If the two systems are not independent, i.e. if they have some parts in common, then the turbine shall automatically be brought to a complete stop or to controlled idling in the event of a failure in the common parts. At least one brake system is required to have an aerodynamic brake unit.

2.2.4 Failure mode and effects analysis

A failure mode and effects analysis is a qualitative reliability technique for systematic analysis of mechanical or electrical systems, such as a wind turbine protection system. The analysis includes examination of each individual component

of the system for determination of possible failure modes and identification of their effects on the system. The analysis is based on a worksheet that systematically lists all components in the system, including:

- component name
- function of component
- possible failure modes
- causes of failure
- how failures are detected
- effects of failure on primary system function
- effects of failure on other components
- necessary preventative/repair measures

The failure mode and effects analysis can be supplemented by a criticality analysis, which is a procedure that rates the failure modes according to their frequency or probability of occurrence and according to their consequences. The assigned ratings can be used to rank the components with respect to their criticality for the safety of the system. An example of a worksheet is given in Table 2-1.

A failure mode and effects analysis can be conducted at various levels. Before commencing, it is thus important to decide what level should be adopted as some areas may otherwise be examined in great detail, while others will be examined at the system level only without examination of the individual components. If conducted at too detailed a level, the analysis can be rather time-consuming and tedious, but will undoubtedly lead to a thorough understanding of the system.

Table 2-1. Example of worksheet.

COMPONENT	FAILURE MODE	FAILURE CAUSE	FAILURE EFFECT	FAILURE DETECTION	FREQUENCY RATING	SEVERITY RATING
Valve	Leak past stem	Deteriorated seal	Oil leak	Visual by ROV	Low	Low
	Fails to close on command	Control system failure	Valve will not shut off flow	Flow does not shut off	Medium	Low

The failure mode and effects analysis is primarily a risk management tool. The strength of the failure mode and effects analysis is that, if carried out correctly, it identifies safety-critical components where a single failure will be critical for the entire system. It is a weakness, however, that it depends on the experience of the analyst and that it cannot easily be applied to cover multiple failures.

2.2.5 Fault tree analysis

A fault tree is a logical representation of the many events and component failures that may combine to cause one critical event such as a system failure. It uses “logic gates” (mainly AND and OR gates) to show how “basic events” may combine to cause the critical “top event”.

Application

Fault tree analysis has several potential uses in relation to wind turbine protection systems:

- In frequency analysis, it is common to quantify the probability of the top event occurring based on estimates of the failure rates of each component. The top event may comprise an individual failure case, or a branch probability in an event tree.
- In risk presentation, it may also be used to show how the various risk contributors combine to produce the overall risk.
- In hazard identification, it may be used qualitatively to identify combinations of basic events that are sufficient to cause the top event, also known as “cut sets”.

Construction of a fault tree

Construction of a fault tree usually commences with the top event and then works its way downwards to the basic events. For each event, it considers what conditions are necessary to produce the event, and it then represents these as events

at the next level. If one of several events causes the higher event, it is joined with an OR gate. If two or more events must occur in combination, they are joined with an AND gate.

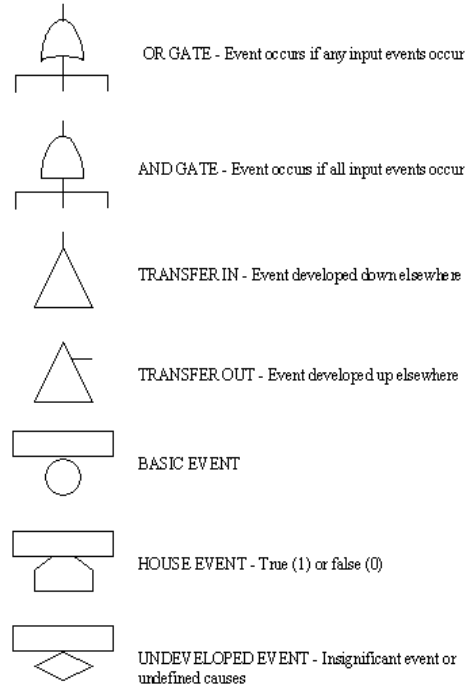


Figure 2-2. Fault tree symbols.

If quantification of the fault tree is the objective, downward development should stop once all branches have been reduced to events that can be quantified in terms of probabilities or frequencies of occurrence.

Various standards for symbols are used – the most typical ones are shown in Figure 2-2. An example of a fault tree is shown in Figure 2-3.

Some types of events, for example a fire or power failure, may affect many components in the system at once. These are known as “common-cause failures” and may be represented by having the same basic event occurring at each appropriate place in the fault tree.

Combination of frequencies and probabilities

Both frequencies and probabilities can be combined in a fault tree, providing the rules in Table 2-2 are followed.

Gate	Inputs	Outputs
OR	Probability + Probability	Probability
AND	Frequency + Frequency	Frequency
	Frequency + Probability	Not permitted
	Probability × Probability	Probability
	Frequency × Frequency	Not permitted
	Frequency × Probability	Frequency

computer programs are used to identify minimal cut sets.

Minimal cut sets can be used in hazard identification to describe combinations of events necessary to cause the top event.

Minimal cut sets can, moreover, be used to rank and screen hazards according to the number of events that must occur simultaneously. In principle, single event cut sets are of concern because only one failure can lead to the top event. In reality, larger cut sets may have a higher frequency of occurrence. Nevertheless, the method can be useful for hazard screening and for suggesting where additional safeguards may be needed.

Quantification of a fault tree

Simple fault trees may be analysed by using a gate-by-gate approach to determine the top event probability, provided that all events are independent and that there are no common cause failures. This gate-by-gate approach is useful for QRA (Quantitative Risk Analysis), because it quantifies all intermediate events in the fault tree and provides a good insight into the main contributors to the top event and the effectiveness of safeguards represented in the tree. However, because it cannot represent repeated events or dependencies correctly, it is normally not used for formal reliability analysis. Reliability analysis of more complex fault trees requires minimal cut set analysis to remove repeated events.

Strengths and weaknesses

Preparation and execution of a fault tree analysis is advantageous in the sense that it forces the wind turbine manufacturer to examine the protection system of his wind turbine systematically. When probabilities can be assigned to events, the fault tree methodology can be applied to assess the overall reliability of the wind turbine

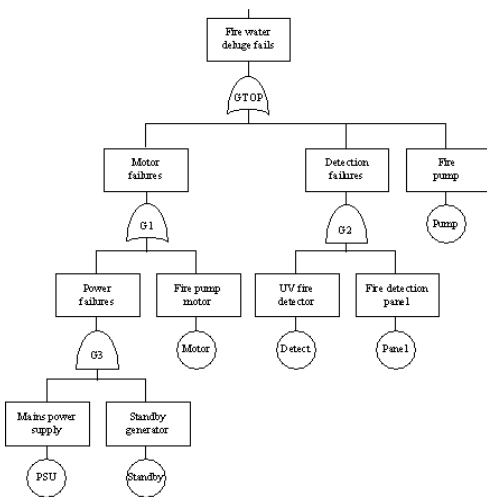


Figure 2-3. Example of fault tree.

Minimal cut set analysis

Cut sets comprise combinations of events that are sufficient to cause the top event. Minimal cut sets contain the minimum sets of events necessary to cause the top event, i.e. after eliminating any events that occur more than once in the fault tree. In case of simple fault trees, with each basic event only occurring once, the minimal cut sets can be identified by means of inspection. For more complex trees, formal methods such as the Boolean analysis are required. Most often,

protection system. Furthermore, it can be used to determine the most critical events and parts of the protection system.

Beware, however, that it is often hard to find out whether a fault tree analysis has been carried out properly. Fault tree analyses become complicated, time-consuming and difficult to follow for large systems, and it becomes easy to overlook failure modes and common cause failures. It is a weakness that the diagrammatic format discourages analysts from stating assumptions and conditional probabilities for each gate explicitly. This can be overcome by careful back-up text documentation. It is a limitation that all events are assumed to be independent. Fault tree analyses lose their clarity when applied to systems that do not fall into simple failed or working states such as human error, adverse weather conditions, etc.

2.3 Structural safety

2.3.1 Limit states

During the lifetime of a structure, the structure is subjected to loads or actions. The loads may cause a change of the condition or state of the structure from an undamaged or intact state to a state of deterioration, damage, or failure. Structural malfunction can occur in a number of modes covering all failure possibilities that can be imagined for the structure. Although the transition from an intact state to a state of malfunction can indeed be continuous, it is common to assume that all states with respect to a particular mode of malfunction can be divided into two sets: 1) states that have failed, and 2) states that have not failed or are safe. The boundary between the safe states and the failed states is referred to as the set of limit states. The safety or reliability of a structure is concerned with

how likely it is that the structure will reach a limit state and enter a state of failure.

There are several types of limit states. Two types are common, ultimate limit states and serviceability limit states. Ultimate limit states correspond to the limit of the load-carrying capacity of a structure or structural component, e.g. plastic yield, brittle fracture, fatigue fracture, instability, buckling, and overturning. Serviceability limit states imply that there are deformations in excess of tolerance without exceeding the load-carrying capacity. Examples are cracks, wear, corrosion, permanent deflections and vibrations. Fatigue is sometimes treated as a separate type of limit state. Other types of limit states are possible, e.g. accidental limit states and progressive limit states.

2.3.2 Failure probability and other measures of structural reliability

In structural design, the reliability of a structural component is evaluated with respect to one or more failure modes. One such failure mode is assumed in the following. The structural component is described by a set of stochastic basic variables grouped into one vector \mathbf{X} , including, e.g. its strength, stiffness, geometry, and loading. Each of these variables are stochastic in the sense that they – owing to natural variability and other possible uncertainties – may take on random degrees of realisation according to some probability distribution. For the considered failure mode, the possible realisation of \mathbf{X} can be separated into two sets: 1) the set for which the structural component will be safe, and 2) the set for which it will fail. The surface between the safe set and the failure set in the space of basic variables is denoted the limit state surface, and the reliability problem is conveniently described by a so-called limit state function $g(\mathbf{X})$, which is defined such that

$$g(\mathbf{X}) \begin{cases} > 0 \text{ for } \mathbf{X} \text{ in safe set} \\ = 0 \text{ for } \mathbf{X} \text{ on limit state surface} \\ < 0 \text{ for } \mathbf{X} \text{ in failure set} \end{cases}$$

The limit state function is usually based on some mathematical engineering model for the considered limit state, based on the underlying physics, and expressed in terms of the governing load and resistance variables.

The failure probability is the probability content in the failure set

$$P_F = P[g(\mathbf{X}) \leq 0] = \int_{g(\mathbf{X}) \leq 0} f_{\mathbf{X}}(\mathbf{x}) d\mathbf{x}$$

where $f_{\mathbf{X}}(\mathbf{x})$ is the joint probability density function for \mathbf{X} and represents the uncertainty and natural variability in the governing variables \mathbf{X} . The complement $P_S = 1 - P_F$ is referred to as the reliability and is sometimes also denoted the probability of survival. The reliability may be expressed in terms of the reliability index,

$$\beta = -\Phi^{-1}(P_F),$$

where Φ is the standardised normal distribution function. The failure probability, the reliability, and the reliability index are all suitable measures of structural safety.

For the simple example that \mathbf{X} consists of two variables, the load L and the resistance R , and the limit state function can be specified as $g(\mathbf{X}) = R - L$, the failure probability becomes a simple convolution integral

$$\begin{aligned} P_F &= P[R - L < 0] = \int_{R-L < 0} f_R(r) f_L(l) dr dl \\ &= \int_{-\infty}^{\infty} \int_{-\infty}^l f_R(r) f_L(l) dr dl \\ &= \int_{-\infty}^{\infty} F_R(l) f_L(l) dl \end{aligned}$$

where f_R and f_L are the probability density functions of R and L , respectively, and $f_R(r) = dF_R(r)/dr$, where F_R is the cumulative distribution function of R .

2.3.3 Structural reliability methods

The reliability index β can be solved in a structural reliability analysis by means of a reliability method which can be any amongst several available methods, including numerical integration, analytical first- and second-order reliability methods, and simulation methods. Reference is made to Madsen et al. (1986). Some of these methods are approximate methods, which will lead to approximate results for the reliability index. Numerical integration is usually only feasible when \mathbf{X} consists of very few stochastic variables such as in the example above. Analytical first- and second-order solutions to the failure probability are often sufficiently accurate, and they are advantageous to simulation results when failure probabilities are small.

A useful by-product of a structural reliability analysis by these methods is the so-called design point \mathbf{x}^* . This is a point on the limit state surface and is the most likely realisation of the stochastic variables \mathbf{X} at failure.

2.3.4 Code format, characteristic values, and partial safety factors

A structural design code specifies design rules that are to be fulfilled during the design of a structure or structural component. The general layout of the design

rules in a design code is known as the code format.

The code format most frequently used in design codes today is a format which is expressed in terms of design values of governing load and resistance variables. These design values are defined as characteristic values of the load and resistance variables, factored by partial safety factors. Such a form of code format results from requirements for an easy and yet economical design and is known as a design value format. Design according to a design value format is sometimes referred to as load and resistance factor design (LRFD).

In its simplest form, a code requirement can be expressed as a design rule in terms of an inequality

$$L_D < R_D$$

in which L_D is the design load effect and R_D is the design resistance. The design load effect is calculated as

$$L_D = \gamma_f L_C$$

where L_C is the characteristic load effect and γ_f is a load factor. Similarly, the design resistance is calculated as

$$R_D = \frac{R_C}{\gamma_m}$$

where R_C is the characteristic resistance and γ_m is a material factor.

Usually, a number of different load effects have to be combined into a resulting load effect, and often the largest of several different such load combinations is used for the load effect in the design rule. An example of such a load combination is the combination of gravitational loads and wind loads.

The characteristic values are usually taken as specific quantiles in the load and resistance distributions, respectively. The characteristic values are often the mean value for dead load, the 98% quantile in the distribution of the annual maxima for variable (environmental) load, and the 2% or 5% quantile for strength. Reference is made to Figure 2-4. The code also specifies values to be used for the partial safety factors γ_f and γ_m .

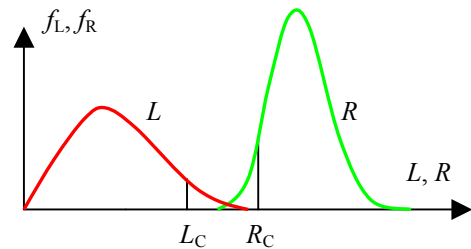


Figure 2-4. Probability density functions and characteristic values for load L and resistance R .

The design equation is a special case of the design rule obtained by turning the inequality into an equality, i.e., $R_D = L_D$ in the example.

2.3.5 Code calibration

Fulfilment of the design rules, as required by a structural design code, is meant to ensure that a particular prescribed structural safety level is achieved. The purpose of a code calibration is to determine the set of partial safety factors to be used with the chosen code format, such that structural designs according to the code will meet this prescribed level of safety.

Structural reliability analysis results, obtained as outlined above, play an important role in codified practice and design. Their application to calibration of partial safety factors for use in structural design codes is of particular interest.

Structural reliability analysis directly capitalises on the variability and uncertainties in load and strength and therefore produces a reliability estimate, which is a direct measure of the structural safety. Because of this, structural reliability analysis forms the rational basis for calibration of partial safety factors, which are used in code checks during conventional deterministic design. With structural reliability method available, it is possible to determine sets of equivalent partial safety factors which, when applied with design rules in structural design codes, will lead to designs with the prescribed reliability.

As a first step, a target reliability index β_T must be selected. The choice of the target reliability index can be derived from a utility-based feasibility study in a decision analysis, or by requiring that the safety level as resulting from the design by a structural reliability analysis shall be the same as the one resulting from current deterministic design practice. The latter approach is based on the assumption that established design practice is optimal with respect to safety and economy or, at least, leads to a safety level acceptable by society.

When the target reliability index β_T cannot be established by calibration against established design practice, or otherwise, then its value may be taken from Table 2-3, depending on the type and consequence of failure. Note that the numbers given in Table 2-3 are given for a reference period of one year, i.e. they refer to *annual* probabilities of failure and corresponding reliability indices. Reference is made to NKB (1978).

In the case of a prescribed reliability index, which is different from the one that results from an actually executed reliability analysis of a structural component, the geometrical quantities of this component must be adjusted. The adjustment is made in such a way that the required reliability index will result from a new reliability analysis of the modified component. The geometrical quantities, which can be adjusted to achieve a specified reliability index, are sometimes denoted design parameters. It is most practicable to operate on just one such design parameter when adjusting the design in order to reach the specified reliability index.

A design case is formed as a specific combination of environmental loading regime, type of material, and type and shape of structure. For a particular design case, which can be analysed on the basis of a structural reliability method, a set of partial safety factors can thus be determined that will lead to a design which exactly meets the prescribed level of reliability. Different sets of partial safety factors may result from different design cases. A simple example of a calibration of partial safety factors is given below for an axially loaded steel truss. A structural design code usually has a scope that covers an entire class of design cases, formed by combinations among multiple environmental loading regimes, different structural materials, and several types and shapes of structures. The design code will usually specify one common set of partial safety factors, which is to be applied regardless of which design case is being analysed. This practical simplification implies that the prescribed level of reliability will usually not be met in full, but only

Table 2-3. Target annual failure probabilities P_{FT} and corresponding reliability indices β_T .			
Failure type	Failure consequence		
	Less serious LOW SAFETY CLASS (small possibility for personal injuries and pollution, small economic consequences, negligible risk to life)	Serious NORMAL SAFETY CLASS (possibilities for personal injuries, fatalities, pollution, and significant economic consequences)	Very serious HIGH SAFETY CLASS (large possibilities for personal injuries, fatalities, significant pollution, and very large economic consequences)
Ductile failure with reserve capacity (redundant structure)	$P_F = 10^{-3}$ $\beta_T = 3.09$	$P_F = 10^{-4}$ $\beta_T = 3.72$	$P_F = 10^{-5}$ $\beta_T = 4.26$
Ductile failure with no reserve capacity (significant warning before occurrence of failure in non-redundant structure)	$P_F = 10^{-4}$ $\beta_T = 3.72$	$P_F = 10^{-5}$ $\beta_T = 4.26$	$P_F = 10^{-6}$ $\beta_T = 4.75$
Brittle failure (no warning before occurrence of failure in non-redundant structure)	$P_F = 10^{-5}$ $\beta_T = 4.26$	$P_F = 10^{-6}$ $\beta_T = 4.75$	$P_F = 10^{-7}$ $\beta_T = 5.20$

approximately, when designs are carried out according to the code. Hence, the goal of a reliability-based code calibration is to determine the particular common set of partial safety factors that reduces the scatter of the reliabilities, achieved by designs according to the code, to a minimum over the scope. This can be accomplished by means of an optimisation technique, once a closeness measure for the achieved reliability has been defined, e.g. expressed in terms of a penalty function that penalises deviations from the prescribed target reliability. For principles and examples of such code optimisation, reference is made to

Hauge et al. (1992), Ronold (1999), and Ronold and Christensen (2001).

2.3.6 Example – axially loaded steel tower

The example given below deals with design of an axially loaded steel tower against failure in ultimate loading. The probabilistic modelling required for representation of load and capacity is presented. A structural reliability analysis of the tower is carried out, and a simple calibration of partial safety factors is performed.

The design of the axially loaded tower is governed by the maximum axial force Q in a

one-year reference period. The maximum axial force Q follows a Gumbel distribution

$$F_Q(q) = \exp(-\exp(-a(q-b)))$$

in which $a = 0.4275$ and $b = 48.65$ correspond to a mean value $E[Q] = 50$ MN and a standard deviation $D[Q] = 3$ MN. The yield strength of steel σ_F follows a normal distribution with the mean value $E[\sigma_F] = 400$ MPa and the standard deviation $D[\sigma_F] = 24$ MPa. The cross-sectional area of the tower is A . Failure occurs when the axial force Q exceeds the capacity $\sigma_F A$, thus a natural format of the design rule is $\sigma_{F,D} A \geq q_D$. The subscript D denotes design value. The limit state function is correspondingly chosen as

$$g = \sigma_F A - Q$$

and the area A is used as the design parameter.

Analysis by a first-order reliability method leads to determination of $A = 0.2007 \text{ m}^2$ in order to meet a target reliability index $\beta = 4.2648$, which corresponds to an annual failure probability $P_F = 10^{-5}$. The characteristic value of the axial force is taken as the 98% quantile in the distribution of the annual maximum force, $q_C = q_{98\%} = 57.78$ MN. The characteristic value of the yield strength is taken as the 5% quantile in the strength distribution, $\sigma_{F,C} = \sigma_{F,5\%} = 360.5$ MPa. One partial safety factor, γ_1 , is introduced as a factor on the characteristic force, and another one, γ_2 , is introduced as a factor on the characteristic capacity. Substitution of the expressions for the design force and the design capacity in the design equation yields

$$\gamma_2 \sigma_{F,C} A - \gamma_1 q_C = \gamma_2 \cdot 360.5 \cdot 0.2007 - \gamma_1 \cdot 57.78 = 0$$

which gives a requirement to the ratio of the partial safety factors $\gamma_1/\gamma_2 = 1.252$. There is thus an infinite number of pairs (γ_1, γ_2) that will lead to the required reliability. This implies an arbitrariness in selecting the partial safety factor set (γ_1, γ_2) for the code. The reliability analysis gives the design point values $q^* = 70.89$ MN for the force and $\sigma_F^* = 353.2$ MPa for the strength. These are the most likely values of the governing variables at failure. A robust choice for the partial safety factors (γ_1, γ_2) can be achieved by designing to the design point values from the reliability analysis. The partial safety factors are therefore selected as

$$\gamma_1 = \frac{q^*}{q_C} = 1.227 \text{ and } \gamma_2 = \frac{\sigma_F^*}{\sigma_{F,C}} = 0.980$$

According to current design practice, a load factor is used as a factor on the characteristic load to give the design load, and a material factor is used as a divisor on the characteristic resistance to give the design resistance. Hence, these factors become

$$\gamma_f = \gamma_1 = 1.227 \text{ and } \gamma_m = \frac{1}{\gamma_2} = 1.021,$$

respectively.

Note that the example is purely tutorial to explain a principle. In reality, the capacity may be more uncertain than assumed here, e.g. owing to model uncertainty not accounted for. Moreover, a larger degree of variability in the axial force may also be expected, depending on the source and type of loading and the amount of data available. The resulting partial safety factors may then become larger than the ones found here.

2.3.7 Example – fatigue of FRP blade root in bending

The example given here deals with design of an FRP blade root against fatigue failure during its design life of 20 years. The probabilistic modelling required for representation of load and resistance is presented. A structural reliability analysis of the blade root is carried out, and a simple safety factor calibration is performed.

The design of the blade root is governed by the long-term distribution of the bending moment range X . In the long term, the bending moment ranges are assumed to follow an exponential distribution

$$F_X(x) = 1 - \exp\left(-\frac{x}{x_0}\right)$$

in which $x_0 = 50$ kNm is recognised as a Weibull scale parameter. The total number of bending moment ranges over the design life $T_L = 20$ years is $n_{tot} = 0.9 \cdot 10^9$. The bending moment ranges X give rise to bending stress ranges $S = X/W$, where W denotes the section modulus of the blade root. Hence, the bending stress range distribution becomes

$$F_S(s) = 1 - \exp\left(-\frac{sW}{x_0}\right)$$

For a given stress range S , the number of bending stress cycles N to failure is generally expressed through an S - N curve, which on logarithmic form reads

$$\ln N = \ln K - m \ln S + \varepsilon$$

where the pair $(\ln K, m) = (114.7, 8.0)$ describes the expected behaviour. The zero-mean term ε represents the natural variability about the expectation and follows a normal distribution with a standard

deviation $\sigma_\varepsilon = 0.86$. The cumulative damage is calculated as the Miner's sum

$$\begin{aligned} D &= \sum_i \frac{\Delta n(s_i)}{N(s_i)} \\ &= \int_0^\infty \frac{n_{tot} \frac{dF_S}{ds} ds}{K \exp(\varepsilon) s^{-m}} \\ &= \frac{n_{tot}}{K \exp(\varepsilon)} \Gamma(m+1) \left(\frac{x_0}{W}\right)^m \end{aligned}$$

where Γ denotes the gamma function.

According to Miner's rule, fatigue failure occurs when the cumulative damage exceeds a threshold of 1.0. A natural format of the design rule is $D_D \leq 1$, where D_D is the design damage. The limit state function is chosen as

$$g = 1 - D$$

and the section modulus W is used as the design parameter.

Analysis by a first-order reliability method leads to determination of $W = 0.00209 \text{ m}^3$ in order to meet a target reliability index $\beta = 3.29$, which corresponds to a target failure probability $P_F = 0.5 \cdot 10^{-3}$ over the design life of 20 years.

For design against fatigue failure it has hardly any meaning to choose the 98% quantile of the annual maximum load, or any other quantile for that matter, as the characteristic load value. A characteristic load *distribution* is needed rather than a characteristic load *value*. The long-term stress range distribution, $F_S(s)$, is chosen as the characteristic stress range distribution, and a load factor $\gamma_f = 1.0$ on all stress ranges according to this distribution is prescribed.

This is based on the assumption that the long-term stress range distribution is known. The validity of this assumption in the context of wind turbines is discussed later. It is also assumed that variability in the individual damage contributions from the individual stress ranges averages out over the many contributing stress ranges in the long-term distribution. This assumption would not hold if the cumulative damage was dominated by damage contributions from only one or a very few large stress ranges, which could be the case for very large m values, say $m > 10$.

The characteristic $S-N$ curve is taken as the expected $S-N$ curve minus two standard deviations. A partial safety factor, γ_m , is applied as a divisor on all stress range values of the characteristic $S-N$ curve.

The design damage D_D is then obtained as

$$D_D = \frac{n_{tot}}{K_C} \Gamma(m+1) \left(\frac{\gamma_m x_0}{W} \right)^m$$

in which $K_C = K \exp(-2\sigma_\epsilon)$ reflects the chosen characteristic $S-N$ curve. Substitution of numbers into the design equation $D_D = 1.0$ leads to the following requirement to the material factor

$$\gamma_m = 1.149$$

Discussion

Note that this example is purely tutorial to explain a principle. In reality, the resistance may be more uncertain than assumed here, e.g. when there is a limited amount of material data available, such that the estimated values of K and m are uncertain. Moreover, model uncertainty may be associated with the application of Miner's rule. With such uncertainties properly accounted for, the value of the resulting material factor, γ_m , will become larger than the one found here.

Note also that with $\gamma_f = 1.0$ prescribed, all levels of uncertainty and variability associated with a fatigue problem such as the present, are accounted for by one single safety factor, γ_m . This factor is thus applied as a safety factor on resistance, regardless of whether some of the uncertainty is associated with load rather than with resistance. This is in accordance with most standards. Note, however, that in the new Danish standard DS409/DS410, a partial safety factor, γ_f , on load is introduced which, under certain conditions, is to be taken as a value greater than 1.0. This applies to situations where the loads causing fatigue damage are encumbered with uncertainty or ambiguity, such as if they are traffic loads, or if the various quantiles of the long-term stress distribution over the design life are statistically uncertain.

As regards design of wind turbines against fatigue, the loads causing fatigue damage are dominated by loads generated by the wind. Whereas the distribution of the 10-minute mean wind speed on a location may be well-known, the distribution of the turbulence intensity is usually not well-determined, owing to local conditions and influence from the presence of the turbine. Nor is the transfer function to stress response in the wind turbine always clear. The distribution of wind-generated loads in a wind turbine can therefore be expected to be known only with some uncertainty, and a load factor γ_f greater than 1.0 would thus be required. However, in practice, one would account for such uncertainty or ambiguity in the load distribution by choosing a load distribution "on the safe side", a conservative "envelope load spectrum", so to speak. In the presented example, this would imply the choice of a conservatively high value of the Weibull scale parameter x_0 , which could then be used in conjunction with $\gamma_f = 1.0$.

2.3.8 Tests and calculations for verification

It is important to demonstrate that the structural strengths or capacities of the various components that constitute the wind turbine structure are sufficient. This can be done by undertaking calculations according to some theory or calculation method, and it can be supported by carrying out full-scale tests of the component in question. Note that a full-scale test of a structural component may give a more accurate estimate of the component strength than theoretical calculations, because model uncertainty and bias, owing to simplifications and limitations associated with the applied calculation method, will be reduced or removed.

When carrying out a full-scale test of a structural component such as a blade, it is important to acknowledge that the loads used in the test are generated and controlled in a completely different manner than the variable natural loads (such as wind loads) which the component will experience in reality and which it should be designed for. For selection of loads to be used in full-scale tests for verification, it is therefore not relevant to apply partial safety factors for loads that are prescribed for design in accordance with particular codes and standards. The loads to be used in tests need to be chosen after thorough consideration of the variability and uncertainty in the strength, given the degree of knowledge about the strength or capacity available prior to the test.

In this context it should be noted that the effect of proof loading represents an increase in confidence in the structural strength or capacity, resulting from prior successful loading of the component.

2.3.9 Inspection and inspection intervals

The design process is only one element in ensuring safe and reliable structures. In fabrication and service, other safety elements can be introduced such as quality control, alignment control, visual inspection, instrumented monitoring, and proof loading. Each of these items provide information about the structure, additional to the information present at the design stage, and may hence reduce the overall uncertainty associated with the structure. The probabilistic model used in design can then be updated and calibrated against reality by including the additional information.

The additional information obtained during fabrication and in service may be obtained either directly as information about some of the governing variables themselves, e.g. strength, or indirectly by observing substitute variables, which are functions of the governing variables, e.g. cracks or deformations.

It is of interest to update the failure probability from its value in the design stage to a value which reflects the additional information gained by inspection. Probability updating by inspection is based on the definition of conditional probability. Let F denote the event of structural failure. In the design process the probability of failure $P_F = P[F]$ is solved according to the procedures described above. Let I denote an event such as the observation of a governing variable or the observation of a function of one or more of the governing variables, obtained by inspection when the structure is in service. The updated probability of failure is the probability of failure conditioned on the inspection event I ,

$$P[F | I] = \frac{P[F \cap I]}{P[I]}$$

The probability in the numerator can be solved by a reliability analysis of a parallel system, for which solutions are available. The probability in the denominator can be solved by a reliability analysis of a structural component as described above, once a suitable limit state function has been defined, and with due account for measurement uncertainty and probability of detection, which are two contributing uncertainty sources of importance in this context.

For some limit states, e.g. crack growth and fatigue failure, the failure probability P_F increases as a function of time. For such limit states, prediction of the failure probability as a function of time can be used to predict the time when the failure probability will exceed some critical threshold, e.g. a maximum acceptable failure probability. This predicted point in time is a natural choice for execution of an inspection. The failure probability can then be updated as outlined above, depending on the findings from the inspection and including improvements from a possible repair following the inspection. The time until the failure probability will again exceed the critical threshold and trigger a new inspection can be predicted and thus forms an inspection interval. This can be used to establish an inspection plan.

Note in this context that for some limit states such as the fatigue limit state, it may actually be a prerequisite for maintaining the required safety level over the design life that inspections are carried out at specified intervals.

2.4 Mechanical safety

There are several mechanical systems in a wind turbine:

- transmission: hub, shaft, gear, couplings, brakes, bearings and generator
- mechanical control systems: pitch system, teeter mechanism, yaw system, hydraulic system and pneumatic system

The safety of mechanical components will usually be determined by their structural safety as described in previous sections. However, as the components are part of mechanical systems, there are several aspects to be considered in addition to the structural safety when the safety of mechanical systems is to be evaluated.

The structural strength will in many cases become limited by surface damages due to wear such as fretting corrosion in connections due to micro movements, or gray staining of gear teeth due to poor lubrication conditions. Hence, aspects like friction and lubrication conditions as well as surface treatment are essential for the mechanical safety.

Mechanical components are often made of rather brittle high-strength material such as case-hardened steel for gears and induction-hardened roller bearing steel. Furthermore, the strength of mechanical components often relies on extremely fine tolerances, e.g. correction grinding of gear teeth or mating surfaces in connections.

Non-metallic materials such as rubber are often used in mechanical components to achieve damping, or they are used as sealing in hydraulic components. Ageing properties and temperature dependence are of importance for such materials.

Mechanical components are in many cases subjected to internal forces such as pressure in hydraulic systems, pretension in bolts and shrinkage stress in shrink fit connections. In other cases, strength requirements rely on

the rotational speed as is the case with an internal gear shaft, which will experience one complete bending cycle for each revolution.

Mechanical safety will thus depend on several more or less well-defined parameters, often in a rather complex combination. It may be difficult to define all governing phenomena adequately, and assumptions may not always hold in practice. In terms of failure probability, it may therefore not always be feasible to take a probabilistic approach to assess mechanical safety.

Due to the complexity of mechanical systems, the required level of safety needs to rely on experience together with the consequences of a given failure. Typically, codes and standards used for mechanical design do not define requirements for safety factors. This also applies to the most commonly used standards, which are the gear standards ISO 6336 and DIN 3990, and the bearing dynamic load rating standard ISO 281. Hence, minimum safety requirements need to be determined on the basis of the manufacturers' experience and, if available, on requirements from authorities, certification bodies and wind turbine developers. As a general guideline, the requirement for structural safety shall at the same time constitute the lower limit for the requirement for mechanical safety.

Machine components may be vulnerable to lightning and may fail as a result. They should therefore be bonded to local ground. DEFU (1999) may be consulted for requirements for cross sections of equipotential bonding connections. Due to their small contact areas, rotating and movable components such as roller bearings may burn if struck by lightning. They can be protected by a protection system consisting of two parts: a diversion of the current via

an alternative part with low impedance, and a reduction of current through the movable components, e.g. by means of electrical insulation.

2.5 Labour safety

The safety of personnel working on a wind turbine or nearby shall be considered when designing a wind turbine, not least when issuing instructions and procedures for transportation and assembly, operation, maintenance and repair.

It shall be possible to operate the control levers and buttons of the wind turbine with ease and without danger. These levers and buttons should be placed and arranged in such a manner that unintentional or erroneous operation, which can lead to dangerous situations, is prevented. The wind turbine shall in general be designed in such a manner that dangerous situations do not occur. If a wind turbine has more than one control panel or control unit, it shall only be possible to operate it from one panel or unit at a time.

The Danish "National Working Environment Authority Regulation No. 561" of June 24, 1994 as later amended, cf. the "National Working Environment Authority Regulation No. 669" of August 7, 1995, regarding design of technical facilities, commonly referred to as "Maskindirektivet", shall be complied with at all times.

Reference is also made to prEN 50308, Wind turbines - Labour safety - December 18, 1998.

2.5.1 Transportation, installation and commissioning

Requirements concerning personnel safety shall be described in the instructions in the

wind turbine manuals and in the procedures for assembly, installation and commissioning.

2.5.2 Normal operation

During normal operation of the wind turbine, the safety of personnel inside and outside the wind turbine shall be considered. Normal operation of the wind turbine shall be possible without accessing the nacelle.

Operational procedures and operation of the wind turbine shall be described in the user manual, which is furnished to the turbine owner or to the person responsible for the operation of the wind turbine. It shall appear from any instructions how personnel safety has been accounted for.

2.5.3 Service, maintenance and repair

The manufacturer or supplier of the wind turbine shall provide instructions and procedures, which consider wind speeds and other external conditions in such a manner that service, maintenance and repair work on the wind turbine can be performed safely. The wind turbine shall be designed with a view to ensuring safe access to and safe replacement of all components to be serviced.

Access

It shall be made clear by means of locks and/or signs that it can be dangerous to ascend the wind turbine. It shall be prevented that unauthorised persons get access to the control panel and the machinery of the wind turbine. Operation of the wind turbine and access to its local control system shall not require access to electrical circuits with a higher voltage than 50V.

Wherever screens and shields are used for protection, it shall be ensured that, during normal operation, personnel cannot get in

contact with any rotating, moving or conducting parts.

The light in access routes shall have an intensity of at least 25 lux. This shall also apply when the main switch of the wind turbine is turned off.

Working conditions

The wind turbine shall be constructed in such a way that replacing components subject to service does not entail working postures or movements which are hazardous to health or otherwise dangerous. It shall be possible to block the rotor and yaw system of the wind turbine in a safe and simple manner other than by using the ordinary brake and yaw system of the turbine. For pitch-controlled turbines, fixation of the pitch setting shall be possible. Blocking of the rotor shall be done by mechanical fixation of the rotor and shall be capable of keeping the rotor fixed at all wind speeds below the defined normal stop wind speed. Blocking of the yaw and pitch systems shall keep the yaw and pitch systems, respectively, fixed at all wind speeds below the defined normal stop wind speed.

Operation of the blocking mechanisms and of their area of application shall be described in the user manual of the wind turbine in order to avoid incorrect use.

It shall be possible to illuminate working areas with a light intensity of at least 50 lux. In addition, the lighting must be designed such that glare, stroboscopic influences and other disadvantageous lighting conditions are avoided.

It shall be possible to initiate emergency shutdown close to the working areas in the wind turbine. As a minimum, it shall be possible to initiate emergency shutdown at the bottom of the tower, i.e. at the control panel, and in the nacelle.

2.6 Codes and standards

DS472

“Load and Safety for Wind Turbine Structures”, DS472, 1st edition, Dansk Ingeniørforening, Copenhagen, Denmark, 1992.

This is the Danish standard for design of wind turbine structures. This standard, with its two annexes A and B, and with the standards DS409 and DS410 and relevant structural codes for materials, forms the Danish safety basis for structural design of horizontal axis wind turbines. The standard is valid for the environmental conditions of Denmark and for turbines with rotor diameters in excess of 5 m.

IEC61400-1

“Wind turbine generator systems – Part 1: Safety requirements”, 2nd edition, International Electrotechnical Commission, Geneva, Switzerland, 1999.

This is an international standard that deals with safety philosophy, quality assurance and engineering integrity. Moreover, it specifies requirements for the safety of wind turbine generator systems. It covers design, installation, maintenance, and operation under specified environmental conditions. Its purpose is to provide an appropriate level of protection against damage from all hazards during the design life. The standard is concerned with control and protection mechanisms, internal electrical systems, mechanical systems, support structures, and electrical interconnection equipment. The standard applies to wind turbines with a swept area equal to or greater than 40 m². The standard shall be used together with a number of other specified IEC standards and together with ISO2394.

NVN11400-0

“Wind turbines – Part 0: Criteria for type certification – technical criteria,” 1st edition,

Nederlands Normalisatie-instituut, The Netherlands, 1999.

This is the Dutch standard for safety-based design of wind turbine structures. It is valid for wind turbines with a swept rotor area of at least 40 m². To a great extent, it is based on IEC61400-1, however, since it is to be used also for type certification of wind turbines in the Netherlands, it covers requirements for additional aspects such as type testing.

DIBt RICHTLINIEN

“Richtlinie. Windkraftanlagen. Einwirkungen und Standsicherheitsnachweise für Turm und Gründung” (in German). Guidelines for loads on wind turbine towers and foundations. Deutsche Institut für Bautechnik (DIBt), Berlin, Germany, 1993.

GL REGULATIONS

“Regulation for the Certification of Wind Energy Conversion Systems,” Vol. IV – Non-Marine Technology, Part 1 – Wind Energy, in “Germanischer Lloyd Rules and Regulations,” Hamburg, Germany, 1993.

REFERENCES

Danske Elværkers Forenings Undersøgelser (DEFU), *Lightning protection of wind turbines*, Recommendation 25, Edition 1, 1999.

Hauge, L.H., R. Løseth, and R. Skjong, “Optimal Code Calibration and Probabilistic Design”, *Proceedings*, 11th International Conference on Offshore Mechanics and Arctic Engineering (OMAE), Calgary, Alberta, Canada, Vol. 2, pp. 191-199, 1992.

Madsen, H.O., S. Krenk, and N.C. Lind, *Methods of Structural Safety*, Prentice-Hall Inc., Englewood Cliffs, N.J., 1986.

Nordic Committee on Building Regulations (NKB), *Recommendations for Loading and Safety Regulations for Structural Design*, NKB Report No. 36, Copenhagen, Denmark, 1978.

Ronold, K.O., “Reliability-Based Optimization of Design Code for Tension Piles,” *Journal of Geotechnical and Geoenvironmental Engineering*, ASCE, Vol. 125, No. 8, August 1999.

Ronold, K.O., and C.J. Christensen, “Optimization of a Design Code for Wind-Turbine Rotor Blades in Fatigue,” accepted for publication in *Engineering Structures*, Elsevier, 2001.

3. External Conditions

3.1 Wind conditions

The wind climate that governs the loading of a wind turbine is usually represented by the 10-minute mean wind speed U_{10} at the site in conjunction with the standard deviation σ_U of the wind speed. Over a 10-minute period, stationary wind climate conditions are assumed to prevail, i.e. U_{10} and σ_U are assumed to remain constant during this short period of time. Only when special conditions are present, such as tornadoes and cyclones, representation of the wind climate in terms of U_{10} and σ_U will be insufficient.

3.1.1 10-minute mean wind speed

The 10-minute mean wind speed will vary from one 10-minute period to the next. This variability is a natural variability and can be represented in terms of a probability distribution function. In the long run, the distribution of the 10-minute mean wind speed can for most sites be taken as a Weibull distribution

$$F_{U_{10}}(u) = 1 - \exp\left(-\left(\frac{u}{A}\right)^k\right)$$

in which the shape parameter k and the scale parameter A are site and height-dependent coefficients. The scale parameter A at height z can be calculated as follows

$$A = A_H \frac{\ln \frac{z}{z_0}}{\ln \frac{H}{z_0}}$$

where z_0 is the terrain roughness parameter which is defined as the extrapolated height at which the mean wind speed becomes zero, if the vertical wind profile has a

logarithmic variation with height. A_H is the scale parameter at a reference height H . A common choice for the reference height is $H = 10$ m. However, in the context of wind turbines, the hub height is a natural choice for H . The expression for A is based on a logarithmic wind speed profile above the ground

$$u(z) = \frac{u^*}{\kappa} \ln \frac{z}{z_0}$$

where u^* is the frictional velocity, $\kappa = 0.4$ is von Karman's constant, and neutral atmospheric conditions are assumed. The frictional velocity is defined as $u^* = (\tau/\rho)^{1/2}$, in which τ is the surface shear stress, and ρ is the air density.

For engineering calculations it may sometimes prove useful to apply the following empirical approximation for the scale parameter A

$$A = A_{10} \left(\frac{z}{H}\right)^\alpha$$

where the exponent α depends on the terrain roughness. Note that if the logarithmic and exponential expressions for A given above are combined, a height-dependent expression for the exponent α results

$$\alpha = \frac{\ln \left(\frac{\ln \frac{z}{z_0}}{\ln \frac{H}{z_0}} \right)}{\ln \left(\frac{z}{H} \right)}$$

Note also that the interpretation of the limiting value $\alpha = 1/\ln(z/z_0)$ is similar to that of a turbulence intensity as z approaches the reference height H , cf. the definitions given

in Sections 3.1.2 and 3.1.3. As an alternative to the quoted expression for α , values for α tabulated in Table 3-1 may be used.

$$u_* = \sqrt{\frac{\tau_0}{\rho}}$$

A homogeneous terrain is characterised by a constant z_0 over the terrain. Typical values for z_0 are given in Table 3-1 for various types of terrain. For offshore locations, where the terrain consists of the sea surface, the roughness parameter is not constant, but depends on:

- wind speed
- upstream distance to land
- water depth
- wave field

is the frictional velocity expressed as a function of the shear stress τ_0 at the sea surface and the density ρ of the air. $A_c = 0.011$ is recommended for open sea. As an approximation, Charnock’s formula can also be applied to near-coastal locations provided that $A_c = 0.034$ is used. Expressions for A_c , which include the dependency on the wave velocity and the available water fetch, are available in the literature, see Astrup et al. (1999). Based on a logarithmic wind speed profile, Charnock’s formula leads to the following expression for the roughness parameter for a water surface

$$z_0 = \frac{A_c}{g} \left(\frac{\kappa U_{10}}{\ln(z/z_0)} \right)^2$$

from which z_0 can be determined implicitly, and from which the dependency on the wind speed in terms of U_{10} is evident. For offshore locations, this implies that determination of z_0 and of the distribution of U_{10} , respectively, involves an iterative procedure. $\kappa = 0.4$ is von Karman’s constant.

The basic wind speed v_B , used in the Danish design code, is the 50-year return value of the 10-minute mean wind speed at 10 m height above land with terrain roughness $z_0 = 0.05$. The 10-minute mean wind speed with a 50-year recurrence period at other heights and with another terrain roughness can be found as

$$v_{10 \text{ min}, 50 \text{ yr}} = v_B k_t \ln \frac{z}{z_0}$$

in which $k_t = 0.19(z_0/0.05)^{0.078}$

Terrain type	Roughness parameter z_0 (m)	Exponent α
Plane ice	0.00001	
Open sea without waves	0.0001	
Open sea with waves	0.0001-0.003	0.12
Coastal areas with onshore wind	0.001	
Open country without significant build-ings and vegetation	0.01	
Cultivated land with scattered buildings	0.05	0.16
Forests and suburbs	0.3	0.30
City centres	1-10	0.40

A widely used expression for the roughness parameter of the open, deep sea far from land is given by Charnock’s formula

$$z_0 = A_c \frac{u_*^2}{g}$$

in which g is the acceleration of gravity, and

3.1.2 Standard deviation of wind speed

For a given value of U_{10} , the standard deviation σ_U of the wind speed exhibits a natural variability from one 10-minute period to another. This variability of the wind speed is known as the turbulence, and σ_U is therefore often referred to as the standard deviation of the turbulence components. Measurements from several locations show that σ_U conditioned by U_{10} can often be well-represented by a lognormal distribution

$$F_{\sigma_U|U_{10}}(\sigma) = \Phi\left(\frac{\ln \sigma - b_0}{b_1}\right)$$

in which $\Phi()$ denotes the standard Gaussian cumulative distribution function. The coefficients b_0 and b_1 are site-dependent coefficients conditioned by U_{10} . See Ronold and Larsen (1999).

The coefficient b_0 can be interpreted as the mean value of $\ln \sigma_U$, and b_1 can be interpreted as the standard deviation of $\ln \sigma_U$. The following relationships can be used to calculate the mean value $E[\sigma_U]$ and the standard deviation $D[\sigma_U]$ of σ_U from the values of b_0 and b_1

$$E[\sigma_U] = \exp\left(b_0 + \frac{1}{2} b_1^2\right)$$

$$D[\sigma_U] = E[\sigma_U] \sqrt{\exp(b_1^2) - 1}$$

These quantities will, in addition to their dependency on U_{10} , also depend on local conditions, first of all the terrain roughness z_0 , which is also known as the roughness length. When different terrain roughness prevails in different directions, i.e. the terrain is not homogeneous, $E[\sigma_U]$ and $D[\sigma_U]$ may vary with the direction. This will

be the case for example if a house is located nearby. Houses and other “disturbing” elements will, in general, lead to more turbulence, i.e. larger values of $E[\sigma_U]$ and $D[\sigma_U]$, than will normally be found in smoother terrain. Figure 3-1 and Figure 3-2 give examples of the variation of $E[\sigma_U]$ and $D[\sigma_U]$ with U_{10} for onshore and offshore locations, respectively. The difference between the two Figures is mainly attributable to the different shape of the mean curve. This reflects the effect of the increasing roughness length for increasing U_{10} on the offshore location.

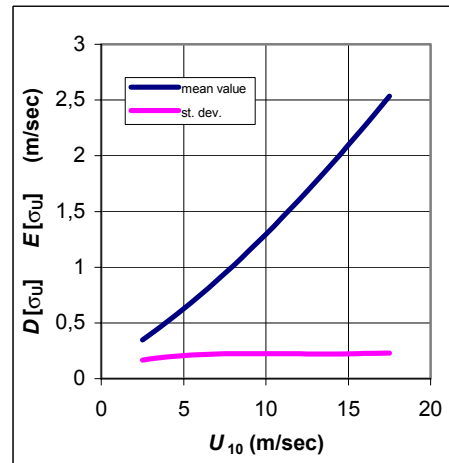


Figure 3-1. Mean value and standard deviation of σ_U as functions of U_{10} – onshore location.

In some cases, a lognormal distribution for σ_U conditioned by U_{10} will underestimate the higher values of σ_U . A Frchet distribution may form an attractive distribution model for σ_U in such cases, hence

$$F_{\sigma_U|U_{10}}(\sigma) = \exp\left(-\left(\frac{\sigma_0}{\sigma}\right)^k\right)$$

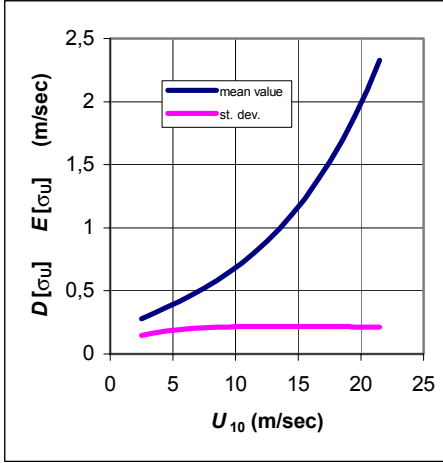


Figure 3-2. Mean value and standard deviation of σ_U as functions of U_{10} – offshore location.

The distribution parameter k can be solved implicitly from

$$\left(\frac{D[\sigma_U]}{E[\sigma_U]}\right)^2 = \frac{\Gamma(1-\frac{2}{k})}{\Gamma^2(1-\frac{1}{k})} - 1$$

and the distribution parameter σ_0 then results in

$$\sigma_0 = \frac{E[\sigma_U]}{\Gamma(1-\frac{1}{k})}$$

where Γ denotes the gamma function.

Caution must be exercised when fitting a distribution model to data. Normally, the lognormal distribution provides a good fit to data, but utilisation of a normal distribution, a Weibull distribution or a Frechet distribution is also seen. The choice of distribution model may depend on the application, i.e. whether a good fit to data is required for the entire distribution, only in the body, or in the upper tail of the distribution. It is important to identify and

remove data, which belong to 10-minute series for which the stationarity assumption for U_{10} is not fulfilled. If this is not done, such data may confuse the determination of an appropriate distribution model for σ_U conditioned by U_{10} .

Based on boundary-layer theory, the following expression for the mean value of the standard deviation σ_U , conditioned by U_{10} , can be derived

$$E[\sigma_U] = U_{10} A_x \kappa \frac{1}{\ln \frac{z}{z_0}}$$

for homogeneous terrain, in which $\kappa = 0.4$ is von Karman's constant, z is the height above terrain, z_0 is the terrain roughness, also known as the roughness length, and A_x is a constant which depends on z_0 . Measurements from a number of locations with uniform and flat terrain indicate an average value of A_x equal to 2.4, see Panofsky and Dutton (1984). Dyrbye and Hansen (1997) suggest $A_x = 2.5$ for $z_0 = 0.05\text{m}$ and $A_x = 1.8$ for $z_0 = 0.3\text{m}$. A conservative fixed choice for σ_U is desirable for design purposes, i.e. a characteristic value, and DS472 suggests

$$\sigma_{U,c} = U_{10} \frac{1}{\ln \frac{z}{z_0}}$$

Note that this value, although higher than the mean value of σ_U , may not always be sufficiently conservative for design purposes.

The IEC61400-1 standard requires utilisation of a characteristic standard deviation for the wind speed

$$\sigma_{U,c} = I_{15} \frac{U_{10,15} + aU_{10}}{a+1}$$

in which $U_{10,15} = 15$ m/s is a reference wind speed, $I_{T,15}$ is the characteristic value of the turbulence intensity at 15 m/s, and a is a slope parameter. $I_{T,15} = 0.18$ and $a = 2$ are to be used in the category for higher turbulence characteristics, while $I_{T,15} = 0.16$ and $a = 3$ are to be used in the category for lower turbulence characteristics. The expression for the characteristic value $\sigma_{U,c}$ is based on a definition of the characteristic value as the mean value of σ_U plus one standard deviation of σ_U .

3.1.3 Turbulence intensity

The turbulence intensity I_T is defined as the ratio between the standard deviation σ_U of the wind speed, and the 10-minute mean wind speed U_{10} , i.e. $I_T = \sigma_U/U_{10}$.

Note that the presence of a wind turbine will influence the wind flow locally, and that the turbulence in the wake behind the turbine will be different from that in front of the turbine. This phenomenon of a wind turbine influenced turbulence is known as a wake effect. Typically, the presence of the wind turbine will lead to increased turbulence intensity in the wake. Wake effects need to be considered for wind turbines installed behind other turbines with a distance of less than 20 rotor diameters. This is of particular interest wherever wind farms with many turbines in several rows are to be installed.

The following method, Frandsen 2001, can be used to take wake effects into account. By this method, the free flow turbulence intensity I_T is modified by the wake turbulence intensity $I_{T,w}$ to give the total turbulence intensity $I_{T,total}$. In the evaluation of the wake effect, a uniform distribution of the wind direction is assumed. The formulas can be adjusted if the distribution of wind direction is not uniform. Reference is made to Frandsen, 2001.

$$I_{T,total} = \sqrt{(1 - N \cdot p_w) I_T^m + p_w \sum_{i=1}^N I_{T,w}^m \cdot s_i}$$

$$p_w = 0.06$$

$$s_i = x_i / D$$

$$I_{T,w} = \sqrt{\frac{1}{(1.5 + 0.3 \cdot s_i \cdot \sqrt{v})^2} + I_T^2}$$

- N number of closest neighbouring wind turbines
- m Wöhler curve exponent corresponding to the material of the considered structural component
- v free flow mean wind speed at hub height
- p_w probability of wake condition
- x_i distance to the i 'th wind turbine
- D rotor diameter
- I_T free flow turbulence intensity
- $I_{T,w}$ maximum turbulence intensity at hub height in the centre of the wake

The number of closest neighbouring wind turbines N can be chosen as follows:

$$2 \text{ wind turbines: } N = 1$$

$$1 \text{ row: } N = 2$$

$$2 \text{ rows: } N = 5$$

$$\text{in a farm with more than 2 rows: } N = 8$$

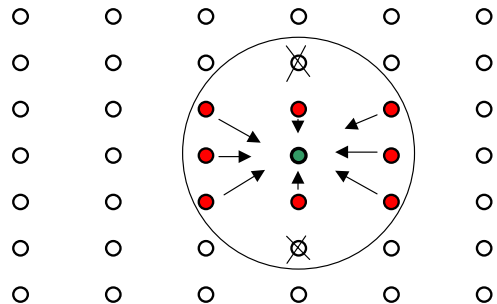


Figure 3-3. Example of determination of neighbouring wind turbines.

If the wind farm consists of more than five rows with more than five turbines in each row, or if the distance between the turbines in the rows that are located perpendicular to the predominant wind direction is less than $3D$, the increase in mean turbulence intensity shall be taken into account. This is done by substituting the free flow turbulence I_T with I_T^* :

$$I_T^* = \frac{1}{2} \sqrt{I_w^2 + I_T^2} + I_T$$

$$I_w = \frac{0.36}{1 + 0.08 \sqrt{s_r s_f v}}$$

$$s_r = x_r / D$$

$$s_f = x_f / D$$

where x_r is the distance within a row, and x_f is the distance between rows.

3.1.4 Lateral and vertical turbulence

The 10-minute mean wind speed, the standard deviation of the wind speed, and the turbulence intensity presented above all refer to the wind speed in the constant direction of the mean wind during the considered 10-minute period of stationary conditions. During this period, in addition to the turbulence in the direction of the mean wind, there will be turbulence also laterally and vertically. The mean lateral wind speed will be zero, while the lateral standard deviation of the wind speed can be taken as $\sigma_{U_y} = 0.75\sigma_U$ according to Dyrbye and Hansen (1997) and as $\sigma_{U_y} = 0.80\sigma_U$ according to Panofsky and Dutton (1984). The mean vertical wind speed will be zero, while the vertical standard deviation of the wind speed can be taken as $\sigma_{U_z} = 0.5\sigma_U$. These values all refer to homogeneous terrain. For complex terrain, the wind speed field will be much more isotropic, and values for σ_{U_y} and σ_{U_z} very near the value of

σ_U can be expected. Beware that calculations for changes in the direction of the wind in complex terrain may come out very wrongly, if values for σ_{U_y} and σ_{U_z} , which are valid for homogeneous terrain, are applied.

Very often, the wind climate at a particular location cannot be documented by site-specific measurements. In such situations, the distribution of U_{10} can usually be well-represented, for example on the basis of wind speed measurements from a nearby location. However, the distribution of σ_U will usually be harder to obtain as it is highly dependent on the local roughness conditions. Thus, it cannot be inferred automatically from known wind speed conditions at nearby locations. On a location where wind speed measurements are not available, determination of the distribution of the standard deviation σ_U of the wind speed is often encumbered with ambiguity. It is thus common practice to account for this ambiguity by using conservatively high values for σ_U for design purposes, viz. the characteristic values for σ_U given in DS472 and IEC61400-1 and referenced above.

3.1.5 Stochastic turbulence models

Wind in one direction is considered, i.e. in the direction of the 10-minute mean wind speed. The wind speed process $U(t)$ within a 10-minute period of constant U_{10} and σ_U is considered and can be assumed to be stationary. The spectral density of the wind speed process expresses how the energy of the wind turbulence is distributed between various frequencies. Several models for the spectral density exist. A commonly used model for the spectral density is the Harris spectrum

$$S_U(f) = \sigma_U^2 \frac{3.66 \frac{L}{U_{10}}}{\left(1 + \frac{3}{2} \left(\frac{2\pi f L}{U_{10}}\right)^2\right)^{5/6}}$$

in which f denotes the frequency, and L is a characteristic length, which relates to the integral length scale L_u by $L = 1.09L_u$. A calibration to full scale data indicates values for L in the range 66-440 m with $L \cong 200$ m used to match the high frequency portion of the spectrum. Based on experience, the Harris spectrum is not recommended for use in the low frequency range, i.e. for $f < 0.01$ Hz.

Another frequently used model for the power spectral density is the Kaimal spectrum

$$S_U(f) = \sigma_U^2 \frac{6.8 \frac{L_u}{U_{10}}}{\left(1 + 10.2 \frac{f L_u}{U_{10}}\right)^{5/3}}$$

in which the integral length scale is given by

$$L_u = 100Cz^m$$

where z is the height and C and m depend on the roughness length z_0 as given in Figure 3-4. This spectrum is used in Eurocode 1.

Towards the high frequency end of the inertial subrange, IEC61400-1 requires that the power spectral density used for design shall approach the form

$$S_U(f) = 0.05 \cdot \sigma_{U,c}^2 \left(\frac{\lambda}{U_{10}}\right)^{-2/3} f^{-5/3}$$

in which the turbulence scale parameter λ depends on the height z above the terrain

$$\lambda = \begin{cases} 0.7z & \text{for } z < 30 \text{ m} \\ 21 \text{ m} & \text{for } z > 30 \text{ m} \end{cases}$$

The turbulence scale parameter is by definition the wavelength where the non-dimensional, longitudinal power spectral density is equal to 0.05.

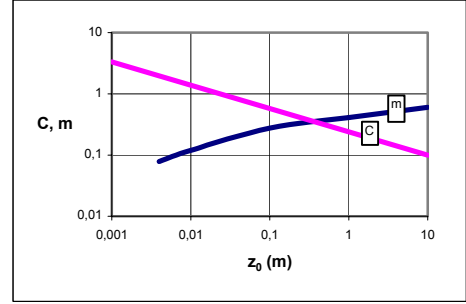


Figure 3-4. Coefficients C and m for the integral length scale of the Kaimal spectrum.

For design purposes it is common to relate calculations to wind conditions at the hub, i.e. U_{10} and σ_U refer to the wind speed at the hub height. Note that the turbulence scale parameter λ relates to the integral length scale L through $L = 4.76\lambda$. This gives the following expression for the Kaimal spectrum, which is well-known from IEC61400-1

$$S_U(f) = \sigma_U^2 \frac{4 \frac{L_k}{U_{10}}}{\left(1 + 6 \frac{f L_k}{U_{10}}\right)^{5/3}}$$

with $L_k = 8.1\lambda$

For calculation of spectral densities for lateral and vertical wind speeds, the above formulas can be used with σ_{U_y} and σ_{U_z} , respectively, substituted for σ_U , and with $\lambda_y = 0.3\lambda$ and $\lambda_z = 0.1\lambda$, respectively, substituted for λ .

Note that there is some arbitrariness in the models for power spectral density. Each model implies idealization and simplification and is usually calibrated to provide a good fit to data within a limited frequency range. At low frequencies, in particular, the models show significant differences. In Figure 3-5 three models for power spectral densities are plotted on dimensionless scales for comparison

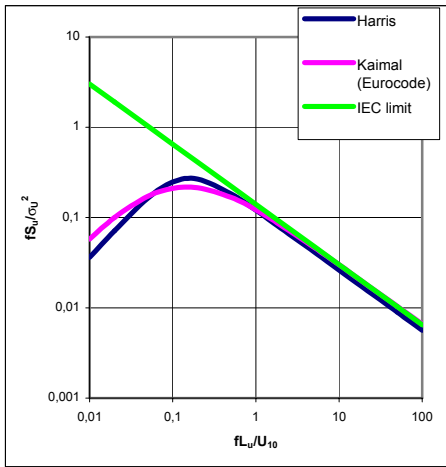


Figure 3-5. Comparison between the Harris, Kaimal and IEC power spectral densities.

Spectral moments are useful for representation of the wind speed process $U(t)$. The j th spectral moment is defined by

$$m_j = \int_0^{\infty} \omega^j S_U(\omega) d\omega$$

In the short term, such as within a 10-minute period, the wind speed process $U(t)$ can usually be represented as a Gaussian process, conditioned by a particular 10-minute mean wind speed U_{10} and a given standard deviation σ_U . The arbitrary wind speed U at a considered point in time will then follow a normal distribution with the mean value U_{10} and the standard deviation σ_U . This is usually the case for turbulence in

a homogeneous terrain. However, for turbulence in a complex terrain it is not uncommon to see a skewness of -0.1 , which implies that the Gaussian assumption has not been fulfilled.

Note that although the short-term wind speed process will be Gaussian for homogeneous terrain, it will usually not be a narrow-banded Gaussian process. This comes about as a result of the spectral density and is of importance for prediction of extreme wind speed values. Such extreme values and their probability distributions can be expressed in terms of spectral moments. Reference is made to textbooks on stochastic process theory.

At any point in time there will be a variability in the wind speed from one point to another. The closer together the two points are, the higher is the correlation between their respective wind speeds. The wind speed will form a random field in space. A commonly used model for the autocorrelation function of the wind speed field can be derived from the exponential Davenport coherence spectrum

$$Coh(r, f) = \exp(-cf \frac{r}{u})$$

where r is the distance between the two points, u is the average wind speed over the distance r , f is a frequency, and c is the non-dimensional decay constant, which is referred to as the coherence decrement, and which reflects the correlation length of the wind speed field. The auto-correlation function can be found as

$$\rho(r) = \frac{1}{\sigma_U^2} \int_0^{\infty} \sqrt{Coh(r, f)} S_U(f) df$$

in which $S_U(f)$ is the power spectral density of the wind speed. The coherence model can be refined to account for different correlation lengths, horizontally and

vertically. Note that it is a shortcoming of the Davenport model that it is not differentiable for $r = 0$. Note also that, owing to separation, the limiting value $\rho(0)$ will often take on a value somewhat less than 1.0, whereas the Davenport model always leads to $\rho(0) = 1.0$.

Note that the integral length scale L_u , referenced above as a parameter in the models for the power spectral density, is defined as

$$L_u = \int_0^{\infty} \rho(r) dr$$

3.1.6 Wind shear

Wind shear is understood as the variation of the wind speed with the height. Its effects

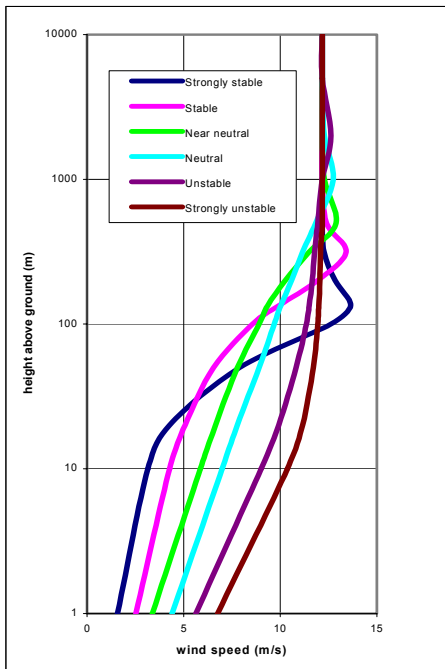


Figure 3-6. Wind shear profiles for various stability conditions on a location with roughness $z_0 = 0.02$ m and geostrophic wind speed $G = 12$ m/s.

are not considered important for small wind turbines, with rotor diameters in the order of 10 m. Wind shear may be important for large and/or flexible rotors. A number of failures have been attributed to blade loads induced by wind shear.

The wind profile depends heavily on the atmospheric stability conditions, see Figure 3-6 for an example. Even within the course of 24 hours, the wind profile will change between day and night, dawn and dusk.

Wind shear profiles can be derived from the logarithmic model presented in Section 3.1.1, modified by a stability correction. The stability-corrected logarithmic wind shear profile reads

$$u(z) = \frac{u^*}{\kappa} \left(\ln \frac{z}{z_0} - \psi \right)$$

in which ψ is a stability-dependent function, which is positive for unstable conditions, negative for stable conditions, and zero for neutral conditions. Unstable conditions

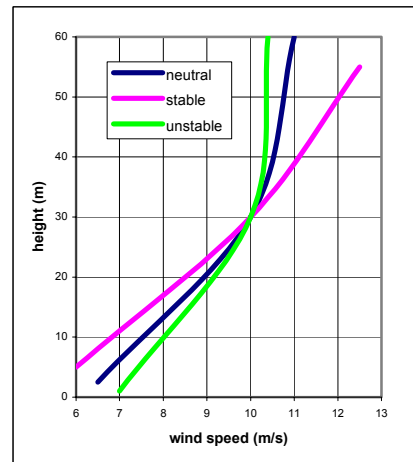


Figure 3-7. Wind profiles for neutral, stable and unstable conditions.

typically prevail when the surface is heated and the vertical mixing is increasing. Stable conditions prevail when the surface is cooled, such as during the night, and vertical mixing is suppressed. Figure 3-7 shows examples of stability-corrected logarithmic wind shear profiles for various conditions on a particular location.

The stability function ψ depends on the non-dimensional stability measure $\zeta = z/L_{MO}$, where z is the height, and L_{MO} is the Monin-Obukhov length. The stability function can be calculated from the expressions

$$\psi = -4.8\zeta \text{ for } \zeta \geq 0$$

$$\psi = 2\ln(1+x) + \ln(1+x^2) - 2\tan^{-1}(x) \text{ for } \zeta < 0$$

$$\text{in which } x = (1 - 19.3 \cdot \zeta)^{1/4}.$$

The Monin-Obukhov length L_{MO} depends on the heat flux and on the frictional velocity u^* . Its value reflects the relative influence of mechanical and thermal forcing on the turbulence. Typical values for the Monin-Obukhov length L_{MO} are given in Table 3-2.

Atmospheric conditions	$L_{MO}(\text{m})$
Strongly convective days	-10
Windy days with some solar heating	-100
Windy days with little sunshine	-150
No vertical turbulence	0
Purely mechanical turbulence	∞
Nights where temperature stratification slightly dampens mechanical turbulence generation	>0
Nights where temperature stratification severely suppresses mechanical turbulence generation	$\gg 0$

If data for the Richardson number R are available, the following empirical relationships can be used to obtain the Monin-Obukhov length

$$L_{MO} = \frac{z}{R} \text{ in unstable air}$$

$$L_{MO} = z \frac{1-5R}{R} \text{ in stable air}$$

In lieu of data, the Richardson number can be computed from averaged conditions as follows

$$R = \frac{\frac{g}{T}(\gamma_d - \gamma)}{\left(\frac{\partial \bar{u}}{\partial z}\right)^2 + \left(\frac{\partial \bar{v}}{\partial z}\right)^2} \left(1 + \frac{0.07}{B}\right)$$

- g acceleration of gravity
- T temperature
- $\gamma = -\partial T / \partial z$ lapse rate
- $\gamma_d \approx 9.8^\circ\text{C/km}$ dry adiabatic lapse rate

Further, $\partial \bar{u} / \partial z$ and $\partial \bar{v} / \partial z$ are the vertical gradients of the two horizontal average wind speed components \bar{u} and \bar{v} , and z denotes the vertical height. Finally, the Bowen ratio B of sensible to latent heat flux at the surface can near the ground be approximated by

$$B \approx \frac{c_p}{L_{MO}} \frac{(\bar{T}_2 - \bar{T}_1)}{(\bar{q}_2 - \bar{q}_1)}$$

in which c_p is the specific heat, LMO is the Monin-Obukhov length, \bar{T}_1 and \bar{T}_2 are the average temperatures at two levels denoted 1 and 2, respectively, and \bar{q}_1 and \bar{q}_2 are the average specific humidity at the same two levels. The specific humidity q is in this context calculated as the fraction of moisture by mass. Reference is made to Panofsky and Dutton (1984).

Topographic features such as hills, ridges and escarpments affect the wind speed. Certain layers of the flow will accelerate

near such features, and the wind profiles will become altered. Theories exist for calculation of such changed wind profiles, see Jensen (1999). An example of effects of a ridge is given in Figure 3-8.

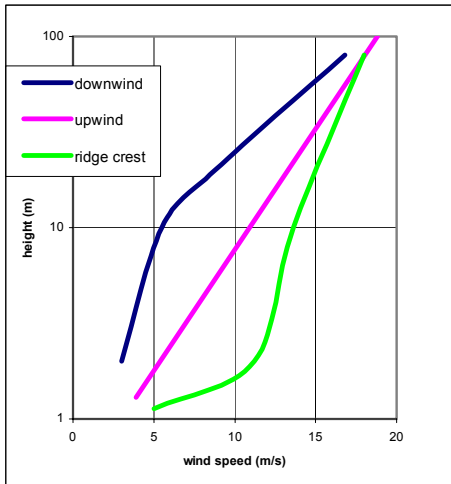


Figure 3-8. Wind profiles observed upwind, at the crest, and at the foot downwind of a two-dimensional ridge.

3.1.7 Wind direction

The wind direction and changes in the wind direction are determined by geography, global and local climatic conditions and by the rotation of earth. Locally, the wind direction will vary with the lateral turbulence intensity and for coast near locations, in particular, the wind direction can vary between day and night.

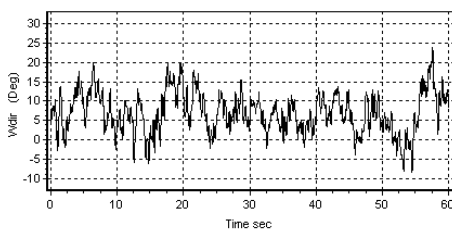


Figure 3-9. Example of fluctuations in the wind direction.

Though the yaw system of the wind turbine will hold the rotor in the direction of the mean wind direction, the short-term fluctuations in the wind direction give rise to fatigue loading. At high wind speeds sudden changes in the wind direction during production can give rise to extreme loads.

Wind rose

The distribution of the wind direction is of particular interest with respect to installation of turbines in wind farms. As can be seen in Section 3.1.3, wind turbines installed behind obstacles, such as for example other turbines, cause a considerable increase in turbulence intensity.

The distribution of the wind direction is often represented by a wind rose as the one seen in Figure 3-10.

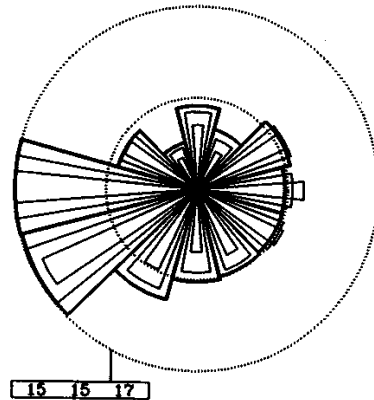


Figure 3-10. Wind rose for Kastrup, Denmark. Lundtang et al. 1989.

The 360° around the site is typically divided into 12 sectors of 30° each. The radius of the outer wedge in each sector represents the relative frequencies of wind from that direction. The middle wedge shows the contribution from each sector to the total mean wind speed, and the inner wedge shows the contribution to the total mean cube of the wind speed. The scale for each

quantity is normalised, thereby allowing the maximum to reach the outer circle. The corresponding frequency in % for each of the three quantities is given in the small box below the wind rose. The inner dotted circle corresponds to half of the value of the outer circle.

3.1.8 Transient wind conditions

It is important to be aware of transient wind conditions which occur when the wind speed or the direction of the wind changes. As these events are rare, usually, there are not many data available. The most important transient wind conditions to consider are listed below:

- extreme of wind speed gradient, i.e. extreme of rise time of gust
- strong wind shear
- simultaneous change in wind direction and wind speed
- extreme changes in wind direction

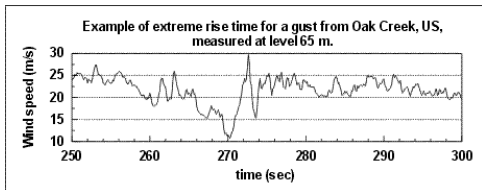


Figure 3-11. Example of extreme rise time for gust. From www.winddata.com.

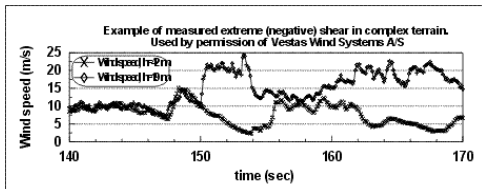


Figure 3-12. Example of strong wind shear. Notice that the wind speed is inversely proportional to the height, i.e. so-called negative wind shear. Courtesy Vestas.

These are all wind events, which by nature fall outside of what can normally be represented by stationary wind conditions. Note that the simultaneous change in wind direction and wind speed occurs when fronts

pass and is usually not covered by commonly available analysis tools for simulation of turbulence. Figure 3-11 to 12 show examples of the most important transient wind events.

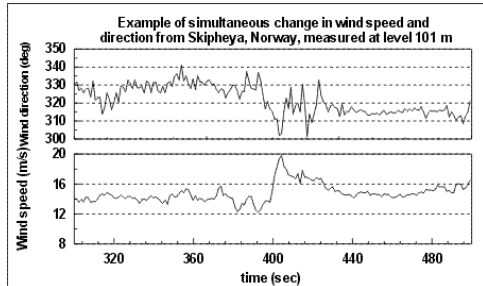


Figure 3-13. Simultaneous change in wind direction and speed. From www.winddata.com.

3.1.9 Extreme winds – gusts

Extreme winds and gusts consist of extremes of the wind speed or of extremes of the short-term mean of the wind speed, e.g. over a 10-second period. Extreme wind speeds can be treated in a traditional manner as extremes of the wind speed process during stationary 10-minute conditions. An example of a wind speed record containing extreme gust is given in Figure 3-14.

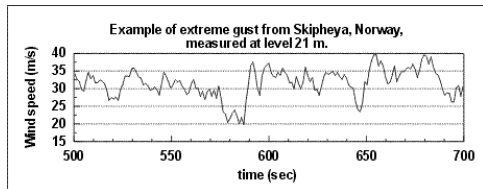


Figure 3-14. Example of extreme gust. From www.winddata.com.

Extreme value analysis

Extreme winds are usually given in terms of 10-minute mean wind speeds, which occur with some prescribed recurrence period, e.g. the 50-year wind speed. The 50-year wind speed is the 10-minute mean wind speed, which, on average, is exceeded once every fifty years. Determination of the 50-year wind speed requires an extreme value

analysis of available wind speed data. It has proven useful to carry out such an extreme value analysis on the friction velocity pressures derived from the wind speed data, rather than on the wind speed data themselves. For this purpose, the observed wind speeds u are transformed to friction velocities u^* by

$$u^* = \frac{\kappa u}{\ln(z/z_0)}$$

$\kappa = 0.4$ von Karman's constant
 Z height over the terrain
 z_0 roughness parameter

More complex formulas for the transformation from u to u^* are available in the literature, by which effects of different terrain roughness in different directions are taken into account, viz. "WASP cleaning".

The friction velocities u^* derived from the above transformation of the original data refer to the prevailing local roughness z_0 . It is often desirable to transform the friction velocities to data that relate to a reference roughness $z_0 = 0.05$ m, which is different from the true local roughness parameter. This can be done by geostrophic mapping, thus utilising the fact that the geostrophic wind speed is constant and equal to

$$G = \frac{u^*}{\kappa} \sqrt{\left(\ln\left(\frac{u^*}{fz_0}\right) - A\right)^2 + B^2}$$

for every roughness z_0 . Here, the Coriolis parameter is $f = 2 \times (\text{earth's rate of rotation in radians per second}) \times \sin(\text{latitude}) \approx 1.2 \cdot 10^{-4}$ rad/s at latitude 55.5° , and the coefficients A and B take on values $A = 1.8$ and $B = 4.5$. The procedure is as follows: the geostrophic wind speed G is calculated explicitly by the given formula when the true roughness z_0 and the corresponding u^* are given. For this value of G , the same

formula is used to implicitly solve a new value of u^* that corresponds to the desired new reference roughness z_0 .

When the friction velocities u^* have been determined from the wind speed data as described above, the corresponding velocity pressure q is calculated from

$$q = \frac{1}{2} \rho u^{*2}$$

where ρ is the density of air.

The original wind speed data u are now transformed into a set of velocity pressure data q . The q data are grouped into n subrecords of a specified duration, e.g. one year, and the maximum value of q in each of the n subrecords is extracted. When the duration of a subrecord is one year, these n maximum values of q constitute an empirical distribution of the annual maximum velocity pressure. The annual maximum of the velocity pressure is expected to follow a Type 1 extreme value distribution, i.e. a Gumbel distribution

$$F(q) = \exp\left(-\exp\left(-\frac{q-b}{a}\right)\right)$$

which has two distribution parameters a and b . The values of a and b are determined by fitting to the n observations of the annual maximum velocity pressure. The shift parameter b is the mode of the distribution and is interpreted as the value of q , which has a recurrence period of one year. The value of q , which has a recurrence period of T years, can be found as

$$q_T = b + a \ln \frac{T}{T_0}$$

where $T_0 = 1$ year. This, in particular, can be used to find the 50-year velocity pressure for $T = 50$ years.

The corresponding 10-minute mean wind speed with the recurrence period T at height z and terrain roughness z_0 can be found as

$$U_{10,T} = \frac{1}{\kappa} \sqrt{\frac{2q_T}{\rho_0}} \ln \frac{z}{z_0}$$

$\kappa = 0.4$ Von Karman's constant
 $\rho_0 = 1.225 \text{ kg/m}^3$ density of air

The above method of extreme value analysis focuses on the maximum wind speed within a specified period of time such as one year, and it is useful for estimation of wind speeds of specified recurrence periods. Note, however, that other methods of extreme value analysis are available, which may also prove useful, the most important of which is the peak-over-threshold method.

When the wind speed with a 50-year recurrence period is given, i.e. $U_{10,50\text{-yr}}$, the wind speed with the recurrence period T years can be found as

$$U_{10,T} = U_{10,50\text{-yr}} \sqrt{0.57 + 0.11 \cdot \ln \frac{T}{\ln(1/p)}}$$

in which $p = \exp(-nT)$ is the probability of no exceedance in T years, and n is the number of exceedances per year. For $T = 50$ years, $n = 0.02$. Reference is made to DS410.

Hurricanes

Saffir-Simpson's hurricane scale, see Table 3-3, groups and ranks hurricanes according to the wind speeds involved and gives consequences in terms of implied storm surges and associated resulting damage.

Table 3-3. Saffir-Simpson Hurricane Scale.

	Wind speed (m/s) *	Storm surge (m)	Damage description
1	33-42	1.0-1.7	Some damage to trees, shrubbery, and unanchored mobile homes
2	43-49	1.8-2.6	Considerable damage to shrubbery and tree foliage; some trees blown down. Damage to poorly constructed signs and roofs on buildings. Major damage to mobile homes.
3	50-58	2.7-3.8	Foliage torn from trees; large trees and poorly constructed signs blown down. Some damage to roofing materials and structures of buildings. Mobile homes destroyed.
4	59-69	3.9-5.6	Shrubs and trees blown down; destruction of all signs and mobile homes. Extensive damage to roofing materials, windows and doors. Complete failure of roofs on many small houses.
5	70+	5.7	Shrubs and trees blown down. Severe damage to windows and doors. Complete failure of roofs on many houses and industrial buildings. Some complete building failures. Small buildings overturned or blown away.

* maximum 1-minute average

Some parts of the world are characterised by having other weather phenomena than those considered here. One such weather phenomenon is cyclones. As this is a weather phenomenon totally different from the storms dealt with above, one cannot just extrapolate results for such storms.

3.1.10 Site assessment

Before a wind turbine is installed, various conditions of the specific site have to be evaluated. It shall be assessed that the environmental, electrical and soil properties are more benign than those assumed for the design of a turbine. If the site conditions are more severe than those assumed, the engineering integrity shall be demonstrated. The environmental conditions include: temperature, icing, humidity, solar radiation, corrosion conditions and possible earthquakes.

The wind conditions shall be assessed from monitoring measurements made on the site, long-term records from a nearby meteorological station or from local codes or standards. Where appropriate, the site conditions shall be correlated with long-term data from local meteorological stations. The monitoring period shall be sufficient to obtain a minimum of six months of reliable data. Where seasonal variations contribute significantly to the wind conditions, the monitoring period shall include these effects.

The two variables U_{10} and σ_U are essential as parameters in the models available for representation of the wind speed. Estimation of wind speed measurements constitutes the most common method for determination of these two parameters. Both U_{10} and σ_U refer to a 10-minute reference period, U_{10} being the 10-minute mean wind speed and σ_U being the standard deviation of the wind speed over the 10 minutes. Note that if wind speed measurements are obtained over

intervals of another duration than 10 minutes, the mean wind speed and standard deviation over these other periods need to be transformed to values referring to a duration of 10 minutes. The following approximate formula applies to transformation of the mean wind speed U_T in the measurement period T to the 10-minute mean wind speed U_{10}

$$U_{10} \approx \frac{U_T}{1 - 0.047 \ln \frac{T}{10}}$$

in which T is to be given in units of minutes. Reference is made to Gran (1992) and DNV (1998).

When the measurement period T is less than 10 minutes, the standard deviation of the wind speed measurements will come out smaller than the sought-after value for σ_U .

The following approximate formula applies to transformation of the standard deviation $\sigma_{U,T}$ obtained from wind speed measurements in the measurement period T to the 10-minute standard deviation σ_U

$$\sigma_U \approx \sqrt{\sigma_{U,T}^2 + U_{10}^2 (0.047 \ln \frac{T}{10})^2}$$

in which T is to be given in units of minutes. The formula is valid for $T < 10$ minutes. In cases where $T > 10$ minutes, the formula to be used reads

$$\sigma_U \approx \sqrt{\sigma_{U,T}^2 - U_{10}^2 (0.047 \ln \frac{T}{10})^2}$$

As described in Section 3.1.1, the long-term distribution of the 10-minute mean wind speed U_{10} can be represented by a Weibull distribution

$$F_{U_{10}}(u) = 1 - \exp\left(-\left(\frac{u}{A}\right)^k\right)$$

For a specific location, the distribution parameters A and k can be estimated from wind speed measurements.

The characteristic value of the turbulence intensity is determined by adding the measured standard deviation of the turbulence intensity to the measured or estimated mean value. If several turbines are to be installed in a wind farm, the influence from the surrounding turbines must be taken into account.

Insofar as regards data processing from climate measurements, reference is made to European Wind Atlas.

Some locations have a topography, which leads to different wind regimes in different directions, and which thus warrants use of different distribution models for U_{10} and σ_U in different directions. A location on the coast is a good example of this phenomenon as wind from the ocean will adhere to one distribution model and wind from land will adhere to another. When two such distributions, conditional on the direction of for example U_{10} , are combined to one unconditional long-term distribution, this may well come out as a bimodal distribution, e.g. represented by parts of two Weibull distributions.

WASP Engineering

Site-specific loads can be derived from site-specific wind conditions, which can be modelled by WASP engineering. WASP – the Wind Atlas Analysis and Application Program – is a method for prediction of wind properties in moderately complex terrain with relevance for loads on wind turbines and other large structures, www.wasp.dk. For detailed wind turbine siting, WASP allows for modelling

complications in the form of terrain inhomogeneity, sheltering obstacles, and terrain height differences. The method is based on theory for attached flow and allows for site-specific prediction of:

- wind shear and wind profiles
- extreme wind speeds
- turbulence

When data for orography and roughness variations are given for the site, and when reference wind data are available from a reference site subject to the same overall weather regime as the prediction site. The mean wind speed can increase considerably on a hill relative to that in a flat terrain. The extreme wind speeds on the hill will be correspondingly higher. The hill will also affect the turbulence structure. Typically, the turbulence in the direction of the mean wind will be attenuated, while the vertical turbulence will be amplified. Separation will usually occur when the hill slope exceeds about 30°, and the assumption of attached flow will then no longer be valid.

In case of very complex, mountainous terrain, the prediction accuracy of WASP can be assessed by means of the so-called RIX number. The RIX number is a site-specific ruggedness index, defined as the fractional extent of the terrain which is steeper than a critical slope. The critical slope is typically chosen as the separation slope of 30°. The RIX number can be estimated from measurements on a topographical map with a sufficiently fine representation of height contours. The RIX number is a coarse measure of the extent of flow separation, and thereby of the extent to which the terrain violates the requirement of WASP, i.e. that the surrounding terrain should be sufficiently gentle and smooth to ensure mostly attached flows. The operation envelope of WASP thus corresponds to $RIX \approx 0\%$. Reference is made to Mortensen and Petersen (1997).

When the prediction site is more rugged than the reference site, the wind speeds at the prediction site will be overpredicted by WASP. Similarly, the wind speeds will be underpredicted when the prediction site is less rugged. The difference in RIX numbers between the two sites is a fairly coarse measure of the significance of the problem and provides estimates of the magnitude and sign of the prediction error. As a rule of thumb, when there is a difference Δ RIX in RIX numbers between the prediction site and the reference site, the approximate magnitude of the relative prediction error in the wind speed will be 2Δ RIX. For example, if $RIX_{\text{prediction}} = 20\%$ and $RIX_{\text{reference}} = 10\%$, then Δ RIX = $20\% - 10\% = 10\%$, and the overall relative error in the predicted wind speeds will be about $2 \times 10 = 20\%$.

Note that WASP engineering can give accurate results outside its operation limits, provided that the difference in RIX numbers between the actual site and the reference site is small and that the topographical data are adequate and reliable.

3.2 Other external conditions

3.2.1 Temperatures

Operational temperatures

A temperature interval for normal operation of the wind turbine is to be chosen. Under normal functional conditions, the wind turbine is considered to be in operation when the temperature of the air is within this interval.

Different structural design codes offer different approaches to how temperatures can be handled. Insofar as regards steel structures, a rather general instruction can be found in DS412 according to which one may set the lowest temperature of operation at -10°C for Danish locations. This is due to the fact that the frequency of low temperatures

is very limited. Insofar as regards wind turbine structures, DS472 gives a temperature interval (-10°C , 30°C) for operation as an example. However, the temperature interval for normal operation should always be chosen in accordance with the specified recommendations for the respective materials which are being used for the construction of the wind turbine. In this context, the following issues may be critical:

- components and connections, which involve two or more materials with different coefficients of expansion. The level of expansion in relation to glass, concrete and steel is more or less the same, whereas plastic expands more.
- choice of fluids for lubrication and hydraulic systems.
- materials whose mechanical properties change when the temperature changes, e.g. rubber for seals, gaskets and dampers becomes brittle at low temperatures, and polyester behaves like glass when the temperature falls below the so-called glass transition temperature.

It is important to consider the temperature interval for normal operation when materials are selected for the construction of the wind turbine and when other conditions of importance for the safety of the turbine are to be evaluated.

Extreme temperatures

For structural parts which can be damaged by extreme temperatures, extreme values of temperatures need to be considered. Extreme values of high and low temperatures should be expressed in terms of the most probable upper or lower values with their corresponding recurrence periods.

Table 3-4 gives values of the daily minimum temperature and the daily maximum temperature for various recurrence periods at two Danish locations. These values are

based on 123 years of temperature observations, reported by Laursen et al. (1999a). Note that the temperature values tabulated for recurrence periods of 1000 and 10000 years are achieved by extrapolation and should therefore be used with caution.

For many materials, peak temperatures such as a daily maximum or a daily minimum temperature have too short a duration to pose any problems for the materials and their behaviour. The duration is too short for the materials to be cooled down or heated up. For such materials it will be more apt to consider extreme values of the one-hour mean temperature, of the daily mean temperature, or of the monthly mean temperature.

Table 3-4. Daily minimum and maximum temperatures at Danish locations.

Recurrence period (years)	Landbohøjskolen		Fanø	
	Daily min. temperature (°C)	Daily max. temperature (°C)	Daily min. temperature (°C)	Daily max. temperature (°C)
1	-13.6	29.3	-13.3	29.2
10	-18.7	31.7	-18.2	32.0
50	-22.3	33.1	-21.5	33.7
100	-23.7	33.7	-23.0	34.3
1000	-28.8	35.3	-27.7	36.3
10000	-33.9	36.8	-32.4	38.0

Table 3-5 gives low and high values of the monthly mean temperature for various recurrence periods at two Danish locations. This is based on 30 years of temperature observations, reported by Laursen et al. (1999b). Note that the temperature values, tabulated for recurrence periods of 100, 1000 and 10000 years, are achieved by extrapolation and should therefore be used with caution.

Note that for a coastal climate like the climate of Denmark, extreme temperatures such as 35°C and -20°C will usually not occur simultaneously with strong winds. The most severe temperature event to be

expected and considered in the context of wind turbine design is an event with extremely low temperature in conjunction with power failure, in particular, power failure of some duration. For Swedish locations, Statens Planverks Författningssamling (1980) gives acceptable design values for the daily mean temperature for structural design against low temperatures. Advice is given on how to transform these values into acceptable one-hour mean temperatures.

Table 3-5. Monthly mean temperatures at Danish locations.

Recurrence period (years)	Kastrup		Fanø	
	Monthly mean temperature (°C) low	Monthly mean temperature (°C) high	Monthly mean temperature (°C) low	Monthly mean temperature (°C) high
1	-0.4	16.4	0.2	16.0
10	-5.0	18.4	-4.2	18.3
50	-6.0	19.3	-6.0	19.5
100	-7.7	19.6	-6.7	19.9
1000	-9.7	20.6	-8.4	21.1
10000	-11.2	21.3	-9.8	22.1

3.2.2 Density of air

The density of air is dependent on temperature and atmospheric pressure. Depending on which standard is used as reference, the standard density of air is set to

$$\rho_{IEC\ 61400-1} = 1.225\ \text{kg/m}^3$$

$$\rho_{DS\ 472} = 1.25\ \text{kg/m}^3$$

The air density averaged over 10 minutes can be determined from the measured absolute air temperature T (in units of °K) averaged over 10 minutes and from the measured air pressure B averaged over 10 minutes by

$$\rho_{10\ \text{min}} = \frac{B}{RT}$$

in which $R = 287.05 \text{ J/kg/}^\circ\text{K}$ is the gas constant. At high temperatures, it is recommended also to measure the humidity and make corrections for it.

High wind speeds usually occur at low pressure, for which the density of air takes on relatively low values. It is important to be aware that the density of air attains high values in arctic regions, whereas it attains low values at high altitudes in tropical regions.

It appears that – depending on temperature and pressure conditions – the density of air will actually follow some probability distribution. This may be important to consider when fatigue assessments are carried out.

3.2.3 Humidity

Humidity is a function of temperature and atmospheric pressure. If the wind turbine is to be located in humid areas or in areas with high humidity part of the day and/or part of the year, components sensitive to such conditions have to be sufficiently protected. A relative humidity of up to 95% should usually be considered for the design.

Increase of corrosion rates due to humidity, and especially cyclic exposure to humidity, should be estimated. Bacterial and fungal growth should be considered for components sensitive to such activity.

3.2.4 Radiation and ultraviolet light

The intensity of solar radiation should be considered for components, which are sensitive to ultraviolet radiation and/or temperature. It is common to consider a solar radiation intensity of 1000 W/m^2 for design. Further details about solar radiation can be found in NASA (1978).

3.2.5 Ice

When the turbine is located in an area where ice may develop, ice conditions should be determined. The density of ice can be set equal to $\rho = 700 \text{ kg/m}^3$. For non-rotating parts, an ice formation of 30 mm thickness on all exposed surfaces can be considered for Denmark, the Netherlands, and Northern Germany. Insofar as concerns the wind turbine at stand-still, it is, furthermore, relevant to consider the rotor blades with an ice cover of this thickness. For the rotating wind turbine, it is relevant to consider a situation with all blades covered by ice, and a situation with all blades but one covered by ice.

For wind turbines on offshore locations, sea ice may develop and expose the foundation of the turbine to ice loads. Loads from laterally moving ice should be based on relevant full scale measurements, model experiments, which can be reliably scaled, or on recognised theoretical methods. When determining the magnitude and direction of ice loads, considerations should be given to the nature of ice, mechanical properties of the ice, ice structure contact area, shape of structure, direction of ice movements, etc. The oscillating nature of ice loads due to build-up and fracture of moving ice should also be considered.

Where relevant, ice loads other than those caused by laterally moving ice, such as loads due to masses of ice frozen to the structure and possible impact loads during thaw of the ice, should be taken into account.

A possible increase in the area due to icing should be considered when determining wind or wave loads on such areas.

3.2.6 Rain, snow and hail

Rain storms should be considered in terms of components that may be subject to water

damage. If no special provisions are made, leakage through covers should be considered. If there is a possibility for accumulation of snow on the wind turbine, the increase of weight due to such accumulation should be considered. The density of heavy snow is in the range 100-150 kg/m³.

In general, caution should be exhibited with regard to installation of wind turbines in areas where hail storms are known to prevail. When designing wind turbines for areas where hail storms are common, possible damage due to impact from hail stones should be considered. The nacelle and the coating on the blades may be especially vulnerable to such damage, in particular, if the hail stones fall during strong winds, i.e. they hit the turbine at an angle different from vertical. The velocity by which a hail stone falls towards the ground is governed by drag and is not influenced by the weight of the hail stone. When the speed of the hail stone is known together with the wind speed, the angle by which the hail stone will hit a wind turbine structure can be determined.

Extreme hail conditions may exist on some locations. Such conditions can be critical for a wind turbine and may force the turbine to stop. Extreme hail events may in some cases govern the design of the leading edges of the rotor blades. The density of hail is usually higher than that of snow. NASA (1978) reports a density of hail of about 240 kg/m³.

3.2.7 Atmospheric corrosion and abrasion

Abrasive action by particles transported by the wind should be considered for exposed surfaces.

The corrosive environment should be represented by generally recognised methods. The classification of the environment should

be such that a sufficient corrosion protection system may be established.

Industrial environments may be rather harsh to wind turbine structures.

Offshore wind turbines will be exposed to corrosion owing to their saline and marine environment. Their foundations will have structural parts whose locations in the wave splash zone will be particularly exposed to corrosion.

The expected corrosion rate depends on the environment.

3.2.8 Earthquake

The effects of earthquakes should be considered for wind turbines to be located in areas that are considered seismically active based on previous records of earthquake activity.

For areas where detailed information on seismic activity is available, the seismicity of the area may be determined from such information.

For areas where detailed information about seismic activity is not generally available, the seismicity should preferably be determined on the basis of detailed investigations, including a study of the geological history and the seismic events of the region.

If the area is determined to be seismically active and the wind turbine is deemed to be affected by a possible earthquake, an evaluation should be made of the regional and local geology in order to determine the location relative to the alignment of faults, the epicentral and focal distances, the source mechanism for energy release, and the source-to-site attenuation characteristics. Local soil conditions need to be taken into account to the extent they may affect the

ground motion. The evaluation should consider both the design earthquake and the maximum credible earthquake.

When a wind turbine is to be designed for installation on a site which may be subject to earthquakes, the wind turbine has to be designed so as to withstand the earthquake loads. Response spectra in terms of so-called pseudo response spectra can be used for this purpose.

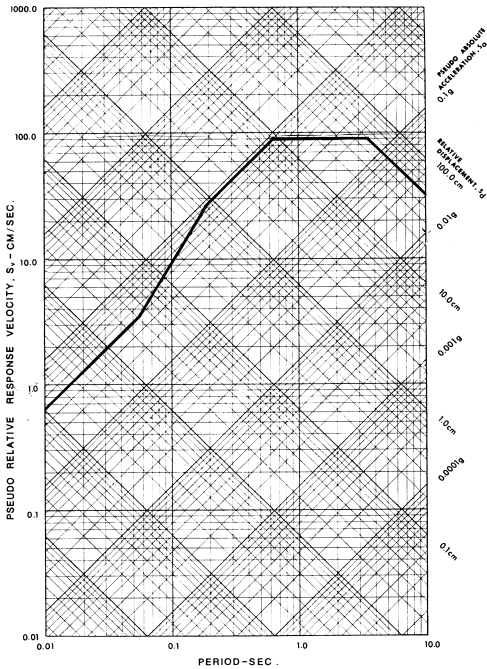


Figure 3-15. Example of pseudo response spectrum.

Pseudo response spectra for a structure are defined for displacement, velocity and acceleration. For a given damping ratio γ and an angular frequency ω , the pseudo response spectrum S gives the maximum value of the response in question over the duration of the response. This can be calculated from the ground acceleration history by means of Duhamel’s integral. The following pseudo response spectra are considered:

- S_D , response spectral displacement
 - S_V , response spectral velocity
 - S_A , response spectral acceleration
- For a lightly damped structure, the following approximate relationships apply

$$S_A \approx \omega^2 S_D \text{ and } S_V \approx \omega S_D$$

such that it suffices to establish the acceleration spectrum and to use this to compute the other two spectra. The three spectra can be plotted together for various γ as shown in the example in Figure 3-15. In this example, the period $T = 2\pi/\omega$ is used as the spectral parameter instead of ω .

It is important to analyse the wind turbine structure for the earthquake-induced accelerations in one vertical and two horizontal directions. It usually suffices to reduce the analysis of two horizontal directions to an analysis in one horizontal direction, due to the symmetry of the dynamic system. The vertical acceleration may lead to buckling in the tower. Since there is not expected to be much dynamics involved with the vertical motion, the tower may be analyzed with respect to buckling for the load induced by the maximum vertical acceleration caused by the earthquake. However, normally the only apparent buckling is that associated with the ground motion in the two horizontal directions, and the buckling analysis for the vertical motion may then not be relevant. For analysis of the horizontal motions and accelerations, the wind turbine can be represented by a concentrated mass on top of a vertical rod, and the response spectra can be used directly to determine the horizontal loads set up by the ground motions. An example of a pseudo response spectrum is shown in Figure 3-15. For a typical wind turbine, the concentrated mass can be taken as the mass of the nacelle, including the rotor mass, plus $1/4$ of the tower mass.

3.2.9 Lightning

Lightning strokes imply discharging of current to the earth following a separation of charge in thunderstorm clouds. Median values of lightning current, charge transfer, and specific energy produced by a single stroke are 30 kA, 10 C, and 50 kJ/Ω, respectively. Maximum recorded values of these quantities are 300 kA, 400 C, and 20 MJ/Ω, respectively.

When lightning strokes hit wind turbines, lightning current has to be conducted through the wind turbine structure to the ground, passing through or near to practically all wind turbine components and exposing them to possible damage. Large wind turbine components, such as blades and nacelle cover, are often made of composite materials incapable of sustaining direct lightning stroke or conducting lightning current, and are therefore vulnerable to lightning damage.

In areas with a high probability of damage to wind turbines due to lightning, a protection system should be installed. The purpose of a lightning protection system is to reduce the damage caused by lightning to a tolerable level.

The design of any lightning protection system should take into account the risk of lightning striking and/or damaging the wind turbine structure. The risk of lightning striking the wind turbine structure is a function of the height of the structure, the local topography, and the local level of lightning activity. The lightning risk is usually higher in low mountainous areas than in coastal areas. For structures taller than 60 m, side flashes occur, i.e. some of the lightning flashes strike the side of the structure rather than the tip. Such side flashes are a cause for concern in connection with wind turbines as blades struck on the sides may be severely damaged.

Statistically, as many as 40-50% of all lightning stroke events for wind turbines cause damage to the control system, whose availability is of vital importance for the operation of a wind turbine.

For detailed information on lightning, reference is made to DEFU (1999).

REFERENCES

Astrup, P., S.E. Larsen, O. Rathmann, P.H. Madsen, and J. Højstrup, “WASP Engineering – Wind Flow Modelling over Land and Sea”, in *Wind Engineering into the 21st Century*, eds. A.L.G.L. Larose and F.M. Livesey, Balkema, Rotterdam, the Netherlands, 1999.

DEFU, *Lightning protection of wind turbines*, Recommendation No. 25, 1st edition 1, DEFU, 1999.

DNV, *Environmental Conditions and Environmental Loads*, Classification Notes No. 30.5, Det Norske Veritas, Høvik, Norway, 1998.

DS410, *Norm for last på konstruktioner*, in Danish, Copenhagen, Denmark, 1999.

DS412, *Norm for stålkonstruktioner*, in Danish, 3rd edition, Copenhagen, Denmark, 1999.

DS472, *Last og sikkerhed for vindmøllekonstruktioner*, in Danish, 1st edition, Copenhagen, Denmark, 1992.

Dyrbye, C., and S.O. Hansen, *Wind Loads on Structures*, John Wiley and Sons, Chichester, England, 1997.

Frandsen, S., *Turbulence and turbulencegenerated fatigue loading in wind turbine clusters*, Report No. Risø-R-

- 1188(EN), Risø National Laboratory, Wind Energy Department, May 2001.
- Gran, S., *A Course in Ocean Engineering*, Elsevier, Amsterdam, the Netherlands, 1992. The Internet version, located at www.dnv.com/ocean/, provides on-line calculation facilities within the fields of ocean waves, wave loads, fatigue analysis, and statistics.
- IEC61400-1, *Wind turbine generator systems – Part 1: Safety requirements*, International Standard, 2nd edition, 1999.
- Jensen, N.O., “Atmospheric boundary layers and turbulence”, in: *Wind engineering into the 21st century. Proceedings of Tenth International Conference on Wind Engineering*, Copenhagen, Denmark, 21-24 June 1999. Larsen, A.; Larose, G.L.; Liversey, F.M. (eds.), A.A. Balkema, Rotterdam/ Brookfield, Vol. 1, pp. 29-42, 1999.
- Laursen, E.V., J. Larsen, K. Rajakumar, J. Cappelen, and T. Schmith, *Observed daily precipitation and temperature from six Danish sites, 1874-1998*, Technical Report No. 99-20, Danish Meteorological Institute, Copenhagen, Denmark, 1999a.
- Laursen, E.V., R.S. Thomsen, and J. Cappelen, *Observed Air Temperature, Humidity, Pressure, Cloud Cover and Weather in Denmark – with Climatological Standard Normals, 1961-90*, Technical Report No. 99-5, Danish Meteorological Institute, Copenhagen, Denmark, 1999b.
- Lundtang, E., Troen, I. , *European Wind Atlas, The Handbook of European Wind Resources*, Risø, Denmark, 1989.
- Madsen, H.O, S. Krenk, and N.C. Lind, *Methods of Structural Safety*, Prentice-Hall Inc., Englewood Cliffs, N.J., 1986.
- Mortensen, N.G., and E.L. Petersen, “Influence of topographical input data on the accuracy of wind flow modelling in complex terrain,” *Proceedings*, European Wind Energy Conference, Dublin, Ireland, 1997.
- National Aeronautics and Space Administration (NASA), *Engineering Handbook on the Atmospheric Environmental Guidelines for Use in Wind Turbine Generator Development*, NASA Technical Paper 1359, 1978.
- Norwegian Petroleum Directorate, *Acts, regulations and provisions for the petroleum activity*, Stavanger, Norway, 1994.
- Panofsky, H.A., and J.A. Dutton, *Atmospheric Turbulence, Models and Methods for Engineering Applications*, John Wiley and Sons, New York, N.Y., 1984.
- Statens Planverks Författningssamling, “Svensk Byggnorm, SBN avd. 2A, Bärande konstruktioner, med kommentarer,” in Swedish, LiberFörlag, Stockholm, Sweden, 1980.

4. Loads

4.1 Load cases

As part of the design process, a wind turbine must be analysed for the various loads it will experience during its design life. A prime purpose in this respect is to verify that the turbine will be able to withstand these loads with a sufficient safety margin. This task is systematised by analysing the wind turbine for a number of relevant load cases.

Load cases can be constructed by combining relevant design situations for the wind turbine with various external conditions. The design situations mainly consist of various operational conditions of the wind turbine. For the most part, the external conditions consist of various wind conditions or wind events.

As guidance, lists of design situations, wind events, and design load cases are provided in the following subsections. These lists are meant as an aid and are not necessarily exhaustive. In the design of a wind turbine, it is important to identify all load cases which are relevant for the wind turbine. Failure mode and effects analysis is a useful tool in assessing which load cases are relevant and which are not, see Chapter 2.

4.1.1 Design situations

The relevant design situations consist of the most significant conditions that a wind turbine is likely to experience. The design situations can be divided into operational conditions and temporary conditions. The operational conditions include:

- normal operation and power production
- cut-in, cut-out, idling, and standstill

The temporary conditions include:

- transportation
- installation, assembly
- faults, such as control system fault

- maintenance and repair
- testing

This list of conditions can be used as a tool to identify design situations, which can be expected to be encountered, and to assess whether listed load cases are relevant, and whether relevant load cases are missing.

4.1.2 Wind events

The wind conditions can be divided into normal and extreme conditions. The IEC-61400-1 standard makes a further distinction and defines the following conditions:

- normal wind profile, see Section 3.1.1
- normal turbulence, see Section 3.1.2
- extreme coherent gust
- extreme direction change
- extreme operating gust
- extreme wind speed, see Section 3.1.9
- extreme wind shear, see Section 3.1.9

4.1.3 Design load cases

The design load cases to be analysed during the design process of a wind turbine are constructed by a combination of relevant design situations and external conditions. The following combinations constitute a minimum number of relevant combinations:

- normal operation and normal external conditions
- normal operation and extreme external conditions
- fault situations and appropriate external conditions, which may include extreme external conditions. Examples of fault situations are generator short circuit or network failure and fault in braking system.
- transportation, installation and maintenance situations and appropriate external conditions

Table 4-1 lists a number of design load cases to consider according to DS472. Table 4-2 presents a similar list extracted from IEC 61400-1. These lists serve as examples, and

it is the duty of the designer to validate their adequacy. When calculating loads it is important to keep in mind a few factors which may influence the involved wind conditions and the magnitude of the loads:

- tower shadow and tower stemming, i.e. the disturbances of the wind flow owing to the presence of the tower

- wake effects wherever the wind turbine is to be located behind other turbines, e.g. in wind farms
- misalignment of wind flow relative to the rotor axis, e.g. owing to a yaw error

Note that some of the load cases that are listed in Table 4-1 and Table 4-2 are load cases which refer to site-specific wind turbines only.

Load case type	Design situation	Wind condition	Limit state		
			Fatigue	Ultimate	Accident
Normal	Power production	Normal	x	x	
	Start and switch	Normal	x	x	
	Stop and transition to idling	Normal	x	x	
	Standstill and idling	Normal	x		
Extra-ordinary	Power production	Extreme stationary wind with $U_{10} = v_{10min,50vr}$	(x)	x	
	Power production	Transient wind conditions for direction change 0-90° and wind speed change 10-25 m/sec in 30 sec.	(x)	x	
	Transport, assembly and erection	Largest allowable U_{10} to be specified		x	
	Manual operation of wind turbine	To be defined according to relevance	x	x	
	Emergency stop	1.3 times cut-out wind speed	x	x	
	Activation of air brakes	1.3 times cut-out wind speed	x	x	
	Idling at yaw error	$0.5v_{10min,50vr}$	x	x	
	Fault conditions	Normal	x	x	
Accidental	Serious failure	Cut-out wind speed	(x)		x

x to be included

(x) to be included unless it can be established as unnecessary for the current design of the wind turbine

Table 4-2. Design load cases, cf. IEC 61400-1.			
Design situation	Wind condition	Other conditions	Type of analysis
Power production	Normal turbulence		Ultimate
	Normal turbulence		Fatigue
	Extreme coherent gust with direction change		Ultimate
	Normal wind profile	External electrical fault	Ultimate
	Extreme operating gust, one-year recurrence period	Loss of electrical connection	Ultimate
	Extreme operating gust, fifty-year recurrence period		Ultimate
	Extreme wind shear		Ultimate
	Extreme direction change, fifty-year recurrence period		Ultimate
	Extreme coherent gust		Ultimate
Power production plus occurrence of fault	Normal wind profile	Control system fault	Ultimate
	Normal wind profile	Protection system fault or preceding internal electrical fault	Ultimate
	Normal turbulence	Control or protection system fault	Fatigue
Start-up	Normal wind profile		Fatigue
	Extreme operating gust, one-year recurrence period		Ultimate
	Extreme direction change, one-year recurrence period		Ultimate
Normal shutdown	Normal wind profile		Fatigue
	Extreme operating gust, one-year recurrence period		Ultimate
Emergency shutdown	Normal wind profile		Ultimate
Parked (standing still or idling)	Extreme wind speed, fifty-year recurrence period	Possible loss of electric power network	Ultimate
	Normal turbulence		Fatigue
Parked and fault conditions	Extreme wind speed, one-year recurrence period		Ultimate
Transport, assembly, maintenance and repair	To be stated by manufacturer		Ultimate

4.2 Load types

The external loads acting on a wind turbine are mainly wind loads. As a wind turbine consists of slender elements such as blades and tower, inertia loads will be generated in addition to the gravity loads that act on these elements. Loads due to operation such as centrifugal forces, Coriolis forces and gyroscopic forces must also be considered.

In most cases, the loads on a wind turbine can thus be classified as follows:

- aerodynamic blade loads
- gravity loads on the rotor blades
- centrifugal forces and Coriolis forces due to rotation
- gyroscopic loads due to yawing
- aerodynamic drag forces on tower and nacelle
- gravity loads on tower and nacelle

Gravity loads on the rotor blades cause bending moments in the blades in the edgewise direction. For a pitch-controlled turbine, gravity loads will also cause bending moments in the flapwise direction. Due to the rotation of the blades, the gravity load effects in the blades will be cyclically varying bending moments. The larger the rotor diameter is, the greater are the gravity load effects. Typically, the bending moment at the blade root will follow a fourth-power law in the rotor diameter. Considering that the rotor area follows a quadratic power law in the rotor diameter, this forms one of the greater challenges in making wind turbines larger.

Centrifugal forces induced by the rotation of the blades can be utilised in conjunction with rearwards coning of the blades to compensate for the effects of some of the wind loads and also to provide more stiffness. Forwards coning of the blades would, in contrast, lead to an increase in the

mean load, i.e. the mean flapwise bending moment, and in a reduction of the stiffness.

The load response in a rotor blade is very dependent on the damping. The total damping is a combination of aerodynamic damping and structural damping. The aerodynamic damping depends on:

- choice of blade aerodynamic profile in conjunction with chosen blade twist
- operational condition
- wind speed
- rotor frequency
- vibration direction of blade cross-section
- motion of blade section relative to incoming flow

The structural damping depends much on the blade material. The aerodynamic load response is very much a result of the lift and drag forces in conjunction with the blade profile properties and damping, and with effects of the motion of the rotor structure included.

The following subsections give a brief introduction to the most important load types encountered for a wind turbine with emphasis on the physics behind them. More details about loads and how to predict them are given in Sections 4.3 through 4.5.

4.2.1 Inertia and gravity loads

The inertia and gravity loads on the rotor are mass dependent loads. The cross-sectional centrifugal force F_c depends on the angular rotor speed, the radial position, and the mass of each blade element. At the blade root, this force is

$$F_c = \sum_{i=1}^n m_i r_i \omega^2$$

in which m_i [kg] is the mass of the i th blade element, ω [rad/s] is the angular rotor speed, and r_i [m] is the radial position of the i th

blade element in a discretisation of the blade into n elements. The gravity force is simply given as

$$F_g = \sum_{i=1}^n m_i g \text{ or } F_g = m_{\text{blade}} g$$

$g = 9.82 \text{ m/s}^2$ acceleration of gravity
 m_i mass of the i th blade element
 m_{blade} total blade mass

In general, gyroscopic loads on the rotor will occur for any flexible rotor support. In particular, gyroscopic loads on the rotor will occur whenever the turbine is yawing during operation. This will happen regardless of the structural flexibility and will lead to a yaw moment M_K about the vertical axis and a tilt moment M_G about a horizontal axis in the rotor plane.

For a three-bladed rotor, the net resulting yaw moment due to the gyroscopic load effects is zero, $M_K = 0$, whereas a non-zero constant tilt moment is produced, $M_G = 3M_0/2$, in which

$$M_0 = 2\omega_k \omega \sum_{i=1}^n m_i r_i^2$$

where ω is the angular velocity of the rotor, ω_k is the angular yaw velocity, and m_i is the i th mass located at radius r_i in a discretisation of the rotor blade into n discrete masses.

For a two-bladed rotor, the gyroscopic load effects lead to a cyclic yaw moment and a cyclic tilt moment

$$M_K = 2 M_0 \cos(\omega t) \sin(\omega t)$$

and

$$M_G = 2 M_0 \cos^2(\omega t),$$

respectively.

In many cases it is possible to neglect gyroscopic effects, because the angular velocity of the yaw system is usually rather small. However, flexible rotor-bearing supports can lead to significant gyroscopic forces (rotor whirl), and gyroscopic forces should never be neglected for present MW turbines.

Note that the quoted formulas for M_K and M_G need to be adjusted for a possible rotor tilt.

4.2.2 Aerodynamic loads

Blades

The true wind flow in the vicinity of the wind turbine rotor is rather complex, because the rotor induces velocities. Hence it is common practice to use a simplified method for calculating rotor loads to be used for a wind turbine design.

The wind velocity conditions at a blade cross-section are illustrated in Figure 4-1.

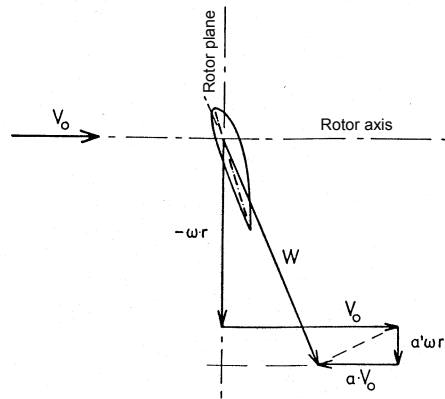


Figure 4-1. Diagram of air velocities at a blade cross-section.

The wind velocity perpendicular to the rotor plane is V_0 . This is the inflow wind velocity. When the wind passes through the rotor

plane, this wind speed becomes reduced by an amount aV_0 due to axial interference. The rotor rotates with angular rotor speed ω . Thus, a blade element at a distance r from the rotor axis will be moving at a speed ωr in the rotor plane. When the wind passes through the rotor plane and interacts with the moving rotor, a tangential slipstream wind velocity $a'\omega r$ is introduced. The resulting relative inflow wind velocity that the rotor blade will experience comes out as shown in Figure 4-1 and is denoted W . This resulting relative wind velocity gives rise to aerodynamic forces on the blade, viz. a lift force

$$F_L = \frac{1}{2} C_L \rho c W^2$$

and a drag force

$$F_D = \frac{1}{2} C_D \rho c W^2$$

C_L lift coefficients
 C_D drag coefficients
 ρ density of air
 c chord length of the blade

For more details about how to calculate aerodynamic forces, see Sections 4.3 through 4.5.

Tower and nacelle

The aerodynamic drag force, F_d on the tower and the nacelle can be calculated on the basis of the projected area perpendicular to the flow

$$F_d = 0.5 \rho A V_0^2 C_D$$

C_D aerodynamic drag coefficient
 A projected area perpendicular to the flow

4.2.3 Functional loads

Functional loads on a wind turbine occur when the turbine is subject to transient operational conditions such as braking and yawing, or when generators are connected to the grid. Further, functional loads from the yaw system may also be present. The most important functional loads can be categorised as follows:

- brake loads from mechanical and aerodynamic brakes
- transient loads in the transmission system, e.g. caused by engagement of the generator
- yawing loads, i.e. loads produced directly by yawing
- loads caused by pitching the blades or engaging the air brakes, initiated by the control system

4.2.4 Other loads

Other loads or load effects to consider are those induced by tower shadow, vortex shedding by the tower, damping, and instabilities like stall-induced blade vibrations. Blade vibrations might be both flapwise and edgewise. Either mode shape (and possibly others) might be excited due to negative aerodynamic damping.

For wind turbine structures installed in water, it is necessary also to consider loads set up by the marine environment such as wave loads, current loads, and ice loads.

A general reference is made to Andersen et al. (1980).

4.3 Aeroelastic load calculations

Load calculations for a wind turbine structure are usually performed by means of a computer program based on an aeroelastic calculation procedure. The purpose of an aeroelastic wind turbine analysis is to solve the equations of motion for a given arbitrary

set of forces acting on the structure and for forces generated by the structure itself. Often, such a code applies a geometrically non-linear finite element approach or a modified modal analysis approach. Reference is made to Figure 4-2.

In any case, it is required that the code must be able to include and simplify the complex mechanical structure of the wind turbine as well as being able to model arbitrary deterministic and stochastic forces acting on the turbine. The general formulation of the differential equations of motion is

$$\mathbf{M}\ddot{\mathbf{x}} + \mathbf{C}\dot{\mathbf{x}} + \mathbf{K}\mathbf{x} = \mathbf{F}$$

- M** mass matrix
- C** damping matrix
- K** stiffness matrix
- F** force vector acting on the structure and typically varying with time
- x** and the derivatives of **x** are unknown vectors containing translations and/or rotations and their derivative

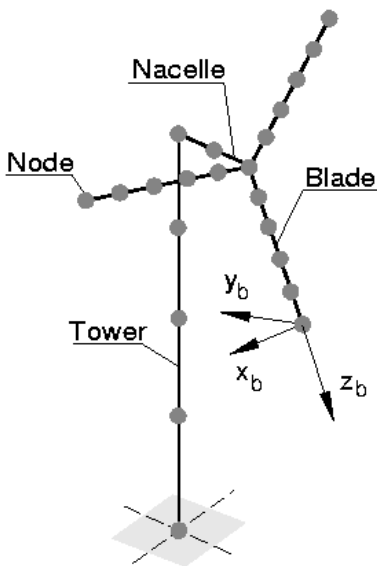


Figure 4-2. Example showing representation of a wind turbine structure by finite element model (HawC).

The loads that are derived from an aeroelastic model are used for design of the various components that constitute the wind turbine structure. In this context, most components are subjected to investigations concerning both extreme loading and fatigue loading.

It is inevitable that some engineering judgment will be involved when preparing for aeroelastic load calculations. It is, therefore, important that the modelling as far as possible is supported by measured data, which may be available from various sources. These include type testing of the rotor blades and prototype testing of an actual turbine, and they are both important to consider when an aeroelastic model is to be validated.

4.3.1 Model elements

Wind field modelling

The wind field contains three wind velocity components:

- longitudinal wind velocity
- transversal wind velocity
- vertical wind velocity

The wind field is usually divided into:

- a mean wind field with shear and slope
- a fluctuating wind field, i.e. turbulence

Wind field simulation is an important part of a structural wind turbine analysis. For wind turbines, spatial variations in the turbulence must be considered, and three-dimensional wind simulation is required. A prime purpose of wind field simulation is to predict time series of the wind speed in a number of points in space, e.g. a number of points across the rotor disc of a wind turbine. Such time series of the wind speed form useful input to structural analysis models for wind turbines.

The parameters used to describe the mean wind field are usually those describing the wind profile and the vertical component of

the wind vector. For flat homogeneous terrain, the vertical component of the wind vector can usually be taken as zero.

The mean wind field is superimposed by a fluctuating wind field, also referred to as the turbulence field, with wind velocity components in three directions, i.e. the longitudinal, transversal and vertical turbulence components, respectively. The parameters used to describe the fluctuating part of the wind field depend on which model is used for its representation.

In order to predict the wind field in a number of points in space, the spatial coherence of the wind field must be properly accounted for. There are two models available for generating a synthetic wind field over a rotor disc:

- the Veers model by Sandia (Veers, 1988)
- the Mann model by Risø (Mann, 1994)

The Veers model uses a circular grid in the rotor plane, while the Mann model applies a quadratic grid. Both models generate a synthetic set of time series of turbulent wind by an inverse Fourier transformation together with a “defactorisation” of the coherence.

The Veers model is based on a method developed by Shinozuka. It is based on a single point spectral representation of the turbulence and a coherence function. A Kaimal formulation is chosen as the spectral model

$$S_i(f) = \sigma_i^2 \frac{6.8 \frac{L_i}{U}}{\left(1 + 10.2 \frac{fL_i}{U}\right)^{5/3}}$$

and an exponential Davenport coherence model is used

$$Coh_i(r, f) = \exp\left(-c_i f \frac{r}{U}\right)$$

index i	identifies the component
F	frequency
R	Distance or spatial separation
L	length scale
σ	Standard deviation of the wind speed
c	coherence decay factor

The original Veers model is extended from a one-component longitudinal turbulence model to a full-field three-dimensional and three-component model by using the calculation method for the longitudinal direction in the transversal and vertical directions as well. No cross-correlation between the three components is modelled. The parameters used in the Veers model are:

- mean wind speed U
- standard deviation of wind speed components $\sigma_u, \sigma_v, \sigma_w$
- integral length scales L_u, L_v, L_w of the turbulence components
- coherence decay factors c_u, c_v, c_w

in which the indices u, v and w refer to the longitudinal, transversal and vertical components, respectively. Reference is made to Section 3.1.5 for details about the integral length scales.

The Mann model is based on a spectral tensor formulation of the atmospheric surface layer turbulence. The model is developed for homogeneous terrain and the parameters used are:

- mean wind speed U
- height above terrain z
- roughness length z_0

The Mann model is capable of representing the cross-correlation between the three wind velocity components.

Measurements are used to establish the parameters that are used in the models. The turbulence intensity, defined from the

standard deviation of the longitudinal wind velocity by $I_T = \sigma_u/U$, is usually measured by means of a cup anemometer. This measurement corresponds to vectorial summation of the longitudinal and transversal wind velocity components. Hence, the turbulence intensity calculated on this basis usually comes out somewhat higher than the sought-after turbulence intensity for the longitudinal component alone. However, it is often used to represent the longitudinal intensity when no other estimate is available.

Data for the relationship between σ_u , σ_v , and σ_w are given in Section 3.1. The longitudinal length scale L_u is in general dependent on the height and the terrain roughness, see Section 3.1 for details. The transverse and vertical length scales can be assumed to relate to the longitudinal length scale by $L_v = 0.3L_u$ and $L_w = 0.1L_u$. Typical values of the longitudinal decay factors c_i are in the range 2-27.

Both the Veers model and the Mann model can be used to simulate time series of the wind speed in a series of points in a plane perpendicular to the mean direction of the wind, e.g. a rotor plane. For details about the models, reference is made to Veers (1988) and Mann (1994, 1998).

Aerodynamic modelling

Aerodynamics deals with the motion of air and the forces acting on bodies in motion relative to the air. Aerodynamic theory makes it possible to perform quantitative predictions of the forces set up by the air flow on the rotor.

On stall-regulated wind turbines, large regions of separated flow will occur during operation at high wind speeds. The stall regulation controls the power output from the turbine by exploiting the decrease in the lift force that takes place when the wind

turbine blades stall and thereby limit the power output and the loads. The overall three-dimensional flow on a rotor is a very complex, unsteady flow depending on a number of variables, which include:

- wind speed
- wind shear
- atmospheric turbulence
- yaw angle
- rotational speed
- rotor radius
- overall layout of the rotor blade
 - twist
 - taper
 - thickness distribution
- airfoil properties
 - thickness
 - camber
 - smoothness of surface
 - leading edge thickness
 - roughness insensitivity
 - blunt/sharp trailing edge

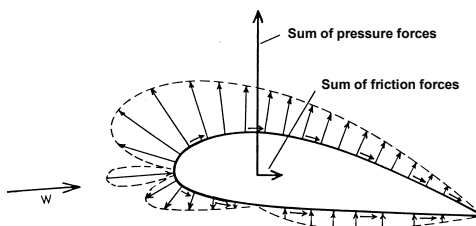


Figure 4-3. Distributions of aerodynamic forces on an airfoil, and their resultants.

A brief introduction to aerodynamic modelling is given in the following with a special view to application to rotor blades. The most important concepts are introduced, and the so-called blade element momentum theory for calculation of aerodynamic forces on a rotor blade is presented. By this method, momentum balance is used for calculation of blade element forces. As with any other method, this method implies a number of simplifications and idealisations, which make it practical for use. Other

methods do exist, but they are time-consuming and not considered any better.

Consider first a two-dimensional flow past a profile. Two-dimensional flow is confined to a plane. The out-of-plane velocity is thus zero. In order to obtain a two-dimensional flow, it is necessary to extrude the profile into a blade of infinite span. For a true blade, the shape, the twist and the profile change over the span, and the blade starts at a hub and ends in a tip. However, for long slender blades, the spanwise velocity component is usually small relative to the streamwise component, such that aerodynamic solutions for two-dimensional flow have a practical interest for wind-turbine rotor blades. The resultant force F from the flow on the blade comes about as the integral of pressure and frictional forces, see Figure 4-3. The resultant force F is decomposed into one component F_L perpendicular to the direction of the resulting relative wind velocity W and one component F_D parallel to this direction. F_L is the lift and F_D is the drag, see Figure 4-4. Both the lift F_L and the drag F_D depend on the inflow angle α .

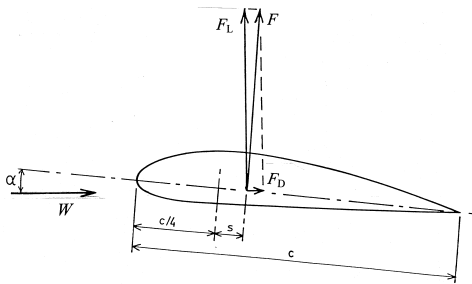


Figure 4-4. Definition of lift and drag on airfoil in 2-D flow.

$c/4$ in Figure 4-4 is referred to as the quarter chord point.

Stall is a nonlinear phenomenon that results in a dramatic loss of flow attachment and airfoil lift when some limiting inflow angle

α_{stall} has been reached. The stall angle α_{stall} is somewhat arbitrary.

Lift and drag coefficients C_L and C_D are defined as

$$C_L = \frac{F_L}{\frac{1}{2} \rho W^2 c}$$

and

$$C_D = \frac{F_D}{\frac{1}{2} \rho W^2 c}$$

- ρ density of air
- c Chord length of the airfoil
- F_L lift forces per unit length
- F_D drag forces per unit length

The lift and drag coefficients are functions of the inflow angle α , as shown in Figure 4-5, of the airfoil shape, and of the Reynolds number $Re = cW/\nu$, in which ν is the kinematic viscosity. C_L increases linearly with α up to the stall angle, α_{stall} , where the profile stalls. For greater values of α , C_L reaches a maximum value, followed by a decrease in C_L for further increases in α . For small α , C_D is almost constant, but increases rapidly after stall. The stall phenomenon is closely related to the separation of the boundary layer from the upper side of the airfoil. The manner in which the profile stalls is dependent on the geometry of the profile. Thin profiles with a sharp nose, i.e. a high curvature around the leading edge, tend to stall more abruptly than thicker airfoils. This is a result of differences in the way the boundary layer separates. Values of the coefficients C_L and C_D can be looked up in tables, calibrated to wind tunnel measurements, see Abbott and von Doenhoff (1959).

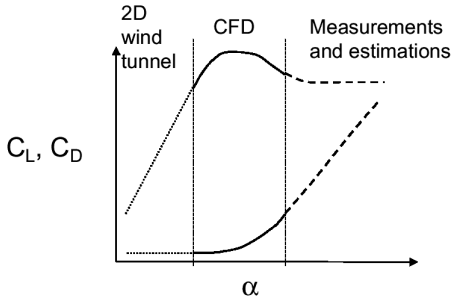


Figure 4-5. Lift and drag curve for an airfoil (Bak et al., 1999a).

An example of the variation of C_L and C_D with the inflow angle α is given in Figure 4-5. It appears that two-dimensional wind tunnel measurements are used to obtain the coefficient values in the pre-stall region. Computational fluid dynamics with corrections for three-dimensional effects is used to obtain these values in the stall region. In the post-stall region, measurements are typically used to determine the coefficient values. Otherwise, a method by Viterna and Corrigan (1981) can be used for their prediction. This method assumes rotors with zero twist angle, and results by the method therefore need modification when this assumption is not fulfilled. By this method, the maximum drag coefficient at inflow angle $\alpha = 90^\circ$ is

$$c_{D,max} = 1.11 + 0.018 \cdot AR$$

in which AR denotes the aspect ratio of the airfoil. The aspect ratio AR is defined for a blade as the ratio between the length of the blade and a representative chord. The drag coefficient in the post-stall region is given by

$$C_D = B_1 \sin^2(\alpha) + B_2 \cos(\alpha), \quad 15^\circ \leq \alpha \leq 90^\circ$$

$$B_1 = C_{D,max}$$

$$B_2 = (1 / \cos(\alpha_s)) \cdot (C_{D_s} - C_{D,max} \sin^2(\alpha_s))$$

The lift coefficient is given by

$$C_L = A_1 \sin^2(\alpha) + A_2 (\cos^2(\alpha) / \sin(\alpha)), \quad 15^\circ \leq \alpha \leq 90^\circ$$

$$A_1 = B_1 / 2$$

$$A_2 = (C_{L_s} - C_{D,max} \sin(\alpha_s) \cos(\alpha_s)) \cdot (\sin(\alpha_s) / \cos^2(\alpha_s))$$

α_s inflow angle at stall onset (usually 15°)

C_{D_s} drag coefficient at stall onset

C_{L_s} lift coefficient at onset of stall

To describe the physics in a mathematical way, the wind turbine rotor can be considered as a disc, which is able to absorb energy from the wind by reduction of the wind speed. The wind speed and the pressure conditions around the disc are illustrated in Figure 4-6.

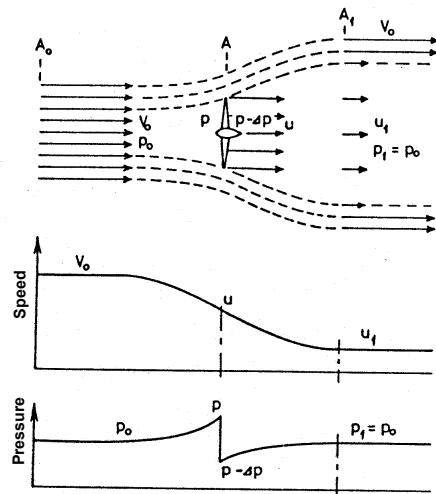


Figure 4-6. Influence of a wind turbine on wind speed and air pressure.

The three-dimensional flow will produce a continuous sheet of tangential vorticity behind the trailing edge of the blade, and the

wake behind the rotor will be rotating. The wake is illustrated in Figure 4-7.



Figure 4-7. Wake illustrated by means of smoke.

Calculation procedure for the blade element momentum method

By the blade element momentum method, the flow area swept by the rotor is divided into a number of concentric ring elements. These elements are considered separately under the assumption that there is no radial dependency between them, i.e. what happens at one element cannot be felt by any other elements. Usually, each ring element is divided into a number of tubes, which are also assumed to be independent. This approach allows for nonsymmetric induction. The wind speed is assumed to be uniformly distributed over each ring element. The forces from the blades on the flow through each ring element are assumed constant. This assumption corresponds to assuming that the rotor has an infinite number of blades. This assumption is corrected for later.

Consider now the ring element of radius r and thickness dr . The thrust on this element from the disc defined by the rotor is

$$dT = 2\pi r \rho u (V_0 - u_1) dr$$

V_0 wind speed before the rotor

u_1 wind speed in the wake behind the rotor

$u = \frac{1}{2}(V_0 + u_1)$ is the wind speed through the rotor plane.

The torque on the ring element is

$$dQ = 2\pi r^2 \rho u C_\theta dr$$

when the tangential wind speed at radius r is zero upstream of the rotor and u_w in the wake. By introducing the axial induction factor $a = 1 - u/V_0$ and the tangential induction factor $a' = \frac{1}{2}u_w/(\omega r)$, where ω denotes the angular velocity of the rotor, the expressions for the thrust and the torque can be rewritten as

$$dT = 4\pi r \rho V_0^2 a(1-a) dr$$

and

$$dQ = 4\pi r^3 \rho V_0 \omega (1-a)a' dr$$

At this point, it is necessary to make an initial choice for a and a' . It is suggested to assume $a = a' = 0$ as an initial guess.

The flow angle ϕ is the angle between the rotor plane and the direction of the relative wind velocity V_{rel} on the rotating blade. The flow angle can be calculated from

$$\tan \phi = \frac{(1-a)V_0}{(1+a')\omega r}$$

The local inflow angle is $\alpha = \phi - \theta$, where the pitch angle θ is the local pitch of the blade relative to the rotor plane. See Figure 4-8.

Determine the lift and drag coefficients C_L and C_D for the blade from adequate tables. They are functions of α and of the blade thickness relative to the chord length. Transform these coefficients to normal and tangential coefficients C_N and C_T by

$$C_N = C_L \cos \phi + C_D \sin \phi$$

$$C_T = C_L \sin \phi - C_D \cos \phi$$

The solidity σ is defined as the fraction of the cross-sectional area of the annular element which is covered by the blades. The solidity depends on the radius r of the annular element and can be found as

$$\sigma(r) = \frac{c(r)B}{2\pi r}$$

in which B denotes the number of blades.

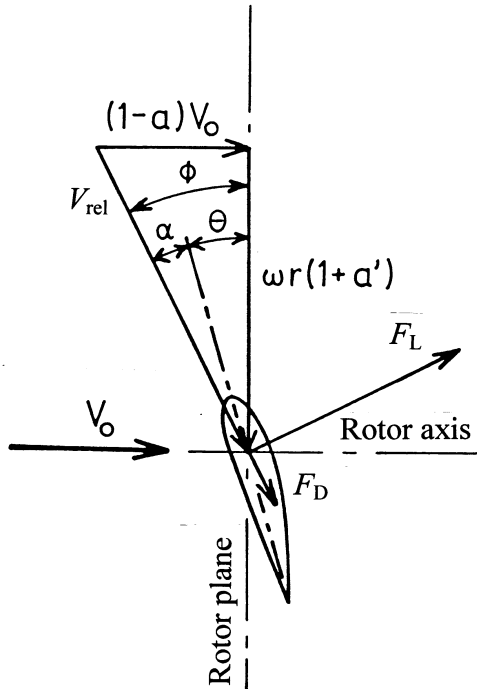


Figure 4-8. Velocity components.

Calculate the influence factors a and a' by

$$a = \frac{1}{\left(\frac{4F \sin^2 \phi}{\sigma C_N} + 1\right)}$$

and

$$a' = \frac{1}{\left(\frac{4F \sin \phi \cos \phi}{\sigma C_T} - 1\right)}$$

in which

$$F = \frac{2}{\pi} \arccos\left(\exp\left(-\frac{B}{2} \frac{R-r}{r \sin \phi}\right)\right)$$

where R is the rotor radius. Note that F is known as Prandtl's tip loss factor. This is a reduction factor, which corrects for the finite length of the blades, implying that it is difficult to fully keep the pressure difference between the top and bottom of the blade profile close to the blade tip. Recalling the assumption of an infinite number of blades sweeping the rotor area, Prandtl's tip loss factor – by its expression – also implies a correction for the actual finite number of blades of the rotor.

Examine these values of a and a' . If they deviate significantly, i.e. by more than some acceptable tolerance, from the values of a and a' assumed for the calculations, go back to where the values for a and a' were initially assumed and use the new values of a and a' to recalculate the flow angle ϕ . Repeat the calculation procedure from there on to obtain a new updated set of a and a' . This iterative procedure needs to be repeated until a convergent set of values for a and a' results. Note that simple momentum theory breaks down when a becomes greater than about 0.3. Formulas exist for correction of a when this situation occurs. Whenever $a > a_c$, where $a_c \approx 0.2$, Glauert's correction can be applied, and implies that a is replaced by

$$a = \frac{1}{2} (2 + K(1 - 2a_c) - \sqrt{(K(1 - 2a_c) + 2)^2 + 4(Ka_c^2 - 1)})$$

in which

$$K = \frac{4F \sin^2 \phi}{\sigma C_N}$$

Note that it is of particular importance to apply Glauert's correction in order to compute the induced velocities correctly for small wind speeds.

Once a convergent set of a and a' has been determined, it can be used to calculate the local forces on a rotor blade at distance r from the axis of rotation, i.e. the force normal to the rotor plane and the force tangential to the rotor plane. The normal force per length unit of the blade is

$$F_N = \frac{1}{2} \rho \frac{V_0^2 (1-a)^2}{\sin^2 \phi} cC_N$$

and the tangential force per length unit of the blade is

$$F_T = \frac{1}{2} \rho \frac{V_0 (1-a) \omega r (1+a')}{\sin \phi \cos \phi} cC_T$$

The procedure is repeated for all ring elements modelled, i.e. for all radius values r , and the result thus consists of distributions along the rotor blade of the normal and tangential forces per unit length. These distributions form the basis for calculating stresses, forces and moments in any cross-section along the blade. In particular, rF_T can be integrated along the blade to give the contribution from one blade to the total shaft torque.

Structural modelling

Rotor blades are slender such that they from a structural point of view will act like beams, and beam theory can be applied. Reference is made to Section 5.1. For analysis of a rotor blade by means of beam

theory, a number of definitions relating to the blade profile are useful. Consider a section of the blade. The elastic axis is perpendicular to the section and intersects the section in a point where a normal force (out of the plane of the section) will not give rise to bending. The shear centre is the point where an in-plane force will not rotate the profile in the plane of section. The two in-plane principal axes are mutually perpendicular and both cross the elastic axis. The principal axes are defined by the phenomenon that whenever a bending moment is applied about one of them, the beam will only bend about this axis. Applying a bending moment about any other axis will induce bending, also about another axis than the one corresponding to the applied moment.

Moments of stiffness inertia about the various axes defined in Figure 4-9 can be calculated by means of standard formulas, which can be found in structural engineering textbooks. The angle α between the reference axis X' and the principal axis X can be calculated as

$$\alpha = \frac{1}{2} \arctan \frac{2[ED_{X'Y'}]}{[EI_{Y'}] - [EI_{X'}]}$$

where

$$[ED_{X'Y'}] = \int_A EX'Y' dA$$

is the deviation moment of inertia, and

$$[EI_{X'}] = \int_A EX'^2 dA \quad \text{and} \quad [EI_{Y'}] = \int_A EY'^2 dA$$

are the bending stiffness properties about the X' and Y' references axes, respectively. The bending stiffness about the principal axes can now be computed as

$$[EI_x] = [EI_{x'}] - [ED_{xy'}] \tan \alpha$$

and

$$[EI_y] = [EI_{y'}] - [ED_{xy'}] \tan \alpha$$

respectively.

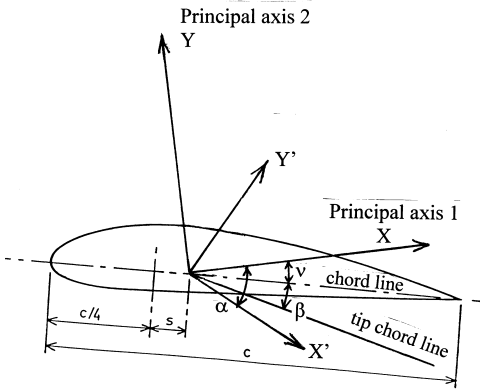


Figure 4-9. Section of blade showing principal axes, chord line, tip chord line, and angles to chord line.

The most important structural stiffness data for a rotor blade have been dealt with here. Note that since present wind turbine blades are usually relatively stiff in torsion, the torsional stiffness has usually not been considered. Note also that this may change in relation to future wind turbine designs.

In structural modelling and analysis, it is important to be aware of the flutter phenomenon, which may result from coupled torsional and flapping motion. Low ratios of torsional and flapwise frequencies and high tip speeds indicate rise of flutter, which may be destructive for the rotor blade. Reference is made to Section 4.3.4.

Control system modelling

The control system is to keep the operating parameters of the wind turbine within specified "normal" limits. This, in turn, is to keep the loads on the wind turbine within certain limits. Because the operating

parameters are usually controlled by monitoring their current values and/or their first or second derivatives, a regulation algorithm can always be set up and coded for use together with an aeroelastic code for load prediction.

For a pitch-regulated turbine with variable speed, a method exists for representation of the control system. The description in the following pertains to the control system of a wind turbine with variable speed.

The mechanical effect of the wind turbine is

$$P = \frac{1}{2} \rho A u^3 C_p(\beta, \lambda)$$

- ρ density of air
- A rotor area
- u wind speed
- C_p rotor efficiency

C_p which is a function of the pitch angle β and of the tip speed ratio $\lambda = \omega_R R / u$. ω_R is the angular frequency of the rotor, and R is the rotor radius.

The pitch angle β and the rotor speed ω_R are the two parameters which can be used for the control of the turbine. The control of the turbine is usually based on one of the following two approaches:

- Optimisation of the power below the nominal power, i.e. the rotor is kept as close as possible to the maximum value of C_p , which occurs for a particular optimal set $(\beta_{opt}, \lambda_{opt})$ of β and λ . This is achieved by choosing β equal to its optimal value β_{opt} , and keeping λ constant at its optimal value λ_{opt} . However, λ cannot be controlled directly, since u is hard to measure with sufficient accuracy. Therefore, instead, information about which power production is optimal for a given value

of ω_r is utilised, and ω_r is used as the parameter to control the turbine and optimise the power rather than λ . This information can be established from the aerodynamic data for the rotor, first of all profile data, and computer software is available for this purpose.

- Limitation of the power by keeping it as close as possible to the nominal power.

The aerodynamic driving torque varies continuously due to the turbulence of the wind. This moment is transferred to electric power by the transmission system and is used as a primary indicator for the loading on the transmission system. By means of the pitch and speed regulation of the turbine, changes in the aerodynamic power are absorbed as changes in the angular velocity of the rotor instead of inducing changes in the torque which is transferred to the gearbox. This implies that relative to a conventional fixed-speed turbine, a lower level of gearbox forces can be kept.

4.3.2 Aeroelastic models for load prediction

Aeroelasticity is a discipline where mutual interaction between aerodynamic and elastic deflections is investigated. Aeroelastic models for load prediction are usually based on the blade element momentum method for transformation of the wind flow field to loads on the wind turbine structure.

Two important and commonly applied methods used for discretisation in connection with structural modelling of wind turbines are the finite element method (FEM) and the modal analysis method (or methods strongly related to modal analysis). Both methods are implemented in computer codes for load prediction. The computer code HawC is an example of an aeroelastic code based on the finite element method. The computer code FLEX4 is an example of

an aeroelastic code based mainly on methods related to modal analysis.

A number of computer programs for aeroelastic analysis with load and deformation prediction for wind turbines exist. Some of these programs are commercially available and can be purchased, while others are developed by wind turbine manufacturers and are not available to the public. Most of the programs provide solutions in the time domain. However, a few programs exist which offer solutions in the frequency domain.

Regardless of which aeroelastic code is applied to prediction of wind turbine loads, it is essential that it is subject to validation. The IEC requires that the load model used to predict loads for design verification of wind turbines be validated for each design load case. This validation of the load prediction is to be based on a representative comparison between measured and predicted loads on a similar wind turbine. This comparison and the subsequent calibration shall include both the peak loads and the fatigue loads.

4.3.3 Aerodynamic data assessment

Choice of aerodynamic coefficients for use as input to any aerodynamic analysis method requires careful consideration. In this context, it is important to give special attention to which regulation strategy is adopted for the wind turbine, which is subject to design.

When the turbine is pitch-controlled, the major task is to program as correctly as possible the regulation routine to be used with the aeroelastic computer code. The aerodynamic coefficients are fairly easy to obtain when the turbine is pitch-controlled, since the turbine will only operate in the linear part of the lift curve and three-dimensional effects are of little importance. However, the initial part of the lift curve in

the stall region should still be correctly modelled, because no pitch regulation mechanism can be considered so perfect that the blades will never experience a stalled condition.

When the turbine is stall-regulated or active-stall-regulated, an appropriate choice of the aerodynamic coefficients is more difficult to achieve. A first step in deriving representative values for the aerodynamic coefficients consists of identifying the profile series used for the rotor blade. When the profiles are well-known, it is easy to find two-dimensional wind tunnel data to support the choice of coefficient values. Data for so-called NACA profiles can readily be found in Abbott and von Doenhoff (1959). When the profiles are not well-known, it is recommended to inspect a visualisation of the profile shape and to find a representative and well-known profile series for which measured aerodynamic two-dimensional data exist.

The next step is to assign values to the aerodynamic coefficients with due consideration to possible three-dimensional effects. It is recommended to evaluate or calibrate the aerodynamic coefficients from power curve data or thrust curve data. A representative thrust curve can easily be derived from the tower bottom bending. When reliable measured data are available, this will provide a good basis for deriving "correct" data.

In most cases, measurements are not available. The assignment of values to the aerodynamic coefficients must be based on a general impression and on experience. Alternatively, it can be considered to apply guidelines for three-dimensional corrections of two-dimensional data according to Bak et al. (1999b). These guidelines can be summarised as follows:

- the lift coefficients are lower at the blade tip in the stall region when 3-D effects are included
- the lift coefficients are unchanged at a distance approximately two thirds of the rotor radius from the rotor axis
- the lift coefficients are higher on the inner part of the blade, i.e. closer to the rotor axis, when 3-D effects are included
- the drag coefficients are unchanged on the outer part of the blade
- the drag coefficients are slightly lower on the inner part of the blade for inflow angles up to approximately 20° when 3-D effects are included. For higher inflow angles, the drag coefficients are higher than indicated by 2-D data.

Beware that these guidelines are based on calibration of computational results for one particular blade, viz. the LM19.1 blade, and cannot necessarily be projected to apply to other blades without validation.

It is usually not possible to find aerodynamic data for inflow angle outside the range -20° - 20° . As high inflow angles outside this range do occur on wind turbines, in particular, during extreme conditions formed by extreme yaw errors or extreme wind speeds, it is often necessary to extrapolate the available aerodynamic data to values for these high angles. A method for such extrapolation can be found in Eggleston and Stoddard (1987). Alternatively, the method by Viterna and Corigan (1981), described in Section 4.3.1, can be used.

Note that proper selection of values for the aerodynamic coefficients is a very important step in the design analyses of a wind turbine, since a reliable prediction of the dynamic response of the wind turbine is very dependent on correct choices of aerodynamic coefficients.

4.3.4 Special considerations

Structural damping

In order to achieve a realistic response from an analysis by an aeroelastic code, specification of the structural damping must be made with caution. The structural damping model is included in the equations of motion in order to assure dissipation of energy from the structural system. Quite often, measurements of the structural damping are only obtained for a limited number of mode shapes, if available at all.

Mode shape	Freq. [Hz]	Damp. [% log.]	
		Mean	Std.dev.
1 st flap	1.636	1.782	0.080
2 nd flap	4.914	2.021	0.011
3 rd flap	9.734	2.468	0.026
4 th flap	16.22	3.227	0.033
1 st edge	2.943	3.603	0.011
2 nd edge	10.62	5.571	0.041
1 st torsion	23.16	5.807	0.062

Table 4-3. Modal damping in logarithmic decrement for a 19m blade.

Experience shows that the structural damping in terms of the logarithmic decrement is usually of the order of 3% for the blades and of 5% for the shaft and the tower. An example of logarithmic decrements found for a 19m rotor blade is shown in Table 4-3. (Baumgart et al, 2000). In order to ensure dissipation of energy, it is required that the part of the damping matrix **C** in the equations of motion that originates from structural damping is positive definite or at least semi-positive definite

$$\mathbf{x}^T \mathbf{C} \mathbf{x} \geq 0$$

Positive definiteness of the structural damping matrices ensures dissipation of energy at all velocities.

A commonly used model for representation of damping is the Rayleigh damping model whose major advantage is a decoupling of

the equations of motion whenever a modal formulation is used. The damping model has the form

$$\mathbf{C} = \alpha \mathbf{M} + \beta \mathbf{K}$$

C damping matrix
M mass matrix
K stiffness matrix
 α, β model constants

Reference is made to Bathe (1982). The Rayleigh damping model enables an accurate fit of two measured damping ratios only. Here, α and β are determined from two damping ratios that correspond to unequal frequencies of vibration.

A disadvantage of the use of the Rayleigh model is that it is known to overpredict the damping at high frequencies of vibration.

In a more general damping model, it is assumed that p damping ratios have been determined. Based on this, the damping matrix is represented by a Caughey series:

$$\mathbf{C} = \mathbf{M} \sum_{k=0}^{p-1} a_k [\mathbf{M}^{-1} \mathbf{K}]^k$$

C damping matrix
M mass matrix
K stiffness matrix
 P number of damping ratios
 a_k model constant

The modelling constants a_k are determined from the p simultaneous equations

$$\xi_i = \frac{1}{2} \left[\frac{a_0}{\omega_i} + a_1 \omega_i + a_2 \omega_i^3 + \dots + a_{p-1} \omega_i^{2p-3} \right]$$

$i = 1, p$, in which ξ_i is the i th damping ratio and ω_i is the angular frequency for the vibration mode that ξ_i was obtained for.

The disadvantage of using this generalised damping model is that the damping matrix C – in the general case – is a full matrix. This may cause the simulations in an aeroelastic analysis to become rather time-consuming. For $p = 2$ this model is reduced to a Rayleigh damping model.

For appreciation of the results presented herein, recall that the i th damping ratio is defined as

$$\xi_i = \frac{c}{2\sqrt{m_i k_i}}$$

- m_i i th mass
- c_i i th damping
- k_i i th stiffness

The corresponding logarithmic decrement is

$$\delta_i = \frac{2\pi\xi_i}{\sqrt{1-\xi_i^2}} \approx 2\pi\xi_i$$

The logarithmic decrement is the natural logarithm of the amplitude decay ratio, i.e. the natural logarithm of the ratio of the amplitudes in two consecutive displacement cycles.

Verification of the structural damping

When some initial guesses of the damping coefficients have been chosen for the aeroelastic model, it must be verified that the model leads to a correct representation of the damping. This is done by fixing all degrees of freedom of the turbine, except the one for which the damping model is to be checked. An external periodic force is applied to the structural component in question (e.g. a blade) using the natural frequency of that component as the excitation frequency. The structure is only excited for a few seconds. The subsequent decay of the induced vibration is measured,

and the damping coefficient is easily determined from a curve fit of the equation

$$f(x) = C \cdot \exp(-\delta \cdot f_n \cdot t)$$

- t time
- f_n excitation frequency
- δ logarithmic decrement
- C calibration constant from the fit

An example of such a fit is shown in Figure 4-10. The dynamic coefficients in the model must be adjusted until the correct logarithmic decrement δ results from this exercise.

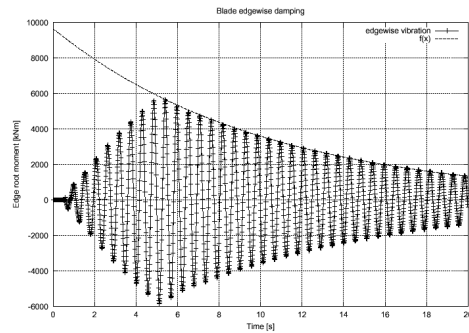


Figure 4-10. Damping test of rotor blade in edgewise vibration.

Upon application of a Rayleigh damping model, it is only possible to fit the correct damping properties at two frequencies. If the damping properties are known at more frequencies, such as in the example in Table 4-3, one is restricted to select some average representation of the damping. In this context, it is important to be aware of the overprediction of the damping by the Rayleigh model at high frequencies, e.g. when analysing high-frequency impulse forces on fibreglass materials.

Stall-induced vibrations of blades

Examples exist of wind turbines, which have developed significant edgewise vibrations of the blades, even during relatively moderate wind situations such as those characterised

by 10-minute mean wind speeds of about 15 m/sec. Such edgewise vibrations are undesirable from a structural point of view and need to be avoided. Edgewise vibrations occur whenever the negative aerodynamic damping exceeds the structural damping. The aerodynamic forces supply more energy to the vibrations than the structural damping can absorb. An example of such vibrations, simulated for a 500 kW turbine, are shown in Figure 4-11 and Figure 4-12. Figure 4-11 shows the vibrations for the basic

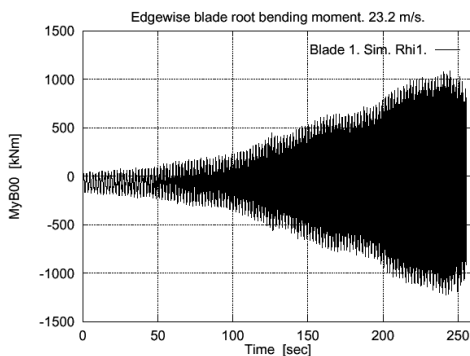


Figure 4-11. Edgewise blade root moment for the 500 kW turbine in basic configuration.

configuration of the turbine, whereas Figure 4-12 shows the vibrations for the new configuration, with increased shaft stiffness. Both figures are extracted from Petersen et al. (1998). Note that flapwise vibrations are equally important to consider.

Recommendations concerning the design of new blades and modification of old blades, when edgewise vibrations pose a problem, are given by Petersen et al. (1998) and are reproduced in the following.

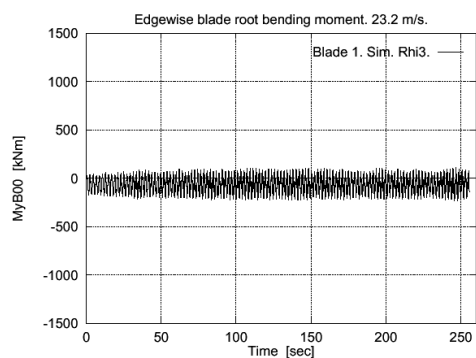


Figure 4-12. Edgewise blade root moment for the 500 kW turbine with an increased shaft stiffness.

For a new turbine design, where a great deal of freedom is at hand, the following procedure is recommended:

1. Base the airfoil on well-documented airfoil data.
2. Choose airfoils, blade planform (chord, aerodynamic twist) and blade structural properties (stiffness, mass, mode shapes – i.e. amplitude and direction of deformation, structural damping, modal mass, modal stiffness and modal natural frequency), considering not only the rotor performance, but also the aerodynamic damping characteristics. Especially, the blade twist should be considered, not only in relation to power performance, but also in relation to mode shape vibration direction.
3. Use a quasi-steady approach (Petersen et al., 1998) to calculate the basic aerodynamic damping characteristics for a single blade, considering both the fundamental flapwise and edgewise mode shapes. If not satisfactory, repeat from Step 2.
4. Extend the quasi-steady analysis and include verified models for dynamic stall on both the airfoil lift and drag, still considering a single blade. If not satisfactory repeat from Step 2.
5. When the single blade analysis results in appropriate aerodynamic damping, continue the analysis by use of the full aeroelastic model, including verified models for stall hysteresis on both airfoil lift and drag. The structural models must have a sufficiently detailed

- representation of the blade bending modes and the rotor whirling modes.
6. Carry out full aeroelastic calculations for the wind speeds of interest. These wind speeds can, to a large extent, be identified through a single blade analysis.
7. Investigate the damping characteristics by looking at the responses at the flapwise and edgewise natural frequencies of the blade, for instance based on the power spectral densities of the blade root bending moments.
8. Repeat from Step 2 if the results are unsatisfactory.

When problems with flapwise and edgewise vibrations have been recorded on a particular turbine, the turbine must be re-designed. In this case, only a limited number of possibilities remain:

1. In general, the scheme above should be applied to the existing design.
2. The aerodynamic properties of the blades may be modified by using different aerodynamic devices, e.g. stall strips and/or vortex generators.
3. The structural properties of the turbine may be changed by adding local masses or increasing local stiffness properties. These changes may alter the relevant mode shapes and natural frequencies in a favourable manner.

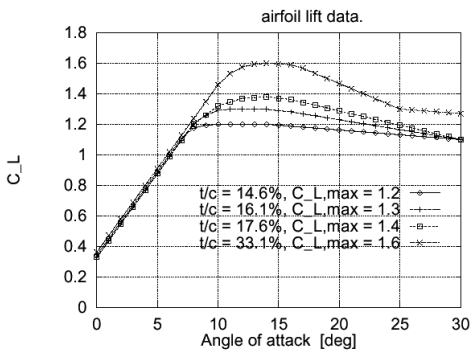


Figure 4-13. Airfoil lift data (unmodified).

4. Mechanical damping devices may be used either on the blades or on the supporting structure. It should be mentioned that these devices do not remove the cause of the vibrations, which is the supply of energy by the aerodynamic forces.

Flutter

Flutter is an aeroelastic instability that may result in large amplitude vibrations of a blade, and possibly in its failure. Flutter vibrations consist of a coupling of flapwise and torsional blade vibrations, which are sustained by the airflow around the blade. There are several undesirable conditions that must exist for flutter to occur. The two most critical conditions occur when the frequencies of a flapwise bending mode and the first torsional mode are not sufficiently separated, and when the centre of mass for the blade cross-sections is positioned aft of the aerodynamic centre, which is approximately at the quarter chord point, which is marked in Figure 4-4 at a distance “ $c/4$ ” from the leading edge. In the design of blades, it is therefore important to ensure a high torsional stiffness (e.g. first torsional frequency larger than ten times the first flapwise frequency), and – if applicable – to ensure that the centre of mass for the blade cross-sections is located between the leading edge and the quarter chord point.

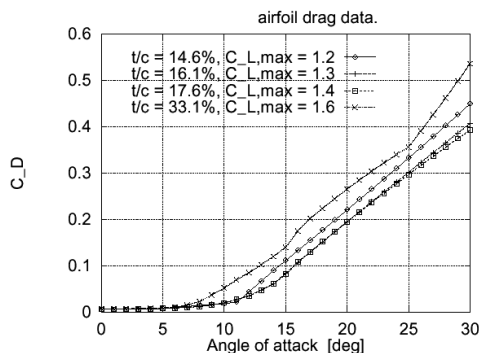


Figure 4-14. Airfoil drag data (unmodified).

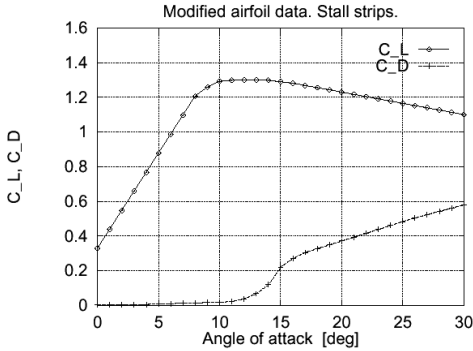


Figure 4-15. Airfoil data with stall strips.

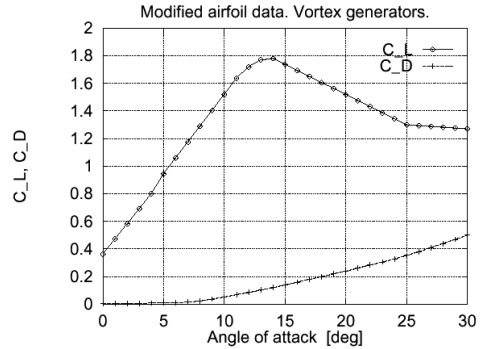


Figure 4-16. Airfoil data with vortex generators.

Use of stall strips and vortex generators

Stall strips can be used on the outer section (typically the far one-third) of a rotor blade as an ‘emergency’ action when problems with heavy vibrations of the blades occur. In general, stall strips increase the damping on local sections of the blade by increasing the drag after the onset of stall.

Vortex generators are often used to increase the lift and thus to improve the aerodynamic properties of the blade. The vortex generators are used on the inner section of the blade and improve the maximum lift of the section. An example of an airfoil with stall strip and vortex generator modifications is shown in Figure 4-13 to 16, (Petersen et al., 1998).

Dynamic stall

The onset of stall becomes delayed when the inflow angle is varying periodically, e.g. according to

$$\alpha(t) = \alpha_0 + \beta \cdot \sin(\omega \cdot t)$$

- α_0 mean inflow angle
- β amplitude
- t time
- ω angular frequency

The phenomenon of delayed onset of stall is denoted dynamic stall, and it influences the

lift and drag coefficients. It is important to account for dynamic stall when it occurs, since lift and drag coefficients are usually derived from wind tunnel tests with constant inflow angle. Various models for dynamic stall can be found in Petersen et al. (1998).

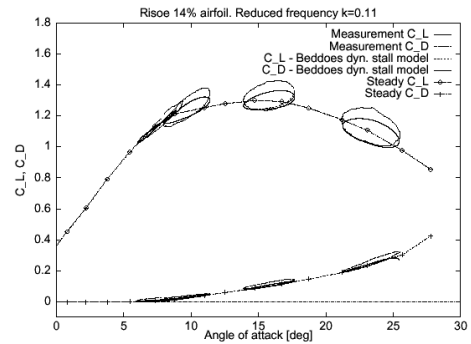


Figure 4-17. C_L and C_D loops, dynamic stall.

An example of dynamic stall measured in a wind tunnel for $\beta = 2^\circ$ is given in Figure 4-17.

4.4 Load analysis and synthesis

4.4.1 Fatigue loads

Fatigue loads are cyclic loads, which cause cumulative damage in the materials of the structural components, and which eventually lead to structural failure. Fatigue loads are usually loads well below the load level that

will cause static failure, and many load cycles are required before a fatigue failure will take place. This is commonly referred to as high-cycle fatigue. However, for some materials with particularly high $S-N$ curve slopes, such as some epoxy materials, the loads of importance for fatigue are close to those that will cause static failure. For such materials fatigue becomes an extreme value problem as far as the loads are concerned with only a few load cycles required to cause fatigue failure. This is commonly referred to as low-cycle fatigue.

The cumulative damage is commonly determined using the Palmgren-Miner rule, as explained in Appendix C. This method requires knowledge of the distribution of the stress ranges, which is dealt with in the following subsections.

Rain-flow counting

Cycle counting methods are used to establish distributions of stress ranges from a stress history. Several methods of cycle counting exist, for example:

- peak counting
- range counting
- rain-flow counting

These three counting methods give the same result for a pure sinusoidal stress history and for an ideal narrow-banded stress history. Rain-flow counting will be considered here and is described for stationary processes. For simplicity, the mean level is taken as zero in the description.

In the rain-flow counting method, the stress history is first converted into a series of peaks and troughs as shown in Figure 4-18 with the peaks evenly numbered. The time axis is oriented vertically with the positive direction downward. The time series is then viewed as a sequence of roofs with rain falling on them. The rain-flow paths are

defined according to the following rules (Wirsching and Shehata, 1977):

1. A rain flow is started at each peak and trough.
2. When a rain-flow path started at a trough comes to the tip of the roof, the flow stops if the opposite trough is more negative than that at the start of the path under consideration (e.g., path [1-8], path [9-10], etc.). A path started at a peak is stopped by a peak which is more positive than that at the start of the rain path (e.g. path [2-3], path [4-5], path [6-7], etc.).
3. If the rain flowing down a roof intercepts flow from a previous path, the present path is stopped (e.g. path [3-3a], path [5-5a], etc.).
4. A new path is not started until the path under consideration is stopped.

Half-cycles of trough-originated stress range magnitudes S_i are projected distances on the stress axis (e.g. [1-8], [3-3a], [5-5a], etc.). It should be noted that for sufficiently long time series, any trough-originated half-cycle will be followed by another peak-originated half-cycle of the same range. This is also the case for short stress histories if the stress history starts and ends at the same stress value.

The rain-flow method is not restricted to high-cycle fatigue but can also be used for low-cycle fatigue where strain range is the important parameter. Figure 4-18 shows a simple example. In this sequence, four events that resemble constant-amplitude cycling are recognised, 1-6-9, 2-3-3a, 4-5-6, and 7-8-8a. These events are closed hysteresis loops, and each event is associated with a strain range and a mean strain. Each closed hysteresis loop can therefore be compared with constant-amplitude data in order to calculate the accumulated damage.

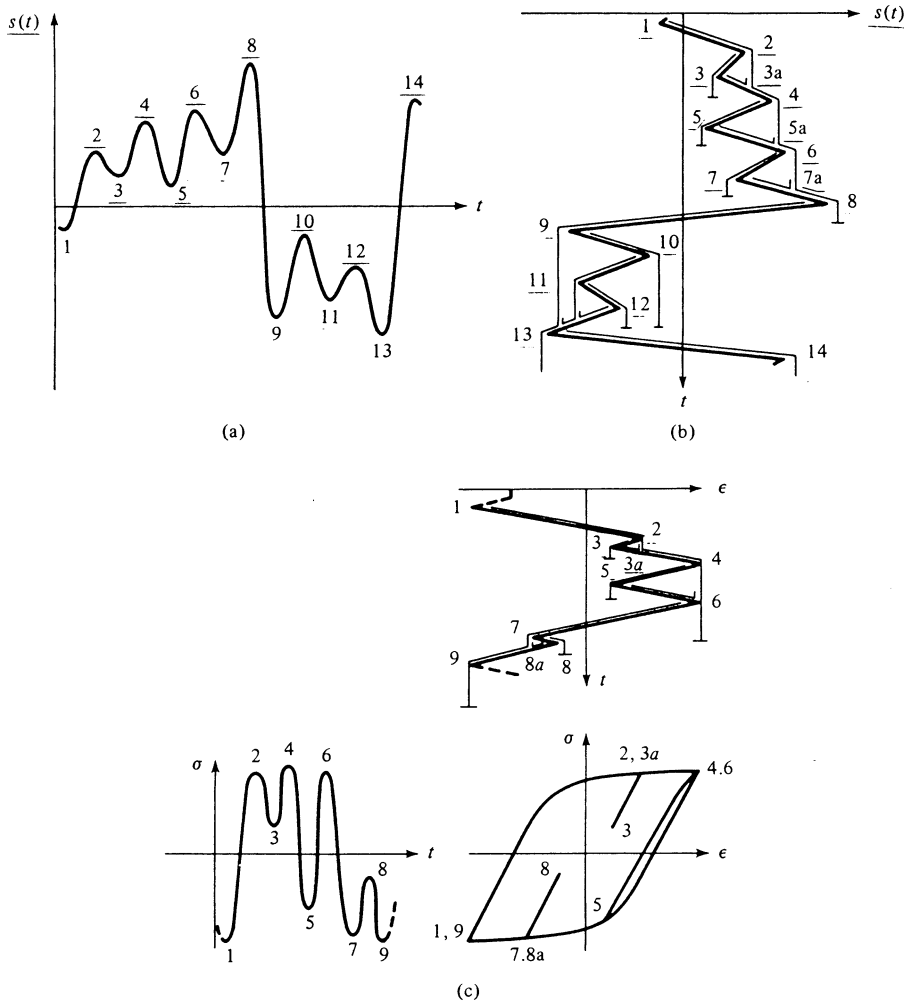


Figure 4-18. Illustration of the rain-flow counting method: (a), (b) application to a stress history, from Wirsching and Shehata (1977); (c) application to a low-cycle strain history, from Madsen et al. (1986).

In the rain-flow method small reversals are treated as interruptions of the larger ranges, and the rain-flow method also identifies a mean stress for each stress cycle. A comparison between test results and results predicted by the three mentioned cycle counting methods shows that the rain-flow counting method generally gives the best results. This method is the only one of the

three that identifies both slowly varying stress cycles and more rapid stress reversals on top of these. The peak counting method will in general assign larger probabilities to larger stress ranges, while the range counting method will assign larger probabilities to smaller stress ranges. Compared to the rain-flow counting method, the peak counting will therefore result in

larger estimates for the accumulated damage, while the range counting method will predict smaller values of the damage. Analytical results for the stress range distribution obtained through rain-flow counting are very difficult to obtain, and the method is generally used with measured or simulated stress histories only.

The rain-flow method identifies a mean stress for each stress cycle. An attractive representation of the resulting stress range distribution from cycle counting by the rain-flow method is therefore to form a matrix with one row for each mean stress level and one column for each stress range. Each element of this matrix will then contain the number of stress cycles associated with a particular stress range and a particular mean stress. Each row of the matrix will contain a discretised stress range distribution conditioned on a particular mean stress. When $S-N$ curves are available for various ratios R between the compressive stress amplitude and the tensile stress amplitude, this representation will allow for prediction of the partial damage in each element of the matrix by applying the appropriate $S-N$ curve for that element. The total fatigue damage D can subsequently be determined by summing up the partial damage over all elements in the matrix,

$$D = \sum_i \sum_j \frac{n_{ij}(S_j)}{N_{ij}(S_j)}$$

in which n_{ij} denotes the number of stress cycles in the matrix element corresponding to the j th stress range, S_j , and the i th mean stress, and N_{ij} is the number of stress cycles to failure in this element. Reference is made to Figure 4-19.

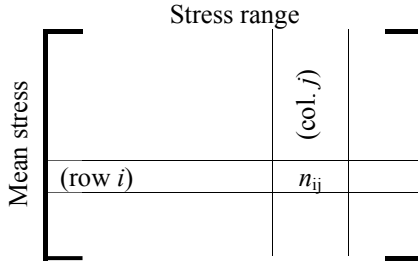


Figure 4-19. Matrix representation of rain-flow counted stress range distribution.

This approach is useful for damage predictions for structural materials, such as blade materials, for which a non-zero mean stress is of importance. For such materials, the dependency on the non-zero mean stress will not be adequately accounted for by a Miner’s sum model, which is based on only one single $S-N$ curve associated with full stress reversals about a zero mean stress.

Stress range distributions

To establish the stress range distributions for a structural component in a wind turbine, it is important to consider the various conditions that the turbine can be in. There are various operational conditions, including:

- production
- start at cut-in and start at cut-out
- stop at cut-in and stop at cut-out
- idling and standstill
- yaw misalignment

Start and stop are transient conditions, for which the stress distributions in the considered structural component are not easily determined. During production, stationary conditions can be assumed to prevail in the short term, e.g. during 10-minute periods. During a 10-minute period, the wind climate parameters such as the 10-minute mean wind speed U_{10} and the turbulence intensity I_T at the hub height can be assumed to be constant. During such short periods of stationary conditions, the load response processes that give rise to the stress ranges in the considered structural

component can be taken as stationary processes. Under stationary conditions, stress ranges are often seen to have distributions which are equal to or close to a Weibull distribution,

$$F_S(s) = 1 - \exp(-(s/S_A)^B)$$

Note that when the exponent B equals 1, this distribution turns into an exponential distribution, and when it equals 2 it becomes a Rayleigh distribution. For representation of stress range distributions, which are not quite Weibull distributions, it will often suffice to apply a somewhat distorted Weibull distribution. The simplest distribution model among this family of distributions is a three-parameter Weibull distribution,

$$F_S(s) = 1 - \exp(-((s-a)/S_A)^B)$$

Other models for moderate distortions of a parent Weibull distribution to form a parametric distribution model, which fits data well, exist (Ronold et al., 1999).

The coefficients a , B and S_A are distribution parameters, and they can often be expressed as functions of the wind climate parameters U_{10} and I_T . When the short-term stress range distributions, conditional on U_{10} and I_T have been established, when the long-term distributions of U_{10} and I_T are known as outlined in Section 3.1, and when the total number of stress cycles during the production life of the turbine is assessed, then the compound distribution of all stress ranges during this production life can be established. This compound distribution can itself often be represented by a Weibull distribution, and it can be represented as shown in Figure 4-20, where n denotes the number of stress cycles which exceed a stress range S during the production life. This distribution forms a significant contribution to the loads that cause fatigue damage. Note that if the curve in the semi-

logarithmic diagram in Figure 4-20 had been a straight line, the distribution would have been an exponential distribution, which is a special case of the Weibull distribution.

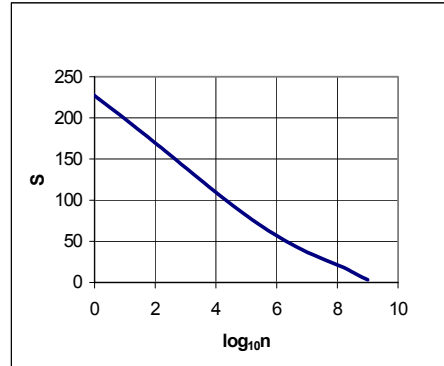


Figure 4-20. Example of compound stress distribution, a so-called load spectrum.

To obtain the distribution of all fatigue loads in the design life, this compound distribution has to be supplemented by the stress ranges owing to start, stop, standstill, idling, and yaw misalignment, to the extent that these are considered to contribute to the cumulative fatigue damage.

For this purpose, information about the duty cycle of the turbine is essential. The duty cycle is a repetitive period of operation, which is characterised by a typical succession and duration of different modes of operation. The duty cycle can be specified by a sequence of parameters, which define the mode of operation for consecutive 10-minute periods for a representative time span. Information about the duty cycle should as a minimum contain the number of starts and stops during the time span, which the duty cycle covers, together with the wind climate parameters in this time span.

Starting the wind turbine is considered to be potentially critical with respect to fatigue. One reason for this is that connection of an electric generator to the grid can cause high

transient loads in the drive train and the rotor blades. It is recommended to distinguish between start at the cut-in wind speed and start slightly below the cut-out wind speed.

When stopping the wind turbine, it is recommended to distinguish between stopping slightly below the cut-in wind speed and stopping at the cut-out wind speed, as the latter is associated with rather large aerodynamic loads.

For standstill and idling below the cut-in wind speed, loads are considered insignificant with respect to fatigue.

Yaw misalignment can be critical with respect to fatigue.

Note that stresses in a particular location of the wind turbine structure, considered critical with respect to fatigue, may be due to a combination of stresses arising from different sources or load processes. When the stress levels are sufficiently low, elastic material behaviour can be assumed for the combination of the stresses before fatigue damage calculations are carried out. It can further – somewhat conservatively – be assumed that load peaks of two load processes occur simultaneously, and that high-amplitude cycles can be combined with high-amplitude cycles. Mean values of two load processes should be combined in the most unfavourable manner to produce the largest mean stress value. For more details on how to combine load spectra, see IEA (1990).

Equivalent loads

Once the load spectrum has been established with contributions from all operational modes over the design life of the wind turbine, it is often convenient to define a so-called damage-equivalent load range S_0 to be used with an equivalent number of cycles

n_{eq} . This is a constant load range S_0 , which in n_{eq} cycles will lead to the same accumulated damage as the true load spectrum that consists of many different load ranges S_i and their corresponding cycle numbers n_i . When the equivalent number of cycles n_{eq} is chosen or specified, the equivalent load range S_0 can be found as

$$S_0 = \left(\frac{\sum_i n_i S_i^m}{n_{eq}} \right)^{1/m}$$

in which m denotes the S - N curve slope of the material in question. This definition of a damage-equivalent load range is well-known in fatigue analysis and is often used in wind turbine load analysis. An example of application can be found in Stiesdal (1991). Note that the equivalent load concept only applies to materials whose S - N curves are described by one slope m , i.e. it can-not be used for materials with bilinear S - N curves.

Uncertainties

Load spectra are usually not known with certainty, but are predicted, e.g. from a limited number of time series of load response, obtained by simulation according to some aeroelastic analysis scheme. Time series of 10-minute duration are usually used for this purpose, and one estimate of the equivalent load range can be obtained from each simulated time series. For a given wind climate (U_{10}, I_T) , the uncertainty in the estimated equivalent load range can be expressed in terms of the coefficient of variance (COV) of the estimate. COV can be expected to be proportional to $1/\sqrt{NT}$, where N is the number of simulated time series for the given wind climate, and T is the duration of the simulated time series, e.g. 10 minutes.

Consider now lifetime load spectra and corresponding equivalent life time load

ranges. Time series of load response are simulated for various wind climates. Compound lifetime load spectra are established on this basis by appropriate weighting according to the long-term distribution of the wind climate parameters. In this way, a total of n simulated lifetime load spectra are established, and one equivalent load range S_{0i} is interpreted from each such simulated lifetime load spectrum. The central estimate of the equivalent lifetime load range is taken as the arithmetic mean

$$\bar{S}_0 = \frac{1}{n} \sum_{i=1}^n S_{0i}$$

The standard deviation of the S_{0i} 's is estimated by

$$s = \sqrt{\frac{1}{n-1} \sum_{i=1}^n (S_{0i} - \bar{S}_0)^2}$$

A Gaussian assumption can usually be made for the simulated equivalent load ranges S_{0i} . On this background, a two-sided confidence interval for the estimated equivalent load range with confidence $1-\alpha$ can be established as

$$\bar{S}_0 \pm \frac{s}{\sqrt{n}} t_{1-\frac{\alpha}{2}, n-1}$$

in which $t_{1-\alpha/2, n-1}$ is the $1-\alpha/2$ quantile in the Student's t distribution with $n-1$ degrees of freedom. Table 4-4 tabulates these quantiles for selected degree-of-freedom values for a couple of common choices for the confidence $1-\alpha$. Quantiles of the Student's t distribution can, in general, be found in most published tables of statistical distributions.

Degrees of freedom, $n-1$	$t_{1-\frac{\alpha}{2}, n-1}$	
	Confidence $1-\alpha$ 0.90	Confidence $1-\alpha$ 0.95
1	6.31	12.71
2	2.92	4.30
3	2.35	3.18
5	2.02	2.57
10	1.81	2.23
20	1.72	2.09
50	1.68	2.01
∞	1.64	1.96

4.4.2 Ultimate loads

Extreme value distributions are of interest when extreme load responses are needed such as for design against failure in ultimate loading. Reference is usually made to a particular load case, e.g.:

- normal operation at a 10-minute mean wind speed near the cut-out wind speed
- standstill at a rare 10-minute mean wind speed such as the one with a 50-year recurrence period
- faulty operation at a high wind speed due to error in the protection system

For the considered load case, it is assumed that a total of n 10-minute time series of the load response X has been generated by aeroelastic simulations. The following quantities associated with the load response X can be interpreted from each of the n time series:

- mean value μ
- standard deviation σ
- skewness α_3
- kurtosis α_4
- rate v_μ of upcrossings of level μ
- maximum x_m in 10 minutes

The maximum value X_m of the load response X in the 10 minutes is of interest. The maximum value will not be a fixed value, but will have a natural variability, which can

be represented by a probability distribution. The natural variability is reflected in terms of different values for x_m in the n simulated time series. The mean value of the maximum load response in 10 minutes is denoted μ_m , and the standard deviation is denoted σ_m . For design purposes, the characteristic load response is usually taken as some quantile of the distribution of the maximum load response in 10 minutes.

There are two fundamentally different approaches to predicting the maximum load response and particular quantiles of its distribution:

- statistical model, which utilises the information about the maximum load response obtained from the n simulated time series in terms of n simulated maximum values x_m
- semi-analytical model, which – based on stochastic process theory – utilises the information about the underlying load response process in terms of the four statistical moments μ , σ , α_3 and α_4 , and the crossing rate ν_μ .

The two approaches are presented in the following sections, and their levels of accuracy is discussed.

Statistical model

The maximum load response X_m in 10 minutes can be assumed asymptotically to follow a Gumbel distribution

$$F_{x_m}(x_m) = \exp(-\exp(-\alpha(x_m - \beta)))$$

in which α is a scale parameter and β is a location parameter. From the n simulated time series there are n observations of the maximum load response X_m . For estimation of α and β , the n values of X_m are ranked in increasing order, $x_{m,1}, \dots, x_{m,n}$. Two coefficients b_0 and b_1 are calculated from the data

$$b_0 = \frac{1}{n} \sum_{r=1}^n x_r \quad \text{and} \quad b_1 = \frac{1}{n} \sum_{r=1}^n \frac{r-1}{n-1} x_r$$

and α and β are estimated by

$$\hat{\alpha} = \frac{\ln 2}{2b_1 - b_0} \quad \text{and} \quad \hat{\beta} = b_0 - \frac{\gamma_E}{\hat{\alpha}}$$

in which $\gamma_E = 0.57722$ is Euler's constant.

The mean value and standard deviation of X_m are estimated by

$$\hat{\mu}_m = \hat{\beta} + \frac{\gamma_E}{\hat{\alpha}} \quad \text{and} \quad \hat{\sigma}_m = \frac{\pi}{\hat{\alpha}\sqrt{6}}$$

respectively.

The θ -quantile in the distribution of X_m can be estimated by

$$\hat{x}_{m,\theta} = \hat{\mu}_m + k_\theta \hat{\sigma}_m$$

in which

$$k_\theta = \frac{\sqrt{6}}{\pi} (-\ln(\ln(\frac{1}{\theta})) - \gamma_E)$$

The standard error in the estimate of the θ -quantile is estimated by

$$se(\hat{x}_{m,\theta}) = \frac{\hat{\sigma}_m}{\sqrt{n}} \sqrt{1 + 1.14k_\theta + 1.1k_\theta^2}$$

This reduces to

$$se(\hat{\mu}_m) = \frac{\hat{\sigma}_m}{\sqrt{n}}$$

for the special case that the θ -quantile is replaced by the mean value μ_m .

Assuming a normal distribution for the estimate of the θ -quantile, the two-sided

confidence interval for the θ -quantile with confidence $1-\alpha$ becomes

$$\hat{x}_{m,\theta} \pm t_{1-\frac{\alpha}{2},n-1} \cdot se(\hat{x}_{m,\theta})$$

in which $t_{1-\alpha/2,n-1}$ is the $1-\alpha/2$ quantile in the Student's t distribution with $n-1$ degrees of freedom. When a characteristic value with a specified confidence is aimed for, it is usually taken as the upper confidence limit, i.e. a one-sided confidence interval is considered. The characteristic value with confidence $1-\alpha$ then becomes

$$\hat{x}_{m,\theta} + t_{1-\alpha,n-1} \cdot se(\hat{x}_{m,\theta})$$

Note that a high number of simulations n may be necessary to achieve a sufficiently accurate estimate of $x_{m,\theta}$ or μ_m .

Example

Consider a load response process X whose extreme value X_{\max} in 10 minutes has been estimated on the basis of $n = 5$ simulated 10-minute time series. The following estimates pertaining to the extreme value distribution have resulted:

$$\hat{\alpha} = 3.69, \hat{\beta} = 3.87, \hat{\mu}_m = 4.02, \hat{\sigma}_m = 0.35.$$

An estimate of the $\theta = 95\%$ quantile of X_{\max} with $1-\alpha = 95\%$ confidence is sought. This gives $k_\theta = 1.866$. The central estimate of the 95% quantile of X_{\max} is

$$\hat{x}_{m,95\%} = 4.02 + 1.866 \cdot 0.35 = 4.673.$$

The standard error in this estimate is

$$se(\hat{x}_{m,95\%}) = \frac{0.35}{\sqrt{5}} \cdot 2.64 = 0.413.$$

The pertinent quantile in the Student's t distribution is $t_{1-\alpha/2,n-1} = 2.78$, and the two-

sided confidence interval for $x_{m,95\%}$ becomes $4.673 \pm 2.78 \cdot 0.413 = 4.673 \pm 1.148$. This indicates a rather wide interval about the central estimate. If n is changed from 5 to 100, the interval is narrowed considerably to 4.673 ± 0.183 .

Semi-analytical model

The semi-analytical model owing to Davenport (1961) utilises more information about the n 10-minute time series of the load response than just the n maximum response values x_m . The load response X can be viewed as a stochastic process during the 10-minute series. The process X can be considered as a quadratic transformation of a parent standard Gaussian process U ,

$$X = \zeta + \eta(U + \varepsilon U^2), \quad \varepsilon \ll 1$$

A first-order approximation gives the following expressions for the coefficients

$$\begin{aligned} \varepsilon &= \frac{\alpha_3}{6} \\ \eta &= \sigma \\ \zeta &= \mu - \varepsilon \sigma \end{aligned}$$

from which it appears that use is made of the mean value μ , the standard deviation σ and the skewness α_3 of the load response process X .

The mean value and standard deviation of X_m are estimated by

$$\begin{aligned} \hat{\mu}_m &= \eta + \zeta (\sqrt{2 \ln(\nu_\mu T)}) \\ &+ \varepsilon 2 \ln(\nu_\mu T) \\ &+ \frac{\gamma_\varepsilon \zeta (1 + 2\varepsilon \sqrt{2 \ln(\nu_\mu T)})}{\sqrt{2 \ln(\nu_\mu T)}} \end{aligned}$$

and

$$\hat{\sigma}_m = \frac{\pi\eta}{\sqrt{6}} \frac{1 + 2\varepsilon\sqrt{2\ln(v_\mu T)}}{\sqrt{2\ln(v_\mu T)}}$$

respectively, where T denotes duration and is usually the length of a simulated time series, i.e. $T = 10$ minutes. Corresponding estimates of the Gumbel distribution parameters α and β can be found as

$$\hat{\alpha} = \frac{\pi}{\hat{\sigma}_m \sqrt{6}}$$

$$\hat{\beta} = \hat{\mu}_m - \frac{\gamma_E}{\hat{\alpha}}$$

The standard error in the mean value estimate $\hat{\mu}_m$ is

$$se(\hat{\mu}_m) = \frac{\hat{\sigma}_m}{\sqrt{n}}$$

where n is the sample size, i.e. the number of 10-minute series available for the estimation of μ_m by the above formula. When σ_m can be considered well-determined by the above formula for $\hat{\sigma}_m$, the two-sided confidence interval for μ_m with confidence $1-\alpha$ becomes

$$\hat{\mu}_m \pm u_{1-\frac{\alpha}{2}} \cdot \frac{\hat{\sigma}_m}{\sqrt{n}}$$

in which $u_{1-\alpha/2}$ is the $1-\alpha/2$ quantile of the standard normal distribution function.

Comparison and recommendations

The semi-analytical results will usually provide a higher accuracy of the extreme value estimates than the statistical results. This comes about because the semi-analytical results utilise much more of the available information than the statistical results do. In other words, a smaller sample size n is required to achieve the same

accuracy when semi-analytical results are used for the extreme value estimates than when only statistical results for the extreme values are used. It is recommended always to predict extreme loads by means of the semi-analytical method, based on the statistics of the simulated load response process, rather than using the observed maximum values only.

Two or more arbitrarily selected simulated 10-minute time series may give considerably different extreme values. This implies that the practice of performing a few simulations and selecting the average extreme load or the largest extreme load as the ultimate load without proper consideration of the stochastic nature of the extremes will not give reproducible results. Further, the results cannot be extrapolated to a characteristic value defined by a quantile or to a different duration of the load case than 10 minutes. The semi-analytical approach takes the stochastic nature of the extremes into account and provides a rationale for analysis of extreme loads from simulated time series of load responses.

As an alternative to the presented quadratic transformation of the parent Gaussian process U to the physical load response process X , a cubic transformation can be applied. This can be made according to a fourth-moment Hermite polynomial expansion as described by Winterstein (1988). This will also allow for representation of the load response process in terms of the kurtosis α_4 .

It is not recommended to consider transformations, which involve higher-order statistical moments of the load response X . This is due to the fact that the lengths of available time series of the load response are usually much too short to allow for a sufficiently accurate estimation of such higher-order statistical moments. In other

words, higher-order moment estimates based on available simulated time series of load response can usually not be trusted.

Correction for periodic loads

The presented semi-analytical model provides good accuracy for prediction of extreme values for wind turbines, which are not in operation. For the operating load cases, the periodic nature of the response mean and standard deviation for some loads must be accounted for. A method, based on azimuthal binning, can be used for this purpose. By such a method, the rotor disc is divided into a number of sectors, each identified by its azimuth angle. When the rotor disc is discretised into M sectors of an equal angle of aperture, sector-specific mean values and standard deviations of the load response process can be established as

$$\mu_i = \mu \left(\frac{2\pi}{M} \left(i - \frac{1}{2} \right) \right)$$

and

$$\sigma_i = \sigma \left(\frac{2\pi}{M} \left(i - \frac{1}{2} \right) \right)$$

in which μ and σ are the mean value and standard deviation, respectively, of the load response X . Let α and β denote the distribution parameters in the Gumbel distribution of the maximum value during the time T of the normalised process $(X-\mu)/\sigma$. They can be determined by the analytical model as described above. The lower bounds of the mean value μ_m of the largest extreme X_{\max} of X in all sectors during the time T are

$$\hat{\mu}_{m,lower} = \max \left\{ \mu_i + \sigma_i \left(\beta - \frac{\ln M - \gamma_E}{\alpha} \right) \right\}$$

The upper bounds of the mean value μ_m of the largest extreme X_{\max} of X in all sectors during the time T are

$$\hat{\mu}_{m,upper} = \max \left\{ \mu_i + \sigma_i \left(\beta + \frac{\gamma_E}{\alpha} \right) \right\}$$

More details about this method can be found in Madsen et al. (1999). A recommended value for discretisation of the rotor disc into sectors is $M = 36$.

4.5 Simplified load calculations

4.5.1 Parametrised empirical models

Various simplified models for load calculation exist and are presented in the following subsections. Today, where available computer resources usually do not prohibit execution of computer-intensive calculations, most load calculations for wind turbines are carried out by means of aeroelastic codes. The simplified models are therefore included mainly for historical reasons and to provide tools for preliminary calculations and quick verification of results.

4.5.2 The simple load basis

Based on a systematisation of measurements and experience from typical stall-regulated wind turbines with active yaw and approximately constant rotor speed, a simplified method for calculation of wind turbine loads has been established. The method is useful for preliminary design of wind turbines with rotor diameters between 5 and 25 m and with rotor speeds between 35 and 50 m/s.

The method is based on the following three load quantities:

- a static horizontal airflow load $F_0 = 300A$, where F_0 is in units of N, $A = \pi R^2$ is the swept area of the rotor, and R is the rotor radius in units of m.

- a driving torque $M_{e,nom} = P_{nom}/(2\pi n_r \eta)$, where P_{nom} is the nominal power of the wind turbine, n_r is the rotor frequency, and η is the nominal efficiency, usually $\eta \leq 0.9$.
- the weight of the rotor mg , where m is the rotor mass and g is the acceleration of gravity

The rotor loads are expressed in terms of these three quantities as summarised in Table 4-5. Moments are based on the assumption that the airflow load F_0 is applied with an eccentricity $e = R/6$.

For calculation of blade loads, it is assumed that the airflow load is distributed evenly between the N_V blades, such that the flapwise airflow load on one blade becomes

Load component	Sym- bol	Static load	Dynamic load amplitude
Horizontal force in rotor plane	F_X	0	0
Moment about horizontal axis in rotor plane	M_X	eF_0	$0.25eF_0$
Horizontal force along rotor axis	F_Y	F_0	$0.25F_0$
Moment about rotor axis	M_Y	$1.3M_{e,nom}$	$0.25 \cdot 1.3M_{e,nom}$
Vertical force	F_Z	$-mg$	0
Moment about vertical axis	M_Z	eF_0	$0.25eF_0$

$$P_V = F_0/N_V$$

This load is assumed to be the resultant of a triangular-shaped flapwise line load along the blade with the maximum value occurring at the blade tip.

For calculation of blade loads in the rotor plane, i.e. edgewise blade loads for the individual blades, the gravity loads need to be considered. For calculation of effects on machinery and tower, the dynamic load amplitudes given in Table 4-5 may be

reduced by 33%. For design of the main shaft, a torque from the mechanical brake of two times the value of M_Y is to be assumed.

The design loads given here are compatible with the Danish codes. Thus, when applied for design purposes, they need to be checked against design capacities calculated according to the Danish codes.

4.5.3 Quasi-static method

The quasi-static method presented in the following gives simple expressions for four different design loads as derived for a still-standing wind turbine in rather severe wind conditions: the blade load is calculated for a vertical blade above the hub. The root moment is used as the design tilt moment. The axial force is determined by summing the wind load over the blades. The yaw moment is determined as the root moment from a horizontal blade.

By the quasi-static method, the load per unit length of the blade is calculated by

$$p(r) = \frac{1}{2} \psi \rho U_{10}^2 D(r) C$$

in which C is the maximum value of the lift coefficient C_L or the drag coefficient C_D . Typical maximum values of C_L and C_D are in the range 1.3-1.5. U_{10} is the 10-minute mean wind speed with a recurrence period of fifty years at a height h . The height h and the coefficient C are given in Table 4-6, depending on which design load is to be calculated. ρ is the density of air, and $D(r)$ is the chord length of the blade at distance r from the hub.

The quasi-static gust factor ψ in the load expression is to be calculated as

$$\psi = \begin{cases} \left(\frac{\ln(\frac{z}{z_0}) + 3.1}{\ln(\frac{z}{z_0})} \right)^2 & \text{for } \frac{n_0 L}{U_{10}} > n^* \\ 1 + 3.9 \frac{2\sqrt{k_b + k_r}}{\ln(\frac{z}{z_0})} & \text{for } \frac{n_0 L}{U_{10}} \leq n^* \end{cases}$$

z hub height
 z_0 roughness length
 L rotor radius
 n^* given in Table 4-6
 n_0 eigenfrequency of the vibration mode associated with the particular design load which is to be calculated

Table 4-6. Quasi-static load specification parameters.

Load	Eigenfrequency n_0 corresponding to	Threshold n^*	C	Height h
Blade load	Blade flapwise bending	1.7	$C_{L,max}$	$z + \frac{2}{3} L$
Axial force	Tower bending	0.45	$C_{D,max}$	z
Tilt moment	Blade flapwise bending	1.7	$C_{L,max}$	$z + \frac{2}{3} L$
Yaw moment	N/A	0	$C_{D,max}$	z

Moreover, the background turbulence effect k_b in the expression for ψ is approximated by

$$k_b = \begin{cases} 0.9 - 2.5 \frac{L}{\ell} & \text{for blade load} \\ 0.75 - 3 \frac{L}{\ell} & \text{for axial force} \end{cases}$$

and the resonance effect k_r in the same expression is given by

$$k_r = \frac{\frac{n_0 \ell}{U_{10}}}{(1 + 1.5 \frac{n_0 \ell}{U_{10}})^{5/3}} F(n_0) \frac{\pi^2}{2\delta}$$

Here, $\ell = 6.8L_u$, in which L_u is the integral length scale of the Kaimal spectrum, see Section 3.1.5. $\delta = 2\pi(\zeta_0 + \zeta_a)$ is the logarithmic increment of damping expressed in terms of the structural damping ratio ζ_0 and the aerodynamic damping ratio ζ_a . $F(n)$ is the aerodynamic admittance function

whose value depends on which design load is being considered

$$F(n) = \begin{cases} \frac{1}{1 + 3 \frac{nL}{U_{10}}} & \text{for blade load} \\ \frac{1}{1 + 12 \frac{nL}{U_{10}}} & \text{for axial force} \\ \frac{2.7 \frac{nL}{U_{10}}}{1 + 4.4 \frac{nL}{U_{10}} + 21.8 (\frac{nL}{U_{10}})^2} & \left\{ \begin{array}{l} \text{for rotor} \\ \text{moments} \end{array} \right. \end{cases}$$

4.5.4 Peak factor approach for extreme loads

Extreme loads are often specified in terms of the load which has a certain recurrence period, such as fifty years, i.e. the load that on average will be exceeded once every fifty years. Two approaches are presented here.

Peak-over-threshold method

By the so-called peak-over-threshold method, the load with a recurrence period T can be estimated by

$$q_T = q_0 + \alpha \ln(\lambda T)$$

in which q_0 is some chosen threshold for the load q , λ is the mean rate of exceedances of the threshold q_0 by the load q , and α is the mean value of the exceedances $\Delta q = q - q_0$.

Periodical maximum method

The distribution of the maximum load in a period of specified duration such as one year can be assumed to be a Gumbel distribution

$$F(q) = \exp(-\exp(-\alpha(q-\beta)))$$

When the distribution parameters α and β refer to the distribution of the maximum load in one year, the load with the recurrence period T years can be estimated by

$$q_T = \beta - \frac{1}{\alpha} \ln\left(\ln\frac{T}{T-1}\right) \approx \beta + \frac{1}{\alpha} \ln T$$

4.5.5 Parametrised load spectra

Parametrised load spectra are useful for calculations where not only the extreme load is of interest, but also the entire load distribution, such as for design against fatigue failure. Parametrised load spectra are simplified and idealised load distributions expressed in terms of a number of characteristic parameters.

A useful parametrised load spectrum is the one which is presented in DS472. This load spectrum is meant for calculation of blade loads and is based on the characteristic aerodynamic line load p_0 . The value of p_0 can be calculated as

$$p_0 = \frac{1}{2} \rho W^2 c C_L$$

$$W^2 = \left(\frac{4\pi}{3} n_r R\right)^2 + V_0^2$$

- ρ density of air
- c characteristic chord length of the blade at a distance $r = 2/3R$
- C_L lift coefficient at a distance $r = 2/3R$
- W resulting wind speed
- n_r rotor frequency
- R rotor radius
- V_0 nominal stall wind speed at the height of the hub

V_0 is defined as the minor of the following two wind speeds:

- the nominal 10-minute mean wind speed V_{nom} at which the turbine reaches its nominal power P_{nom}
- the 10-minute mean wind speed at which stall just extends to the entire blade for airflow parallel to the rotor shaft

The load distribution along the blade is represented as a triangular line load whose value is 0 at the hub and p_0 at the blade tip a distance R away from the hub, such that the value of the line load at a distance r from the hub can be calculated as

$$p = \frac{p_0 r}{R}$$

and such that the resulting bending moment at the blade root becomes

$$M_{root} = p_0 \frac{R^2}{3}$$

For fatigue calculations, loads are, in general, represented by some mean load, which is superimposed by some cyclically varying load. The cyclically varying load is

considered in the following. The load ranges F_{Δ} of the cyclically varying load are represented by a probability distribution. This probability distribution is expressed such that $F_{\Delta}(N)$ is the load range which is exceeded N times during the design life of the wind turbine.

The cyclically varying load consists of a deterministic part owing to gravity loads and a stochastic part owing to aerodynamic loads. The cyclically varying deterministic load appears for example as a cyclically varying edgewise bending moment at the blade root and results from the rotation of the blades about the hub. The corresponding load range distribution consists of load ranges of constant magnitude, and their number is equal to the total number of rotations N_R of the rotor during the design life. The constant magnitude load range of this deterministic load will typically be a function of the mass m per unit length of the rotor blade and of the acceleration g of gravity.

The cyclically varying stochastic load appears for example as a cyclically varying flapwise bending moment at the blade root and results from the airflow forces set up on the blades by the wind. The corresponding load range distribution is represented by a generic standardised distribution, whose unitless range values F_{Δ}^* are to be multiplied by a design constant, which depends on load type and direction, to give the sought-after load range F_{Δ} .

According to DS472, the generic standardised load range distribution to be used for the stochastic load ranges is given by the following expression

$$F_{\Delta}^*(N) = \beta(\log_{10}(N_F) - \log_{10}(N)) + 0.18$$

with the additional condition $F_{\Delta}^*(N) \leq 2k_{\beta}$

in which

$$\beta = 0.11k_{\beta}(I_T + 0.1)(A + 4.4)$$

I_T is the characteristic turbulence intensity at the hub height according to the formula in DS472, see Sections 3.1.2 and 3.1.3. Note that this generic standardised load range distribution is valid for rotor diameters less than 25 m. Application to larger rotor diameters may lead to overconservative results.

In general, $k_{\beta} = 1$ such as for loads on individual blades, however $k_{\beta} = 2.5$ for calculation of rotor pressure from all three blades.

$$N_F = n_C T_L (\exp(-(V_{\min}/A)^k) - \exp(-(V_{\max}/A)^k))$$

is the number of load ranges in the design life T_L of the turbine corresponding to a characteristic load frequency n_C .

A and k are scale and shape parameters, respectively, in the long-term Weibull distribution of the 10-minute mean wind speed U_{10} , see Section 3.1.1.

V_{\min} and V_{\max} are cut-in and cut-out wind speeds, respectively, for the operation of the wind turbine, see Section 2.2.

For combination of deterministic loads, a harmonic variation with time can be assumed, and the following formula can be used, based on the assumption that the blade is vertical at time $t = 0$:

$$p(t) = \bar{p} + \frac{1}{2} p_{\Delta C} \cos(2\pi n_C t) + \frac{1}{2} p_{\Delta S} \sin(2\pi n_C t)$$

where p may denote, for example, line load for blades. \bar{p} is then the mean line load,

and $p_{\Delta C}$ and $p_{\Delta S}$ are load ranges for cosinusoidal and sinusoidal load components, respectively.

The characteristic frequency n_C to be used is also indicated and expressed in terms of the rotor frequency n_R .

For combination of deterministic load ranges and stochastic load ranges, it is recommended, conservatively, to simply add the load range values from the two distributions. The largest deterministic load range value is then added to the largest stochastic load range value, the second-largest deterministic load range value is added to the second largest stochastic load range value, and so on, until all load range values of the two distributions have been combined to form the combined distribution. An example of such a combination of a deterministic and stochastic load range distribution is given in Figure 4-21 for the edgewise line load on a rotor blade.

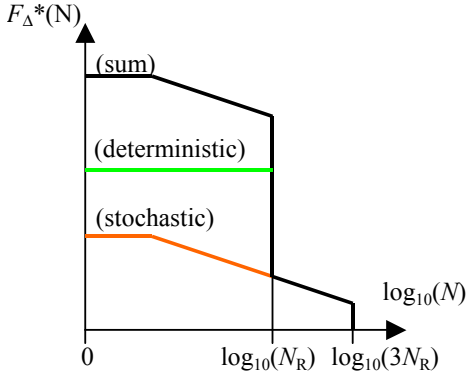


Figure 4-21. Standardised distribution.

Table 4-7 gives expressions for deterministic and stochastic load components for line loads for rotor blades.

Rotor loads

Rotor loads are expressed as the sum of a deterministic mean load and a harmonically varying load with stochastic range.

Table 4-7. Line load on rotor blade.

Direction	Mean	Load range distributions		
		Deterministic	Stochastic	
	\bar{p}	$p_{\Delta C}$	$p_{\Delta S}$	$p_{\Delta, stochastic}$
Edgewise	$2M_{nom}/(3R^2)$	0	$+2mg$	$0.3F_{\Delta}^*(N)p_0$
Flapwise	$1.5p_0r/R$	0	0	$F_{\Delta}^*(N)p_0r/R$
Along blade	$(2\pi n_R)^2 mr$	$-2mg$	0	0
Frequency n_C		n_R	n_R	$3n_R$

Load component	Symbol	Deterministic mean \bar{F}	Stochastic load range F_{Δ}	Frequency n_C	Lowest resonance frequency n_0 (oscillation form)
Horizontal force in rotor plane	F_X	0	0		
Moment about horizontal axis in rotor plane	M_X	0	$0.33F_{\Delta}^*(N)k_R p_0 R^2$	$3n_R$	n_{ROTOR} (rotor, tilt, asymm.)
Horizontal force along rotor axis	F_Y	$1.5p_0 R$	$0.5F_{\Delta}^*(N)p_0 R$	$3n_R$	n_{TOWER} (tower, bending)
Moment about rotor axis	M_Y	$0.5M_{\text{nom}}$	$0.45F_{\Delta}^*(N)p_0 R^2$	$3n_R$	
Vertical force	F_Z	$-Mg$	0		
Moment about vertical axis	M_Z	0	$0.33F_{\Delta}^*(N)k_R p_0 R^2$	$3n_R$	n_{ROTOR} (rotor, yaw, asymm.)

$$F = \bar{F} + \frac{1}{2} F_{\Delta} \cos(2\pi n_C t)$$

t time
 n_C frequency

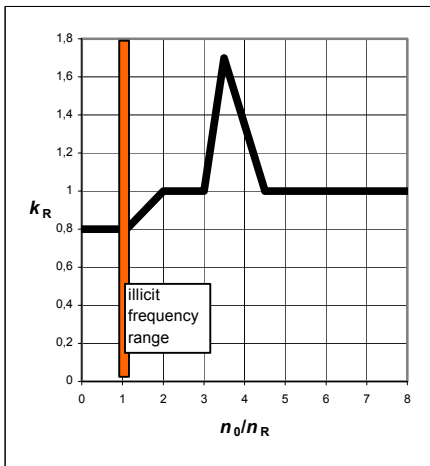


Figure 4-22. Amplification factor k_R vs. frequency ratio n_0/n_R .

Table 4-8 gives expressions for deterministic and stochastic load components for rotor loads. The expressions are based on the blade line load p_0 , the nominal torque M_{nom} , the rotor mass M , and the standardised load

range distribution given in terms of $F_{\Delta}^*(N)$ as outlined above. Some of the expressions include a correction factor k_R that accounts for amplification effects, which are a function of the ratio between the resonance frequency n_0 and the rotor frequency n_R . The correction factor k_R is given in Figure 4-22. The resonance frequency n_0 is the lowest resonance frequency for the associated oscillation form, i.e. n_{TOWER} for towers in bending and n_{ROTOR} for the collective asymmetric rotor oscillation at standstill, where one blade oscillates out of phase with the two other blades.

4.6 Site-specific design loads

As part of a scheme to reduce the cost of produced energy, site-specific characteristics can be included directly in the design process of wind turbines. The idea is to optimise the wind turbine design by minimising the cost of produced energy, given the characteristics at a particular site. Extreme loads and fatigue loads on a wind turbine are site-dependent. Site-specific design loads will therefore form part of such a cost-optimal design process.

Two approaches to site-specific designs are envisaged:

- adaptation of existing wind turbine designs to specific site by minor adjustments
- design from scratch

Site-specific design has a potential whenever wind turbines are to be installed in complex terrain such as in mountainous areas, where special conditions may prevail, or for large offshore wind farms where a large number of identical turbines are to be installed at the same site. It can be used to verify that all relevant load cases have been considered.

Using site-specific design loads and carrying out site-specific wind turbine designs is somewhat in contrast with the current trend within the wind turbine industry. In order to keep down manufacturing costs, the current trend is not to site-optimize wind turbines, but rather to produce a selection of standard wind turbines. The task is then to choose a standard wind turbine from this selection and verify that it is suitable for a given location. The tower and the foundation may still be site-optimized if desirable, and site-specific loads will be required for this purpose. The foundation design will always have to be site-specific in that it needs to be designed for the prevailing local soil conditions.

Reference is made to Section 3.1.10 on the subject of site assessment.

4.7 Loads from other sources than wind

Installation of wind turbines in shallow waters of up to 15 m water depth can be foreseen. A support structure or foundation structure is used for transfer of loads from the wind turbine and its tower to the supporting soils at the seabed. The

foundation structure will be exposed to wave loads, current loads and ice loads. The prediction of wave loads is dealt with in the following. A brief introduction to current loads and ice loads is also given.

4.7.1 Wave loads

Wave climate

Usually, the wave climate at a location can be considered stationary within periods of typically three hours duration. The wave climate is represented by the significant wave height H_S and the peak period T_P . The significant wave height H_S is a measure of the intensity of the wave climate and is defined as four times the standard deviation of the sea elevation process η . Some sources define the significant wave height as the average of the highest one third of the wave heights. For a narrow-banded Gaussian sea elevation process, the two definitions converge. The peak period T_P is related to the mean zero-crossing period of the sea elevation process. The significant wave height and the peak period can be taken as constant within each three-hour period.

Long-term distributions of H_S and T_P are site-dependent. The long-term distribution of H_S can often be represented well by a Weibull distribution, whereas the distribution of T_P conditioned on H_S is usually well-represented by a lognormal distribution whose distribution parameters are functions of H_S . Examples can be found in Bitner-Gregersen and Hagen (2000).

Wave spectrum

The frequency content of the sea elevation process can be represented by the power spectral density. The spectral density of the sea elevation process can be represented by the JONSWAP spectrum

$$S_{\eta}(\omega) = \frac{5}{32\pi} H_s^2 T_p \left(\frac{\omega T_p}{2\pi} \right)^{-5} \cdot \exp\left(-\frac{5}{4} \left(\frac{\omega T_p}{2\pi} \right)^{-4}\right) \cdot C(\gamma) \gamma^{\exp\left(\frac{1}{2\sigma^2} \left(\frac{\omega T_p}{2\pi} - 1 \right)^2\right)}$$

$$C(\gamma) = 1 - 0.287 \cdot \ln \gamma$$

$$\sigma = 0.07 \text{ for } 0 < \omega < 2\pi/T_p$$

$$\sigma = 0.09 \text{ for } \omega > 2\pi/T_p$$

The peak-enhancement factor γ can be taken as

$$\gamma = \exp(5.75 - 1.15 \frac{T_p}{\sqrt{H_s}}); \quad 3.6 \leq \frac{T_p}{\sqrt{H_s}} \leq 5$$

in which H_s is in metres and T_p in seconds. The following approximate relationship exists between the peak period T_p and the zero-crossing period T_z

$$T_z = T_p \sqrt{\frac{5 + \gamma}{11 + \gamma}}$$

Reference is made to Gran (1992) and DNV (2000).

Wave heights

In deep waters, the sea elevation process η is a Gaussian process, and the individual wave heights H , measured from trough to crest, will follow a Rayleigh distribution when H_s is given

$$F_H(h) = 1 - \exp\left(-\frac{2h^2}{(1 - \nu^2)H_s^2}\right)$$

ν spectral width parameter

The maximum wave height H_{\max} during some time span T_L is often of interest for design. Let N denote the number of zero-upcrossings of the sea elevation process in this period of time, i.e. $N = T_L/T_z$. The distribution of H_{\max} can then be approximated by

$$F_{H_{\max}}(h) \approx \exp\left(-N \exp\left(-\frac{2h^2}{(1 - \nu^2)H_s^2}\right)\right)$$

and the expected value of the maximum wave height can be approximated by

$$E[H_{\max}] \approx H_s \sqrt{\frac{(1 - \nu^2) \ln N}{2}}$$

A first-order approximation yields the following value for the spectral width parameter, $\nu = 0.43$. With this value of ν , the following relationship between the maximum wave height H_{\max} and the maximum wave crest Z_{\max} holds

$$H_{\max} \approx 1.8 \cdot Z_{\max}$$

In shallow waters, shoaling effects imply that wave crests become more peaked while wave troughs become flatter and not quite as deep. The sea elevation process has become somewhat "skewed" and will not quite be Gaussian, and the individual wave heights will not quite be Rayleigh distributed. Techniques are available to account for the skewness introduced by the shoaling. Reference is made to Winterstein et al. (1991) and to U.S. Army Coastal Engineering Research Center (1973).

Note that in shallow waters, the wave heights will be limited by the water depth, d . The maximum possible wave height at a water depth d is approximately equal to the water depth

$$H_{\max, \text{lim}} \approx d$$

and the Rayleigh distribution of the wave heights will become distorted in the upper tail to approach this limit asymptotically.

Wave periods

Once the significant wave height H_S is given, the zero-upcrossing period T_Z is usually well-represented by a shifted lognormal distribution

$$F_{T_Z}(t) = \Phi\left(\frac{\ln(t - \delta) - a_1}{a_2}\right); t \geq \delta$$

in which Φ denotes the standardised normal distribution function, the distribution parameters a_1 and a_2 are functions of H_S , and the shift parameter δ can be approximated by

$$\delta \approx 2.2\sqrt{H_S}$$

when H_S is given in metres and δ is given in seconds. This is based on braking considerations, see Haver (1990).

The mean zero-upcrossing period T_Z is an average wave period associated with a sea state of a given significant wave height H_S . The wave period T associated with the maximum wave height H_{\max} in this sea state can be represented by a Longuet-Higgins distribution

$$F_T(t) = \frac{\Phi\left(\left(1 - \left(\frac{T_Z}{t}\right)^2 (v^2 + 1)\right) \frac{h_0}{2v}\right)}{\Phi\left(\frac{h_0}{2v}\right)}$$

- Φ standardised normal distribution function
- v spectral width parameter as referenced above
- h_0 normalised maximum wave height in deep water

$$h_0 = H_{\max} \frac{4\sqrt{2\pi}}{H_S} \sqrt{\left(1 + \frac{2kd}{\sinh[2kd]}\right) \tanh[kd]}$$

in which k is the wave number, which results implicitly as the solution to

$$\omega^2 = gk \tanh[kd]$$

where $L = 2\pi/k$ and $\omega = 2\pi/T$

- g acceleration of gravity
- L wave length
- k wave number
- ω angular velocity
- T wave period

Wave forces by Morison's equation

Wave forces on slender structural members, such as a cylinder submerged in water, can be predicted by Morison's equation. By this equation, the horizontal force on a vertical element dz of the structure at level z is expressed as

$$\begin{aligned} dF &= dF_M + dF_D \\ &= C_M \rho \pi \frac{D^2}{4} \ddot{x} dz + C_D \rho \frac{D}{2} |\dot{x}| \dot{x} dz \end{aligned}$$

- C_M inertia coefficients
- C_D drag coefficients
- D diameter of the cylinder
- ρ density of water
- \dot{x} horizontal wave-induced velocity of water
- \ddot{x} horizontal wave-induced acceleration of water

The first term in the formula is an inertia force and the second term is a drag force. The level z is measured from stillwater level, and the z axis points upwards. Thus, at seabed $z = -d$, when the water depth is d . The movement of the structure is considered to be very small.

According to first-order linear wave theory, the horizontal wave-induced velocity is

$$\dot{x} = A_w \omega \frac{\cosh[k(z+d)]}{\sinh[kd]} \sin(\omega t)$$

and the acceleration is

$$\ddot{x} = A_w \omega^2 \frac{\cosh[k(z+d)]}{\sinh[kd]} \cos(\omega t)$$

A_w wave amplitude

The resulting horizontal force F on the cylinder can be found by integration of Morison's equation for values of z from $-d$ to 0

$$\begin{aligned} F &= F_M + F_D \\ &= \int_{-d}^0 (C_M \rho \pi \frac{D^2}{4} \frac{H}{2} \omega^2 \cos(\omega t) \cdot \frac{\cosh[k(z+d)]}{\sinh[kd]}) dz \\ &\quad + \int_{-d}^0 (C_D \rho \frac{D}{2} \frac{H^2}{4} \omega^2 \sin(\omega t) |\sin(\omega t)| \cdot \frac{\cosh^2[k(z+d)]}{\sinh^2[kd]}) dz \end{aligned}$$

Note that the integration from $-d$ to 0 ignores contributions to the force from the wave crest above the stillwater level at $z = 0$. However, this is a minor problem for the inertia force F_M , since this has its maximum

when a nodal line at the stillwater level passes the structure. The drag force F_D , on the other hand, reaches its maximum when the crest passes the structure, and if this force is dominating, a significant error can be introduced by ignoring the contribution from the wave crest.

Note also that Morison's equation is only valid when the dimension of the structure is small relative to the wave length, i.e. when $D < 0.2L$, and that it is only valid for nonbreaking waves. In deep water, waves break when H/L exceeds about 0.14.

The inertia coefficient depends on the cross-sectional shape of the structure and of the orientation of the body. Typically, C_M is in the range 1.6-2.5. For a vertical cylinder, $C_M = 2.0$. For a cylinder with in-service marine roughness, e.g. owing to marine growth, C_M should normally not be less than 1.8. The drag coefficient C_D is never less than 0.6, and for a smooth cylinder $C_D = 1.0$.

An example of application of Morison's equation is given in Figure 4-24 for a cylinder with 4 m diameter in 10 m water depth. The upper part of this figure shows the sea elevation process, the middle part shows the horizontal water particle velocity and acceleration at the stillwater level, and the lower part of the figure shows the resulting horizontal wave force and overturning moment at the seabed. The example is based on $C_M = 2$ and $C_D = 1.2$.

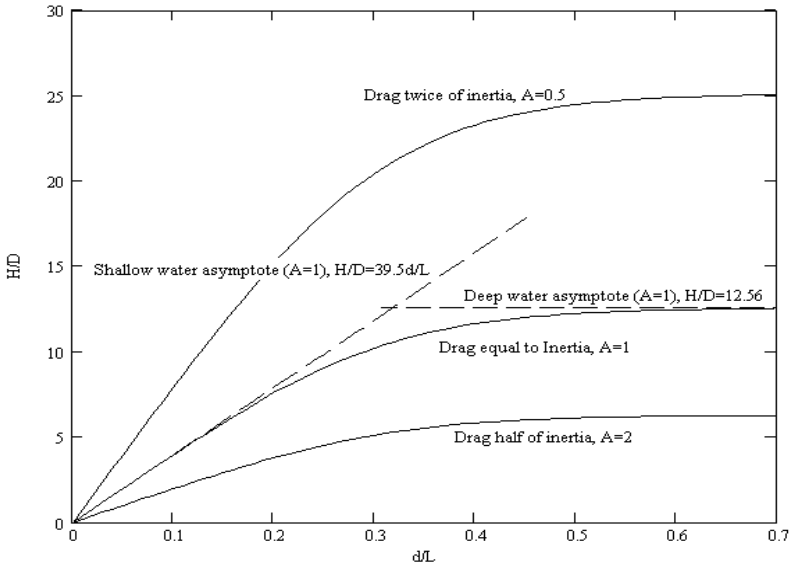


Figure 4-23. Relative magnitude of inertia and drag forces.

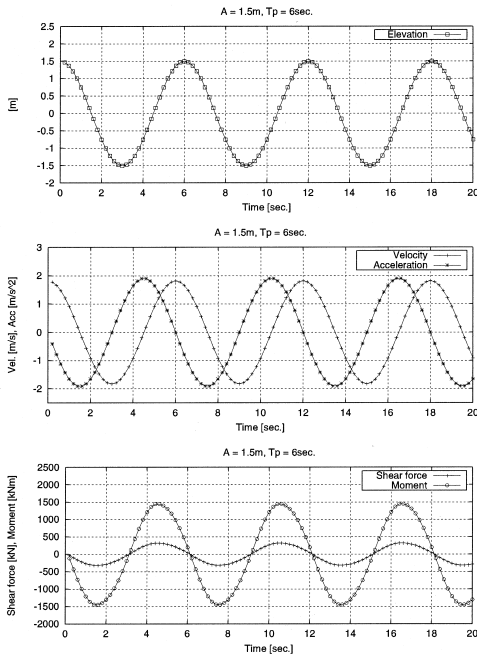


Figure 4-24. Example of sea elevation process, associated water particle velocities and accelerations, and resulting Morison forces at the seabed for a cylindrical example structure.

The inertia force can be expressed as

$$F_M = A_M \cos(\omega t)$$

and the drag force as

$$F_D = A_D \sin(\omega t) |\sin(\omega t)|$$

A_M amplitudes of inertia force

A_D amplitudes of drag force

Let A denote the ratio between the amplitudes, $A = A_M/A_D$. The following relationship can be established

$$\frac{H}{D} = \pi \frac{C_M}{C_D} \frac{\sinh^2[kd]}{((\sinh[2kd])/4 + kd/2)A}$$

and can be represented as shown in Figure 4-23. For a given structure and location, Figure 4-23 can be used to quickly establish whether the inertia force or the drag force is the dominating force, once the ratios H/D and d/L have been calculated.

With reference to Figure 4-23, structures located above the curve for $A = 1$ experience loads which are dominated by the drag term in Morison's equation. Structures located below the curve for $A = 1$ are dominated by inertia loads. The two dashed asymptotes in Figure 4-23 are valid for shallow water waves ($d/L < 1/20$) and deep water waves ($d/L > 0.5$), respectively. The asymptotes are derived from asymptotic results for small-amplitude wave kinematics.

Example

A cylinder with diameter $D = 5$ m is considered subjected to the wave climates at the Middelgrunden and Rødsand sites in Danish waters. Water depths and wave data for a number of cases at these two locations are tabulated in Table 4-9 with the resulting ratios H/D , d/L and A . It appears that for H/D , d/L and A . It appears that for both sites A values occur, which indicate that the inertia force dominates the loading.

Table 4-9. Examples of ratio between inertia force and drag force.

Site	Wave height H (m)	Depth d (m)	Wave length L (m)	H/D	d/L	A
MG	3.8	5.5	40	0.76	.138	7.1
MG	2.6	5.5	28	0.46	.196	16.2
RS	3.5	8.0	45	0.70	.178	9.8
RS	3.5	9.5	47	0.70	.202	10.9
RS	3.5	11.0	50	0.70	.220	11.7
RS	6.2	8.0	64	1.24	.125	4.0
RS	6.7	9.5	76	1.34	.125	3.7
RS	6.7	11.0	88	1.34	.125	3.7

MG = Middelgrunden
RS = Rødsand

Wave forces by diffraction theory

When the dimension of the structure in question is large compared with the wave length, typically when $D > 0.2L$, Morison's equation is no longer valid. The inertia force will then be dominating and can be predicted by means of diffraction theory. For a cylinder of radius $R = D/2$ installed in water of depth d and subjected to a wave of

amplitude A , this theory gives the following maximum horizontal wave force

$$F_{x,max} = \frac{4\rho g A}{k^2} \frac{\sinh[k(d + A \sin \alpha)]}{\tanh[kd]} \xi$$

whose vertical arm measured from the sea floor is

$$h_F = d \frac{kd \sinh[kd] - \cosh[kd] + 1}{kd \sinh[kd]}$$

The coefficients ξ and α are given in Table 4-10, extracted from Gran (1992).

Table 4-10. Coefficients ξ and α .

kR	ξ	$\alpha(^{\circ})$	kR	ξ	$\alpha(^{\circ})$
0.02	0.0063	0.018	0.2	0.06433	1.816
0.04	0.00252	0.072	0.4	0.25808	6.972
0.06	0.00568	0.162	0.6	0.54230	13.618
0.08	0.01012	0.289	0.8	0.83373	18.734
0.10	0.01586	0.453	1.0	1.07726	20.504
0.12	0.02290	0.653	1.2	1.26842	18.940
0.14	0.03126	0.889	1.4	1.42148	14.804
0.16	0.04095	1.162	1.6	1.54958	8.844
0.18	0.05197	1.471	1.8	1.66133	1.611
0.20	0.06433	1.816	2.0	1.76191	-6.522
0.22	0.07802	2.195	2.2	1.85448	-15.306
0.24	0.09304	2.609	2.4	1.94099	-24.572
0.26	0.10937	3.056	2.6	2.02275	-34.201
0.28	0.12701	3.534	2.8	2.10063	-44.112
0.30	0.14591	4.043	3.0	2.17524	-54.245
0.32	0.16606	4.581	3.2	2.24705	-64.555
0.34	0.18740	5.145	3.4	2.31641	-75.009
0.36	0.20989	5.733	3.6	2.38360	-85.581
0.38	0.23347	6.343	3.8	2.44882	-96.253
0.40	0.25808	6.972	4.0	2.51228	-107.007
0.42	0.28364	7.617	4.2	2.57411	-117.832
0.44	0.31008	8.276	4.4	2.63444	-128.717
0.46	0.33732	8.944	4.6	2.69340	-139.654
0.48	0.36526	9.619	4.8	2.75107	-150.637
0.50	0.39381	10.298	5.0	2.80754	-161.659
0.52	0.42287	10.976	5.2	2.86288	-172.716
0.54	0.45234	11.650	5.4	2.91717	-176.196
0.56	0.48214	12.318	5.6	2.97045	-165.081
0.58	0.51216	12.975	5.8	3.02280	-153.941
0.60	0.54230	13.618	6.0	3.07425	-142.779
0.62	0.57249	14.245	6.2	3.12485	-131.598
0.64	0.60262	14.852	6.4	3.17465	-120.399
0.66	0.63263	15.438	6.6	3.22368	-109.183
0.68	0.66244	15.998	6.8	3.27197	-97.953
0.70	0.69197	16.532	7.0	3.31956	-86.710
0.72	0.72118	17.036	7.2	3.36648	-75.454
0.74	0.75000	17.510	7.4	3.41275	-64.188
0.76	0.77839	17.952	7.6	3.45841	-52.910
0.78	0.80631	18.360	7.8	3.50348	-41.624
0.80	0.83373	18.734	8.0	3.54797	-30.328
0.82	0.86062	19.073	8.2	3.59192	-19.025
0.84	0.88697	19.376	8.4	3.63533	-7.714
0.86	0.91276	19.643	8.6	3.67824	-3.604
0.88	0.93797	19.874	8.8	3.72064	-14.929
0.90	0.96261	20.068	9.0	3.76258	-26.260
0.92	0.98667	20.226	9.2	3.80405	-37.596
0.94	1.01016	20.349	9.4	3.84508	-48.938
0.96	1.03308	20.435	9.6	3.88567	-60.284
0.98	1.05545	20.487	9.8	3.92585	-71.635
1.00	1.07726	20.504	10.0	3.96562	-82.991

This can be used for prediction of wave forces on foundation structures shaped like cylinders, such as monopiles and some

gravity-based structures. Note, however, that the formulas may lead to erroneous results if the structural geometry deviates much from the assumed cylindrical shape, such as when a conical structural component is present in the wavesplash zone to absorb or reduce ice loads.

Note also that in shallow waters waves may break locally over a sloping seabed, if they are large enough, and thereby violate the kinematic assumptions behind the presented formulas. For a horizontal seabed, however, such local breaking is not expected as too large waves will have broken prior to arriving at the particular location. The assumed wave kinematics of these waves will regenerate before the waves arrive at the location, while the heights of waves will conform to the limit given by the water depth.

Wave loads are strongly dependent on the water depth. For this reason it is important to consider effects of local variations in the water depths, including astronomical tides and storm surges.

4.7.2 Current loads

Morison's equation can be used to predict current loads. Note in this context that the velocity \dot{x} and the acceleration \ddot{x} in Morison's equation need to be taken as the resulting combined current and wave velocity and acceleration, respectively. As in the case of pure wave load prediction, Morison's equation is only applicable as long as the wave length is longer than five times the diameter of the cylindrical structure.

4.7.3 Ice loads

It is current practice to distinguish between static ice loads and dynamic ice loads. For conical structures, Ralston's formula for ice loads can be applied, see Ralston (1977).

For ice loads in general, reference is made to API (1995).

4.7.4 Earthquake loads

For prediction of earthquake loads, reference is made to Section 3.2.8.

4.8 Load combination

Principles for how to combine loads arising from different concurrent load processes are outlined in this section.

When several load processes are acting concurrently, their combined load response in the structure needs to be considered for design. For example, the foundation structure of an offshore wind turbine will be subject to the combined action from wind and wave loads, and the resulting structural response from this action governs the design. Another load combination, which is possible, is the combination of wind and ice loads, and current may combine with any of the other load types mentioned.

Consider the combination of wind and wave loads. The short-term wind climate is usually represented by the 10-minute mean wind speed U_{10} , and the short-term wave climate is usually represented by the significant wave height H_S . U_{10} and H_S may be interpreted as intensities of the corresponding wind speed and sea elevation processes, respectively. The wind and the waves at a particular location often have a common cause such as a low pressure. The waves are driven by the wind and often generated locally. At the same time, the roughness implied by the wave-affected sea surface influences the wind. A high wave intensity will imply a high wind intensity, and vice versa.

It is important to consider this usually strong dependency – the simultaneous occurrence

of wind and wave climates of high intensities – in design. In a probabilistic analysis, this can practically be done by modelling one of the climate variables as a so-called independent variable by means of its marginal cumulative distribution function, and then model the other variable as a dependent variable by means of a distribution conditioned on the independent variable. For the considered wind and wave example, one could represent the significant wave height H_S by its marginal long-term distribution, typically a Weibull distribution, and then model the 10-minute mean wind speed U_{10} conditional on H_S . The distribution of U_{10} conditioned on H_S will typically be a lognormal distribution

$$F_{U_{10}|H_S}(u) = \Phi\left(\frac{\ln u - b_1}{b_2}\right)$$

Φ standard normal distribution function
 b_1, b_2 functions of the significant wave height H_S , i.e. $b_1 = b_1(H_S)$ and $b_2 = b_2(H_S)$

In some cases, other generic distribution types than the lognormal distribution may provide the best representation of U_{10} conditional on H_S , e.g. a Weibull distribution.

Once the wind and wave climates are given in terms of a specific set of concurrent U_{10} and H_S values, the wind speed process conditioned on U_{10} and the wave process conditioned on H_S can be considered independent. It is therefore, for example, not reasonable to expect that the maximum wind speed will occur at the same time as the maximum wave height.

For design, it is reasonable to consider some relatively rare combination of wave and wind climate as the characteristic climate and then to find the maximum load response

that occurs for this climate over its duration. Practically, one may for example consider the wave climate for the significant wave height with a 50-year recurrence period in combination with a wind climate conditioned on this wave climate, e.g. the expected value of U_{10} conditional on the 50-year significant wave height, or some higher quantile of U_{10} . With such a rare characteristic wave and wind climate in mind, the following paragraphs outline how the combined load response, e.g. the horizontal force in some section of the foundation structure, during this climate can be found.

For linear load combinations, Turkstra's rule plays a central role. The rule states that the maximum value of the sum of two independent random processes occurs when one of the processes has its maximum value. Application of Turkstra's rule to the combination of two load processes, e.g. wave load and wind load, implies that the combined load will have its maximum either when the wave load has its maximum or when the wind load has its maximum. Let Q_1 and Q_2 denote the two load processes. Mathematically, the maximum combined load Q_{\max} over a time span T will be

$$Q_{\max} = \max \left\{ \begin{array}{l} \max_{0 \leq t \leq T} Q_1(t) + Q_2(t) \\ Q_1(t) + \max_{0 \leq t \leq T} Q_2(t) \end{array} \right.$$

Turkstra's rule indicates that a natural code format for a combination of two loads for use in deterministic design is

$$q_{\text{design}} = \max \left\{ \begin{array}{l} \gamma_1 q_{1k} + \gamma_2 \psi_2 q_{2k} \\ \gamma_1 \psi_1 q_{1k} + \gamma_2 q_{2k} \end{array} \right.$$

in which q_{1k} and q_{2k} are characteristic values of Q_1 and Q_2 , γ_1 and γ_2 are associated partial safety factors, and the ψ -factors are load combination factors.

For a wind turbine structure, loads do not always combine linearly to give the sought-after maximum load response. Aeroelastic wind load calculations may be nonlinear, and the combined wave and wind load response may not necessarily come out as the linear combination of the separately calculated wave load response and the separately calculated wind load response. For such nonlinear cases, the combined response is to be calculated from some appropriate structural analysis for the concurrent characteristic wave and wind load processes without applying any partial load factors. The resulting maximum load response from this analysis can be interpreted as a characteristic load response, which reflects the combined wave and wind loading. A common partial safety factor is then to be applied to this characteristic load response to give the design value q_{design} , i.e. it will no longer be possible to distinguish between different partial safety factors for wave loads and wind loads.

REFERENCES

- Andersen, P.S., U. Krabbe, P. Lundsager, and H. Petersen, *Basismateriale for beregning af propelvindmøller*, Report No. Risø-M-2153 (in Danish), Risø National Laboratory, revised version, 1980.
- Abbott, I.H., and A.E. von Doenhoff, *Theory of Wing Sections*, Dover Publications Inc., New York, N.Y., 1959.
- API, *Recommended practice for planning, designing and constructing structures and pipelines for arctic conditions*, RP2N, 2nd edition, American Petroleum Institute, 1995.
- Bak, C., P. Fuglsang, N.N. Sørensen, H.A. Madsen, Wen Zhong Shen, J.N. Sørensen, *Airfoil Characteristics for Wind Turbines*, Risø R-1065(EN), Risø National Laboratory, 1999a.
- Bak, C., H.A. Madsen, and N.N. Sørensen, *Profilkoefficienter til LM19.1 vingen bestemt ud fra 3D CFD*, 1999b.
- Bathe, K.J., *Finite Element Procedures in Engineering Analysis*, Prentice-Hall, 1982
- Baumgart, A., I. Carlén, M. Hansen, G. Larsen, S.M. Petersen, *Experimental Modal Analysis of a LM 19.1 m blade*, unpublished work.
- Bitner-Gregersen, E., and Ø. Hagen, *Aspects of Joint Distribution for Metocean Phenomena at the Norwegian Continental Shelf*, ASME Paper No. OMAE-2000-6021, *Proceedings*, International Conference on Offshore Mechanics and Arctic Engineering, 2000.
- Davenport, A.G., *The Application of Statistical Concepts to the Wind Loading of Structures*, Proc. Inst. of Civil Engineers, Vol. 19, 1961.
- DNV, *Environmental Conditions and Environmental Loads*, Classification Notes No. 30.5, Det Norske Veritas, Høvik, Norway, 2000.
- Eggleston, D.M, and F.S. Stoddard, *Wind Turbine Engineering Design*, Van Nostrand Reinhold Co. Inc., New York, N.Y., 1987.
- Gran, S., *A Course in Ocean Engineering*, Elsevier, Amsterdam, the Netherlands, 1992. The Internet version, located at <http://www.dnv.com/ocean/>, provides on-line calculation facilities within the fields of ocean waves, wave loads, fatigue analysis, and statistics.

- Hallam, M.G., N.J. Heaf, and L.R. Whootton, *Dynamics of Marine Structures: Methods of Calculating the Dynamic Response of Fixed Structures Subject to Waves and Current Action*, CIRIA Underwater Engineering Group, 6 Storey's Gate, London SW1P 3AU, Report UR8, 1978.
- Haver, S., *On a Possible Lower Limit for the Spectral Peak Period*, Statoil Report No. F&U-MT 90009, Stavanger, Norway, 1990.
- IEA, *Expert Group Study on Recommended Practices for Wind Turbine Testing and Evaluation, 3. Fatigue Loads*, 2nd edition, 1990.
- Larsen, G., and P. Sørensen, "Design Basis 2," *Proceedings*, IEA Symposium "State-of-the-Art of Aeroelastic Codes for Wind Turbine Calculations," pp. 137-145, Lyngby, Denmark, 1996.
- Madsen, H.O., S. Krenk, and N.C. Lind, *Methods of Structural Safety*, Prentice-Hall Inc., Englewood Cliffs, N.J., 1986.
- Madsen, P.H., K. Pierce, and M. Buhl, "The use of aeroelastic wind turbine response simulations for prediction of ultimate design loads," *Proceedings*, 3rd ASME/JSME Joint Fluids Engineering Conference, Paper No. FEDSM99-S295-10, San Francisco, Cal., 1999.
- Mann, J., "Wind field simulation," *Probabilistic Engineering Mechanics*, Elsevier Science Ltd., Vol. 13, No. 4, pp. 269-282, 1998.
- Mann, J., "The spatial structure of neutral atmospheric surface-layer turbulence," *Journal of Fluid Mechanics*, No. 273, pp. 141-168, 1994.
- Petersen, J.T., *Geometric nonlinear finite element model for a horizontal axis wind turbine*, Risø National Laboratory, 1990.
- Petersen, J.T., H.A. Madsen, A. Björk, P. Enevoldsen, S. Øye, H. Ganander, D. Winkelaar, *Prediction of Dynamic Loads and Induced Vibration in Stall*, Risø-R-1045, Risø National Laboratory, 1998
- Ralston, T.D., "Ice Force Design Considerations for Conical Offshore Structures," *Proceedings*, Fourth POAC Conference, Vol. 2, pp. 741-752, St. John's, Nfld., Canada, 1977.
- Ronold, K.O., J. Wedel-Heinen, and C.J. Christensen, *Reliability-based fatigue design of wind-turbine rotor blades*, Engineering Structures, Elsevier Science Ltd., Vol. 21, No. 12, pp. 1101-1114, 1999.
- Stiesdal, H., "Rotor Loadings on the BONUS 450 kW Turbine," *Proceedings*, EWEC'91, Amsterdam, the Netherlands, 1991.
- U.S. Army Coastal Engineering Research Center, *Shore Protection Manual*, Vols. I-III, Washington, D.C., 1973.
- Veers, P.S., *Three-Dimensional Wind Simulation*, Report No. SAND88-0152, Sandia National Laboratories, Albuquerque, N.M., 1988.
- Viterna, L.A. and R.D. Corrigan, *Fixed pitch rotor performance of large horizontal axis wind turbines*, DOE/NASA Workshop on Large Horizontal Axis Wind Turbines, Cleveland, Ohio, July 28-30, 1984.
- Winterstein, S.R., "Nonlinear Vibration Modes for Extremes and Fatigue," *Journal of Engineering Mechanics*, ASCE, Vol. 114, No. 10, pp. 1772-1790, 1988.

Winterstein, S.R., E. Bitner-Gregersen, and K.O. Ronold, “Statistical and Physical Models of Nonlinear Random Waves,” *Proceedings*, International Conference on Offshore Mechanics and Arctic Engineering (OMAE), Vol. II , pp. 23-31, Stavanger, Norway, 1991.

Wirsching, P.H., and A.M. Shehata, “Fatigue under Wide Band Random Stresses Using the Rain-Flow Method,” *Journal of Engineering Materials and Technology*, ASME, July 1977, pp. 205-211.

5. Rotor

5.1 Blades

Rotor blades are usually made of a matrix of fibreglass mats, which are impregnated with a material such as polyester, hence the term glass fibre reinforced polyester, GRP. The polyester is hardened after it has impregnated the fibre-glass. Epoxy is sometimes used instead of polyester. Likewise, the basic matrix is sometimes made wholly or partly of carbon fibres, which form a lighter, but more expensive material with a high strength. Wood-epoxy laminates are sometimes used in large rotor blades.

5.1.1 Blade geometry

The design of the outer contour of a wind turbine rotor blade is based on aerodynamic considerations. The cross-section of the blade has a streamlined asymmetrical shape, with the flattest side facing the wind. Once the aerodynamic outer contour is given, the blade is to be designed to be sufficiently strong and stiff. The blade profile is a hollow profile usually formed by two shell structures glued together, one upper shell on the suction side, and one lower shell on the pressure side. To make the blade sufficiently strong and stiff, so-called webs are glued onto the shells in the interior of the blade, thus forming a boxlike structure and cross-section, see Figure 5-1. From a structural point of view, this web will act like a beam, and simple beam theory can be applied to model the blade for structural analysis in order to determine the overall strength of the blade.

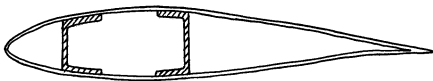


Figure 5-1. Section of a blade showing upper and lower shells and two webs, respectively.

It is important that the blade sections near the hub are able to resist forces and stresses from the rest of the blade. Therefore, the blade profile near the root is both thick and wide. Further, along the blade, the blade profile becomes thinner so as to obtain acceptable aerodynamic properties. As the blade speed increases towards the tip, also the lift force will increase towards the tip. Decreasing the chord width towards the tip will contribute to counteract this effect. In other words, the blade tapers from a point somewhere near the root towards the tip as seen in Figure 5-2. In general, the blade profile constitutes a compromise between the desire for strength and the desire for good aerodynamic properties. At the root, the blade profile is usually narrower and tubular to fit the hub.

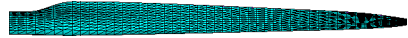


Figure 5-2. Side view of a blade.

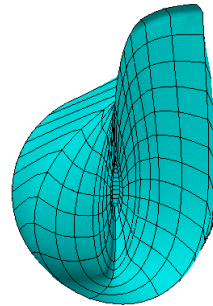


Figure 5-3. View of a blade from the tip, illustrating the twist of the blade: the wind comes in from the left, and the pitch is 0° at the tip and about 25° at the hub.

The blade is twisted along its axis so as to enable it to follow the change in the direction of the resulting wind along the blade, which the blade will experience when it rotates. Hence, the pitch will vary along the blade. The pitch is the angle between the chord of the blade profile and the rotor plane, see Chapter 4. Figure 5-3 illustrates

the twist of a blade. Note in this context that the *pitch angle*, which is referred to throughout this document, usually refers to the collective rotation of the entire blade relative to the rotor plane.

For a blade, four non-coincident trajectories can be defined:

- mass axis, the spanwise locus of section mass centres
- elastic axis, the spanwise locus of points about which no section is exposed to bending deflection
- control axis, the axis of mechanical feathering, which is determined by the blade retention and pitching mechanism
- aerodynamic axis, the blade section quarterchord for a conventional airfoil shape within linear performance limits

These four trajectories are not axes in the true sense, since they – owing to the geometry of the blade – are not straight lines. However, for calculations for a particular section of the blade, four axes, perpendicular to the section, can be defined as the tangents to the trajectories at their respective intersections with the section.

5.1.2 Design loads

In principle, the same airflow conditions would apply at all sections along a blade as long as the profile stays the same, while the magnitude and direction of the forces would change depending on the distance to the tip. However, in practice, the profile and the blade thickness vary along the blade and thereby make the airflow conditions more complex.

At stand-still, the wind pressure force will – depending on the load case – be somewhat larger at the root than at the tip. This is due to the fact that the blade is wider at the root. The force is acting roughly at a right angle to the flat side of the blade profile. As the blade is more twisted at the root, a larger component of the force will act in the

direction of rotation at the root than at the tip. Relative to the rotor axis, the force at the root has a smaller torque arm than the force at the tip and will therefore give about the same contribution to the starting torque as the force at the tip.

During operation, the wind approaching the blade profile constitutes the vectorial sum of the farfield wind speed perpendicular to the rotor plane and the head wind due to the rotational movement of the blade through the air. Smaller aerodynamic forces are produced near the root than at the tip. However, the forces produced near the root are more aligned with the direction of rotation than the forces near the tip. The change in magnitude and direction of the forces along the blade contributes to determine the shape and design of the blade, including the width, thickness and twist of the blade.

The design loads for a blade can be determined by means of blade momentum theory and aeroelasticity. For details, reference is made to Chapter 4.

5.1.3 Blade materials

Wind turbine blades are made of lightweight materials to minimise the loads from rotating mass.

A rotor blade is built up of the following elements:

- external panels - form the aerodynamic shape and carry a part of the bending load
- internal longitudinal spars/webs – carry shear load and a part of the bending load, restrain the cross section against deformation and the panels against buckling.
- inserts like bushings - transfer the loads from the panels and spars into the steel hub.

- lightning protection – carries a lightning hitting the blade tip to the root
- aerodynamic brake – for some types of turbines with fixed pitch an aerodynamic brake is part of the protection system. The aerodynamic brake is typically the tip turning on a shaft.

Fibre reinforced plastics (FRP) is the favoured group of materials for external panels, internal spars/webs and shafts for aerodynamic brakes.

FRP is materials where fibres are used for transferring the global loads and a polymeric resin is used to distribute the load between the fibres and to restrain the fibres against local relative displacements.

FRP is often used on both sides of a cellular core in a sandwich structure. The core in a sandwich structure is used for increasing the local bending stiffness of the panel or web. An increased local bending stiffness may be required to avoid buckling when subjected to compressive or shear loading.

Gelcoats and topcoats are used to protect the FRP against abrasion, UV radiation and moisture and to give the right colour.

Wood is a natural material with the same type of structure as FRP. Wood is used as an alternative to FRP in design of blade panels and spars/webs.

Further information about FRP can be found in Mayer (1992), in DNV (1999) or on www.marinecomposites.com.

FRP Reinforcements

Both glass fibre and carbon fibre is used in manufacturing the blade panels and internal spars.

Carbon fibre is used for aerodynamic brake shafts.

Glass and carbon fibres come in different types having different chemical compositions. The most important type of glass is E-glass.

The mechanical properties, modulus and tensile strength, may vary significantly between different types of fibres and can also vary considerably within each type of fibre. There are for example low, medium and high strength carbon fibres. The selection and qualification of fibres is part of the blade design.

It is important to realise that the final properties of a FRP laminate not only depend on the properties of the fibres. The properties of the matrix, the structural interaction between fibres and matrix and the volume fraction of fibres are also important.

Sizing is deposited on the surface of the fibre during production. The purpose of the sizing is to increase the strength of the bond between the fibre and the resin. Sizing can also be applied to enable easy handling without inducing defects in the fibres during blade manufacturing. A particular sizing that has been developed for one type of application or one type of resin is not necessarily adequate for another application or another resin. It is important that the supplier of the fibre material provides adequate information about this and that the supplier's recommendations are followed during blade manufacturing.

The reinforcement fibres for FRP panels are supplied in fabrics/mats.

The basic building blocks of reinforcement fabrics are:

- roving where long fibre strands are arranged in bundles with little or no twist.
- Chopped Strand Mat (CSM) where the orientation of relatively short fibre strands is random. Only glass fibres are supplied as CSM.

From these the following basic types of fabrics are pre-fabricated: unidirectional (UD), woven roving, angle-ply and multiaxial fabrics. Woven rovings and multiaxial fabrics often have a light (100 g/m^2 or 300 g/m^2) CSM bonded to one or both sides to enhance the interlaminar bond to adjacent plies in which case they are called combination mats. Fabrics may be bonded together by a bonding agent (which later is dissolved in the polyester) or mechanically by stitching a yarn through the thickness.

Different types of fibres, e.g. glass and carbon, may be combined in one fabric. Such fabrics are referred to as hybrid fabrics.

A complete set of reinforcement or fabrics in one laminate is defined by its stacking sequence. The stacking sequence specifies the sequence of plies (starting from one side of the laminate) and their respective orientation, with respect to a reference direction.

Fabrics are defined, apart from the type and stacking sequence, also by the total weight of reinforcement per unit area, usually expressed as g/m^2 .

Note that carbon fibres used as reinforcement of the rotor blades will cause galvanic corrosion of any steel parts they get in touch with, unless stainless steel is used for the making of these parts.

Resins

Polyester, vinylester and epoxy are the most commonly used resins in wind turbine blades. Polyester is dominating with epoxy being used in structurally more demanding applications.

The resin consists of a base into which hardener is mixed to initiate the cross-linking process (sometimes aided by the addition of a catalyst). In addition accelerators or inhibitors may be added to adjust the gel-time and cure time to the working temperature and the characteristics of the operation to be carried out. The possibility for adjusting the gel-time and cure time is relatively large for polyester. For epoxy variation of these parameters will normally have an effect on the properties of the cured resin. Waxes may be added to polyester to control evaporation of styrene and exposure to oxygen during curing.

In addition other compounds may be added for specific reasons, e.g. low cost fillers, pigments and thixotropic agents which can stabilize the resin on a vertical surface. The effect of such additives on the properties of the resin can be significant and shall be evaluated.

Core materials

The most common core materials are structural foams and wood products.

Foams are based on thermoplastics, e.g. PVC, and are delivered in a range of densities. The most important mechanical properties are the shear modulus, shear strength and ductility or yielding behaviour. Stiffness and strength increases with the density. Different types and grades of foam can have significantly different properties. Detailed information on the properties is given in the manufacturer's product specification. PVC foams may be supplied in a "heat stabilised" condition, which

provides better dimensional stability and reduces the chance of outgassing. Outgassing is the release of volatile gasses from the core when the panel has been completed.

Wood core materials include balsa, conventional wood and plywood. Balsa is by far the most commonly used and is supplied in different densities, stiffness and strength increasing with density.

Core/Sandwich adhesives are used to bond the sheets/pieces together and to fill the voids between pieces/sheets of core. A good bond is necessary to maintain the shear capacity of the core. The bond should have at least the same shear strength and fracture elongation as the core material. A high ductility of the adhesive normally increases the strength of the joint.

Wood

Several species of wood can be used for wind turbine blades.

Wood is applied as plywood or in lamellas to minimize the impact of imperfections like knots on the strength.

It is important for the resistance of the wood that the water content is low. A high water content will result in low mechanical values, rot and fungus. The humidity shall be controlled during storage and manufacturing. Coating and sealing shall be qualified as part of design to govern the long-term water content in the wood.

Adhesives

Adhesives are used for joining blades that are manufactured in parts and to bond metallic inserts like steel bushings at the root. It is important for adhesive joints that the surfaces are clean and absolutely free from wax, dust and grease. Sandblasting and

cleaning by solvents may be necessary to meet this requirement for bushings.

The thickness of adhesive joints shall be controlled as it has an impact on the strength.

5.1.4 Manufacturing techniques

Several manufacturing techniques are applied in manufacturing of wind turbine blades.

Wet hand lay-up

A layer of resin is applied in a mould. (The mould has previously been covered with a release agent and a layer of gelcoat). The first ply of reinforcement fabric is then applied in the wet resin. Subsequently the remaining plies are applied (according to the laminate schedule) alternating with application of resin.

During the course of application of all plies the fabrics are worked using metallic or bristle rollers to ensure a thorough wetting out of the fibres, to compact/consolidate the laminate and to make sure that all entrapped air is removed. In addition superfluous resin is removed using an elastic scraper. For glass the colour indicates whether satisfactory wet-out has been achieved. This colour/opacity change is not apparent when carbon fibre is used.

Since the quality of the material is entirely dependent on the system for laying, any form of automation is beneficial to quality control. Systems involving automatic resin / catalyst mixing pumps, wet out machines (where cloth is weighed dipped in resin and squeezed through rollers and then reweighed to verify resin ratio before being laid), gel time measuring machines, etc. will be of great benefit.

If the preceding ply has cured completely the operation is no longer a wet-in-wet

lamination and the new bond shall be treated as a new bond. The surface preparation for a new bond is critical since there will be no effective crosslinking between the laminates. The new applied resin will in this case act as an adhesive.

Wet lay-up may be carried out with vacuum bagging where an airtight (plastic) membrane is applied over the hand laid-up laminate or core. The air under the membrane is sucked out by means of a pump such that an overpressure (from the atmosphere) acts over the entire laminate.

The vacuum bagging technique is used to improve the compacting of the laminate and thus to increase the volume fraction of reinforcement and to improve the consistency of the finished laminates. Normally a porous mat is applied on top of the laminate and under the membrane to facilitate even resin distribution and the escape of the air. Vent holes may be required through the core for the same purpose.

Pre-pregs

Plies are supplied as fabric saturated with resin that will cure when heated. The plies are stored cold. The complete stack of plies is laid-up in the mould. The laminates in the mould is vacuum bagged and cured by heating the mould. The applied vacuum consolidates the laminate and removes entrapped air.

Vacuum-assisted resin transfer moulding (VARTM)

The technique has similarities to vacuum-bagging. The complete set of reinforcement plies is applied to the mould, but without adding the resin. The airtight membrane is put on top and vacuum drawn. The resin is then transferred via piping/hoses from a container of premixed resin by the suction created by the vacuum.

The advantage of this technique is the good control of, and the relatively high, volume fraction of fibres one achieves and thus consistency in the properties of the laminates and a lower laminate weight.

It is important that the gel time is sufficiently long such that the resin has time to infuse the whole mould before it gels.

Filament winding

Shafts for aerodynamic brakes are typically manufactured by filament winding where fibres or tapes are pre-impregnated with a resin and wound on a rotating mandrel.

Internal spars can also be fabricated by filament winding

5.1.5 Quality assurance for blade design and manufacture

The blade manufacturer, not the supplier of the raw materials, controls the final properties of the laminates.

The blade designer shall consider the qualification of FRP materials. Properties to be considered in this context include, but are not limited to:

- stiffness, ultimate and fatigue strength at relevant temperatures
- toughness (at low temperatures if appropriate)
- creep
- ageing characteristics (considering humidity and temperature)
- resistance of wood to rot and fungus

Note that for some materials, some of these properties may not be relevant. Guaranteed property values may be given in terms of:

- manufacturer's nominal value,
- manufacturer's specified value, or
- manufacturer's specified minimum value.

A type approval of a given material, e.g. in accordance with DNV standards, can be used as part of the quality control and design documentation, but is in itself not sufficient for approval of the material for its intended use.

Full-scale tests of a sample blade are required to verify the strength of the blade, statically as well as in fatigue as not all aspects can be covered by the material qualification.

FRP material specimens for testing shall be manufactured with a curing cycle that is representative for the blade and have a representative fibre to resin ratio.

Test specimens should be wide enough to cover at least four repetitions of the structure of the weave/fabric/mat.

Ultimate strength of FRP and wood shall be investigated in both tension and compression. Fatigue testing shall cover both the effects of stress width and the mean stress.

The fibre alignment is important for the load carrying capacity of FRP in compression. The work instructions for blade manufacturing shall control the fibre alignment.

5.1.6 Strength analyses

Structural analyses of the rotor blades must be carried out for all relevant load cases in order to verify that the strength of the blades is sufficient to withstand the loads that these load cases exert on the blades. By the strength calculations in these analyses, it must be verified that both the ultimate strength and the fatigue strength, for a given design life, are sufficient. For structural parts in compression, stability against buckling must also be considered.

For each load case, a set of design loads is established by multiplying the relevant characteristic loads by partial safety factors for load. The standards applied for this purpose should be quoted when the design loads are documented. In principle, each load case can be defined in terms of six load components and their variation over the blade span. The resolution used to specify this variation must be fine enough to allow for sufficiently accurate calculations in all points of interest along the blade, especially in all critical areas, e.g. wherever changes in geometry or material occur.

Environmental conditions, which affect the material behaviour, should be considered and taken into account. In particular, such conditions include humidity and temperature, which may both lead to degradation of strength and stiffness, and their design effects calculated by multiplying characteristic effects by appropriate partial safety factors should be applied in the strength analysis.

Loads on critical components such as tip brakes are often different in character from the general loads on the blades and may thus need extra attention.

As blades are getting larger, large unsupported panels will be present between the webs and the leading and trailing edges. This may have an impact on the stability of the blades. Therefore, the buckling capacity of a blade must be verified by a separate calculation, in addition to the full-scale test. For this calculation, a FEM analysis will normally be required. Furthermore, buckling of the webs may also have to be considered.

As rotor blades become longer, evaluation of the stability against buckling becomes still more important because of the large unstiffened panel segments, which are usually involved.

Standards

The following standards are normally used for verification of wind turbine blades:

- DS472, “Last og sikkerhed for vindmøllekonstruktioner” (“Load and Safety for Wind Turbine Structures”, in Danish), DS472, 1st edition, the Danish Society of Chemical, Civil, Electrical and Mechanical Engineers (Dansk Ingeniørforening), Copenhagen, Denmark, 1992.
- DS456 “Konstruktioner af glasfiberarmeret umættet polyester” (“Structural Use of Glass Fibre Reinforced Unsaturated Polyester”, in Danish), DS456, 1st edition, the Danish Society of Chemical, Civil, Electrical and Mechanical Engineers (Dansk Ingeniørforening), Copenhagen, Denmark, 1985.

Ultimate strength

When the direction of the load is time-dependent, information about phase and frequency should be given. For each section of interest along the blade, the design loads have to be calculated. In principle, all six load components need to be calculated. Normally, the bending moments and the shear forces are most critical, but also the torsional moment and the axial force can, in some cases, be important for the design.

Once the necessary information regarding material strength and stiffness, geometry of blade and lay-up of laminate is established, the capacity of the blade can be calculated section by section. This can be done more or less by hand, or by some calibrated finite element programs. In principle, all six capacity components need to be calculated, e.g. flapwise and edgewise bending moment capacities. When characteristic values for material strength are used as input, characteristic capacity values result. The design capacities are then found by dividing the characteristic capacities by a materials

factor, i.e. a partial safety factor for materials, cf. Section 2.3.

In general, each section of interest along the blade should be checked, as well as all six load components in that section, to ensure that the calculated design load does not exceed the corresponding calculated design capacity.

In this context, the tensile strength $\sigma_{F,T}$ in the direction of the fibres is one of the strengths, which is important to consider. This strength is dominated by the strength $\sigma_{F,B}$ of the fibre bundles. The strength $\sigma_{F,B}$ of a fibre bundle is proportional to the mean failure stress $\bar{\sigma}$ of the individual fibres

$$\sigma_{F,B} = \bar{\sigma} \frac{\exp(1/m)}{m^{1/m} \Gamma(1 + \frac{1}{m})}$$

m material constant

Γ the gamma function

Reference is made to Beaumont and Schultz (1990). The individual fibre strengths σ very often follow a Weibull distribution, however, their mean will under the central limit theorem follow a normal distribution. $\bar{\sigma}$ and hence also $\sigma_{F,T}$ can then be deduced to be normally distributed. The normal distribution prerequisite for $\sigma_{F,T}$ is important when a particular lower-tail quantile of the distribution of $\sigma_{F,T}$ is to be interpreted and used as the characteristic value for $\bar{\sigma}_{F,T}$. Note that very erroneous numbers may result for the characteristic values of $\bar{\sigma}_{F,T}$, if they are interpreted on the basis of a Weibull distribution assumption for $\sigma_{F,T}$.

The characteristic value for a strength property is usually defined as a particular quantile in the probability distribution of the property. This is often a quantile in the

lower tail of the distribution, e.g. the 2% or 5% quantile. Note that different standards may define the characteristic value differently, i.e. it is not always defined as the same percentile in the different standards. Accordingly, different standards may prescribe different partial safety factors to be used with their respective characteristic values for design. As an example, DS472 defines the characteristic value of an FRP material as the 5% quantile and requires a materials factor of 1.7, while DS456 defines the characteristic value as the 10% quantile and requires a materials factor of 1.8. In design, it is essential that the characteristic value of a strength-property in question is combined with the correct partial safety factor. It is not licit to combine the characteristic value of one standard with the partial safety factor of another as this can lead to erroneous results and unsafe designs.

Stability

The longer the blades are, the more likely it is that stability against buckling will govern the design of the blades instead of ultimate strength. The stability against buckling can most easily be verified by calculations by means of a properly calibrated finite element program. Performing such a calibration by hand is more difficult owing to the complex geometry of a rotor blade, and well-proven tools for this purpose, such as closed-form solutions for the buckling capacity, are not available.

When designing for a sufficient stability against buckling, it is a standard approach to apply an extra design margin to take effects of geometrical imperfection, fibre misalignment, workmanship, etc. into account.

Fatigue strength

Sufficient fatigue strength must be documented. This applies to all sections along the blades and to all directions in each location. For this purpose, all load

components should be given in all points of relevance along the blade, including phase and frequency information. This requirement is automatically fulfilled when the six load components are given as time series. From the time series of the six load components, long-term stress distributions can be established in all points of relevance. In principle, this includes distributions of the mean stress as well as distributions of the stress range that represents the variation about the mean stress. Rain-flow counting is a commonly used method for this purpose. The total number of stress cycles in the design life can also be extracted from the time series and can be used to transform the stress range distribution into a design lifetime histogram of stress ranges. A sufficiently fine discretisation of the stress range axis needs to be chosen for this purpose.

In each section of interest along the blade it must be verified that the fatigue strength is not exceeded. This is in practice done by checking that the Miner's sum, calculated for the design stress range histogram in conjunction with the design *S-N* curve, does not exceed a critical value, usually equal to 1.0. See Appendix C for further reference.

Fatigue in edgewise bending is dominated by gravity loads and depends, to a large extent, on the weight of the blade and on the actual number of rotations of the rotor during the design life. Fatigue in flapwise bending is dominated by the blade response to aerodynamic loads exerted by the wind. Note that transient loads during start/stop and loads due to yaw errors may give significant contributions to the cumulative fatigue damage and need to be given thorough consideration in addition to the loads that occur during normal operation. For an example of fatigue calculations and fatigue design, see Section 2.3.7.

Frequency

As a minimum, the two lowest eigenfrequencies of the rotor blade, both in flapwise and edgewise oscillation, should be calculated. These eigenfrequencies should be compared to the rotational frequencies of the wind turbine. A sufficient margin to these frequencies must be available to avoid resonance of the blade. It is recommended to keep the eigenfrequencies outside a range defined as the rotational frequency $\pm 12\%$.

Calibration of design tools

It is essential only to use well-proven and properly calibrated design tools. Especially in case of advanced computer programs, such as finite element programs, it is important to tune or calibrate the results from use of the computer program models against results achieved from full-scale tests on rotor blades, thereby obtaining the models which the best possible reflect reality. As calibration results obtained from a one bladed model cannot automatically be transported and rendered valid for a model of another type of blade, caution must be exercised when it comes to generalisation of model calibration results.

Delamination

Delamination may occur if the shear strength of the fibre reinforced laminate is insufficient to withstand the shear loads that occur in the blades. It is in this context important to consider also a sufficient fibre strength perpendicular to the blade axis.

5.1.7 Tip deflections

A deflection analysis of a blade must be carried out. As part of the deflection analysis it must be proven, for all load cases, that the ultimate tip deflection (caused by a static load or by an interaction of dynamic loading and structural response) is acceptable.

The tip deflection can normally be calculated by means of an aeroelastic

computer code, but it can also be calculated by hand or by some finite element program. Knowing the initial distance from the blade tip to the tower in the no-load condition, this allows for determination of the clearance between the rotor blade and the tower. The clearance should be determined by using the most unfavourable combination of geometrical tolerances and characteristic stiffness properties of the rotor blade and its supports. The effect of damping may be important and should be considered. Further, if the rotor or its supports is subject to creep, shrinkage, temperature deformations or degradation with time, this must be allowed for in the clearance measure.

When comparing the resulting available clearance between the rotor blade tip and the tower, a specified minimum clearance must be met. Danish rules require that the clearance shall be calculated for the characteristic extreme load on the blade times a safety factor of 1.3, and that this clearance shall at least be 0, i.e. the blade shall not hit the tower when subjected to the extreme design load. Dutch rules have a similar requirement, but this is stricter in the sense that the safety factor on the load is to be taken as 1.5 rather than 1.3.

In order to increase the distance between the blade tip and the tower during operation, the rotor can be coned, the blade can be produced with a predeflection, and the rotor plane can be tilted. A tilt angle of about 5° between the rotor axis and the horizontal plane is quite common.

Normally, the stiffness and mass properties of the blade, as used in the tip deflection calculations, have to be verified through the test of the blade.

5.1.8 Lightning protection

Lightning striking a rotor blade may cause damage to the blade such as – in the extreme

case – peeling at the back edge. Lightning protection of rotor blades can, in principle, be designed in two different ways:

- the lightning can be prevented from penetrating into the blade by diverting the current along a prepared current path, such as a conductive tape, on or in the surface of the blade.
- the lightning can be directed from the point of stroke on the blade through the blade by way of a conductor cable.

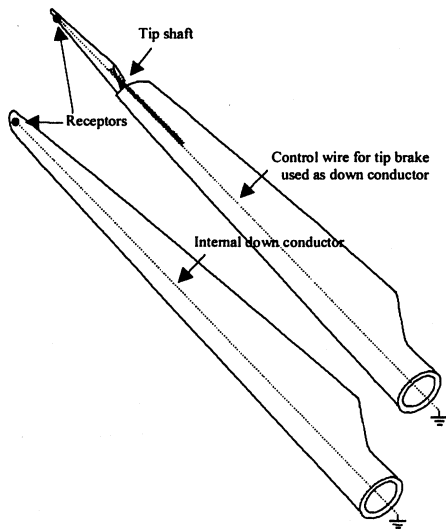


Figure 5-4. Examples of how lightning protection of blades can be arranged From DEFU (1999).

The latter approach is the most common approach. By this approach, a lightning conductor is mounted in the blade tip, and through a commutator lug in the interior of the blade, the current is directed to the blade root. The effectiveness of this method is expected to be highly dependent on the size of the blade and on the amount of metals or carbon fibres used in the blade. Note that a lightning protection like the ones presented here cannot be expected to work in all cases. A blade may be hit by many lightning strokes over its design life, and there may be cases for which the protection will fail, e.g. if the conductor cable fuses. For large

blades, i.e. blades longer than about 20 m, it may be necessary to secure the blades against damage from lightning that strikes the blade in other locations than the blade tip. Note also that it is necessary to account for the limited conductivity of the carbon fibre materials that are used in tip shafts. From the aircraft industry, methods exist for lightning protection of glass fibre and carbon fibre materials by which these materials are made electrically conductive by means of metallic sheets, nets, or threads, rather than by mounting metallic conductors on the material surfaces. Reference is made to DEFU (1999). Examples are shown in Figure 5-4.

5.1.9 Blade testing

The purpose of rotor blade testing is to verify that the laminates in the blade are structurally safe, i.e. that the plies of the rotor blade do not separate by delamination in static or cyclic loading. The purpose is also to verify that the fibres do not fail under repeated loading. Full-scale blades are used for the rotor blade tests, and tests are carried out for verification of fatigue strength as well as static strength.

For every new type of blade to be manufactured, one blade is to be tested statically and dynamically to verify the strength of the blade design.

The production of a test blade is to be inspected in order to verify that the blade is representative of the blade design. Alternatively, the blade may be sampled at random from the blade production. However, this alternative approach is usually not feasible, because it is often desirable to carry out the blade test in the early phases of a production. Therefore, the test blade is often selected on a deterministic basis as one of the first blades in the production series.

The test blade is to be equipped with strain gauges and displacement transducers. The measurement results from the strain gauges are continuously monitored on computers. Nonlinear variations in the pattern of bending may reveal a damage in the rotor blade structure.

The blade is to be tested statically by a static load in two opposite directions flapwise and in two opposite directions edgewise. The static load must at least equal the extreme design load. Tests in two opposite directions instead of just in one direction are necessary due to lack of symmetry in the blade. Measurements by means of the strain gauges and displacement transducers are used to monitor and verify that the strains and displacements stay within the design limits and design calculations during the entire test. Nonlinearity in the measured strains may indicate buckling or damage to the blade.

Dynamic testing is also carried out for loading in both flapwise and edgewise directions. Normally, the blade is tested for loading in one direction at a time, but a load with simultaneous components in both directions may also be applied. The dynamic testing is carried out as an accelerated test, i.e. at a load level, which causes the same damage to the blade as the true load spectrum, including a test factor of 1.3. Normally, the test is carried out at a fixed load level and for a number of load cycles of between $2 \cdot 10^6$ and $5 \cdot 10^6$ cycles.

Infrared cameras can be used to reveal local build-up of heat in the blade. This may either indicate an area with structural damping, i.e. an area where the blade designer has deliberately laid out fibres which convert the bending energy into heat in order to stabilise the blade, or it may indicate a zone of delamination, or a zone where the fibres are close to failure.

Furthermore, the lowest natural frequencies and corresponding damping ratios of the blade are measured as these are important input parameters for the load calculations. This is achieved by excitation of the blade at different frequencies and in different directions. It is essential that the natural frequencies of the blade do not coincide with the rotational frequencies of the wind turbine. The purpose of this part of the test is to make sure that the natural frequencies of the blade differ from the rotational frequency with sufficient margin. Note that the aerodynamic damping is also measured, in particular, in the flapwise direction.

In case the natural damping of the blade is insufficient to avoid vibrations, e.g. edgewise vibrations, a damper may be built into the blade. The damper may consist of materials with high internal damping, which is built into the blade, or it may be a mechanical damper. It is essential that this damper is also included in the test blade, since the design of the connection between the damper and the blade may introduce weak areas or large stiffness changes.

A rotor blade can also be tested for its residual static strength (and thus its ability to withstand extreme loads in the long term) by being bent once by a very large force. The magnitude of this force is usually determined by the load level of the static test described above. The residual strength test is usually performed after the blade has been subject to fatigue testing, and the purpose is to verify that the static strength of a blade, which has been in operation for a substantial amount of time, is sufficient and that the stiffness – although it may have changed – is still acceptable.

A test specification for the blade test should be worked out. The specification should specify the loads and the measurement set-up, including means of avoiding overload of

the blade. This is an important aspect, as the dynamic test is normally carried out at a frequency close to the lowest flapwise/edgewise natural frequency, at which even small variations in the energy input may significantly alter the load amplitude. The test loads must be determined in such a way that it is ensured that major parts of the blade are tested to the required load level. Note that in case the test is running outdoor, weather conditions such as sun and rain may influence the resulting blade deflections.

During testing the stiffness of the test rig must be considered. Ideally, the stiffness of the test rig should be comparable to that of the blade hub connection when the blade is installed on the turbine. As a minimum, the stiffness of the test rig must be measured to allow for adjustment of the measured deflections.

Guidance on blade testing is given in IEC 61400-23 TS Ed. 1: “Wind turbine generator systems - Part 23. Full-scale structural testing of rotor blades for WTGS’s”.

5.1.10 Maintenance

The blade should be kept clean to ensure that the aerodynamic properties of the blade remain unchanged.

5.2 Hub

The hub is the fixture for attaching the blades to the rotor shaft. It usually consists of nodular cast iron components for distribution of the blade loads to the wind support structure, i.e. ultimately to the tower. A major reason for using cast iron is the complex shape of the hub, which makes it hard to produce in any other way. In addition hereto, it must be highly resistant to metal fatigue. Thus, any welded hub structure is regarded as less feasible.

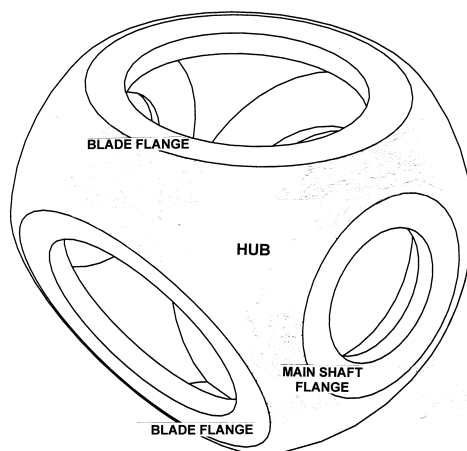


Figure 5-5. View of wind turbine hub.

The moments and forces transmitted to the hub and tower depend on the type of hub. Three types of hub are common:

- hingeless rigid hub, has cantilevered blades and transmits all moments to the tower.
- teetering rotor, has two rigidly connected blades supported by a teeter-pin joint, which can only transmit in-plane moments to the hub. Flapwise moments are not transmitted.
- articulated hub, has free hinges in flapping and lead-lag, so there is no mechanical restraint moment on the blades in either flapping or lead-lag.

The hingeless hub is the most common configuration for wind turbine hubs.

Figure 5-5 shows an example of such a hub, and Figure 5-6 and Figure 5-7 show the hub in the context of the transmission system, in which it forms part of the link between the rotor blades and the generator. Figure 5-6 and Figure 5-7 provide examples of two different bearing arrangements with one and two main bearings, respectively. For details, see Section 6.2.

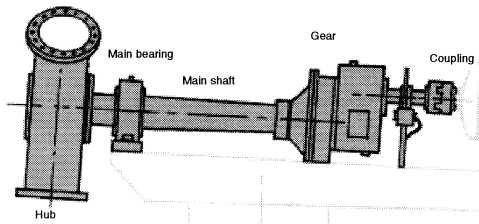


Figure 5-6. Transmission system consisting of hub, one main bearing, main shaft, gear and coupling. Courtesy Bonus Energy A/S.

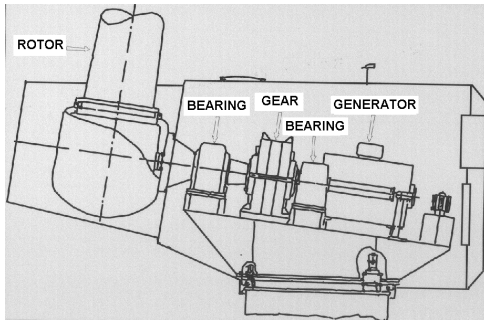


Figure 5-7. Transmission system consisting of hub, two main bearings, main shaft and gear, and with the generator marked out.

5.2.1 Determination of design loads

The loads at the blade-hub interfaces to be considered at the blade root for design of the hub consist of the following:

- full flapping moment
- flapping shear, resulting thrust on one blade
- lead-lag moment, power torque of one blade, and gravity loads
- lead-lag shear, in-plane force that produces power torque
- centrifugal forces
- pitching moments of one blade

Design loads can be calculated from the blade loads in accordance with this list.

Obviously, it is structurally beneficial to reduce the loads at the blade-hub interfaces, in particular, the large blade-flapping moment. The blade-root flapping moment can be traded off against tip deflection.

Flexible blades have the advantage of relieving some of the load into centrifugal terms. Since yaw stability and fatigue life are both significantly affected by blade flexibility, other considerations apply in this context.

The hub should be constructed in such a way that it will be possible to adjust the tip angle of the blade and tighten up the bolt connections.

5.2.2 Strength Analysis

Cast components should be designed with smooth transitions and fillets in order to limit geometrical stress concentrations.

The characteristic resistance for cast iron components can be taken as the 5th or 95th percentile of test results, whichever is the most unfavourable.

The structural resistance in the ultimate limit state is to be determined by elastic theory. When design is carried out according to the allowable stress method, the maximum allowable stress should be taken as the characteristic resistance divided by a safety factor.

Fatigue design can be carried out by methods based on fatigue tests and cumulative damage analysis. When design is carried out according to the allowable stress method, the allowable fatigue stress range is to be taken as the characteristic resistance divided by a safety factor. The characteristic resistance for a given number of cycles to failure is defined as the stress range that corresponds to 95% survival probability. The characteristic resistance should be modified to account for size effects, surface conditions and mean stress. When limited test data are available for estimation of the characteristic resistance, the characteristic resistance should be given with 95% confidence.

The layout of a wind turbine hub often makes it difficult to determine which section is the structurally most critical section of the hub. In this context, the Finite Element Method (FEM) forms a suitable tool for strength analysis of the hub and can be used in conjunction with state-of-the-art fatigue analysis techniques to determine the fatigue life and to optimise the design with respect to strength and cost. It is advisable to qualify the loading assumptions for such FEM analyses by measurements.

The FEM analyses can, in particular, be used to document that a satisfactory strength is available in critical sections, such as at stress concentrations and stiffness transitions, as well as at the shaft-hub connection and the interfaces to the blades.

5.2.3 Analysis of bolt connections

The blades are usually bolted to the hub. There are two techniques for mounting the bolts in the blades:

- a flange is established at the blade root by moulding the glass fibre reinforced plastics to form a ring, in which steel bushes for the bolts are embedded.
- treaded steel bushes are mounted directly into the blade root and fixed to the blade by glue.

In both cases, the bolts from the blade pass through a flange on the cast hub. The bolt holes in this flange can be made somewhat elongated to enable adjustment of the tip angle.

For these bolt connections, a bolt tension procedure is usually required. Such a procedure should usually specify:

- bolt, nut, washer type, dimension and quality
- flatness tolerances for surfaces
- roughness of surface
- surface treatment and protection
- bolt tensioning sequence and method

- treatment of treads, e.g. waxing
- torque to be applied

The relation between bolt torque and bolt tension may be subject to test.

5.2.4 Hub enclosure

The hub enclosure, which is sometimes referred to as the nose cone, is usually made of glass fibre reinforced polyester. In cases where the hub enclosure is large, it is recommended to consider the wind load it will be exposed to.

5.2.5 Materials

Spheroidal graphite cast iron, also known as nodular cast iron, is the preferred material for the hub. Cast iron is classified according to its mechanical properties, such as strength and hardness, in EN1563. Cast hubs are usually tested by non-destructive testing (NDT) for verification of the mechanical properties and for detection of possible defects and internal discontinuities. The following NDT methods are available:

- ultrasonic inspection
- magnetic particle inspection
- visual inspection
- hardness measurements

Ultrasonic inspection can be carried out as point testing or, more thoroughly, as complete scanning. For ultrasonic inspection, it is common to assign different acceptance criteria, e.g. in terms of different allowable defect sizes, to different areas of the cast hub. These areas and the assigned acceptance criteria should be indicated on the drawing of the casting. Usually, a strict acceptance criterion is assigned to an area with high stresses, whereas a more lax acceptance criterion is assigned to an area with low stresses. The stricter the acceptance criterion is in a particular area, the more thorough is the ultrasonic inspection in that area, and the stricter are the requirements to the allowable size of detected discontinuities.

It is important to consider whether the chosen structural material possesses the necessary ductility. Low temperatures can be critical for cast hubs in this respect, and the choice of hub material should, therefore, be made with due consideration to the temperatures of the surroundings.

Note that repair of cast hubs by means of welding is not permitted.

5.2.6 Standards

EN1563 Founding – Spheroidal graphite cast irons. CEN, 1997.

EN1369 Founding – Magnetic particle inspection. European Standard. CEN, 1996.

REFERENCES

Beaumont, P.W.R., and J.M. Schultz, “Statistical Aspects of Fracture,” Chapter 4.6 in *Failure Analysis of Composite Materials*, Volume 4, ed. by P.W.R. Beaumont, J.M. Schultz, and K. Friedrich, Technomic Publishing Co., Inc., Lancaster, Penn., 1990.

Danske Elværkers Forenings Undersøgelser (DEFU), *Lynbeskyttelse af vindmøller. Del 7: Vinger* DEFU Report No. TR394-7 (in Danish), 1999.

DNV, *Rules for Classification of High Speed and Light Craft, Materials and Welding*, Part 2, Chapter 4, Composite Materials, Det Norske Veritas, Høvik, Norway, 1999.

Hück, M., *Berechnung von Wöhlerlinien für Bauteile aus Stahl, Stahlguss und Grauguss*, Verein Deutscher Eisenhüttenleute Bericht Nr. ABF 11 (in German), July 1983.

Hück, M., W. Schütz, and H. Walter, “Modern Fatigue Data for Dimensioning Vehicle Components of Ductile and Malleable Cast Iron,” first published in *Automobiltechnische Zeitschrift* 86, Nos. 7, 8 and 9, 1984.

Mayer, R.M. “Design with reinforced plastics”, The Design Council, London, 1992.

6. Nacelle

6.1 Main shaft

The main shaft transmits the rotational energy from the rotor hub to the gearbox or directly to the generator. Moreover, the purpose of the main shaft is to transfer loads to the fixed system of the nacelle. In addition to the aerodynamic loads from the rotor, the main shaft is exposed to gravitational loads and reactions from bearings and gear.

The main shaft is also subjected to torsional vibrations in the drive train. Such vibrations will usually be of importance to possible frictional couplings like shrink fit couplings between shaft and gear.

A wind turbine can be exposed to large transient loads. Therefore, it has to be considered whether the chosen structural material possesses the necessary ductility. This is particularly important if the turbine is to be operated at low temperatures. Since corrosion may imply a considerable reduction of the assumed fatigue capacity, it should be ensured that the shaft is protected against corrosion. Suitable quality assurance should be implemented to make sure that the geometrical and mechanical assumptions for the design are fulfilled, e.g. surface roughness, that the specified values of material parameters are met, and that the imperfections of the material do not exceed any critical level.

6.1.1 Determination of design loads

In the following, it is assumed that all relevant load cases are taken into consideration. Selection of the relevant load cases and determination of the characteristic values of the individual load components on the rotor can be made according to procedures given in Sections 4.4 - 4.8 for both extreme loads and fatigue loads.

Figure 6-1 illustrates the loads and reactions that the main shaft is subjected to. Under normal circumstances, reactions in the main shaft can be calculated from equilibrium considerations.

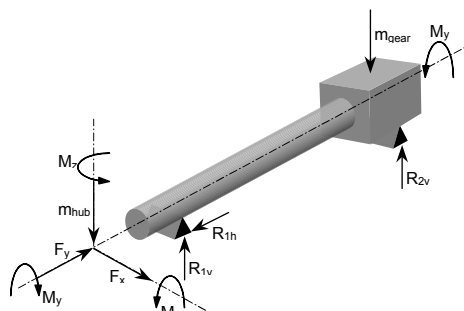


Figure 6-1. Loads and reactions on the main shaft.

For each load case, a set of design loads are established by multiplying the relevant characteristic loads by a partial safety factor for loads. The loads can be combined by simple superposition.

Fatigue loads consist of histories of stress amplitudes. One history per load component exists. Hence, a combination of fatigue loads implies a combination of stress histories. Unless the phase differences between the individual load components are known, the largest stress amplitude of one load component is to be added to the largest stress amplitude of each of the other load components, the second largest amplitude is to be added to the second largest amplitude of each of the other load components, and so forth.

6.1.2 Strength analysis

Structural analysis of the main shaft shall be carried out for all relevant load cases in order to verify that the strength of the shaft is sufficient to withstand the loads to which it is subjected.

It shall be verified that both the ultimate strength and the fatigue strength are sufficient for the actual design life.

6.1.3 Fatigue strength

The fatigue strength can be expressed in terms of the particular stress amplitude that leads to failure after a specified number of constant-amplitude stress cycles. This can be expressed in terms of an $S-N$ curve, also known as a Wöhler curve, which gives the number of cycles N to failure at stress amplitude S .

Various factors influence the strength relative to reference values determined from small specimens in laboratory tests, and may lead to a reduction of this strength. In this respect, the following elements of importance should, as a minimum, be considered:

- technological size effect
- geometrical size effect
- surface roughness
- stress concentrations
- stress ratio R , defined as the ratio between the minimum stress and the maximum stress with tensile stresses defined as positive and compressive stresses as negative.

Technological size effect

Reduction due to the technological size effect is based on the fact that specimens of identical dimensions, made of materials of the same kind but of different dimensions, have different fatigue properties. Test specimens are made with relatively small dimensions (typical diameter $d = 5-10$ mm) and have had their mechanical properties improved as a result of the reduction of the cross-section by forging or rolling. The technological size effect can be accounted for by means of the influence factor K_1 , applied to the fatigue strength. K_1 can be determined from Figure 6-2.

Geometrical size effect

The reduction due to the geometrical size effect is based on the fact that specimens of different dimensions exhibit differences in their fatigue properties, despite the fact that they are made of materials of identical initial dimensions. This can be accounted for by means of the influence factor K_2 , applied to the fatigue strength. K_2 can be determined from Figure 6-3. If fatigue strength in pure tension-compression is considered as a basis for the calculations, K_2 can be set equal to 1.

Effects of surface roughness

Fatigue cracks are often initiated from unevenness in the surface and from small surface cracks. An ideal “reference surface” for the test specimens corresponds to a polished surface with a surface roughness of $R_a = 0.05-0.1\mu\text{m}$. The surface roughness that can be expected from a careful machining is $R_a = 0.4-1.6\mu\text{m}$. A reduction factor K_r to account for the effect of surface conditions deviating from the reference surface can be determined from Figure 6-4.

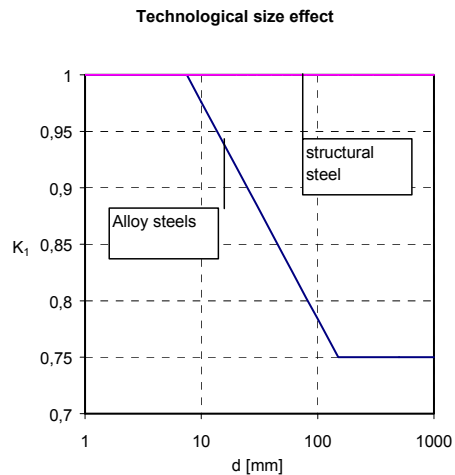


Figure 6-2. Technological size effect (d denotes diameter of considered part of shaft), from Roloff and Matek (1994).

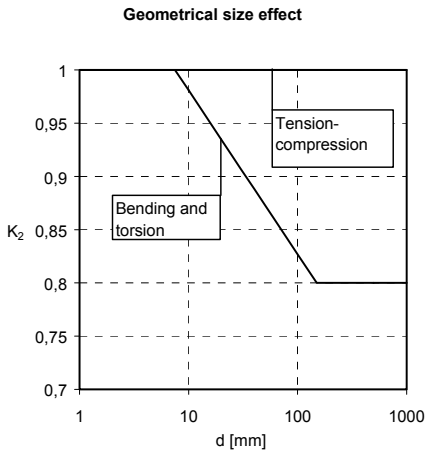


Figure 6-3. Geometrical size effect (d denotes diameter of considered part of shaft), from Roloff and Matek (1994).

Note that R_a denotes an average surface roughness. In some literature on the subject, the peak surface roughness R_z is given rather than R_a . There is no unambiguous relation between R_a and R_z , but for preliminary calculations one may consider the peak surface roughness R_z equal to approximately 6 times R_a .

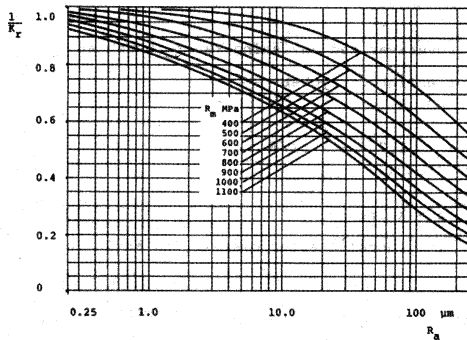


Figure 6-4. Reduction factor K_R vs. surface roughness R_a , from Sundström (1998).

Stress concentrations

Stress concentrations will occur at local changes in geometry, e.g. where cross-sections alter. This is also the case at shrink

fit couplings and tight bearing fits. A considerably amount of stress concentration factors for various common shapes are given in Peterson (1974). The sensitivity of the material to such stress concentrations depends primarily on the ratio between the yield strength and ultimate strength of the material, and on the stress gradient in the considered part of the structure. This so-called notch sensitivity can be accounted for by means of the notch sensitivity factor q

$$q = \frac{1}{1 + \sqrt{A/\rho}}$$

- ρ notch radius
- A Neuber factor, which can be determined from Figure 6-5

Note that the notch radius appears as “rc” in the drawing in Figure 6-6.

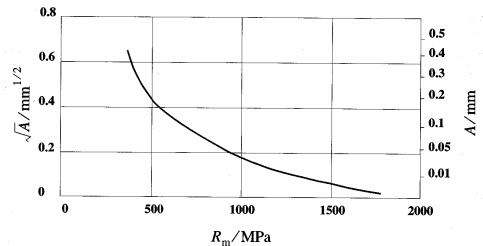


Figure 6-5. Notch sensitivity factor q , from Sundström (1998).

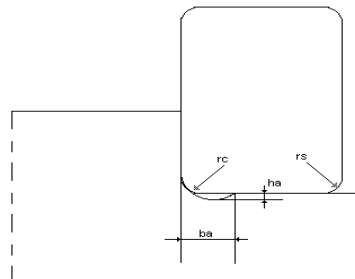


Figure 6-6. Shaft lay-out in vicinity of bearings, from SKF (1989).

Whenever a notch is encountered, the notch sensitivity factor q can be used to convert the stress concentration factor α into a notch factor β to be used instead

$$\beta = 1 + q(\alpha - 1)$$

A commonly encountered notch is found by the recess, which is to transfer the axial load from a main bearing. A common lay-out of a shaft in the vicinity of bearings is shown in Figure 6-6, and data for the involved geometrical quantities are given in Table 6-1.

Table 6-1.

r_s Mm	b_a Mm	h_a mm	r_c mm
1	2	0.2	1.3
1.1	2.4	0.3	1.5
1.5	3.2	0.4	2
2	4	0.5	2.5
2.1	4	0.5	2.5
3	4.7	0.5	3
4	5.9	0.5	4
5	7.4	0.6	5
6	8.6	0.6	6
7.5	10	0.6	7

Stress concentration factor, bending

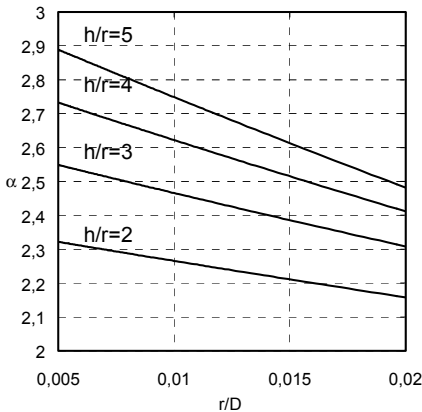


Figure 6-7. Stress concentration factor, from Roloff and Matek (1994).

The geometrical stress concentration factor is denoted α and can be determined from Figure 6-7 and Figure 6-8.

Stress concentration factor, torsion

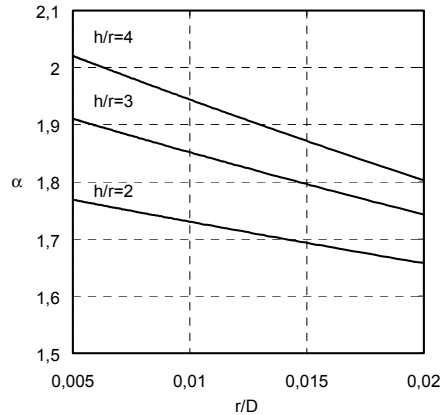


Figure 6-8. Stress concentration factor, from Roloff and Matek (1994).

The following symbols are used in the figures:

- D Larger diameter of shaft
- d Smaller diameter of shaft
- h $(D-d)/2$
- r radius of notch

Stress concentrations due to tight bearing fits, corresponding to the ISO 286 shaft tolerances from m to r , can be accounted for by a stress concentration factor $\alpha = 1.1-1.2$.

For shrink fit couplings a stress concentration factor $\alpha = 1.7-2.0$ can be used.

Influence of mean stress

Most material data are obtained from tests carried out as either fully reversed bending tests or as pulsating tension-compression tests, i.e. the stress ratio $R = \sigma_{\min}/\sigma_{\max}$ is -1 . For tests in torsion, R is usually equal to -1 . When other stress ratios prevail than those represented in available tests, it may be

necessary to reduce the maximum allowable stress range. However, for main shafts the stress ratio often assumes values near to –1 such that it may not be necessary to consider any such reduction. In more accurate calculations, one may take into account the influence of the mean stress by means of methods available for this purpose, e.g. a Haig diagram. Reference is made to Gudehus and Zenner (1999), Bergmann and Thumser (1999) and VDI.

Fatigue resistance and characteristic $S-N$ curve

In lack of endurance tests of the actual material, a number of different methods to establish a synthetic characteristic $S-N$ curve are available. Each method has its own advantages and disadvantages. Some of the methods can be found in Gudehus and Zenner (1999), Bergmann and Thumser (1999) and Sundström (1998). General aspects of fatigue calculation can be found in Appendix C. In general, it is not recommended to combine two different methods because this may cause the assessment of the overall safety level to become nontransparent.

In the following, one of several methods for establishment of a characteristic $S-N$ curve will be referenced, which is simple and suitable for preliminary calculations.

It may be difficult to establish $S-N$ curves for alloy steel. If test data are available, the test assumptions are often not documented. If reliable $S-N$ curves for the applied steel quality are not available, a synthetic $S-N$ curve may be used, based on static strength data for the material in conjunction with fatigue strength σ_D under rotational bending and torsion (and possibly tension-compression). Such data are always available for standard reference materials. When σ_D is not available for the actual material, one may for tension-compression

use the following estimate, which refers to the mean $S-N$ curve with 50% failure probability

$$\sigma_{D50\%} = (0.436 \times R_e + 77)$$

R_e yield strength in MPa

$\sigma_{D50\%}$ in units of MPa applies to polished test specimens of small dimensions, 7-10 mm, made of mild steel or low-alloy steel.

To achieve results corresponding to 2.3% failure probability rather than 50% failure probability, $\sigma_{D50\%}$ has to be reduced as follows

$$\sigma_{D2.3\%} = \sigma_{D50\%} - 2 \cdot s$$

in which s represents a standard deviation. For mild steel and low-alloy steel, s can be taken as 6% of $\sigma_{D50\%}$, see Sundström (1998).

Determination of design $S-N$ curve

On a $\log S - \log N$ scale, the $S-N$ curve can be considered linearly decreasing from $(10, R_m)$ to $(10^6, \sigma_D)$, where R_m denotes the ultimate strength. For $N > 10^6$, the curve may be taken as a horizontal line at $S = \sigma_D$.

Stresses exceeding the yield stress R_e are usually not allowed in a structure subjected to fatigue loading. Consequently, the $S-N$ curve is cut off at R_e .

Due to the variation of the influence factors from point to point within the shaft, the $S-N$ curve to be used for the actual shaft is unique for each individual location considered within the shaft.

One may, conservatively, use the following design rules

$$\sigma \cdot \gamma_f < \sigma_{D2.3\%} \cdot K_1 \cdot K_2 / (K_r \cdot \beta \cdot \gamma_m)$$

$$\tau \cdot \gamma_f < \tau_{D2.3\%} \cdot K_1 \cdot K_2 / (K_r \cdot \beta \cdot \gamma_m)$$

in which σ and τ are the actual characteristic normal stress and torsional stress, respectively, in the observed cross-section. $\sigma_{D2.3\%}$ is the characteristic value for the endurance limit, calculated from $\sigma_{D50\%}$ as specified above.

For the notch factor β , a somewhat better approximation can be achieved by accounting for the smaller sensitivity of the material to notches at lower numbers of cycles. At $N = 10$ one can set $\beta = 1$ and then let β increase linearly with $\log N$ to $\beta = 1 + q(\alpha - 1)$ at $N = 10^6$ as shown in Figure 6-9.

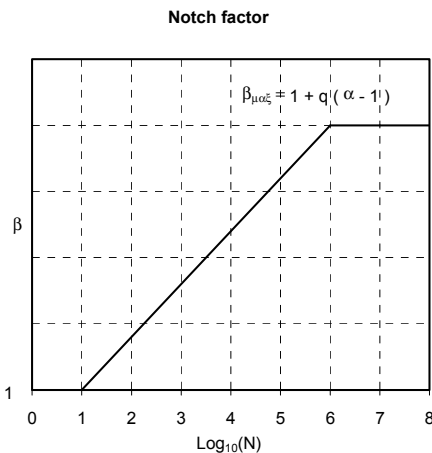


Figure 6-9. Notch factor.

Fatigue loads are usually specified in terms of a distribution of stress amplitudes, i.e. a so-called load spectrum, which on discretised form gives the number of stress cycles in each interval of a suitably discretised stress amplitude axis. The stress cycles in each stress amplitude interval contribute to the total fatigue damage. The total fatigue damage can be calculated by Palmgren-Miner’s method and has to be less than 1.0 in order to ensure a sufficiently low failure probability in the design life of the shaft. Reference is also made to Appendix C.

For main shafts, both bending and torsion occur at the same time. One can take this into account by using the reference stress

$$\sigma_{i,ref} = \sqrt{\sigma_i^2 + 3\tau_i^2}$$

in which σ_i is the normal stress, and τ_i is the torsional stress. As the bending stress is oscillating with a stress ratio near -1 , while the shear stress is oscillating with a positive stress ratio between 0 and approximately 0.8, use of the reference stress $\sigma_{i,ref}$ implies an approximation. A more accurate approach can be found in Gudehus and Zenner (1999).

6.1.4 Ultimate strength

Stress calculation is to be carried out according to standard mechanical engineering methods and is usually straightforward. For materials with a high ultimate strength, it may be necessary to account for stress concentration in extreme load cases. The influence of the ultimate strength can be accounted for by the following factor

$$\beta_{extreme} = 1 + (\alpha - 1) \cdot (R_m / 1000)^2$$

R_m ultimate strength in Mpa

α stress concentration factor taken from Figure 6-7 and Figure 6-8

The following criterion is to be fulfilled in design

$$\sigma \cdot \gamma < R_e / (\gamma_m \cdot \beta_{extreme})$$

σ actual stress in the observed section

R_e yield strength

For stress ratios > 0 and dissimilar stress distribution, a plastic strain up to 0.2% may be allowed for single extreme load cycles. Reference is made to Gudehus and Zenner (1999). The amount of plastic strain may be estimated from Neuber’s correction, see

Gudehus and Zenner (1999) and Sundström (1998). For repetitive extreme load cycles with stress ratios < 0 , a low-cycle fatigue calculation should be conducted, see Gudehus and Zenner (1999) and Sundström (1998).

Partial safety factors

The requested safety level is normally achieved by multiplying the characteristic loads by a load safety factor γ_f and reducing the characteristic material properties with a material safety factor γ_m .

The load safety factor accounts for the random nature of the load components (e.g. fatigue loads, extreme loads, gravitational loads, etc.) and the uncertainty in the calculation method. The material safety factor accounts for the scatter in the material properties and for the level of quality control of the material.

The values of these safety factors are normally given in the relevant wind turbine regulations, e.g. DS472, and in the associated material standards. For machine components, the certifying bodies or the owner sometimes define their own values for γ_m .

6.1.5 Main shaft-gear connection

In cases where the main shaft does not constitute an integral part of the gear and in cases where it forms the generator shaft in multi-polar generators, the main shaft should somehow be connected to the transmission input shaft. Formerly, hollow-axis gears were used by which the torsional moment was transferred from the main shaft to the shaft bushing of the gear by means of a keyway connection. This principle for torsional moment transfer has now been abandoned, except for small simple wind turbines, as keyway connections are only poorly suited to transfer varying and reversing loads. Assembly and dismantling

can also be difficult. Usually, some kind of shrink fit coupling is used, e.g. in conjunction with a shrink disk.

Shrink disks

A correct functioning of clamp couplings requires careful dimensioning and assembly. If the coupling, in addition to torque, also is to transfer bending moments, it is important to include this in the calculations. When applying catalogue values for transferred torque, it is recommended to apply a safety factor of 1.5 to the peak torque in order to be on the safe side.

To achieve the prescribed level of safety, it is important to make sure that the roughness conditions of the surface and the tolerances for both parts are in accordance with the recommendations of the manufacturer. During assembly, correct bolt pretensions shall be applied, and the required cleanness of the frictional surfaces shall be accounted for.

Couplings

In certain cases where the gear is rigidly mounted on the machine foundation, a coupling is applied which can only transfer torque and which is flexible with respect to bending moments. In these cases, the hub parts of the couplings are usually shrunk both on main shaft and on gear shaft. Insofar as regards the design of the coupling itself, reference is made to special literature.

6.1.6 Materials

In most cases, non- or low-alloyed machinery steels are used, i.e. steel with a carbon content of 0.3-0.7% and with less than 5% alloy of metals such as Mn, Cr, Mo, Ni and V.

This classification covers steel with rather different mechanical properties, ranging from non-alloyed steel with an ultimate strength of about 500 MPa and failure

elongation of 15% to low-alloyed steel with an ultimate strength of up to 1500 MPa and failure elongation less than 10%.

In addition to obtaining an adequate ultimate strength, the material should exhibit a high fracture toughness and a low brittle transition temperature. Steel within this category is standardised in DIN 17200.

Such steel is suitable also as a basis for forged materials for main shafts. This is a very common design approach, which implies an improvement of the structure and a good transition to the flange for the rotor hub.

In some cases, cast main shafts are used. The casting provides a great degree of freedom as far as the shaping of the shafts is concerned, whereas it poses some limits in terms of relatively low ultimate strength and failure elongation.

Usually, nodular iron in the qualities GGG.40 or GGG.50, according to DIN 1693, is used.

The main shaft is one of the most critical components in a wind turbine structure. Thus, it is important to make sure, by means of appropriate quality assurance, that the assumed material quality is met, and that the manufacturing has not caused development of surface cracks or other imperfections. This implies that the material is checked for imperfections by some suitable non-destructive testing procedure, such as ultrasonic testing, and that the shaft is delivered with a materials certificate.

6.1.7 Standards

Materials:

Structural steels EN 10 025

Tempered steels DIN 17200

Nodular irons DIN 1693, Parts 1 and 2.

Technical terms of delivery and testing:

DIN 1690, Parts 1 and 2, DIN 54111, Part 2.
Magnetic particle inspection SIS 114401;
Capillary Liquid Testing: Non-destructive Testing, PI-4-2 Liquid Penetrant testing.
General Dynamics.

Certificates:

EN 10 204.

6.2 Main Bearing

The main bearing of a wind turbine supports the main shaft and transmits the reactions from the rotor loads to the machine frame. On account of the relatively large deformations in the main shaft and its supports, the spherical roller bearing type is often used, see Figure 6-10 for an example.

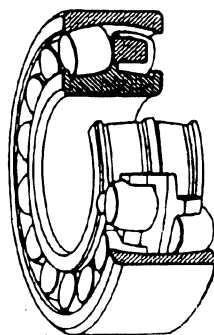


Figure 6-10. Spherical roller bearing, from Bonus (1999).

Spherical roller bearings have two rows of rollers with a common sphered raceway in the outer ring. The two inner ring raceways are inclined at an angle to the bearing axis. The bearings are self-aligning and consequently insensitive to errors in respect of alignment of the shaft relative to the housing and to shaft bending. In addition to high radial load capacity, the bearings can accommodate axial loads in both directions.

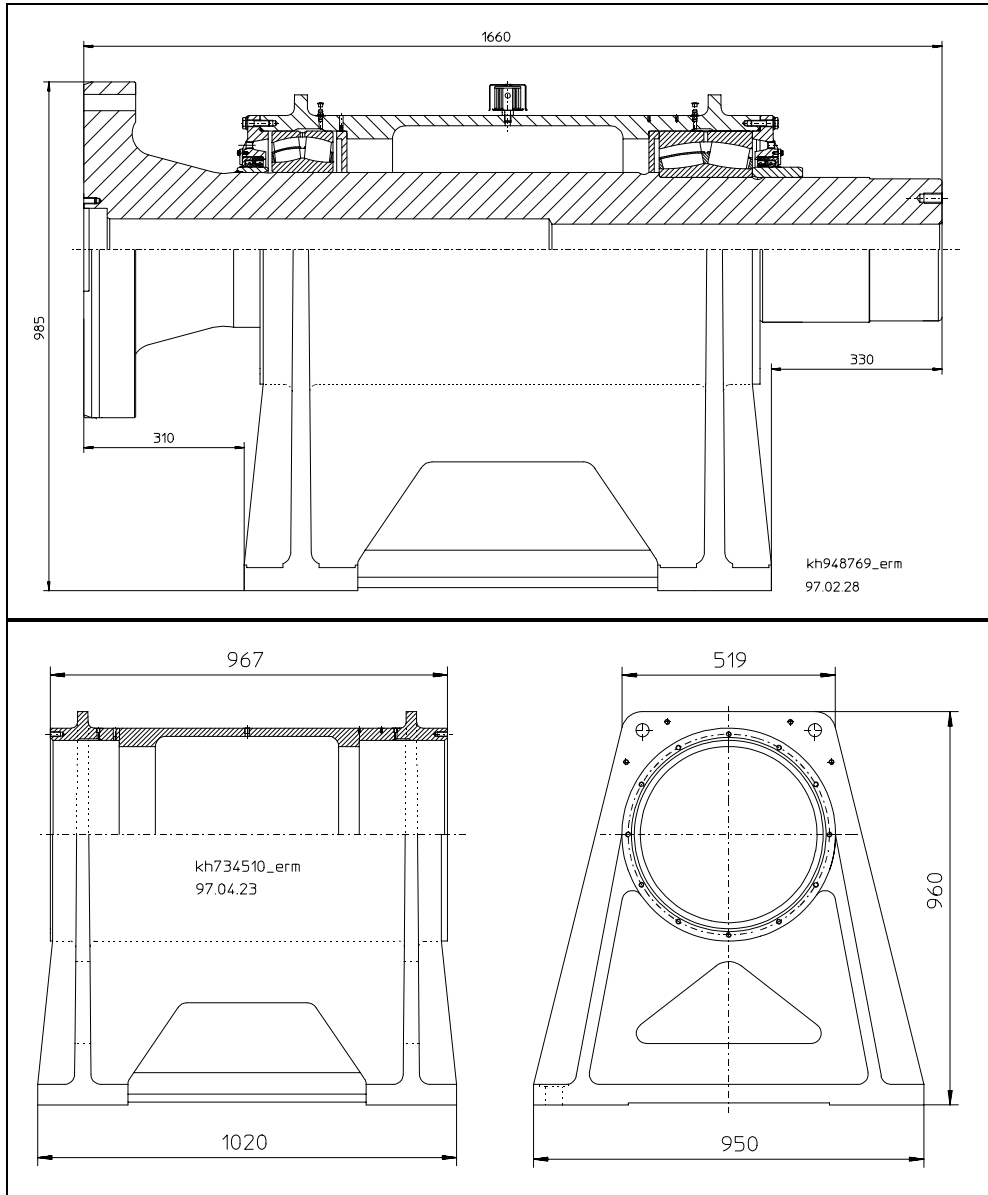


Figure 6-11. Bearing frame with main shaft and bearing arrangement for wind turbine with two main bearings; courtesy Vestas.

The allowable angular misalignment is normally 1-2.5 degrees depending on the bearing series. This is sufficient to compensate for deformations in shafts, housing and machine frame caused by the

rotor loads and, subsequently, to prevent excessive edge loads, which would result in possible damage to the bearing.

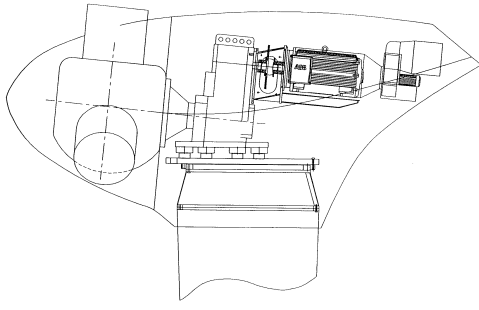


Figure 6-12. Nacelle with transmission system for which the main bearing is integrated in the gearbox. Courtesy NEG Micon.

The main bearings are mounted in bearing housings bolted to the main frame. The quantity of bearings vary among the different types of wind turbines. Many wind turbines have two bearings, each with its own flanged bearing housing. Some turbines with two bearings use the hub as a housing. Some turbines have only one main bearing, given that the gearbox functions as a second main bearing. Each bearing arrangement has its own advantages and disadvantages. Figure 6-11 shows an example of the main shaft and bearing arrangement for a turbine with two main bearings in the same housing. Two other examples are given in Figure 6-12 and Figure 6-13. A couple of additional examples appear from illustrations of the hub and transmission system in Section 5.2.

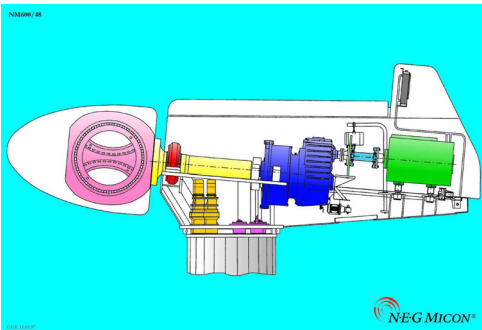


Figure 6-13. Nacelle with transmission system with two main bearings. The second bearing on the main shaft forms the foremost bearing in the gearbox. This

arrangement makes it easy to replace the gearbox. Courtesy NEG Micon.

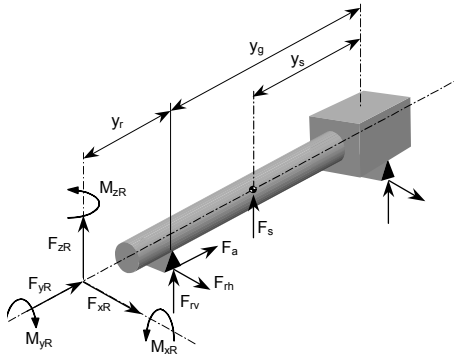


Figure 6-14. Main shaft.

F_{xR}	side force on rotor and nacelle
F_{yR}	thrust on rotor
F_{zR}	weight of rotor
M_{xR}	tilting moment at rotor
M_{yR}	driving torque at rotor
M_{zR}	yaw moment at rotor
F_s	shaft mass
y_r	distance rotor to bearing centre
y_g	distance bearing centre to gear stay
y_s	distance shaft centre of gravity to gear stay

6.2.1 Determination of design loads

Figure 6-14 shows the conventional design of a rotor shaft. The shaft is supported by a bearing placed adjacent to the rotor. Another bearing at the opposite end of the rotor shaft is integrated in the main gearbox.

The loads in Figure 6-14 are drawn in directions according to a conventional coordinate system, and not in the direction that they will normally have.

From the example in Figure 6-14, the front main bearing loads can be calculated from simple beam theory as

$$F_a = -F_{yR}$$

$$F_r = \frac{1}{y_g} \sqrt{M_1^2 + M_2^2}$$

with

$$M_1 = M_{xR} - F_S y_S - F_{zR} (y_r + y_g)$$

$$M_2 = F_{xR} (y_r + y_g) + M_{zR}$$

The loads are usually specified in terms of a load spectrum or distribution of loads, which on discretised form gives the number of hours of operation within each defined load interval in the discretisation. For each interval, the associated operational and environmental conditions have to be taken into account. All relevant load cases are to be included in this load spectrum.

6.2.2 Selection of bearing types

The main bearing must be able to accommodate axial as well as radial forces from the rotor. Further, the bearing must allow misalignment from deflection of the shaft and the support. These requirements are fulfilled by means of spherical roller bearings, see Figure 6-10.

6.2.3 Operational and environmental conditions

The main shaft speed range of a conventional wind turbine of rated power in the range 500-2500 kW is about 10 to 30 rpm at nominal load. Depending on the operational strategy, the wind turbine will experience all speeds from standstill to nominal speed for varying periods of time. These conditions have to be included in the load spectrum for the bearing. The temperature range can vary considerably and has to be evaluated with due consideration to the actual site. In the IEC 61400-1 standard, a normal ambient temperature range from -10° C to +40° C is specified. Environmental conditions such as salinity,

chemically active substances and abrasive particles have to be considered.

Lightening currents passing through the bearings may have to be considered for some sites.

6.2.4 Seals, lubrication and temperatures

Seals

Bearing seals are needed, partly to hold back bearing lubrication, and partly to keep out contaminants. As the main bearing is often placed relatively unprotected and quite close to the outside, this is of particular importance because dirt and rainwater can easily come in contact with the bearing.

Non-rubbing seals (labyrinth seals) are appropriate since they exhibit practically no friction and no wear. A labyrinth seal forms a good supplement to other seals.

When using rubbing seals it should be aimed at mounting the seal on the shaft and to let the bearing housing form the sealing surface. This is done to reduce the risk of scratches in the shaft. The compatibility of the grease with the seal material has to be checked.

Lubrication

The main purpose of lubrication is to create a lubricant film between the rolling elements to prevent metal-to-metal contact. This is to avoid wear and premature rolling bearing fatigue. In addition, lubrication reduces the development of noise and friction, thus improving the operating characteristics of a bearing. Additional functions may include protection against corrosion and enhancement of the sealing effect of the bearing seals.

When selecting lubrication, some of the matters that need to be considered are viscosity, consistency, operating temperature

range, the ability of protection against corrosion and the load carrying ability.

Water in the lubrication leads to corrosion, degradation of the lubrication, formation of aggressive substances together with oil additives, and it affects the formation of a load carrying lubricating film.

Since the rotational speed varies from zero to the nominal speed, a boundary lubrication condition will consist a considerable part of the operational time. This will normally call for a lubricant with EP (extreme pressure) additives and as high a viscosity as practically possible. In this respect, it is essential to consider possible load cases where the radial load is low or even zero combined with low temperatures (high viscosity), because it may cause sliding in the bearing.

Grease lubrication

The most commonly used lubrication in the main bearings is grease.

Grease has the advantage of being easily retained in the bearing arrangement, it contributes to sealing the bearing arrangement from contamination, and the use of an expensive circulation system is avoided. Rolling bearing greases are standardised in DIN 51825.

Grease consists of a base oil with thickeners and possibly additives added. The following grease types are distinguished:

- mineral oil with metal soaps as thickener.
- mineral oil with non-soap thickener
- synthetic oils with non-soap thickener

A possible choice of grease lubrication would be a lithium soap base grease of penetration class 2-3 with EP additives and maybe corrosion and oxidation inhibitors.

Lithium soap base grease has the quality of being waterproof and usable at a wide of range temperatures $-35\text{ }^{\circ}\text{C}$ to $+130\text{ }^{\circ}\text{C}$.

Other possibilities are sodium grease or calcium soap base grease.

Sodium grease absorbs large quantities of water and is useful in environments with condensation. It may, however, soften to such an extent that it flows out of the bearing.

Calcium soap base greases of penetration class 3 do not absorb any water. This is advantageous in situations where bearing seals are exposed to splash water.

The stiffness of the grease is determined by the consistency class. A stiff grease, which belongs to consistency class 3 or higher, can contribute to the sealing of the bearing and keep out contaminants by lying in a labyrinth seal or in the contact area of a rubbing seal.

However, for high P/C load ratios, greases of consistency class 1-2 should be selected. In a dusty environment, a stiff grease of penetration class 3 should be used.

The relubrication interval corresponds to the minimum grease life F_{10} of standard greases in accordance with DIN 51 825. The grease service life is dependent on the type and amount of grease, bearing type and size, loading, speed, temperature and mounting conditions. For fairly large bearings ($> 300\text{ mm}$) the relubrication interval is recommended to be more frequent than F_{10} . In some cases, continuous lubrication is established.

Great care should be exercised if the grease type is to be changed. If incompatible greases are mixed, their structure can change

drastically, and the greases may even soften considerably.

As regards the amount of grease to be used, a rule of the thumb is to fill the bearing completely with lubrication while the housing is half filled (SKF, 1989).

Oil lubrication

Since temperatures are normally relatively low, the lubricant does not need to function as heat dissipator. In that case, there is no need for circulation of the lubricant, which simplifies the design. On the other hand, when the lubrication is not circulated, there is no possibility of filtering, and relubrication is therefore necessary.

Oil lubrication makes it necessary to monitor the lubrication system because of the risk of leakage. A disadvantage compared to grease lubrication is that it demands a better sealing and a circulation system.

Straight oils and preferably corrosion- and deterioration-inhibited oils can be used. If the recommended viscosity values are not maintained, oils with suitable EP additives and anti-wear additives should be selected. If the bearings are heavily loaded (i.e. the load ratio $P/C > 0.1$), or if the operating viscosity v is smaller than the rated viscosity v_1 , oils with anti-wear additives should be used. EP additives reduce the harmful effects of metal-to-metal contact, which occurs in some places. The suitability of EP additives varies and usually depends largely on the temperature. Their effectiveness can only be evaluated by means of tests in rolling bearings. (FAG WL-81 115/4.)

The intervals between oil changes depend on the specific lubrication system and circulation, contamination and ageing of the oil.

Before going into operation, oil must be supplied to the bearing. In case of circulating oil lubrication, the oil pump should be started before the turbine goes into operation. In other cases, the bearing must be manually lubricated before first start-up, and total drain of the bearing during service must be avoided.

6.2.5 Rating life calculations

The fatigue load carrying capacity of the bearing is characterised by the basic dynamic load rating C . This quantity can be calculated according to ISO 281 (1990).

The static load carrying capacity of the bearing is characterised by the static load rating C_0 . This quantity can be calculated according to ISO 76 (1990).

The general methodology for selecting and calculating rolling bearings is given in Section 6.3 for both dynamic and static loads. In general, for a design life of 20 years, the required basic rating life L_{10h} should equal or exceed 300,000 hours. The modified rating life L_{10mh} should at the same time reach 175,000 hours. In the context of grease lubrication and oil lubrication without filter, the contamination factor η_C should not be chosen higher than 0.2 if special precautions are not taken to obtain and verify higher values. For oil lubrication with off-line filtering, a contamination factor η_C of 0.5-0.7 may be obtained. The C/P ratio should not exceed 2.5 for the largest load interval.

The above-mentioned figures apply to medium size wind turbines (600-1000 kW). It should be borne in mind that large bearings are relatively less sensitive to contamination particles of a certain size than smaller bearings.

The static safety factor C_0/P_0 based on the extreme load cases should not be lower than 4.

6.2.6 Connection to main shaft

The thrust from the rotor should be considered to be taken up by shoulder or by friction, or a combination of both. One should then be aware of the stress concentration in the main shaft at the shoulder.

In cases where there is a possibility of the wind turbine being in a situation where the wind is coming from the back, one should consider a stop ring as shown in Figure 6-15.

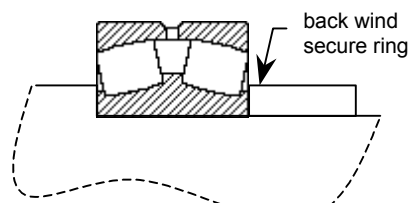


Figure 6-15. Back wind stop ring.

A tight fit, i.e. complete support of the bearing ring over its entire circumference, makes a full utilisation of the bearing's load carrying capacity possible.

The bearing clearance should be as small as possible to ensure accurate guidance, however, large enough in order not to get stuck in any situation. When considering the bearing clearance things to take into account will be a possible difference in temperature and expansion of inner ring and compression of outer ring during mounting, respectively.

The bearing clearance should always be checked after mounting on the shaft.

6.2.7 Bearing housing

The bearing must be firmly supported by the whole circumference to achieve a proper load transmission.

For bearings with normal tolerances, the dimensional accuracy of the cylindrical seating in the housing should be at least IT grade 7, and on the shaft at least IT grade 6.

The tolerance for cylindrical form should be at least one IT grade better than the dimensional tolerance.

Since cast bearing houses will often have a complex geometry, an obvious method to be used for verification would be a finite element analysis, see Appendix D.

6.2.8 Connection to machine frame

The connection between the bearing housing and the machine frame will most likely be a bolt connection. The connection should be capable of transferring the combination of axial and radial forces from the bearing to the main frame by friction or by shear in bolts by tight fit, depending on the geometry of the connection (see Appendix A).

6.2.9 Standards

ISO 76 Roller bearings – Static load ratings.

ISO 281 Roller bearings – Dynamic load ratings and rating life + Amendment 1 and 2.

IEC 61400-1 Wind generator systems, Part 1. Safety requirements.

6.3 Main gear

The purpose of the main gear is to act as a speed increaser and to transmit energy between the rotor and the generator.

6.3.1 Gear types

The most common gear types used in main gears for wind turbines can be identified and classified as follows, based on their geometrical design:

- *spur and helical gears* consist of a pair of gear wheels with parallel axes. Spur gears have cylindrical gear wheels with radial teeth parallel to the axes. In helical gears, the teeth are helical, i.e. they are aligned at an angle with the shaft axes. Double-helical gears have two sets of helical teeth on each wheel. Helical gears are sometimes referred to as spiral gears or oblique gears. See Figure 6-16.
- *epicyclic or planetary gears* consist of epicyclic trains of gear wheels, i.e. gears where one or more parts – so-called planets – travel around the circumference of another fixed or revolving part. See Figure 6-17.

Planetary gears in combination with one or more parallel axis gears form the most commonly applied gear type for the main gear in wind turbines. Gears in which the power is transferred from one wheel to two or more meshing wheels are referred to as gears with a split power path.

Other types of gears, rarely or never used in wind turbine main gears, include the following, which are listed here merely for completeness:

- *bevel gears* consist of a pair of toothed conical wheels whose working surfaces are inclined to nonparallel intersecting axes. Bevel gear wheels can be designed with spur teeth, helical teeth, and curved spiral teeth. Spiral bevel gears result when the teeth are helical or curved. See Figure 6-18.
- *worm gears* consist of a worm-thread wheel, or “endless screw”, working in conjunction with a cylindrical toothed

wheel. The axes are nonparallel and nonintersecting, see Figure 6-19. Worm gears are not used for main gears in wind turbines, but are sometimes used as yaw gears in yaw systems.

- *hypoid gears* constitute a cross between worm gears and bevel gears in that they are similar to bevel gears but have nonintersecting axes. Hypoid gears are turned into spiral bevel gears in the limiting case when the offset between the axes approaches zero. Reference is made to Figure 6-20.

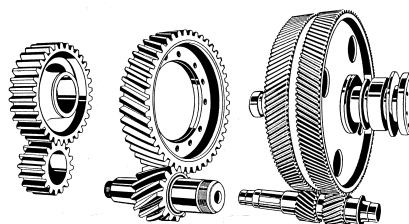


Figure 6-16. Examples of spur and helical gears, from Niemann and Winter (1985).

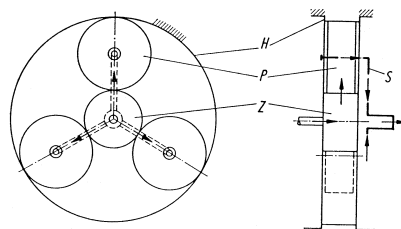


Figure 6-17. Planetary gear principle, outer fixed annulus with three revolving planets and one rotating planet carrier in the middle, from Niemann and Winter (1985).

Tooth form

The tooth forms used practically universally in spur, helical, bevel and worm gears are so-called involute teeth. This tooth form implies that rotation of the base circle at a uniform rate is associated with uniform displacement. The path of contact is a straight line, which coincides with the line of action.

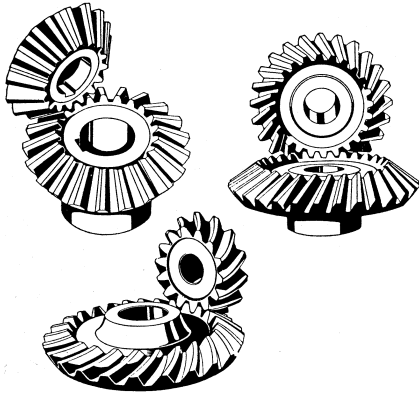


Figure 6-18. Examples of bevel gears, from Niemann and Winter (1985).

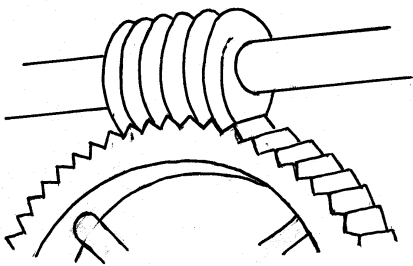


Figure 6-19. Worm gear.

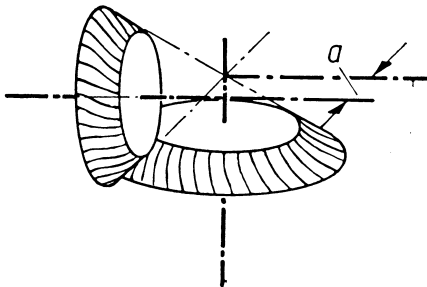


Figure 6-20. Hypoid gear, from Niemann and Winter (1985).

Bearing types

Bearings for wind turbine gears should all be rolling element, anti-friction type bearings. Different bearing types applied in gears include:

- ball bearings
- cylindrical roller bearings
- spherical roller bearings

- tapered roller bearings

Examples of bearings are shown in Figure 6-21. Two bearings should be used to support each gear shaft, one for support of both radial and thrust forces, the other for support of only radial forces and free to allow for axial growth under thermal changes. Bearing fits should be tight to prevent damage to the bearing or the housing and to prevent spinning of inner and outer bearing races.

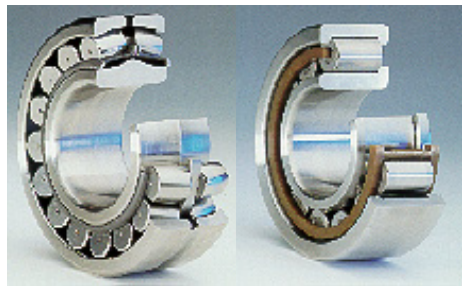


Figure 6-21. Examples of roller bearings: Spherical bearing (left) and cylindrical bearing (right). From SKF (1997).

The bearing fits should be carefully selected in order to avoid spinning bearing rings as well as squeezing of the rollers.

For roller bearings in gears, it is normally sufficient to have a predicted L_{10h} lifetime of at least 100,000 hrs referring to the cubic mean load, or 30,000 hrs referring to the nominal power.

The loads should be specified in terms of a load duration spectrum, which on discretised form gives the number of hours of operation within each of a number of suitably chosen load intervals. The equivalent power, which is defined as the cubic mean power, can be calculated as follows

$$P_{eq} = \left(\sum_i (P_i^3 \frac{h_i}{h_t}) \right)^{1/3}$$

- P_i power in the i th defined load interval
- h_i number of hours of operation in the i th interval
- h_t total number of hours of operation

Rolling bearings

The design of roller bearings for a gear is made using a load duration spectrum. The load duration spectrum may be transformed to an equivalent cubic mean load, P_{eq} . According to ISO281/1, the basic rating life is defined as

$$L_{10} = \left(\frac{C_{dyn}}{P_{eq}} \right)^p \cdot 10^6 \text{ revolutions}$$

- C_{dyn} basic dynamic capacity of the bearing
- $p = 10/3$ for roller bearings
- $p = 3$ for ball bearings

The bearing manufacturers usually quote values for C_{dyn} . The index 10 refers to a 10% failure probability associated with the bearing life L_{10} . ISO 281/1 suggests the following formula for calculation of adjusted rating life

$$L_{na} = a_1 a_2 a_3 \left(\frac{C_{dyn}}{P_{eq}} \right)^p \cdot 10^6 \text{ revolutions}$$

in which the suffix n denotes the associated probability of failure. The corresponding survival probability is $1-n$, which is also referred to as the reliability. The coefficient a_1 is a reliability factor, which depends on the actual reliability, see Table 6-2. The coefficients a_2 and a_3 are factors of the bearing material and service conditions, respectively. For a commonly applied reliability of 90%, a conventional bearing material and normal operating conditions, $a_1 = a_2 = a_3 = 1.0$.

Failure probability n (%)	Reliability $1-n$ (%)	Reliability factor a_1
10	90	1.00
5	95	0.62
4	96	0.53
3	97	0.44
2	98	0.33
1	99	0.21

Bearing manufacturers recommend values for the factor product $a_{23} = a_2 a_3$. These values may vary from manufacturer to manufacturer, and a_{23} will usually depend on the viscosity ratio

$$\kappa = \frac{\nu}{\nu_1}$$

in which ν is the operational viscosity of the lubrication, and ν_1 is the viscosity required for an adequate lubrication, i.e. a lubrication which is sufficient to avoid metallic contact between the rolling elements and the race ways.

New methods for bearing life prediction are being developed, e.g. by SKF and INA. SKF defines a modified rating life

$$L_{naa} = a_1 a_{SKF} \left(\frac{C_{dyn}}{P} \right)^p \cdot 10^6 \text{ revolutions}$$

in which the adjustment factor a_{SKF} depends on the cleanliness of the lubricant and the load ratio P_u/P , where P_u denotes the endurance load limit, and P is the actual load. Since the a_{SKF} factor will vary from one load level to another, use of this approach to lifetime predictions requires application of the entire load spectrum of loads P_i , not only an equivalent load P_{eq} . The total rating life can accordingly be obtained as follows

$$L_{10mh} = \frac{h_i}{\sum_i \frac{h_i}{L_{10mh,i}}}$$

in which the numerator h_i denotes the total number of hours of operation, and the denominator denotes the sum of all relative life consumptions over a suitable discretisation of the load spectrum.

Other methods exist which require advanced calculation programs developed by the major bearing manufacturers.

Lubrication conditions are essential for the bearing design. The oil viscosity should preferably result in a viscosity ratio $\kappa > 1.0$. In the region from $\kappa = 0.4$ to $\kappa = 1.0$, the bearing manufacturers recommend lubrication oils with approved EP (extreme pressure) additives.

The oil supplied to bearings should have a cleanliness and a temperature corresponding to the design assumptions. The cleanliness of the lubricant as defined in ISO 4406 consists of three numbers, for example 17/14/12, which corresponds to certain numbers of particles per 100 ml sample greater than $2\mu\text{m}$, $5\mu\text{m}$ and $15\mu\text{m}$, respectively.

The static capacity of roller bearings is defined in ISO 76 and is the load for which the total permanent deflection of the bearing is 1/10000 times the rolling element diameter. The margin to this capacity should not be less than 4.0 for extreme design loads.

Materials

Gears should preferably be made from separate steel forging. Heat treatment and case-hardening can be used to harden the steel.

The major function of the material selection and subsequent heat treatment of steel materials to be used for gears is to achieve the desired microstructure at the critical locations so that, in particular, the teeth will have the desired contact and tooth root strength capacity. Common heat treatments for steel include:

- preheat treatments (anneal, normalise, temper)
- heat treatments
 - through-hardening (anneal, normalise, normalise and temper, quench and temper)
 - surface hardening (flame and induction harden, carburise, carbonitride, and nitride)
- subsequent heat treatment (stress relief)

Case-hardening implies that carburisation is carried out after a prior heat treatment and is followed by hardening and tempering. The case-hardening implies that the surface layer becomes harder than the interior.

Requirements to materials and hardening treatments for gear transmissions can be found in DNV Rules for Classification of Ships, Part 4, Chapter 2.

6.3.2 Loads and capacity

Insofar as regards gears, the load levels are in focus rather than the load ranges. This is in contrast with what is otherwise the case for many structural details. Procedures for calculation of loads and for prediction of load capacities for gears are outlined in the following and include prediction of surface durability, tooth strength, and scuffing load capacity. Other damage such as wear, gray staining (micropitting) and fractures starting from flanks may also limit the gear capacity, although limited or no calculation procedures are given for the associated capacities.

The nominal tangential load is given as

$$F_T = \frac{2T}{d}$$

T applied torque
d reference diameter

Surface durability

Contact stress. The design contact stress σ_H is derived from the nominal tangential load as follows

$$\sigma_H = Z \sqrt{\frac{F_T(u+1)}{d_1 b u}} K$$

u gear ratio per stage
b face width
d₁ reference diameter of the pinion

The factors *K* and *Z* are compound influence factors to account for various effects. The factor *K* is defined as the product

$$K = K_A K_\gamma K_V K_{H\beta} K_{H\alpha}$$

K_A application factor, defined as the ratio between maximum repetitive torque and nominal torque, and accounts for dynamic overloads external to the gearing
K_γ load-sharing factor, defined as the ratio between the maximum load through the actual path and the evenly shared

load, and accounts for the maldistribution of load in multiple-path transmissions

K_V Internal dynamic factor to account for internally generated dynamic loads in the gear
K_{Hβ} face load factor of contact stress and scuffing
K_{Hα} transverse load distribution factor of contact stress and scuffing

The factor *Z* is defined as the product

$$Z = Z_{BD} Z_H Z_E Z_\epsilon Z_\beta$$

Z_{BD} zone factor for inner point of single pair contact for pinion or wheel
Z_H zone factor for pitch point
Z_E elasticity factor that accounts for influence of modulus of elasticity and Young's modulus. This is a factor whose squared value is in units of stresses
Z_ε contact ratio factor that accounts for influence of transverse contact ratio and overlap ratio
Z_β helix angle factor

Note that all factors, except *Z_E*, are dimensionless. Formulas and details for calculation of the various factors can be found in ISO6336, DIN3990, and DNV CN41.2

Table 6-3. Endurance limits.

Steel grade	σ_{Hlim} (N/mm ²)
Alloyed case-hardened steel of special approved high grade	1650
Alloyed case-hardened steel of normal grade	1500
Nitrided steel of approved grade	1250
Alloyed quenched and tempered steel, bath or gas nitrided	1000
Alloyed, flame or induction hardened steel (HV = 500-650 N/mm ²)	0.75HV+750
Alloyed quenched and tempered steel	1.4HV+350
Carbon steel	1.5HV+250

Note that these values refer to forged or hot-rolled steel. For cast steel, values need to be reduced by 15%. HV denotes surface hardness.

Capacity. The characteristic endurance limit σ_{Hlim} for contact stresses is the stress that can be sustained for $5 \cdot 10^7$ cycles without the occurrence of progressive pitting. This limit usually defines the beginning of the endurance stress range, i.e. it defines the lower knee of the σ - N curve. Values of σ_{Hlim} are given in Table 6-3, but should only be used for materials which are subjected to relevant quality control. Results of suitable fatigue tests may also be used to establish values of σ_{Hlim} .

The design endurance strength, also known as the permissible contact stress, is

$$\sigma_{HP} = \frac{\sigma_{Hlim}}{S_H} Z_N Z_L Z_V Z_R Z_W Z_X$$

- S_H required safety factor
- Z_N life factor for endurance strength, reduces the endurance strength when the design life of the gear is greater than $5 \cdot 10^7$ cycles, and increases it when the design life is less than $5 \cdot 10^7$ cycles
- Z_L lubricant factor referring to various aspects of oil film influence
- Z_V speed factor referring to various aspects of oil film influence
- Z_R roughness factor referring to various aspects of oil film influence
- Z_W work hardening factor
- Z_X size factor

Formulas and details for calculation of the various factors can be found in ISO6336, DIN3990 and DNV CN41.2.

Design rule. The design rule to be fulfilled is

$$\sigma_H \leq \sigma_{HP}$$

Tooth root strength

Tooth stress. The following section deals with the tooth root strength as limited by tooth root cracking. The local tooth stress σ_F for pinion and wheel can be predicted as

$$\sigma_F = \frac{F_T}{bm_n} Y_F Y_S Y_\beta K_A K_V K_{F\beta} K_{F\alpha}$$

- Y_F tooth form factor
- Y_S stress concentration factor
- Y_β helix angle factor
- b face width at the tooth root, either for pinion or for wheel
- m_n normal module

Other coefficients and variables are defined elsewhere, see Section 6.3.1. Expressions for the tooth form factor, the stress concentration factor and the helix angle factor can be found in ISO6336, DIN3990 and DNV CN41.2.

Capacity. The permissible local tooth root stress σ_{FP} for pinion and wheel can be predicted as

$$\sigma_{FP} = \frac{\sigma_{FE} Y_d Y_N}{S_F} Y_{\delta_{relT}} Y_{R_{relT}} Y_X Y_C$$

- σ_{FE} local tooth root bending endurance limit of the reference test gear. The stress concentration factor for the test gear is normally 2.0
- Y_d design factor, which accounts for other loads than constant load direction, e.g. idler gears, temporary change of load direction, prestress due to shrinkage, etc.
- Y_N life factor for tooth root stresses related to the reference test gear dimensions. It is used to take into account the higher load bearing

	capacity for a limited number of load cycles, and a reduced load bearing capacity when the number of load cycles is large
S_F	required safety factor
$Y_{\delta_{relT}}$	relative sensitivity factor of the gear, related to the reference test gear
$Y_{R_{relT}}$	relative surface condition factor of the gear, related to the reference test gear
Y_X	size factor
Y_C	case depth factor considering subsurface fatigue

Formulas and details for calculation of the various factors can be found in ISO6336, DIN 3990 and DNV CN41.2.

Design rule. The design rule to be fulfilled is

$$\sigma_F \leq \sigma_{FP}$$

Scuffing load capacity

High surface temperatures due to high loads and sliding velocities can cause lubricant films to break down in the gear. This will lead to seizure or welding-together of areas of tooth surfaces between the wheel and the pinion. This phenomenon is known as scuffing and may lead to failure. In contrast to pitting and fatigue failure, which both exhibit a distinct incubation period, a single short overloading can lead to scuffing failure.

Two criteria are to be fulfilled to ensure a sufficient level of safety against scuffing failure. Both criteria are formulated in terms of criteria on temperature, i.e. the local contact temperature may not exceed some permissible temperature. The one criterion is a so-called flash temperature criterion, based on contact temperatures, which vary along the path of contact. The other criterion is an integral temperature criterion, based on the

weighted average of contact temperatures along the path of contact. Usually, the flash temperature criterion will govern the design against scuffing failure.

Two inequalities should be fulfilled to meet the flash temperature criterion

$$\theta_B \leq \frac{\theta_s - \theta_{oil}}{S_s} + \theta_{oil} \quad \text{and} \quad \theta_B \leq \theta_s - 50^\circ$$

θ_s	scuffing temperature as determined from FZG tests
θ_{oil}	oil temperature before it reaches the mesh, i.e. the normal alarm temperature
θ_B	maximum contact temperature along the path of contact, calculated as the sum of the bulk temperature θ_{MB} and the maximum flash temperature θ_{flamax} along the path of contact
S_s	required safety factor, usually taken as 1.50.

The integral temperature criterion reads

$$\theta_{int} \leq \frac{\theta_s}{S_s}$$

$$\theta_{int} = \theta_{MC} + 1.5 \cdot \theta_{flaint}$$

θ_{int}	integral temperature
θ_{MC}	bulk temperature
θ_{flaint}	mean flash temperature along the path of contact

Formulas for calculation of θ_s , θ_{MB} , θ_{flamax} , and θ_{flaint} can be found in DNV CN41.2.

Note that gray staining may occur under the same conditions that may lead to scuffing, and that this may even happen without or before the occurrence of a literal scuffing failure.

Capacity of shaft/wheel connections

Several types of couplings between shaft and wheel appear in the context of gears. The major types are listed in Section 6.4 dealing with issues of importance for their design.

Other capacities

Other capacities to be considered in the context of gears include:

- bearing calculations
- shaft capacities for torsional loads and tooth loads
- gearbox housing and suspension. The capacity of the gearbox is highly dependent on the type of gearbox, e.g. whether it is cast or welded, whether it is small or large, and whether it is one- or two-pieced. The gearbox housing shall have sufficient strength and stiffness to avoid mesh misalignment due to deflection of the gearbox housing.

6.3.3 Codes and standards

DIN 3990, “Tragfähigkeitsberechnung von Stirnrädern”, Part 1-5, Deutsches Institut für Normung e.V., 1987.

ISO 6336-1 to 6336-5

AGMA, “Recommended Practices for Design and Specification of Gearboxes for Wind Turbine Generator Systems,” American Gear Manufacturers Association, Alexandria, Virginia, 1997.

6.3.4 Lubrication

The functioning of a gear involves relative motion of surfaces in contact under load. Separation of the surfaces by a thin film of oil is a key factor in achieving smooth operation and a good service life. Lubrication is used for this purpose. Oils for the lubrication of gearing have to meet diverse performance requirements, including

stability, resistance to foaming, separation from water, and prevention of corrosion. However, the principal function of the oil is the protection of the rubbing surfaces of the gear teeth. There are many requirements for the lubrication system. The following items are recommended as a minimum.

The choice of a lubricant and lubrication system should be the joint responsibility of the gearbox manufacturer and the gear box purchaser.

Wind turbine gears have a relatively low pitchline velocity and high gear tooth loads. These conditions require either synthetic or mineral gear oil with antiscuff additives and the highest viscosity that is practical. The choice of lubricant depends on many factors, including viscosity, viscosity index, pour point, additives and costs.

It is recommended to evaluate the ability of a lubricant to resist micropitting.

Viscosity classes for lubricants according to ISO are given in Table 6-4, and recommended criteria for acceptance of gear lubricants are given in Table 6-5.

Monitoring

Oil level indication by means of a sight glass or dipstick or equivalent is to be provided.

The lubrication oil temperature is to be monitored. A temperature in excess of the approved maximum should result in automatic shutdown. The monitoring system should be arranged so as to imply shutdown in case of malfunction.

For gears with a forced lubrication system, the pressure is to be monitored. Oil pressure below minimum, with a running gear, should result in automatic shutdown. This requirement does not apply if the forced system is mainly arranged for oil cooling, and if the gear can work satisfactorily with

splash lubrication. However, an indication of the insufficient oil pressure is to be provided.

Table 6-4. Viscosity classes according to ISO.

Viscosity class	Average viscosity at 40°C (mm ² /s)	Limits of kinematic viscosity at 40°C (mm ² /s)	
		min.	max.
VG 2	2.2	1.98	2.42
VG 3	3.2	2.88	3.52
VG 5	4.6	4.14	5.06
VG 7	6.8	6.12	7.48
VG 10	10	9.0	11.0
VG 15	15	13.5	16.5
VG 22	22	19.8	24.2
VG 32	32	28.8	35.2
VG 46	46	41.4	50.6
VG 68	68	61.2	74.8
VG 100	100	90	110
VG 150	150	135	165
VG 220	220	198	242
VG 320	320	288	352
VG 460	460	414	506
VG 680	680	612	748
VG 1000	1000	900	1100
VG 1500	1500	1350	1650
VG 2200	2200	1980	2420
VG 3200	3200	2880	3520

Installation of gearing

The gear is to be installed so that appropriate alignment and running conditions for the gear are maintained under all operating conditions. In case of flexible mounting, harmful vibrations are to be avoided. Excessive movements of flexibly mounted gears are to be limited by stopper arrangements. Design of the oil systems and maintenance methods with respect to changing the oil should be developed to minimise oil leaks and spills.

Assembly and testing in the workshop

The accuracy of meshing is to be verified for all meshes. The journals should be in their expected working positions in the bearings. The mesh contact should be consistent with that which would result in the required load distribution at full load.

The gear transmission is to be spin tested in the workshop and checked with regard to oil tightness. The spin test can also be used for gear mesh verification. As regards the prototype gear as well as selected gears from serial production, special testing will be necessary, in particular, with respect to face load distribution, lubrication/temperatures and vibrations.

Assembly and testing in the nacelle

The functioning of the lubrication oil system and monitoring system is to be tested.

If the arrangement is made so that external bending moments (e.g. due to the rotor or torque reaction) can influence the gear mesh alignment, the contact pattern has to be verified under real or simulated conditions for some gears in a series. This can be achieved by applying a thin suitable lacquer to the teeth before the test. The tooth contact pattern at the actual test load is to be analysed with respect to load distribution at the rated load. This requirement also applies to gears where no part load or full load testing has been made in the workshop.

6.3.5 Materials and testing

The quality requirements for materials and heat treatment for gears are divided into three levels according to DIN3990 T5 and ISO6336-5. The three levels are denoted ME, MQ and ML, respectively, and ME is the highest quality level.

Specific requirements for quality control and material requirements and testing are given for each material type and quality level. The

strength values for both pitting and bending fatigue are dependent on the quality level. Values are given in DIN3990 T5 and ISO6336-5. The DNV Classification Note

N41.2 is based partly on ISO6336. The material and testing requirements that the Classification Note 41.2 is based on are given below.

Parameter	Methodology	Recommended criteria for acceptance
Viscosity (mm ² /s)	ISO 3104	±10%
Viscosity indices	ISO 2909	Min. 90
Oxidation stability	ASTM D 2893	Increase in viscosity of a test sample oxidised at 121°C should not exceed 6% of reference value
Corrosion properties, iron	ISO 7120	No rust after 24 hours with synthetic sea water
Corrosion properties, copper	ISO 2160	#1b strip after 3 hours at 100°C
Foaming properties	ASTM 892	Sequence 1: max. 75/10 10:00 Sequence 2: max. 75/10 10:00 Sequence 3: max. 75/10 10:00
Load carrying property	DIN 51 354	Load stage min. 12
Micropitting resistance test	FVA. No. 54	Stage 10
Filterability	ISO/DIS 13357-1,2	As stated in standard

Testing and inspection of gearing

Requirements to testing and inspection of gearing depend on which type of heat treatment is applied. The following types of heat treatment are dealt with in separate subsections:

- case-hardened
- alloyed through-hardened (quenched and tempered)
- nitrided

Case-hardened gears

For wind turbine gears, the test requirements for case-hardened steel normally correspond to ordinary and intermediate grades of quality as defined in DNV Classification Note 41.2. A higher level of material and heat treatment quality control may result in acceptance of increased endurance values (see Classification Note 41.2).

Certificates are required for:

- chemical composition

- mechanical properties (including Charpy-V)
- ultrasonic test

For steel that will be case-hardened, the mechanical properties need not be documented before the heat treatment process, as they are generally documented after the final heat treatment.

The impact energy (KV) at ambient temperature in tangential direction to pinion/wheel is not to be less than specified for the approved material type and in no case less than 30 J.

For case-hardening the following is required:

- core hardenability (Jominy) is randomly checked
- suitable heat treatment is made prior to machining in order to avoid excessive distortions during quenching
- carburisation is made by gas in a controlled atmosphere furnace. The furnace shall be equipped with carbon

potential controls and continuously recorded

The entire case-hardening process is checked at regular intervals with regard to:

- The case microstructure: to be martensite with allowance for up to 15% retained austenite and fine dispersed individual carbides. (Higher percentage of retained austenite may be accepted provided increased safety factor against scuffing).
- Decarburisation: not to be visible at a magnification of 500.
- The core microstructure: to be martensitic/bainitic with no free ferrite in critical tooth root area.

The case-hardening process is normally to be documented for each hardening batch and each material charge with a certificate, which includes the following:

- hardness profile
- core impact energy (KV)

If no alternative procedure is approved, the certificate is to be based on a coupon test. The coupon is normally to be made of material from the same charge as the actual gear and heat-treated along with this charge. The coupon is to be sampled in the tangential direction and is not to be separately forged. If it is not possible to sample coupons tangentially, longitudinal or radial samples may be accepted.

The coupon diameter is not to be less than 2 times the normal modulus, minimum 20 mm. Further, the size is to be sufficient for making 2 test pieces for impact energy (KV) of the core.

The hardness profile (hardness as a function of depth) is to be determined by hardness measurements with a load of 10-50 N. The measurements are to be made from the surface to the core. The expected amount of grinding is to be subtracted.

It is required that the depths to 550 HV, 400 HV and 300 HV and the core hardness are documented to be within the approved specification. Further, the hardness at any point below the surface is not to exceed the surface hardness (before grinding) with more than 30 HV. The core impact energy is not to be less than the approved specification, and in no case less than 30 J.

As mentioned above, the case-hardening process (the coupons) is normally to be documented for each hardening batch and each material charge. The use of coupons made of the same material type but not same charge may be accepted provided that the manufacturer has a quality assurance system which ensures sufficient reproducibility. In particular, the limits of elements in the chemical composition combined with the respective heat treatment processes must ensure that the required core properties are obtained. This part of the quality assurance system has to undergo special evaluation. A reduced extent of impact testing may also be considered.

Case-hardened gears are to have a minimum tooth root space hardness of 58 HRC over the entire face width. Otherwise, a reduction of permissible tooth root stresses applies, see Classification Note 41.2 Part 3, Section 7.

Depending on the specific material type, this may be difficult to obtain for large gears and control testing may be required. Therefore, manufacturers may carry out special procedure tests in order to document the permissible sizes for their various material types. Components of smaller sizes than those tested need no documentation of tooth root hardness.

If a component exceeds the tested size, or if the manufacturer has not carried out a procedure test, the tooth root space hardness

is to be checked at mid face. If this hardness is less than the specified minimum (58 HRC if nothing else is specified), this measurement is to be carried out over the entire face width.

Nitrided gears

For nitrided gears the process is to be documented for each nitriding batch and material charge with a certificate containing:

- hardness profile
- white layer thickness

If no alternative procedure is specified, the certificate is to be based on a coupon test. The coupon is to be made of material from the same charge as the actual gear and heat-treated along with this charge.

The coupon diameter is not to be less than 2 times the normal modulus. The hardness profile (hardness as a function of depth) is to be determined by means of hardness measurements with a load of 10-50 N. The measurements are to be made from the surface to the core. If further grinding is intended (and is approved), the expected amount is to be subtracted.

It is required that the depth to 400 HV and the core hardness are documented to be within the approved specification.

The white layer thickness is not to exceed 10µm.

As mentioned above, the nitriding process (the coupons) is normally to be documented for each hardening batch and each material charge. The use of coupons made of the same material type but not from the same charge may be accepted provided that the manufacturer has a quality assurance system, which ensures sufficient reproducibility.

Inspection

100% surface crack detection by means of wet fluorescent magnetic particle method is required for the toothed area, including the ends of the teeth. Upon request, liquid penetrant may be considered.

The tooth accuracy of pinions and wheels is to be documented with reference to ISO 1328-1975 or to a corresponding national standard.

Visual inspection is to be carried out with respect to:

- surface roughness of flanks
- surface roughness of root fillets
- tooth fillet radius
- possible grinding notches of root fillet. Any grinding in the root fillet area, and in particular when leaving notches will result in reduction of permissible stresses. See Classification Note 41.2 Part. 3, Section 7.

6.4 Couplings

The major types of couplings are listed in the following along with issues of importance for their design.

6.4.1 Flange couplings

The flange thickness just outside the flange fillet is normally to be at least 20% of the required shaft diameter.

Coupling bolts are to be prestressed so that a suitable amount of prestress remains even under the most severe running conditions, in particular, with regard to bending moments. The level of safety is to be demonstrated in both the ultimate limit state and the fatigue limit state. The same minimum safety factors as those for shaft design apply, see Section 6.1.

If the torque transmission is based only on friction between the mating surfaces of flange couplings, the friction torque (including the influence of axial forces and bending moments) is not to be less than 1.5 times the characteristic peak torque.

The torque transmission may also be based on a combination of shear bolts and friction between the mating flange surfaces. A basic principle is that both the friction alone (including the influence of axial forces and bending moments) and the shear bolts alone should be able to transmit the characteristic peak torque.

6.4.2 Shrink fit couplings

The friction connection is to be able to transmit at least 1.5 times the characteristic peak torque without slipping. Bending moment influence is to be considered.

For tapered mating surfaces where a slippage due to torque and/or axial force may cause a relative axial movement between the tapered members, the axial movement is to be prevented by a nut or similar. When a nut is required, the pre-stress is to be of the same magnitude as the axial force component from the tape.

The permissible material stress depends on the relative wall thickness, material type, and whether the coupling is demountable or not, and the usual range of permissible equivalent stress (von Mises) is 70% to 110% of the yield strength of the hub.

6.4.3 Key connections

The connection is to be able to transmit the characteristic peak torque.

The shear stress in the key is not to exceed 50% of the yield strength in shear. The pressure on the side of the keyway is not to exceed 85% of the yield strength of the key.

The yield strength to be applied in checks according to these two criteria is not to exceed 2/3 of the tensile strength of the key, and it is not to exceed twice the yield strength of the shaft or the hub, whichever is involved.

In principle, there is to be no clearance between the hub and the shaft, however, a certain amount of minimum interference fit is required, e.g. approximately 0.02% of the shaft diameter.

6.4.4 Torsionally elastic couplings.

Rubber couplings are to be designed such that a failure of a rubber element does not cause loss of the connection between the rotor and the brake.

6.4.5 Tooth couplings

Tooth couplings are to have a reasonable degree of safety with respect to surface durability and tooth strength. This is subject to special consideration.

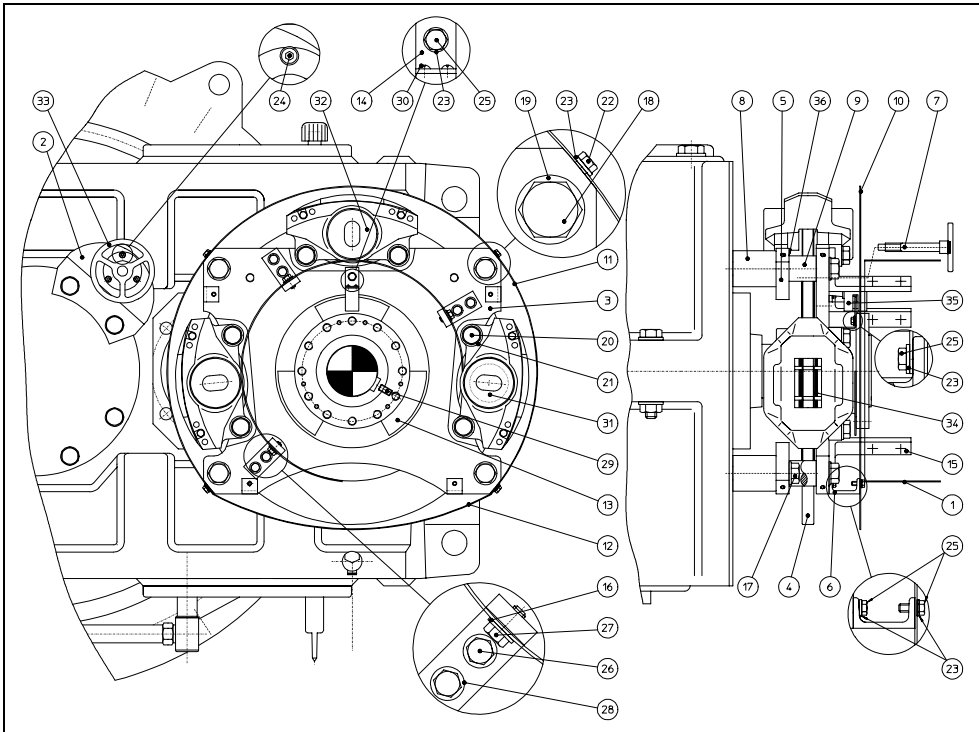
6.5 Mechanical brake

Mechanical brakes are usually used as a backup system for the aerodynamic braking system of the wind turbine and/or as a parking brake, once the turbine is stopped, e.g. for service purposes. Mechanical brakes are sometimes also used as part of the yaw system. In a mechanical brake, brake callipers, brake discs and brake pads form crucial parts. A hydraulic system is usually used for the actuation and release of the brake.

6.5.1 Types of brakes

Mechanical brakes can be active or passive, depending on how the hydraulic system of the brake is applied:

- active brake: the pressure of the hydraulic system actively pushes the brake pads against the brake disc.



- | | | | |
|----|--|----|---------------------------------------|
| 1 | cover for cardan | 19 | washer |
| 2 | suspension for screw pump | 20 | set screw |
| 3 | foundation plate for brake arrangement | 21 | washer |
| 4 | brake disc for hub | 22 | set screw |
| 5 | middle plate for distance pipe | 23 | washer |
| 6 | fitting for cover | 24 | hexagonal socket head cap screw |
| 7 | lock screw for brake disc | 25 | set screw |
| 8 | bushing | 26 | set screw |
| 9 | bushing | 27 | set screw |
| 10 | cover for brake | 28 | washer |
| 11 | side cover for brake, top | 29 | hexagonal head bolt |
| 12 | side cover for brake, bottom | 30 | slotted raised countersunk head screw |
| 13 | sensor pick-up plate at cardan | 31 | brake calliper |
| 14 | fitting for sensor | 32 | blade calliper air bleed |
| 15 | angle iron for cover | 33 | screw pump |
| 16 | washer | 34 | brake lining |
| 17 | hexagonal head bolt | 35 | fork sensor |
| 18 | hexagonal head bolt | 36 | shims |

Figure 6-22. Example of brake arrangement. Courtesy Vestas.

- passive brake: the pressure of the hydraulic system keeps a spring tight. Once the pressure is released, the spring is also released and will push the brake pads against the brake disc.

In either case, the hydraulic pressure of the hydraulic system is crucial in order to be able to operate the brake as intended. The hydraulic pressure is usually provided by means of an accumulator. For active systems, it is particularly important to make sure that the pressure in the accumulator is always available, and it is important to have redundancy in this respect, i.e. an extra pressure source is necessary for backup.

The type of spring used in a mechanical brake to keep up a pressure is often a coil spring of the disc spring type. This type of spring is nonlinear and has the advantage that it is capable of maintaining an approximately constant spring pressure over a considerable range of deflection.

An example of a brake arrangement is given in Figure 6-22.

6.5.2 Brake discs and brake pads

Brake discs and brake pads must be able to withstand temperature loading, since the friction during braking leads to dissipation of energy in terms of heat and causes high temperatures to develop locally.

Brake pads may be made of different kind of materials. Ceramic brake pads do not withstand high temperatures (temperatures in excess of 300-400°C) very well, in the sense that they lose their frictional resistance. For high temperatures, brake pads made of sinter bronze can be used.

Brake discs must be subject to temperature calculations or temperature measurements. They must meet requirements to planarity in order to work properly, i.e. they must not warp when subjected to temperature loading.

In general, the thicker the disc is, the better is its ability to absorb temperature loading.

The possible variation in the frictional coefficient poses a problem, which must be given due consideration when the brake system is being dimensioned. If the frictional coefficient is too big, the brake force will become too large. If the frictional coefficient is too small, the brake system will be unable to brake.

6.5.3 Brake torque sequence

The rise time from zero to maximum brake torque will influence the dynamic response of the turbine heavily. Since the turbine is rotating when the brake is actuated, full brake force will be mobilised immediately upon the actuation of the brake.

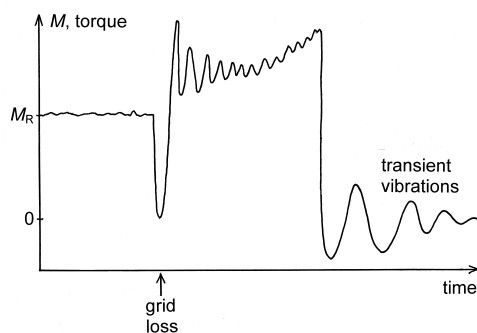


Figure 6-23. Temporal evolution of torque at and after grid loss with subsequent actuation of the brake.

In the design of the brake system, it is important to consider the maximum torque during the course of the braking. Depending on the dynamics, the maximum torque may well occur towards the end of this course, and transient vibrations may sometimes follow. An example of the temporal evolution of the torque during the course of braking is given in Figure 6-23. The turbine is rotating when a grid loss occurs, and the torque drops to zero. When the connection to the grid is lost, the brake is actuated, and

the torque raises and develops as shown in the figure.

6.6 Hydraulic systems

In a hydraulic system, power is transmitted and controlled through a liquid under pressure within an enclosed circuit. Hydraulic systems are used in wind turbines, for example in terms of a hydraulic accumulator for pitching of the rotor blades. A hydraulic system must be protected against exceeding the maximum admissible pressure. A pressure release valve can be used for this purpose and will prevent explosion in the event of fire. All components of the hydraulic system must be easily accessible for assembly, adjustment and maintenance.

Pressure shocks should be kept to a minimum. Pressure shocks or a large pressure drop must not lead to a dangerous condition. A safe condition must be guaranteed in the event of power supply failure and in the subsequent event of restoration of the power supply.

The following external factors must not affect the operation of a hydraulic system:

- salt and other corrosive substances
- sand and dust
- moisture
- external magnetic, electromagnetic and electric fields
- sunlight
- vibrations

When a hydraulic system forms part of the protection system, grid failures and extreme temperatures must not compromise the operation of the system.

6.6.1 Arrangement

Hydraulic systems should have no connections with other piping systems. The

hydraulic fluid is not to have a flash point lower than 150°C and is to be suitable for operation at all temperatures that the system may normally be exposed to. Means for filtration and cooling of the fluid are to be incorporated in the system wherever necessary.

6.6.2 Accumulators

For gas and hydraulic fluid type accumulators, the two media are to be suitably separated if their mixture would be dangerous or would result in the contamination of the hydraulic fluid and/or loss of gas through absorption.

Each accumulator is to be protected on both its gas side and its hydraulic fluid side by a safety device such as a relief valve, a fuse plug or a rupture disc to prevent excessive pressure if overheated. When the accumulator forms an integral part of a system with such a safety device, the accumulator itself need not be supplied with such a safety device.

6.6.3 Valves

Valves are used in hydraulic systems to control the hydraulic effect between a pump and an engine, cylinder, or actuator. The purpose of valves is to govern the direction and amount of the volume flow rate or to block the volume flow rate, and it is also to limit or control the pressure of the fluid. A distinction can be made between four major types of valves, viz.

- shut-off valves, which block flow in one direction and allow for partly or full flow in the opposite direction
- directional control valves, which control the direction of the volume flow rate, and which can block the volume flow rate or adjust the amount of volume flow rate
- pressure valves, which limit or control the hydraulic pressure

- flow control valves, which adjust the volume flow rate to the hydraulic actuator such that the desired speed of the hydraulic actuator is achieved.

6.6.4 Application in protection systems

If a hydraulic system forms part of a protection system, the design and construction of the hydraulic system must comply with the requirements to the protection system, and it must be designed, constructed and used as a fail-safe or redundant system. Hydraulic systems, which form parts of protection systems, can be divided into three categories as follows:

1. Systems in which the brake is actively released by a hydraulic or pneumatic pressure medium.
2. Systems in which the brake is actively released (mechanically, hydraulically, pneumatically or electrically), but actuated hydraulically or pneumatically. The active release thus takes place against a "passive" oil or air pressure.
3. Systems in which the brake is released in the neutral state (passively released) and is actuated hydraulically or pneumatically.

It is recommended to comply with the following requirements to these three types of hydraulic systems:

1. When brakes (mechanically or aerodynamically) are actively released, the pressure medium shall be able to flow away in a reliable manner during a braking action. In the hydraulic system, the following features shall be present as a minimum:
 - two valves must be placed parallel to one another as a switching element. An incorrect switch position of a valve must lead to a safe situation. It must be possible to test each valve individually.

- the return pipes must be made sufficiently strong by their design and construction, or by protection, such that they cannot be closed off by external damage.

- filters must be installed on the pressure side of the pump and should be avoided in the return pipe. If filters are installed in the return pipe, a bypass is required.

- no components must be installed in the return pipe which can lead to blockage of the pipe as the result of maloperation.

2. For actively released brakes, which are being actuated hydraulically or pneumatically, the actuation must be accomplished by means of a pressure accumulator, and the following additional requirements apply:

- the connecting pipe between the accumulator and the actuated component, e.g. the blade adjustment mechanism, must be as short as possible.

- no other components, such as valves, couplings and rotating elements, are allowed in this connection.

- the pressure in the accumulator must be monitored at a level which is sufficiently high to guarantee independent braking action.

- the other protection system of the wind turbine must be actuated mechanically, and the actuating element shall be designed and constructed "safe-life", e.g. a mechanical spring.

3. The use of a passively released braking system, by which the braking action takes place by means of build-up of pressure, is only permissible when the following conditions are met:

- the monitoring, control and actuation systems are designed and constructed with redundancy, i.e.

they are designed and constructed at least in duplicate, and function independently of the electrical grid.

- the pressure build-up is supported by a pressure accumulator to which the same requirements apply as those stated above.
- the other protection system of the wind turbine must be equipped with a "safe-life" actuation element.

In addition, for Categories 2 and 3, an actively operated hydraulic or pneumatic installation shall not be used to keep a wind turbine in a safe state for a long period after a protection system has been actuated.

6.6.5 Additional provisions

It is recommended to take the necessary steps to ensure that failure of a redundant system can be detected. Long-term standby redundancy should be avoided. In the case of oil leaks in hydraulic systems, other wind turbine components or other systems must not be affected.

6.6.6 Codes and standards

The following guidelines and standards deal with design of hydraulic systems.

Teknisk Forlag, *Hydraulik Ståbi*, (in Danish), ed. T. Rump, Teknisk Forlag a.s., Copenhagen, Denmark, 1996.

ISO, "Hydraulic fluid power – General rules for the application of equipment to transmission and control systems," International Standard, ISO4413, 1st edition, 1979.

ISO, "Hydraulic fluid power – Gas-loaded accumulators with separators – Range of pressures and volumes, characteristic quantities and identification," International Standard, ISO5596, 1st edition, 1982.

6.7 Generator

6.7.1 Types of generators

The generator is the unit of the wind turbine that transforms mechanical energy into electric power. While the blades transfer the kinetic energy of the wind to rotational energy in the transmission system, the generator provides the next step in the supply of energy from the wind turbine to the electrical grid.

This section deals with the safety aspects of the generator and its interaction with the rotor and the transmission system. The functioning of the generator and its interaction with the grid is dealt with in Chapter 9. An example of a generator is shown in Figure 6-24.

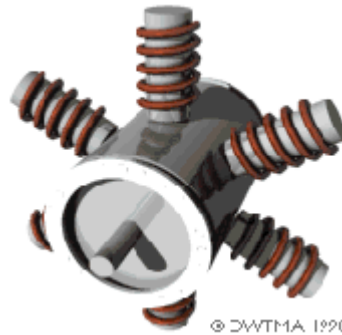


Figure 6-24. Six-pole generator © Danish Wind Turbine Manufacturers Association

The rotational speed of the generator is dependant on the grid frequency and the number of poles

$$n_s = 60 \cdot \frac{f}{p}$$

- f grid frequency in Hz
- p number of pole pairs
- n_s synchronous rotational speed in rpm.

The produced alternating current, which is transmitted to the electrical grid, must match the frequency of the grid. The required rotational speed of the generator's rotor is achieved by means of the gearbox of the wind turbine, since the wind turbine rotor itself is not allowed to rotate at this high speed for physical reasons. Rotation of the wind turbine rotor at the high rotational speed of the generator rotor would cause aerodynamic problems and supersonic speeds. Noise would also be a problem, and excessive centrifugal forces would be generated. A multi-pole generator has the advantage of reducing the mechanical complexity of the generator and makes it possible to reduce the gearbox and sometimes even to omit it.

There are two major types of generators:

- synchronous generators
- asynchronous generators

A synchronous generator operates at a constant speed, dictated by the frequency of the connected grid, regardless of the magnitude of the applied torque. The speed dictated by the frequency of the grid is also known as the synchronous speed.

An asynchronous generator is a generator, which allows slip, i.e. deviations from the rotational speed dictated by the frequency of the connected grid. In other words, the rotational speed is allowed to vary somewhat with the applied torque. This is the most common generator type used in wind turbines. A variant with coiled rotors is prevalent. The slip is defined as the difference between the rotational speed of the generator and the rotational speed dictated by the frequency of the grid. The slip is sometimes expressed in percent of the latter. When a slip of up to about 1% is possible, the operation mode for the asynchronous generator is referred to as constant speed, given that this slip is rather

insignificant. When a larger slip is allowed, say within 10%, and can be varied electronically, e.g. by a rotor current controller, it is referred to as variable slip. The pitch or stall control of the wind turbine is meant to ensure that the allowable slip of the generator is not exceeded.

The advantage of the variable slip comes about when the wind turbine is operated at its rated power. At the rated power, power fluctuations caused by changes in the wind speed are undesirable. When a wind gust hits the wind turbine rotor, the slip enables the generator speed to increase a little in response to the gust without causing a corresponding increase in the generated power output. Thus, the slip ensures a smooth power output and at the same time contributes to keeping the loads on blades, main shaft and gearbox down.

The variation of the operating speed with the applied torque for an asynchronous generator is beneficial because it implies a smaller peak torque and less wear and tear on the gearbox than for a synchronous generator. This is one of the most important reasons for using an asynchronous generator rather than a synchronous generator in a wind turbine, which is connected directly to the electrical grid. Another reason for using asynchronous generators is that the involved slip is beneficial when there is flexibility in the structural system.

Traditionally, the active materials in a generator consist of magnetically conducting iron and electrically conducting thread arranged in a coil. Permanent magnets are becoming increasingly common, and electrical components, such as temperature sensors, are becoming integral parts of the generator.

With a view to switches and power failure, the generator must be able to withstand

switching on in phase opposition at 100% residual voltage, or it must be secured against the occurrence of this situation by means of a special arrangement in the control system.

Generators are to be constructed in such a way that when running at any working speed, all revolving parts are well-balanced. Suitable fixed terminal connectors are to be provided in an accessible position with sufficient space for convenient connection of the external cables.

6.7.2 Climate aspects

Temperature

The generator shall be designed to be fully functional at the temperatures that are likely to occur locally, when the external ambient temperature is within the range $[-10,30]^{\circ}\text{C}$ for normal operation. These limits refer to Danish conditions. For other countries, this range is typically expanded to $[-20,30]^{\circ}\text{C}$. The ambient temperature is the instantaneous value of the temperature of the air outside the wind turbine. The temperature range for the location of the generator should be documented, and the self-heating of the generator should also be documented. When the generator is assembled at its intended location, it needs to be ensured that it is not placed near heat dissipating components, or it has to be designed to withstand the associated temperatures.

Relative humidity of air

To avoid leak currents, i.e. low insulation resistance, corrosion and other damaging influences on the components, these components should – either by their design or by climate control in the wind turbine – be secured so that damaging condensation cannot occur.

The electrical components of the turbine shall be fully functional at a relative

humidity in the external ambient air of 95% within the entire temperature range as specified above.

The influence of the humidity of air on the electrical components is always dependent on other climatic parameters, in particular, on the temperature and on changes in the temperature. Creation of condensation can be remedied by means of heating when the generator is not running, and by heating of closets when the self-heating is insufficient to avoid damaging condensation of water.

Resistance toward saline atmospheres

When the wind turbine is to be located near a coastline or offshore, the electrical equipment shall be constructed in such a way that it will not be damaged by the impact from the saline and moist environment. The encapsulation, the cooling and the insulation of the generator are all to be designed in such a manner that the wind turbine can withstand these impacts. As regards equipment in the turbine, this can be achieved by applying climate control in terms of desalination and dehumidification systems or by heating to avoid condensation and saline deposit.

Electrical immission and emission

Electric and electronic equipment, whose functions can be affected by electrical immission, shall meet the requirements given in the EMC directive as described in DS/EN50082-2, Generic Immunity Standard, Industrial Environment. Electric and electronic equipment, from which electrical emission can occur, shall meet the requirements laid down in the EMC directive as described in DS/EN50081-2, Generic Emission Standard, Industrial Environment.

6.7.3 Safety aspects

The generator forms one of several links in the transmission between the rotating system

and the electrical system of a wind turbine, i.e. between the blades and the grid. Failure of any link in this chain implies a risk. This risk is absorbed by the protection system, which brings the wind turbine to a safe condition in which it remains until normal operation can be resumed. The number of failures that demand activation of the protection system should be minimised in order to reduce the burden on the protection system. The probability of breakdown results from the probability of failure of the protection system combined with the probability of a critical error that requires the intervention of the protection system. The probability of breakdown shall be less than 0.0002 per machine year. The target for the reliability of the protection system is a number, which is large enough to keep the probability of breakdown below this level.

The grid-connected asynchronous generator with short-circuited cage winding in the rotor has been the basis for the safety considerations behind the Danish Approval Scheme and for the associated recommendations.

For a stall-controlled wind turbine with asynchronous generator, it is the generator and its relatively simple control that most of the time constitute the system that keeps the turbine in a safe condition. If the generator is disconnected due to an error or due to intervention by the protection system, at least one of the two fail-safe brake systems, which are part of the protection system, shall begin working. These are usually pitchable blade tips and mechanical brakes. “Fail-safe” is defined as a design philosophy by which the safety of the turbine is maintained even during component failure or grid failure.

Insofar as regards a turbine with variable speed and pitchable blades, and thus a relatively complex control, it is the

interaction between these features and the generator which ensures that the turbine is kept in a safe condition. If the generator is disconnected due to an error or due to intervention from the protection system, or if an error occurs in the blade pitch system or the speed control, at least one of the two fail-safe brake systems, which form part of the protection system, shall begin working. These are usually pitchable blades and mechanical brakes. Note that for turbines with pitchable blades, one of the two brake systems – the pitchable blades – forms part of both the protection system and the control system. Errors which have common root causes need to be given special attention. Neither blade pitch nor mechanical brake will have the required effect if the blades are locked at a position of, for example, +15°.

For such concepts, the target reliability quoted above still applies. Components which form part of both control and protection functions are to be fail-safe designed, or their probability of failure is to be minimised.

The generator is to be designed such that it can produce a sufficiently large torque to keep the turbine within its defined range of operation, see Section 2.2.1. Disconnection (switching off) of the generator should be based on reverse power, on zero-power, or on a signal from the relay protection against electrical errors. The purpose is to utilise the braking power of the generator in all situations.

When a frequency converter is used, it needs to be considered together with the generator with respect to safety and frequency of errors.

The generator is to be designed for the mechanical impacts it will be exposed to. At start-up of a turbine with fixed unpitchable blades in high wind speeds, the cut-in of the

generator should be performed at an undersynchronous number of revolutions to limit the acceleration until the full number of revolutions is achieved. At pitch control of the blades, a control strategy is to be applied which ensures limitation of the acceleration.

6.7.4 Cooling and degree of sealing

The cooling system of the generator should as a minimum correspond to IC41 for jacket cooling according to DS/EN60034-6.

The generator, including its possible external encapsulation and its external cooling system with cooling agents such as air or water, should as a minimum be protected against external impacts corresponding to degree of sealing IP54 in accordance with DS/EN60034-5.

The machine cabin of the wind turbine is not considered as a sufficient enclosure of the generator for protection against unintended intrusion of objects such as tools, dust from brakes, and hydraulic liquids. The internal shielding in the cabin is to provide safety for personnel and protection against unintended objects. The temperature can be higher in the cabin than outside the turbine, in which case the generator is to be designed for the temperature within the cabin, unless some other external cooling system is in place.

6.7.5 Vibrations

The generator shall be balanced such that it as a minimum fulfils the requirements to Class N according to DS/IEC60034-14. The generator shall be capable of withstanding vibrations from other parts of the wind turbine.

6.7.6 Overspeed

The generator is to be constructed such that it fulfils the requirements to overspeed according to DS/EN60034-1 and DS/EN

60034-3. For stall-controlled turbines with pitchable blade tips, a typical upper limit for overspeed in the context of grid failure and activation of the blade tips will be about 1.4 times the operational number of rotations.

Synchronous generators may produce overvoltage, which may be damaging to the frequency converter. To prevent overvoltage, the voltage should be adjusted downward. When permanent magnets are used, the generator terminals may be short-circuited or loaded by brake resistances.

Generators are to be capable of withstanding the following overspeed during two minutes: 1.25 times the rated maximum speed.

6.7.7 Overloading

The wind turbine is to be automatically controlled in such a way that it will be brought to either standstill or idling at a low rotational speed if the average produced power in 10 minutes exceeds 115% of the nominal (rated) power P_{nom} . For a stall-controlled wind turbine with a conventional asynchronous generator, it is in addition required that it shall be brought to a standstill or idling if the produced one-second mean power exceeds 140% of the nominal (rated) power. The corresponding limiting value for a pitch-controlled turbine with a conventional asynchronous generator is 200% of the nominal (rated) power P_{nom} .

For a passively controlled generator, the instantaneous value of the torque shall as a minimum be 1.35 times the one-second value. For an actively controlled generator, which forms part of the protection system, the overload capacity of the generator shall be documented for each individual concept. At short-circuiting of the grid and at short-term grid failure, the generator shall be capable of absorbing the thermal and dynamic forces.

6.7.8 Materials

Permanent magnets

Permanent magnets shall be designed in such a manner that the minimum induction locally in the magnet during an electrical fault will not fall short of the break point value, at which irreversible demagnetisation sets in at some extreme temperature. It is recommended to keep a margin to the break point value of at least 0.1 Tesla for NeBFe and 0.05 Tesla for ferrite materials. Mechanical stability of NeBFe magnets can be protected against corrosion by means of coating by tin, zinc or similar.

Coils

Coils are to be constructed with an insulation, which as a minimum meets the requirements to Class F according to IEC60085. The temperature rise at maximum load must not exceed the limits set forth for the chosen class of insulation in IEC60034-1. This refers to coils in air-cooled generators. The allowable temperature rise values are reproduced in Table 6-6 together with acceptable values for the total temperature.

Insulation class	Temperature rise (°C)	Total temperature (°C)
A	50	105
E	65	120
B	70	130
F	90	155
H	115	180

When a frequency converter is used, the coil insulation becomes exposed to a large impact due to large voltages U and large time derivatives dU/dt of the voltage. The impact can be reduced by application of filters for smoothing of the voltage. It shall always be ensured that the insulation of the generator can resist the impacts that it is

exposed to. A frequently applied maximum value for dU/dt is 1 kV/ μ sec. However, in some cases up to 5 kV/ μ sec is used. As a minimum, the insulation shall be capable of resisting impulse voltages of 1300 V as measured on the generator clamps. Alternatively, a different wire can be used to obtain extra insulation.

If there is a risk that the internal heating is insufficient to avoid damaging condensation of water in the generator, in particular at standstill, the generator shall be furnished with at-rest heating (heating system for use at standstill). In case of grid failure and longer periods of standstill, it must be ensured that the coil has dried out before the turbine is restarted. Note that for a generator in protection class IP54, at-rest heating is normally not considered necessary.

Bearings

When frequency converters are used, capacitive couplings might produce flow paths through the bearings. This might imply a reduced lifetime for the bearings. The impact shall be reduced to a level that the bearings can withstand, e.g. by insulation of the bearings, or by dU/dt filtering.

Bearings are to be efficiently and automatically lubricated at all running speeds and within the service intervals specified by the manufacturer. Provisions are to be made to prevent the lubricant from gaining access to windings or other insulated or exposed conducting parts.

6.7.9 Generator braking

By controlling a frequency converter, the generator can be used to reduce the rotational speed to the level that corresponds to the minimum frequency of the converter. This is referred to as generator braking. By means of external brake resistances, braking by means of the generator can form part of

the protection system brakes as well as of the operational brake system, provided that the generator remains magnetised during the braking and that braking to bring the turbine to a safe condition is fail-safe. Generator braking is suitable for synchronous generator types, including permanently magnetised generators and multiple-poled generators without gearbox, for which mechanical braking is made difficult by large dimensions.

6.7.10 Lifetime

The generator shall be designed for the same lifetime as the rest of the wind turbine. The design lifetime shall be at least 20 years. This requirement does not apply to components subject to wear, for which replacement intervals are specified in the user's manual for the actual type of wind turbine.

6.7.11 Testing of generators

For new generators, it is recommended that the manufacturer carries out tests as specified in the following. The tests may be arranged as type tests, as production sample tests, or as routine tests.

The manufacturer's test reports should provide information about make, type, serial number, insulation class, all technical data necessary for the application of the generator, and the results of the tests.

Recommended tests:

- temperature test at full load (minimum 1.15 times rated load)
- overload test
- overspeed test
- high-voltage test
- measurement of insulation resistance
- measurement of resistance of windings
- measurement of air gap
- open-circuit voltage characteristics
- short-circuit current resistance

- measurement of excitation current at rated current, voltage and power factor (if possible also at $\cos\phi = 0$ lag, where ϕ denotes phase angle)
- short-circuit test

Generators should withstand terminal short-circuits at least during one second without damage to the generator itself or to its excitation equipment. This can be verified by means of type tests or random tests.

Generators should have sufficient momentary and steady short-circuit current in relation to the release characteristics of switch and fuse gear on the installation, thereby ensuring a reliable release by short-circuits anywhere in the grid. This can be verified by random tests.

It is recommended that the steady short-circuit current should normally not be less than 3 times the full-load current.

6.8 Machine support frame

The machine support frame is located on top of the tower and supports the machinery, including the gear box. Usually, it also provides support for the nacelle cover. In contrast to the tower, the machine support frame is usually a very turbine-specific structure, which can be constructed in many different ways and according to many different layouts. It can be a welded, bolted or cast steel structure. Sometimes it is formed as an integral part of the gear box, i.e. the gear box itself acts as the machine frame. Sometimes it is integrated with the yaw system. Sometimes it is as simple as a big plate. It is, in general, a much less standardised product than a tower.

For design of the machine support frame, the following issues are important to consider:

- a sufficient stiffness of the frame must be ensured in order to meet the stiffness

requirements for the machinery. The gear box should not be able to move relative to the bearings, and the yaw system will not get sufficient mesh with the gear rim if the frame is not sufficiently stiff.

- sufficiently fine tolerances must be met during the manufacturing of the frame in order to facilitate the proper positioning and assembly of the yaw system and the transmissions.
- the frame must be designed against fatigue owing to its exposure to the rotor forces.
- access to the nacelle is obtained through the tower and the machine support frame, which implies that the machine support frame must include a hole of convenient size for personnel to pass.

The machine support frame is exposed to rotor loads consisting of thrust, yaw moment and tilt moment. These load components are not necessarily in phase. In addition hereto comes weight. Also, local forces wherever forces are being transmitted should be considered, i.e. forces at bearing housings, gear shafts, and yaw system. It is recommended to use finite element methods for structural analysis of the machine support frame.

6.9 Nacelle enclosure

The purpose of the nacelle enclosure is to protect the machinery and the control system of the wind turbine against rain and moisture and against salt and solid particles, such as sand grains in the air. The nacelle enclosure is also meant to protect against noise and is therefore often covered with some noise-reducing material. The enclosure needs to be tight to fulfil its purpose. However, it also needs to have ventilation to allow for adequate cooling of the gear system. The nacelle enclosure is to be designed for wind

load. In this context, it is important to choose correct lift and drag coefficients.

The nacelle enclosure is usually used also as a walkway and needs to be designed with sufficient dimensions for this purpose. In this context, it is particularly important to consider the design of the fixtures of the enclosure.

Moreover, it is important that the nacelle enclosure can be opened to allow for removal of damaged components for replacement, for example, by means of a helicopter.

Artificial light has to be installed to ensure safe access and working conditions.

6.10 Yaw system

Yaw denotes the rotation of the nacelle and the rotor about the vertical tower axis. By yawing the wind turbine, the rotor can be positioned such that the wind hits the rotor plane at a right angle. The yaw system provides a mechanism to yaw the turbine and to keep the rotor axis aligned with the direction of the wind. If situations occur where this alignment is not achieved, yaw errors are produced. The yaw error, or the yaw angle, is defined as the angle between the horizontal projections of the wind direction and the rotor axis.

The yaw system can be either passive or active. A passive yaw system implies that the rotor plane is kept perpendicular to the direction of the wind by utilisation of the surface pressure, which is set up by the wind and which produces a restoring moment about the yaw axis. For upwind turbines, this usually requires a tail vane in order to work properly. Also, coning of the rotor can help keeping the nacelle in place. Note that a passive yaw system may pose a problem in

terms of cable twisting if the turbine keeps yawing in the same direction for a long time. An active yaw system employs a mechanism of hydraulic or electrically driven motors and gearboxes to yaw the turbine and keep it turned against the wind. Such active

positioning of the turbine relative to the wind is also referred to as forced yaw. Most large horizontal axis wind turbines use forced yaw to align the rotor axis with the wind. An example of an active yaw system is given in Figure 6-25.

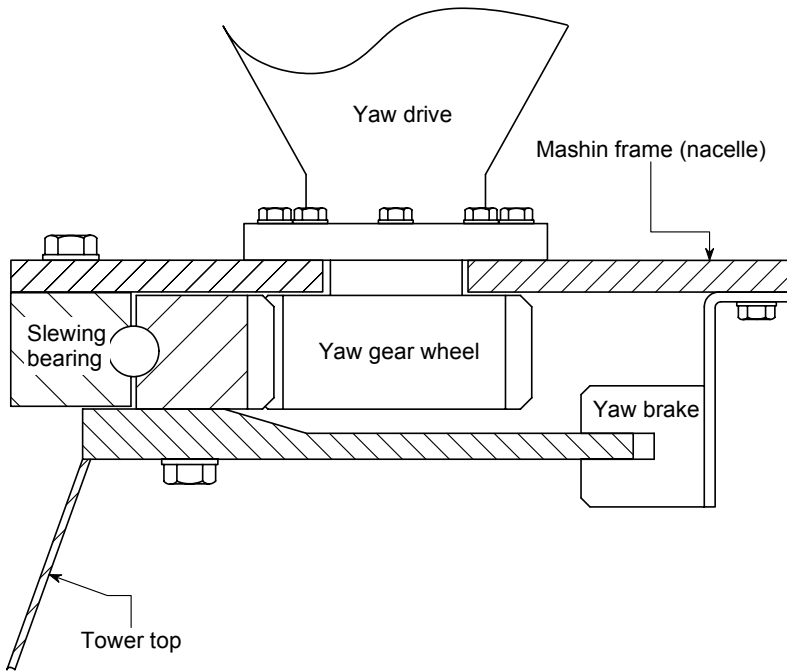


Figure 6-25. Typical active yaw system involving a slewing bearing

The mechanism used for an active yaw system usually consists of a number of electrically operated motors in conjunction with a gear that actuates a large toothed yaw ring in the tower circumference. Together with yaw brakes and yaw bearings, these components are most often delivered as standard components from a supplier, who also provides the pertaining design documentation. When used in a yaw system, it should be noted that these components may be exposed to conditions which have not been taken into account by the supplier. The following sections deal with the different components of an active yaw

system, including the yaw ring, the yaw drive with the yaw motors, the yaw bearing, and the yaw brakes.

The yaw error is usually measured by means of direction sensors such as one or more wind vanes. The wind vanes are usually placed on top of the nacelle. Whenever the wind turbine is operating, an electronic controller checks the orientation of the wind vanes and activates the yaw mechanism accordingly. In addition to this automated yaw of the wind turbine, it should be possible to yaw the nacelle manually. Manual yaw is needed during start-up,

service of the yaw system, and testing of the turbine.

6.10.1 Determination of design loads

Yaw is characterised by the maximum angular yaw velocity ω_k and the fraction of the design life during which yaw takes

place. When the duration of yaw is not known for design, DS472 specifies that yaw can be assumed to take place during 10% of the time for all wind speeds that occur. Assuming yaw in 10% of the time is, however, quite conservative for most sites.

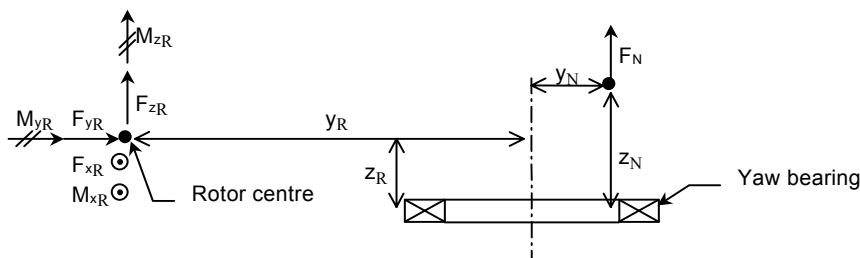


Figure 6-26. Loads acting on the rotor and the yaw bearing.

The static load consists of the weight of the nacelle and rotor, acting as an axial force on the bearing. This load is superimposed by the wind load on the rotor as illustrated in Figure 6-26.

In Figure 6-26, the rotor loads are drawn in directions according to a conventional coordinate system and not in the direction that they will normally have.

- F_{xR} side force on rotor and nacelle
- F_{yR} thrust on rotor
- F_{zR} weight of rotor
- M_{xR} tilting moment at rotor
- M_{yR} driving torque at rotor
- M_{zR} yaw moment at rotor
- F_N weight of nacelle
- y_N horizontal distance to nacelle c.o.g.
- y_R horizontal distance to rotor c.o.g.
- z_N vertical distance to nacelle c.o.g.
- z_R vertical distance to rotor c.o.g.

From these quantities, the static loading on the yaw bearing, tilt moment M_{tilt} , yaw moment M_{yaw} , radial force F_r and axial force F_a , can be calculated as

$$M_{\text{yaw}} = M_{zR} + F_{xR} \cdot y_R + M_{\text{brake}} + M_{\text{friction}}$$

$$M_{\text{tilt}} = \sqrt{M_1^2 + M_2^2}$$

with

$$M_1 = M_{yR} + F_{xR} z_R$$

$$M_2 = M_{xR} - F_{zR} y_R - F_{yR} z_R + F_N y_N$$

$$F_r = \sqrt{F_{yR}^2 + F_{xR}^2}$$

$$F_a = F_{zR} + F_N$$

The yaw moment depends on the magnitude of the yaw error and the wind speed. The direction of the yaw moment depends on the direction of the rotation of the rotor in conjunction with the direction of the yaw error.

The extreme design yaw moment, which is the design basis for yaw drives and yaw brakes, is likely to appear during operation at a maximum wind speed with a maximum yaw error. Dynamically, the yaw moment will have a tendency to oscillate with a frequency of x times the rotor frequency, where x denotes the number of blades.

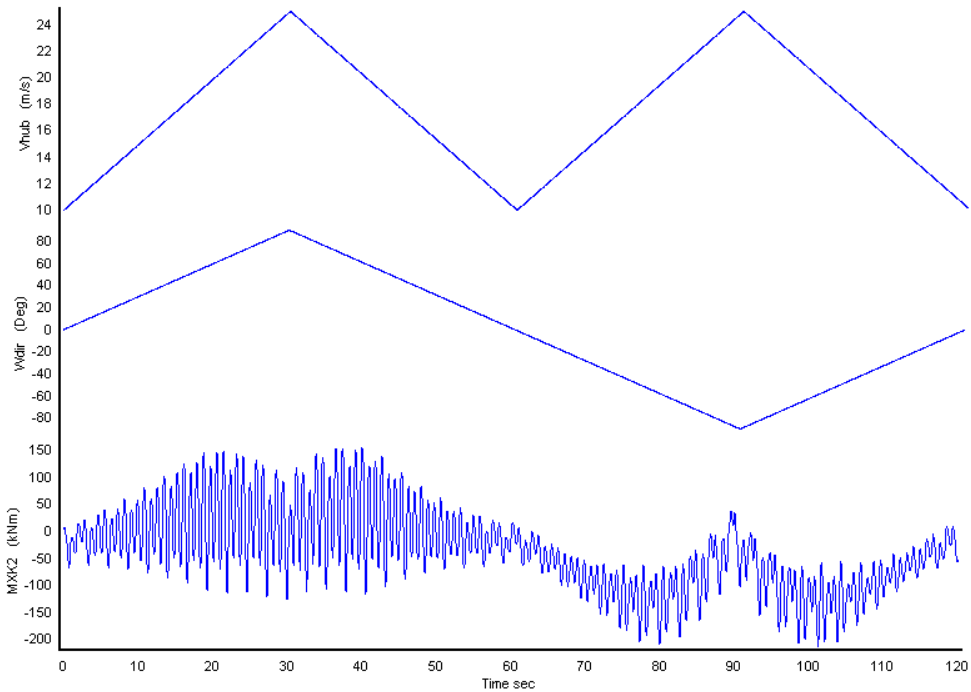


Figure 6-27. Relation between wind speed, yaw error and yaw moment.

Figure 6-27 shows a computer simulation of the yaw moment as a function of the yaw error and wind speed for a three-bladed wind turbine. It appears that the yaw error oscillates with frequencies equal to the rotor frequency and three times the rotor frequency. It also appears that the sign of the yaw moment changes when the yaw direction changes, and – not surprisingly – the yaw moment increases when the yaw error and the wind speed increase.

6.10.2 Yaw drive

The yaw drive is the system of components used to cause the yaw motion. A large yaw speed will produce gyro effects that will result in large loads on the wind turbine. The yaw speed must therefore be small enough

for gyro effects to become negligible. Reference is made to Section 4.2.1.

A passive yaw system will normally require some sort of damping arrangement to reduce the yaw speed.

For large turbines with active yaw systems, the yaw speed is usually lower than 1°/sec, which is small enough for the gyro effects to be ignored. To achieve such a low yaw speed, the yaw motors needs to be connected through a gearbox.

Such drives can be delivered as standard equipment from manufacturers of electrically operated motors.

The yaw drives must have sufficient power to overcome the largest mean yaw moment

occurring plus friction in the yaw bearing. Installation, lubrication and service should be undertaken in accordance with the specification from the manufacturer.

Pinion shaft, pinion and mounting must be designed to withstand the maximum yaw moment, including partial safety factors.

6.10.3 Yaw ring

The yaw drive is normally mounted on the nacelle in such a way that it is in gear with a toothed yaw ring mounted on the top of the tower. Yaw rings are normally toothed on the inner surface as this provides a better protection from the surroundings and implies a slightly better mesh.

The gears connected to the drive and the yaw ring must be designed in such a manner that tooth failure for the maximum peak yaw moment is prevented.

Bending stress in a tooth can be calculated according to DIN 3990, Part 3 from

$$\sigma_F = \frac{F}{b \cdot m} \cdot Y_f \cdot Y_e \leq \frac{\sigma_{Fl}}{S_F}$$

Y_f	tooth shape factor
Y_e	load reduction factor
F	tooth force
b	tooth width
m	module
σ_{Fl}	tooth yield stress
S_F	safety factor

Scuffing might occur in gears with hardened pinions whose tip edges act as scrapers. Damage due to wear and fatigue should be considered.

It should be noted that the yaw ring is not only loaded during yawing. Even though yaw brakes might be applied a part of the

yaw moment might be transmitted through the yaw drive.

6.10.4 Yaw brake

During power production, turbulence, wind shear and fairly small inevitable yaw errors will give rise to a torque moment about the tower axis. To keep the nacelle in position and to spare the gears, it is common to mount a brake disc in connection with the yaw bearing. Braking can then be performed by means of hydraulic activated callipers. Passive hydraulic callipers, i.e. spring-applied brake callipers, are preferable because they can ensure braking also in the case of a leakage in the hydraulic system.

The brake calliper manufacturer will provide surface tolerances and geometrical tolerances for the brake disc. These tolerances must be complied with.

The yaw brake callipers, discs and mounting bolts shall be designed to withstand the maximum occurring yaw moments. For turbines with yaw brake systems designed with limited safety ($S = 1.15$), it shall be proven that the turbine will withstand free yaw operation, i.e. inertia forces due to acceleration of the nacelle.

The brake is to be protected against dust, corrosion, oil and any other influence that might alter the friction. The brake and control system shall be designed such that a situation where pads are worn out is avoided.

In addition to using the ordinary yaw brake, it must be possible to block the yaw mechanism to enable service and maintenance adjacent to the yaw mechanism without any personal risk.

Blocking of the yaw system can be done by mechanical fixation of the yaw ring or the yaw motor shaft. Blocking of the yaw system must not be dependent on external

power supply. Only in the case of negative callipers, the motor is allowed to be electrically braked. A fixation of the ring is preferable because a possible backlash in the yaw gear can be large enough to cause the nacelle to jerk during service.

The locking mechanism must be designed for wind speeds up to the defined stop wind speed, above which maintenance, which demands locking of the yaw mechanism, is not permissible.

6.10.5 Yaw bearing

The yaw bearing is the bearing that supports the nacelle in a horizontal axis wind turbine. It is located between the rotating nacelle and the stationary tower and transmits wind loads from the nacelle to the tower. As regards the yaw bearing, it has been common in the past to choose between two different solutions – slide plates or rolling bearings.

Rolling bearings will often be designed as slewing bearings, which are capable of accommodating combinations of axial, radial and moment loads. Yaw motion is generated by gears mounted in the nacelle and being in gear with the toothed bearing. Slewing bearings, as seen in Figure 6-28, are mounted by means of bolting to the seating surfaces. Usually, bolts of quality 10.9 are recommended, see Appendix A.

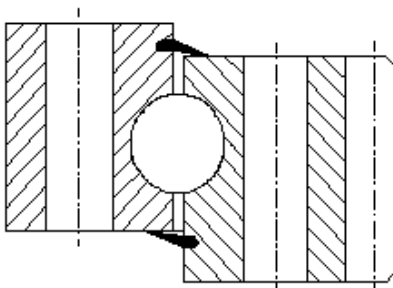


Figure 6-28. Four Point Ball Bearing.

Tolerances for the mounting surfaces should be in accordance with specifications from the bearing manufacturer. To prevent the bearing from becoming distorted, the contact surfaces must be carefully machined and attention must be drawn to the stiffness of the surrounding structure. Application of a plastic grouting may compensate for irregularities in the contact surfaces.

Slewing bearings used in yaw systems are different from normal bearings in that they are exposed to oscillatory motion. This oscillatory motion and the low rotational speed imply that slewing bearings have a tendency to exhibit a relatively low ratio between the lubrication film thickness and the surface roughness.

Calculation of the load rating for bearings in oscillatory motion is described in NWTC. It is quite complex and involves the variation of load and the bearing rotational position as a function of time. In practice, it is common that the bearing manufacturer provides the design calculation or means for how to verify the design.

Unlike regular rolling bearings, whose strengths are represented by the load rating C , the strength of a slewing bearing will normally be represented in terms of a curve that gives the relation between the allowable equivalent tilt moment and the equivalent axial load. Reference is made to Figure 6-29 for an example.

The equivalent axial load F_{eq} is calculated from the radial load F_r and the axial load F_a in the same way as for ordinary rolling bearings,

$$F_{eq} = (X \cdot F_a + Y \cdot F_r) \cdot K_A \cdot K_S$$

in which X and Y are combination factors which depend on the bearing type and the ratio between F_a and F_r . Values of X and Y

will be provided by the manufacturer. K_A is an application factor and is recommended to be in the range 1.7-2.0 for yaw bearings. The safety factor K_S equals the partial safety factor for the load of the relevant load case.

The tilt moment as calculated in Section 6.10.1 is denoted M_t , and the equivalent tilt moment M_{eq} is calculated as

$$M_{eq} = M_t \cdot K_A \cdot K_S$$

in which K_A and K_S are to be taken as for the axial load.

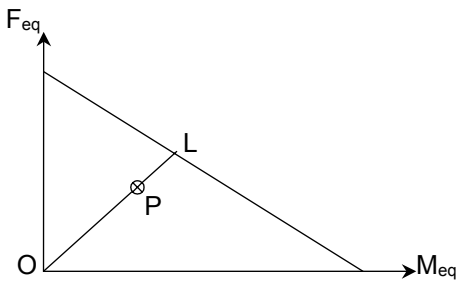


Figure 6-29. Bearing life curve.

The service life curve, which is exemplified in Figure 6-29, is usually provided by the manufacturer of the bearing. The service life curve represents the combinations of equivalent tilt moment and equivalent axial load for which the failure probability at a specified number of revolutions is 10%. Note that different manufacturers specify different numbers of revolutions for their respective service life curves. The number of revolutions is a measure of the bearing life. When M_{eq} and F_{eq} have been calculated, the corresponding point P can be plotted as shown in Figure 6-29. The extension of the line OP intersects with the service life curve in the point L. The bearing life, specified by the manufacturer in terms of a number of revolutions, can now be increased by multiplication by a factor which is to be calculated as the line length ratio $|OL|/|OP|$.

As for any other component in the wind turbine, the dynamic loading of the bearing can be represented by one or more load spectra, or – on a simpler form – by a number of load cases that are assumed to adequately represent the loading that the bearing will experience over the design life of the turbine. In the latter case, at least four load cases should be modelled. The equivalent load for a specified load spectrum or a set of representative load cases can be calculated according to the formula

$$P = \sqrt[p]{\frac{\sum_i P_i^p \cdot O_i}{\sum O_i}}$$

in which P denotes either the equivalent axial force F_{eq} or the equivalent tilt moment M_{eq} , depending on whether axial force or tilt moment is considered. O_i denotes the duration of the load P_i corresponding to the i th load block in a discretisation of the load spectrum or the i th load case when a load case representation is adopted. The exponent p is referred to as the bearing exponent and is to be taken as 3 for ball bearings and as 10/3 for roller bearings.

A curve similar to the one shown in Figure 6-29 is used to calculate the stress reserve factor during extreme loading of the bearing. Calculation of equivalent loads F_{eq} and M_{eq} is also analogue. The different application factors, X , Y , etc. will, however, differ.

When slewing bearings are provided with spur gears, the manufacturer will normally specify the allowable tangential force with reference to the bending stress at the root of the tooth in order to prevent tooth failure.

The friction torque moment in a slewing bearing can be calculated as

$$M_{yaw} = \mu \cdot (a \cdot M_t + b \cdot F_a \cdot D_r + c \cdot F_r \cdot D_r),$$

M_{yaw}	friction moment
μ	friction coefficient
M_t	tilting moment
F_a	axial force (gravity)
F_r	radial force (thrust + side)
D_r	raceway diameter

For a four-point ball bearing the coefficients can be set to

$$\mu = 0.006, a = 2.2, b = 0.5 \text{ and } c = 1.9$$

Proper lubrication of the yaw bearing is of great importance. It is advised to follow the bearing manufacturer's instructions regarding type and amount of grease, and relubrication intervals.

One way of improving the lubrication in a bearing is periodically to let the bearing rotate through an angle equal to at least one bearing segment.

Bearing seals should be checked every six months.

DNV (1992) recommends that the safety against failure for the slew ring toothing is to be 1.6.

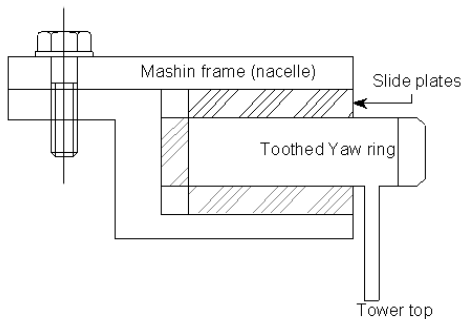


Figure 6-30. Schematic diagram of slide bearing.

An alternative to a slewing bearing is a slide bearing, which is often designed as a

number of plates and claws that engage the nacelle to the tower, see Figure 6-30.

The materials used for slide bearings are cast polyamide plates or similar materials which are relatively strong, with good sliding and hard-wearing properties.

Table 6-7 gives properties for a few types of relevant materials. The mechanical properties listed apply to the unreinforced material. The data given are only to be considered as guidance, since data from different manufacturers vary considerably.

Polyurethane (PUR) has a high ultimate strength combined with a large elongation at failure, i.e. it exhibits a ductile behaviour. It has good wearing properties and exhibits constancy towards oil and grease. Different types of PUR are categorised according to their "Shore hardness". The Young's modulus of elasticity of polyurethanes grows exponentially with the Shore hardness.

Polyamide (PA) is characterised by a combination of mechanical strength and chemical resistance, good sliding properties and high fatigue strength. PA is categorised according to the number of C-atoms in its molecules.

Acetal (POM) offers excellent inherent lubricity, fatigue resistance, and chemical resistance. Acetals suffer from outgassing problems at elevated temperatures, and they are brittle at low temperatures.

Polyethylene Terephthalate (PET) exhibits good creep constancy, which means that it can absorb large static loads. It also exhibits good dimensional stability, wear properties and low friction. On the negative side, it is sensitive to notches.

Plates used for slide bearings will normally need to be greased to obtain a sufficiently low friction torque and for corrosion protection of the steel parts.

A major difference between rolling bearings and slide bearings is that slide bearings involve larger frictional resistance. Slide bearings therefore require larger yaw motors but less brake capacity than rolling bearings.

	PA 66	PUR	PET	POM
Tensile strength	52 MPa	83 MPa	46 MPa	61 MPa
Compressive strength	60 MPa	NA	97 MPa	31 MPa
Flexural module	1379 MPa	3447 MPa	2758 MPa	2620 MPa
Hardness Rockwell R	100	119	120	107
Temperature				
Maximum	121 °C	110 °C	100 °C	N/A
Minimum	-79 °C	-40 °C	-15 °C	N/A

Source: www.plasticsusa.com

6.10.6 Yaw error and control

Yaw errors have a significant impact on the blade loads, the rotor loads and the power production. Hence, it is important that the yaw mechanism is efficient and reliable. Even small yaw errors give rise to increased fatigue loads in the blades due to the variation in the inflow angle during the rotation of the rotor that they cause.

If the yaw error becomes too big, i.e. if it falls outside the specified or assumed range of operation, the wind turbine must be stopped.

Special arrangements to prevent long-term yaw errors can be made. One such arrangement is formed by using a set of independent wind vanes. In case one of the vanes gets stuck, the vanes will misalign. An error message will then be produced, and the wind turbine will be stopped.

6.10.7 Cable twist

In large power producing turbines, cables are needed to conduct the current from the wind turbine generator down through the tower. The cables will become twisted if the turbine keeps yawing in the same direction

for a long time. The wind turbine must, therefore, be equipped with a cable twist sensor, which monitors the number of revolutions and informs the controller when it is time to untwist the cables, usually after 2 to 4 revolutions. The sensor can be designed quite simply as a switch on the yaw drive which is activated once per revolution.

With regard to redundancy in the cable twist monitoring system, the wind turbine can also be equipped with a pull switch which becomes activated when the cables become too twisted.

To emphasise the importance of preventing cable twisting, it suffices to note that the turbine can easily experience 50-100 rotations in the same direction during one year, if it is allowed to rotate unrestricted.

6.10.8 Special design considerations

Due to yaw moments being cyclic as mentioned in Section 6.10.1, loose fits should be avoided.

REFERENCES

- AGMA, *Recommended Practices for Design and Specification of Gearboxes for Wind Turbine Generator Systems*, American Gear Manufacturers Association, Alexandria, Virginia, 1997.
- Bergmann, J., and R. Thumser, *Forschung für die Praxis P 249, Synthetische Wöhlerlinien für Eisenwerkstoffe*, Studiengesellschaft Stahlanwendung e.V., Verlag und Vertriebsgesellschaft mbH, Düsseldorf, Germany, 1999.
- Bonus, *Bonus Info, Special Issue, the Wind Turbine Components and Operation*, Autumn, Brande, Denmark, 1999.
- The Danish Energy Agency, *Technical Criteria for the Danish Approval Scheme for Wind Turbines*, Copenhagen, Denmark, April 2000.
- Dansk Ingeniørforening, *Last og sikkerhed for vindmøllekonstruktioner*, (in Danish), DS472, 1st edition, Copenhagen, Denmark, 1992.
- Det Norske Veritas, *Calculation of Gear Rating for Marine Transmissions*, DNV Classification Note No. 41.2, Høvik, Norway, 1993.
- Det Norske Veritas, *Guidelines for Certification of Wind Turbine Power Plants*, Copenhagen, Denmark, 1992.
- DIN 743, *Tragfähigkeitsberechnung von Wellen und Achsen*, 1998.
- DIN 743, Part 1-3, *Tragfähigkeitsberechnung von Welle und Achsen*.
- FAG Technical Information, *FAG Rolling Bearings*, TI No. WL 43-1190 EA.
- FAG OEM und Handel AG, *Rolling Bearing Lubrication*, Publ. No. WL 81 115/4 EA.
- Gudehus, H., and H. Zenner, *Leitfaden für eine Betriebsfestigkeitsrechnung*, 4. Auflage, Verein Deutscher Eisenhüttenleute, Düsseldorf, Germany, 1999.
- IEC, *Wind turbine generator systems – Part 1: Safety requirements*, International Standard, IEC61400-1, 2nd edition, 1999.
- ISO, *Rolling bearings – Dynamic load ratings and rating life*, International Standard, ISO281, 1st edition, 1990.
- ISO, *Rolling bearings - Static load ratings*, International Standard, ISO 76, 2nd edition, 1987.
- Niemann, G., and H. Winter, *Maschinenelemente, Band II, Getriebe allgemein, Zahnradgetriebe – Grundlagen, Stirnradgetriebe*, Springer-Verlag, Berlin, Germany, 1985.
- NWTC, *Guideline DG03, Wind Turbine Design, Yaw & Pitch Rolling Bearing life*, National Renewable Energy Laboratory, NWTC – Certification Team.
- Peterson, R.E., *Stress Concentration Factors*, John Wiley and Sons, New York, N.Y., 1974.
- Pilkey, W.D., *Peterson's Stress Concentration Factors*, 2nd edition, John Wiley and Sons, New York, N.Y., 1997.
- Roloff, H., and W. Matek, *Maschinenelemente. Formelsammlung*, Vieweg Verlag, Braunschweig/Wiesbaden, Germany, 1994.
- SKF, *General catalogue*, SKF, Denmark, 1989.

SKF, *Roller Bearings in Industrial Gearboxes, Handbook for the gearbox designer*, SKF, Denmark, 1997.

Sundström, B., *Handbok och formelsamling i Hållfasthetslära*, Institutionen for hållfasthetslära, KTH, Stockholm, Sweden, 1998.

VDI Berichte 1442, *Festigkeitsberechnung Metallischer Bauteile*.

7. Tower

The tower of a wind turbine supports the nacelle and the rotor and provides the necessary elevation of the rotor to keep it clear off the ground and bring it up to the level where the wind resources are. The towers for large wind turbines are typically made of steel, but concrete towers are sometimes used. Nowadays, most towers are tubular towers, however, lattice towers are also in use. Guyed towers are used for relatively small wind turbines only. The tower is usually connected to its supporting foundation by means of a bolted flange connection or a weld.

In the context of wind turbines, the tower constitutes a low-technology component whose design is easy to optimise, and which therefore – during the design process – lends itself easily as an object for possible cost reduction. This may come in useful as the cost of a tower usually forms a significant part of the total cost of a wind turbine.

Figure 7-1 shows an array of the most common tower structures. The main features of the different tower types are briefly dealt with below.

Tubular towers

Most large wind turbines are delivered with tubular steel towers, which are manufactured in sections of 20-30 m length with flanges at either end. The sections are bolted together on the site. The towers are conical, i.e. their diameters increase towards the base, thereby increasing their strength towards the tower base, where it is needed the most, because this is where the load response owing to the wind loading is largest. Since the necessary shell thickness is reduced when the diameter increases, the conical shape allows for saving on the material consumption.

The maximum length of the tower sections is usually governed by requirements to allow for transportation. Also, the upper limit for the outer diameter of the tower is usually governed by such requirements, at least for land-based turbines – the maximum clearance under highway bridges in



Figure 7-1. Various tower structures. From www.windpower.org, © Danish Wind Turbine Manufacturers Association.

Denmark is 4.2 m. An advantage of tubular towers compared to other towers is that they are safer and more comfortable for service personnel and others that have to enter and climb the towers.

Lattice towers

Lattice towers are manufactured by means of using welded steel profiles or L-section steel profiles. Since a lattice tower requires only about half as much material as a freely standing tubular tower with a similar stiffness, the basic advantage of lattice towers is reduced cost. It also gives less wind shade than a massive tower. The major disadvantage of lattice towers is their visual appearance, although this is a debatable issue. Nevertheless, for aesthetic reasons lattice towers have almost disappeared from use for large, modern wind turbines.

Guyed pole towers

Many small wind turbines are built with narrow pole towers supported by guy wires. The advantage is weight savings and thereby reduced costs. The disadvantages include difficult access around the towers, which make them less suitable in farm areas. Finally, this type of tower is more prone to vandalism, thus compromising the overall safety.

Other types

Some towers are designed as hybrids of the above types, for example the three-legged tower for a 95 kW turbine in Figure 7-1.

7.1 Load cases

The load cases to be investigated for tower design are described in Section 4.1. However, some special load cases may apply particularly to the tower, for example those that need to be considered when a long tower is to be transported. In addition, the erection of the tower on site may involve

critical loads. Such special cases should be investigated as appropriate.

7.2 Design loads

As described in Section 4.3, the design loads are most often determined on the basis of an aeroelastic analysis or – less frequently – by a simplified calculation, see Section 4.5. Regardless of which analysis approach is used for these calculations, the loads should be calculated from a model, in which the tower properties (geometry, materials, stiffness) are in agreement with the ones used in the final design. Thus, the design of the tower may demand an iterative procedure to get from an initial design to the final design with the correct stiffness.

The design loads for fatigue are to be determined by calculations, which are to be supplemented and verified by actual measurements from a prototype turbine. Since load measurements cannot be made until the turbine has been designed and constructed, it is recommended to apply an additional partial safety factor of 1.2 on fatigue loads until measurements are carried out and become available. The use of an additional safety factor as an extra precaution is meant to avoid a major redesign in the event of increased design loads.

The extreme design loads can only be determined by calculations, because these loads cannot be measured due to the long recurrence period between events.

When designing a turbine with fixed speed, the frequency of the rotor revolution is of the utmost importance. This frequency, often referred to as ‘1P’, may induce increased dynamic loads, e.g. due to rotor unbalances, wind shear and tower shadow. In addition, the higher ‘P’s’ are of importance, e.g. the ‘2P’ and the ‘3P’, which

are the frequencies of blades passing the tower on a two- and three-bladed turbine, respectively. When designing a turbine with variable speed, one must verify that the rotor speed of the turbine does not operate in or near the first natural frequency of the tower, see Section 7.3.1.

i.e. the 1P and 3P frequencies, respectively. If it is confirmed that the tower frequency is kept outside ranges defined as the rotor frequency $\pm 10\%$ and the blade passing frequency $\pm 10\%$, respectively, then there will normally not be any problems due to load amplification arising from vibrations at or near the natural frequency.

7.3 General verifications for towers

7.3.1 Dynamic response and resonance

The first natural frequency of the tower should always be measured in connection with the erection of a prototype turbine.

For turbines with two generators or two generator speeds, this investigation should be performed for both corresponding blade-passing frequencies. Special attention should be given to variable-speed turbines, in which cases the turbine should not be allowed to operate in a frequency interval defined as the eigenfrequency of the tower $\pm 10\%$.

It should be verified that the first natural frequency of the tower does not coincide with the rotor and blade-passing frequencies,

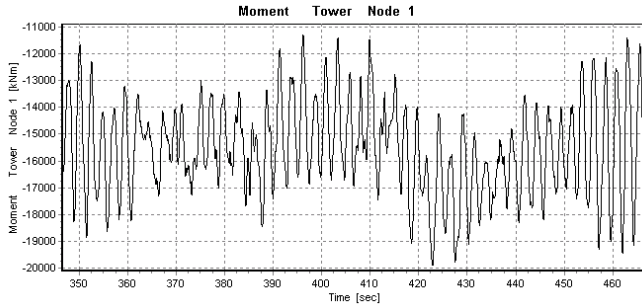


Figure 7-2: Time series: response at tower bottom

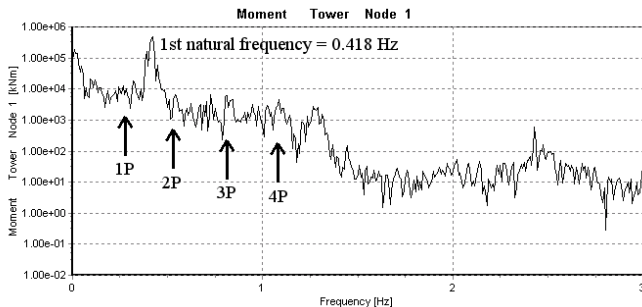


Figure 7-3: Power spectrum: response at tower bottom

When turbines are operating in an over-synchronous mode, i.e. where the 1P frequency is larger than the first tower natural frequency, one must include a proper analysis of the start-up and stopping sequences. This should be done in order to account for the increased dynamic loading that occurs when the rotor frequency is passing through the first natural frequency of the tower.

An example for a 1.8 MW turbine is shown in Figure 7-2 and Figure 7-3. From the power spectrum it appears that the major part of the energy is found at the natural frequency of the tower at 0.418 Hz. The 1P to 4P passing frequencies are not close to the first natural frequency. Furthermore, only a small quantity of energy is found on the passing frequencies in the response spectrum.

It should be noted that the natural frequency of the tower is very dependent on the ‘efficiency’ of the presumably fixed support at the foundation level. If the calculation model assumes that the tower is completely fixed, then the error in the natural frequency of the tower may be up to 20%. Guidelines for selection of elastic springs as supports for a tower whose foundation is not rigid can be found in Chapter 8. Note that it is becoming practice to use tower dampers to compensate for low damping perpendicular to the direction of the wind.

When large variations in the foundation stiffness are encountered within a particular project, such as the development of a wind farm, the natural frequency in bending should be measured at all installations.

7.3.2 Critical blade deflection analysis

The distance between tower and the blade tip should comply with the following condition

$$d_0 - \gamma \cdot u_{\max} > F$$

- d_0 distance between the tower and the blade tip in the unloaded/undeflected condition
- u_{\max} maximum deflection of the blade considering all relevant load cases and based on characteristic load values and characteristic material properties
- γ partial safety factor on the maximum deflection of the blade, to be chosen according to the relevant load case
- F requirement to the residual clearance between the tower and blade tip, usually 0.0

The definition of the safety factor γ depends on which set of standards is used for the critical blade deflection analysis.

According to IEC61400-1, the safety factor on the maximum deflection is taken as equal to the corresponding partial safety factor for load γ_f times the material factor γ_m . The value of γ_m to be used for this purpose depends on the coefficient of variation of the strength and on the definition of the characteristic strength. For example, when the coefficient of variation is 10% and the characteristic strength is defined as the 5% quantile with 95% confidence, then $\gamma_m = 1.1$. The value of γ_f to be used depends on which load case governs the design.

When considering the blade-to-tower distance, one should be aware that not only the blades but also the tower will deflect when exposed to wind loading, and the deflection of the tower may be out of phase with the deflection of the blades.

Note that the clearance between blade and tower is not only governed by the structural deflections, but also by a possible slip at the yaw bearing, by the perpendicularity of the tower flange, and by the tolerances on the tilt and on the rotor plane.

Large blade deflections are typically encountered in extreme wind situations, but also in the operating condition when the yaw angle is large or when the terrain is sloping. Atypical wind profiles may also give rise to large blade deflections. Special attention should therefore be given to wind turbine designs that are sensitive to special load cases such as negative wind shear in complex terrain.

The current Danish practice uses validated stiffness data in the aeroelastic calculations for analysis of deflections. Validated stiffness data are blade stiffness data, which comply with the experimental data from static tests of the blades. This implies that one may have to produce two sets of aeroelastic calculations. The first is a load calculation, in which the model is tuned to the correct natural frequencies and damping properties of the structural system. The second is a special deflection model where the deflections are tuned to be in agreement with the static experiments. Ideally, the two models would be the same, but in practice, this is not always the case.

7.4 Tubular towers

7.4.1 Loads and responses

For the purpose of calculating section loads in the tower, the tower can be viewed as a cantilever beam as shown in Figure 7-4. External loads, denoted by index T in this figure, are applied at the tower top flange, which is located at a height H above the tower base. Note that this height may deviate somewhat from the hub height.

Section loads in the tower at height h can be calculated from the loads applied at the top of the tower:

$$F_z(h) = F_{zT} + \rho_t \int_h^H A(z) dz$$

$$M_z(h) = M_{zT}$$

$$F_y(h) = F_{yT} + F_w(h)$$

$$M_x(h) = M_{xT} + F_{yT} \cdot (H - h) + M_w(h) + F_{zT} \cdot (\delta(H) - \delta(h))$$

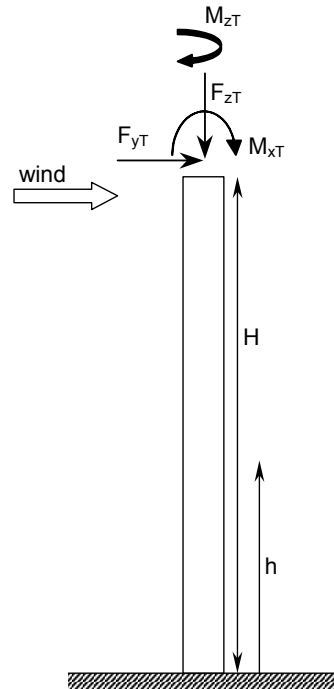


Figure 7-4. Cantilever beam model of a tubular tower subject to loading at the level of the hub.

F_y	thrust from wind load
M_x	bending moment from wind load
F_z	gravity force
M_z	torsional moment
ρ_t	density of tower including appurtenances
$A(z)$	cross-sectional area as a function of height z
δ	deflection of tower due to thrust from wind

External loads, here denoted by index T , are assumed to include the dynamic effect or gust factor (referring to a quasi-static approach).

In M_{xT} , it is particularly important to include the contribution from the possible eccentricity of the nacelle.

The section force $F_w(h)$ and the moment $M_w(h)$ from the wind load on the tower can be calculated as

$$F_w(h) = \frac{1}{2} \rho \int_h^H V(z)^2 \varphi D(z) C(z) dz$$

$$M_w(h) = \frac{1}{2} \rho \int_h^H (H - h - z) V(z)^2 \varphi D(z) C(z) dz$$

ρ	air density
$V(z)$	wind speed
$D(z)$	outer tower diameter
$C(z)$	form factor
φ	gust factor

$C(z)$ depends on the Reynold's number, $Re = VD/\nu$, in which ν denotes the kinematic viscosity of air. At 20°C, $\nu = 15.09 \cdot 10^{-6}$ m²/sec. For painted steel towers, $C(z)$ can be set to 0.6.

7.4.2 Extreme loads

For identification of the loads that govern the design, the specific combination of load components that produces the highest stress must be found. This can be quite a task when an aeroelastic analysis program is used that simulates a large number of load cases in 10-minute time series. Further, determination of which load case actually governs the design will most likely vary from different sections of the tower.

Alternatively, loads must be combined by taking the maximum of each load component from the particular load case where the most dominant load has its maximum, or more conservatively they can be combined by combining the maxima of the various load components regardless of which load case they actually appear in.

7.4.3 Fatigue loads

Combining fatigue loads is an even more complicated task. When using the rain-flow method as described in Section 4.4.1, the load spectra for the different load components are normally not directly combinable.

Therefore it might be a good idea, if possible, to combine the time series of the various load components resulting from the aeroelastic simulation. For example, the resulting bending moment in the direction θ relative to the y -axis can be calculated as

$$M_{res} = M_x \sin \theta + M_y \cos \theta$$

in which M_x and M_y are the bending moments associated with the load components in the x and y directions, respectively.

This could be taken even further to calculate the stress at relevant sections in the tower for every time step during the simulation and subsequently rain-flow count the resulting time series of the stress.

7.4.4 Vortex induced vibrations

The turbine must be checked for vortex induced vibration. The vortex excitation may occur during mounting of the turbine, i.e. in a situation where the rotor and nacelle have not yet been mounted on the tower. A suggested procedure to be followed for this purpose can be found in Eurocode 1, Section 2.4, Annex C or alternatively in the Danish

DS410, according to which the critical wind speed v_r can be calculated as

$$v_r = \frac{n \cdot D}{St}$$

- n tower natural frequency
- D tower diameter
- St Strouhal number

For conical towers, D should be set equal to the top diameter.

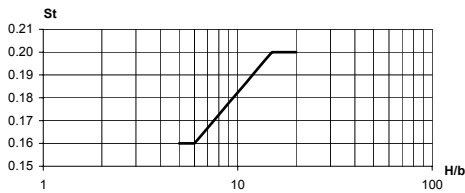


Figure 7-5. The Strouhal number vs. ratio between tower height H and tower diameter b .

The analysis might prove that certain wind velocities should be avoided when erecting the tower. However, the sensitivity to vortex vibrations may be changed by temporary guy wiring of the tower or by mounting a temporary mass near the top of the tower.

Normally, vortex-induced vibrations do not pose any problems after installation of the tower and the wind turbine. Once the nacelle is in place, its weight will lower the critical wind speed for vortex-induced vibrations to a low level – typically below 10 m/s – which is within the interval of power production.

When the blades rotate and pass the tower, they will reduce the wind speed and create turbulence in the wind that passes the tower behind the blades, thereby obstructing the generation of vortices.

Another aspect, which contributes to reducing the effect of vortex-induced

vibrations, is the aerodynamic damping of the blades and the nacelle.

7.4.5 Welded joints

Welds are, in general, treated in the same manner as the rest of the structure when a proper reduction factor for the weld quality and base material is included.

Table 7-1 shows the recommended detail categories for bolts with rolled threads after heat treatment and common welds in tubular towers according to the standards Eurocode 3 and DS412. The given detail categories assume 100% controlled full penetration butt welds of quality level B according to DS/ISO 25817.

Weld	Categories
plate to plate	80
plate to flange	71
plate to door frame	80
axially loaded bolts	71

Table 7-1. Detail categories for bolts and common welds in tubular towers.

Figure 7-6 shows typical welds in a tubular tower.

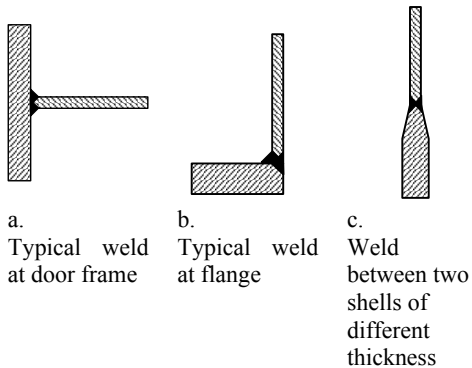


Figure 7-6. Typical weld details in tubular tower

Note that for the weld between the tower shell and the flange in Figure 7-6b, the given detail category assumes a small shell thickness relative to the flange thickness.

Note also that a weld between two shells of different thickness as shown in Figure 7-6c is symmetrically tapered to avoid stress concentrations. The slope of the tapering should not be greater than 1:4.

In case of single-sided tapering, as shown in Figure 7-7, a stress concentration is introduced.

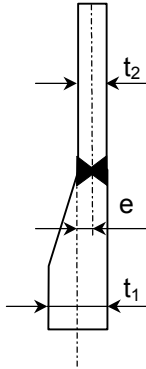


Figure 7-7. Single-sided plate tapering in tubular tower

According to DNV (1987), the stress concentration factor for the single-sided plate tapering can be calculated as

$$SCF_{taper} = 1 + 6 \frac{e}{t_2 \left(1 + \left(\frac{t_1}{t_2} \right)^{2.5} \right)}$$

in which t_1 and t_2 are the plate thickness of the lower and upper part of the tower shell, respectively, and the eccentricity e is given by

$$e = \frac{1}{2}(t_1 - t_2)$$

When using quality levels poorer than B according to DS/ISO 25817, it is recommended to apply detail categories a corresponding number of levels lower.

The fatigue damage can be calculated using the Palmgren-Miner's rule as described in Appendix C.

Whenever the weld is perpendicular to the direction of loading and the material thickness t is greater than 25 mm, the fatigue strength σ_{fatd} should be reduced in accordance with the following formula

$$\sigma_{red,fatd} = \sigma_{fatd} \cdot (25/t)^{0.25}$$

In cases where it is not possible to achieve the required design lifetime for a detail in an analysis that includes partial safety factors, inspection of the detail is required. However, it is still necessary to meet the requirements to the nominal lifetime when calculations are made without partial safety factors on the material properties included. Note that this approach is only allowed in Danish standards.

The period of time until the first inspection is carried out should at the most be set equal to the calculated design lifetime in the event that partial safety factors are included. Once one or more inspections have been carried out, subsequent inspection intervals should be chosen depending on the results of the previous inspections.

7.4.6 Stress concentrations near hatches and doors

The doors and hatches induce stress concentrations near the openings. This stress concentration is traditionally represented by a stress concentration factor (SCF), which expresses the stress ratio between a sample with and a sample without the opening. The SCF could be determined from parametric equations, from a finite element analysis or by model experiments. A study by Jørgensen (1990) found a SCF of about 1.8 for a door opening. However, it is recommended that an individual SCF analysis

should be performed for each detail in question.

It is important to consider stress concentrations at the tower door. Especially, as they depend heavily on how the door flange is carried out, i.e. whether it is straight, or whether it is curved in order to follow the curvature of the tower wall at the top and bottom of the door. Moreover, they depend on how the flange is aligned with the tower wall, and whether it is placed externally or internally with respect to the tower wall.

Further, it must be considered to what extent the door frame replaces the missing tower shell regarding the cross-sectional area, moment of inertia and centre of gravity. Finally, it might be relevant to consider local stability of the door region.

For unstrengthened circular holes, like inspection holes and port holes, the stress concentration factor for bending will normally be about 3.

For small holes like bolt holes, detail categories can be found in structural steel codes.

Nowadays, the fatigue loading often governs the design near openings. In this case, a suitable fatigue strength curve is to be selected. This should be done in agreement with Section 9.6.3 of Eurocode 3, which specifies the use of a “Category 71 curve” for a full penetration butt with permitted welds defects acceptance criteria satisfied. The fatigue damage is calculated using a Palmgren-Miner’s approach.

7.4.7 Stability analysis

The buckling strength of the tower usually governs the tower design as far as the shell thickness is concerned. The buckling strength of the tower can be analysed using

the approach described in Annex D of DS449 combined with DS412, DIN 18800 or other recognised standards.

In the following, the method suggested in the Danish standard is presented.

Stresses owing to the axial force, σ_{ad} , and owing to the bending moment, σ_{bd} , are given by

$$\sigma_{ad} = \frac{N_d}{2\pi R t}$$

$$\sigma_{bd} = \frac{M_d}{\pi R^2 t}$$

A reduction factor ϵ is calculated as

$$\epsilon_a = \frac{0.83}{\sqrt{1 + 0.01 \frac{R}{t}}}$$

$$\epsilon_b = 0.1887 + 0.8113 \epsilon_a$$

$$\epsilon = \frac{\epsilon_a \sigma_{ad} + \epsilon_b \sigma_{bd}}{\sigma_{ad} + \sigma_{bd}}$$

According to theory of elasticity, the critical compressive stress is

$$\sigma_{el} = \frac{E_d}{\frac{R}{t} \sqrt{3(1-\nu^2)}}$$

The relative slenderness ratio for local buckling is

$$\lambda_a = \sqrt{\frac{f_{yd}}{\epsilon \sigma_{el}}}$$

If $\lambda_a \leq 0.3$, the critical compressive stress σ_{cr} is given by

$$\sigma_{cr} = f_{yd}$$

If

If $0.3 < \lambda_a \leq 1$, the critical compressive stress σ_{cr} is given by

$$e > \frac{2}{1000} H$$

$$\sigma_{cr} = (1.5 - 0.913\sqrt{\lambda_a}) f_{yd}$$

then an additional increment

However, if the tower height H does not exceed $1.42 R\sqrt{R/t}$, then

$$\Delta e = (e - \frac{2}{1000} H)$$

$$\sigma_{cr} = f_{yd}$$

is to be added to e .

From theory of elasticity, the Euler force for a cantilever beam is given by

Finally, the following inequality must be fulfilled

$$N_{el} = \frac{\frac{1}{4} \pi^2 E_d \pi R^3 t}{H^2}$$

$$\frac{N_d}{2\pi R t} + \frac{N_{el}}{N_{el} - N_d} \cdot \frac{M_d + N_d e}{\pi R^2 t} < \sigma_{cr}$$

The relative slenderness ratio for global stability is

- N_d design axial force
- M_d design bending moment
- R tower radius
- t tower shell thickness
- H tower height
- E_d design modulus of elasticity
- ν Poisson's ratio
- f_{yd} design yield stress

$$\lambda_r = \sqrt{\frac{\sigma_{cr}}{\left(\frac{N_{el}}{2\pi R t}\right)}}$$

The core radius k of a tube is given by

7.4.8 Flange connections

$$k = \frac{R}{2}$$

The tower sections and the connection to the foundation are often adjoined with L or T flange connections.

For cold-formed welded towers, the equivalent geometrical imperfection can now be calculated as

Figure 7-8 shows an L flange connection along with the deformed shape of the upper side of the connection. Using the model in Figure 7-8, the tension force Z in the tower shell and the bolt force F are calculated from

$$e = 0.49(\lambda_r - 0.2)k$$

$$Z = \frac{4 \cdot M}{D \cdot n}$$

For welded towers, it can be calculated as

and

$$e = 0.34(\lambda_r - 0.2)k$$

However, if $\lambda_r \leq 0.2$ then $e = 0$.

$$F = Z + R = Z \frac{a+b}{a}$$

respectively.

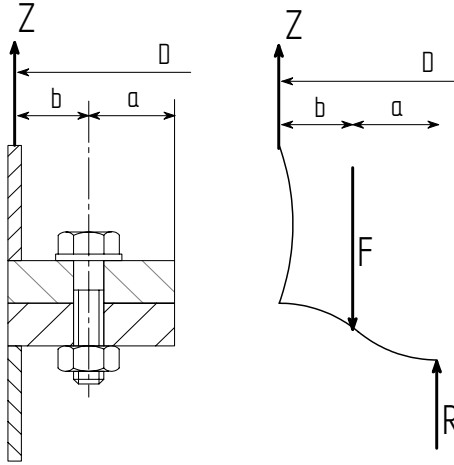


Figure 7-8. L flange connections.

The bolt stress, disregarding pretension, in the L flange connection is given by

$$\sigma_L = \frac{F}{A_{st}}$$

- M_d design bending moment
- D diameter of tower shell
- n number of bolts
- A_{st} bolt stress area

Since tower flanges often have a considerable thickness, the risk of brittle fracture should be considered. This can be done according to Eurocode 3, Annex C or DS412, Annex A.

7.4.9 Corrosion protection

Corrosion protection of the tower should be in accordance with DS/R 454 and for offshore turbines according to DS/R 464 or similar recognised standards. The most

common type of corrosion protection used for tubular towers is paint.

7.4.10 Tolerances and specifications

Whatever standard is used for the stability analysis, the calculations assume certain maximum imperfections. These tolerances are concerned with maximum deviations from nominal longitudinal and circumferential dimensions and must be respected. Otherwise, when a tolerance is exceeded, the excess must be included in the factor e in the stability calculations.

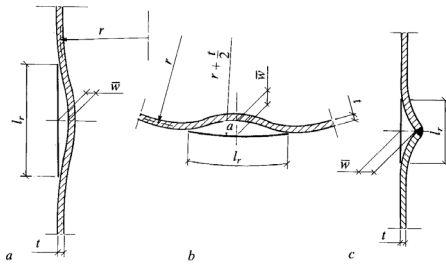


Figure 7-9. Tower shell dent tolerances.

When using the buckling strength analysis approach, as described in Section 7.4.7, the assumed maximum dent tolerances are as follows with reference to Figure 7-9:

Between circumferential seams

- measured along an arbitrary production with a straight bar of length $l_r = 4\sqrt{rt}$, however, not longer than 95 % of the distance between adjoining circumferential seams, the maximum deviation from w should fulfil: $w/l_r < 0.01$ (Figure 7-9 a).
- measured along an arbitrary circumference with a shape with curvature equal to the nominal outer radius of the cylinder and length $l_r = 4\sqrt{rt}$, the maximum deviation from w should fulfil $w/l_r < 0.01$ (Figure 7-9 b).

At circumferential seams

- measured along an arbitrary production across a weld with a straight bar of length $l_r = 25t$, the maximum deviation w should fulfil $w/l_r < 0.01$ (Figure 7-9 c).

Elements of large thickness, such as tower flanges, should be checked for stratification. Further, the flanges must satisfy certain tolerances regarding straightness and circularity to enable correct tightening of the connection. The stresses in the flange should be based on the smallest flange thickness, cf. the tolerance specifications.

7.5 Access and working environment

When designing the tower it must be verified that proper access to the nacelle is possible. It must be assured that the access complies with the requirements for personnel safety and maintenance. In addition, the working environment during blade inspection using an inspection hatch in

the tower side must be dealt with. Turbines erected in Denmark should comply with the requirements specified by the Danish Working Environment Service.

7.6 Example of tower load calculation

7.6.1 Loads and responses

The behaviour of the tower during extreme loading is illustrated through an aeroelastic calculation for a reference turbine with a rated power of 1800 kW. The main characteristics of this turbine are given in Table 7-2, and its dynamics are given in Table 7-3.

No. of blades	3
Hub height	71.5 m
Rotor diameter	66 m
Rotational speed	15.9 rpm
Rated power	1800 kW
Tower	tubular

Table 7-2. Main characteristics of reference wind turbine.

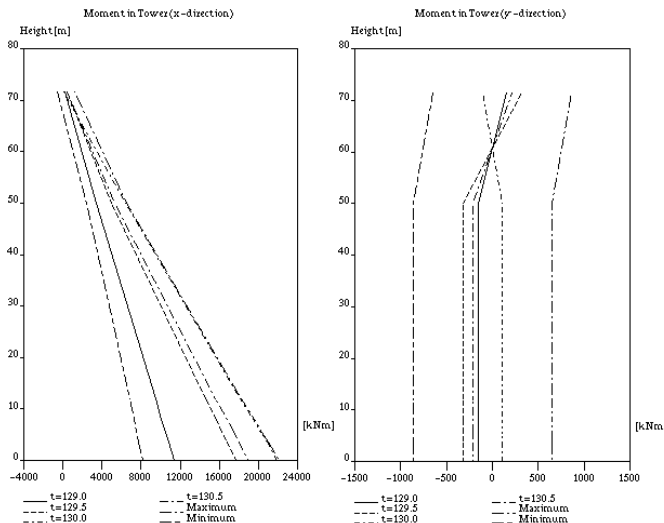


Figure 7-10. Tower response from analysis of a 1.8 MW turbine (left = alongwind response, right = transverse wind response). Operational loads for 24 m/s wind speed.

An aeroelastic response calculation for an operating turbine – showing the bending moments – is shown as a function of time in Figure 7-10. The response is calculated for a 10-minute mean wind speed $U_{10} = 24$ m/s, which is near the cut-out wind speed, and a turbulence intensity $I_T = 11\%$. From Figure 7-10 it appears that the response is highly fluctuating with time, thus the design responses are to be determined from the probability distribution of the extreme response, see Section 4.4. This fluctuation is due to the dynamics of the turbine in conjunction with the stochastic turbulence field.

7.6.2 Occurrence of extreme loads during normal power production

The results of a response analysis based on 49 realisations (calculations with different seeds) of the turbulence field are shown in Table 7-4. The load case is analysed for $U_{10} = 24$ m/s and $I_T = 11\%$, and the simulation time for each realisation is 10 minutes.

Table 7-4 shows results for four important processes as interpreted from the 49 calcula-

tions. These processes constitute the wind speed process, the electric power and the horizontal force and moment at the foundation level. Considering the variation of the processes and the time of operation, it is obvious that a proper selection of the characteristic value must be rooted in probabilistic methods as described in Section 4.3.1.

Table 7-4 provides simulated estimates of the first four central moments of the moment and horizontal force responses, viz. the mean, the standard deviation, the skewness and the kurtosis of these two responses. The bottom lines in the table give estimates of the maximum moment and the simultaneous value of the force, and of the maximum force and the simultaneous value of the moment. The central estimates are denoted by μ in the table. Statistical uncertainty in the estimates is also included in terms of the standard deviations of the estimates, denoted by σ in the table. It appears that the maximum of the moment response process and the maximum of the force response process do not occur at the same time.

Mode shape	Configuration of turbine		
	Blades: In normal position		Blades: 90° pitched
	Freq. [Hz]	Damp. (%)	Freq. [Hz]
1 st tower transversal	0.418	6.0	0.417
1 st tower longitudinal	0.419	6.0	0.420
1 st rotor torsion	0.805	5.0	0.704
1 st rotor torsion	0.979		1.002
1 st asymmetric rotor (yaw)	1.000		1.064
1 st symmetric rotor (flap)	1.067	3.1	1.769
1 st edgewise mode	1.857	3.1	1.032
2 nd edgewise mode			1.045

Table 7-3. Dynamic properties of reference wind turbine.

The characteristic extreme response and the design extreme response for an operating turbine should be selected according to the following scheme:

1. Simulate/calculate the extreme responses for the codified load cases and, if necessary, include other load cases that might be critical for the considered concept (e.g. variable speed,

etc.). For each load case at least five different seeds should be used.

Run statistics	Wind	Power	Moment M	Horis. force, F
Mean μ	24.09	1810	14323	210
σ	0.00	5.5	28.8	0.413
Std. dev. μ	2.63	119.6	2046	30.9
σ	0.01	4.2	152	2.3
Skewness μ	-0.052	-0.187	-0.028	-0.055
σ	0.218	0.085	0.127	0.239
Kurtosis μ	2.953	6.650	2.950	2.953
σ	0.377	0.550	0.256	0.239
Upcross. period μ	6.703	1.714	2.520	1.678
σ	0.881	0.052	0.748	0.896
max[M] and simul. μ	28.2	1986.7	21018	312
σ	2.9	90.2	777	12
max[H] and simul. μ	27.4	1978.0	20907	314
σ	1.9	95.9	812	12

Table 7-4. Extreme loads during power production (simulation time: 10 minutes).

2. Calculate the statistics (as exemplified in Table 7-4) for each executed simulation (at least 10 minutes).
3. Use the procedures in Section 4.4.2 to project the responses calculated from a 10-minute simulation to a longer period of operation (e.g. more days – calculated from the mean wind speed distribution – see Chapter 3).
4. Choose the characteristic value of the response as described in the code. (Not many codes deal with this issue, and those that do, do not necessarily define the characteristic value in the same manner).
5. Apply a safety factor as described in the codes (the revised edition of the Danish code of practice DS472 specifies $\gamma_f = 1.5$) to calculate the design value of the response.

7.6.3 Extreme loads – parked turbine

An extreme load analysis is also performed with the reference turbine in a parked

configuration. The wind is acting perpendicular to the nacelle, i.e. with a full drag on the nacelle, and the blades are pitched to give a full drag also on the blades.

The extreme loads calculated from 60 simulations of the response processes are shown in Table 7-5. The mean wind speed is 34 m/s and the turbulence intensity is 10%. The central estimates are denoted by μ in the table. Statistical uncertainty in the estimates is also included in terms of the standard deviations of the estimates, denoted by σ in the table. From the data it appears that the statistical variations of the various responses under consideration are significant also in the parked condition.

Run statistics	Wind	Moment M	Horis. force, F
Mean μ	33.51	12293.7	234.2
σ	0.001	23.3	0.45
Std. dev. μ	3.333	2555.2	45.79
σ	0.005	79.3	1.09
Skewness μ	-0.027	0.208	0.206
σ	0.205	0.203	0.210
Kurtosis μ	2.939	3.091	3.055
σ	0.248	0.266	0.233
max[U] and simul. μ	43.74	17515.3	331.5
σ	1.03	2362.6	26.4
max[M] and simul. μ	40.30	21490.8	395.9
σ	1.72	1052.0	17.4
max[H] and simul. μ	40.38	21449.9	396.5
σ	1.67	1056.4	17.0

Table 7-5. Extreme loads for parked turbine (simulation time: 10 minutes)

The characteristic extreme response should be chosen equal to the expected maximum response in a 10-minute period. This approach is justified only if the coefficient of variation on the maximum value is sufficiently low, see Mørk. An approach by Davenport can be used for this purpose, see Section 4.4.2. The corresponding design value is found by applying the appropriate

partial safety factor (the current edition of DS410 and the revised edition of DS472 specify $\gamma_f = 1.5$).

7.6.4 Fatigue loading

The fatigue loads are also fluctuating loads, thus one must assure that a sufficient number of simulations are performed before the design of the tower can be carried out. A 1.5 MW stall-controlled turbine with a tubular tower as reported in Thomsen (1998) is considered as an example, and the fatigue loads are as shown in Table 7-6. The table is calculated with the Wöhler curve exponent $m = 3$, which is the value traditionally selected for steel, and the equivalent number of cycles is 600. The turbulence intensity is set to 15%.

Table 7-6 shows the variation in the equivalent load as a function of the mean wind speed. The table is based on a large number of simulations for each wind speed, and both the mean and the coefficient of variation of the load estimates are included, denoted by μ and COV, respectively. The coefficient of variation appears to be rather large (greater than 10%) in this example, despite the large number of simulations used for the estimations. This indicates the importance of carrying out a sufficient number of simulations. It is recommended not to use less than five simulations, see Danish Energy Agency (2000), however, five simulations may in many cases be insufficient.

The equivalent load as shown in Table 7-6 must be corrected with respect to the proper operation time at different wind speeds (adjusting for the distribution of the mean wind speed – resulting in the lifetime equivalent load). The mean wind velocity is assumed to follow a Weibull distribution with scale parameter $A = 10$ m/s and slope parameter $k = 2.0$. The lifetime fatigue equivalent load for a 20-year lifetime is

given in Table 7-7, calculated for 10^7 equivalent load cycles. Note that the uncertainty in the lifetime fatigue loading is still significant with a coefficient of variance of 6%. This may call for a safety factor for fatigue loading different from 1.0.

Wind speed [m/s]	Statistical parameter	Equivalent load [kNm]
7	μ COV	828.7 17%
10	μ COV	1511.1 10%
15	μ COV	3151.1 13%
20	μ COV	6059.4 15%
24	μ COV	7703.1 15%

Table 7-6. Equivalent load for tower bending in a 10-minute simulation.

Quantity	Stat. Par.	Eq. load [kNm]
R_{eq}	μ COV $n_{eq,L}$	10292.42 6% 10^7

Table 7-7. Equivalent load for tower bending in a 10-minute simulation.

The dependency of the damage-equivalent load on the wind speed and on the turbulence intensity is shown in Figure 7-11. The upper half of the figure shows the equivalent load in a 10-minute simulation period as a function of the wind speed. Also, three levels of turbulence intensity are analysed. From the figure, it is clearly seen that the fatigue damage increases with the wind speed and turbulence intensity. Moreover, the uncertainty in the damage increases with increasing wind speed and turbulence. The error bars in Figure 7-11 illustrate the mean of the fatigue load plus/minus one standard deviation.

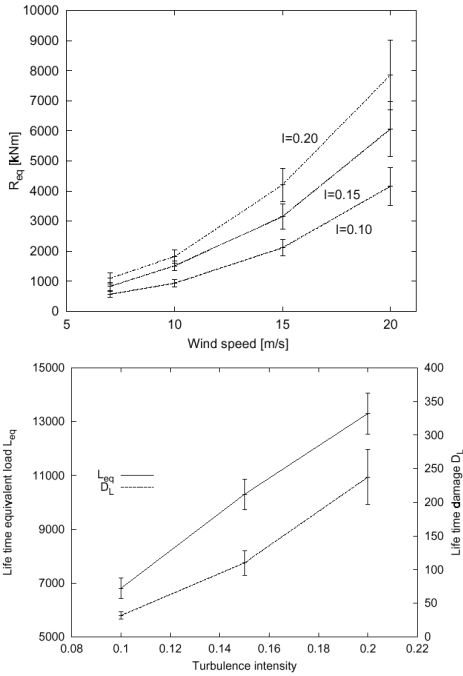


Figure 7-11. Sensitivity of 10-minute equivalent load to wind speed (above) and lifetime equivalent fatigue load to turbulence intensity (below). Error bars correspond to \pm one standard deviation in estimates.

The lower half of Figure 7-11 gives the lifetime damage and the lifetime equivalent load as functions of the site-specific design turbulence intensity. The figure shows that the lifetime equivalent load increases from about 6000 kNm to about 14000 kNm when the turbulence intensity increases from 10% to 20%. The fatigue damage is correspondingly – due to the nonlinearity in the fatigue Wöhler curve – increased by a factor of 8.

An analysis of a 500 kW stall-controlled turbine gives the relative contribution to the fatigue damage from different load cases and is reported in Thomsen et al. (1997). The results of this investigation are reproduced in Table 7-8, from which it appears that the major fatigue contribution arises from the ‘normal production’ load combinations. Load combinations involving failures or errors do hardly influence the fatigue damage at all. The load combinations are identical to those specified in DS472.

	LC no.	U_{10} [m/s]	Yaw [deg]	I_T [%]	Cont. [%]	Comment
LC's: normal power production	1	6	-10	18	0,9	
	2	8	-10	18	1,7	
	3	10	-10	18	3,1	
	4	12	-10	18	4,1	
	5	14	-10	18	5,0	
	6	16	-10	18	6,5	
	7	18	-10	18	6,4	
	8	20	-10	18	6,1	
	9	22	-10	18	5,9	
	10	24	-10	18	5,6	
	11	6	+10	18	0,9	
	12	8	+10	18	2,3	
	13	10	+10	18	4,1	
	14	12	+10	18	5,0	
	15	14	+10	18	5,3	
	16	16	+10	18	6,6	
	17	18	+10	18	6,6	
	18	20	+10	18	6,1	
	19	22	+10	18	5,9	
	20	24	+10	18	5,3	
LC's: starts/stops	21	Low		Start	0,0	
	22	Nom		Start	0,1	
	23	High		Start	0,1	
	24	Low		Stop	0,0	
	25	Nom		Stop	0,1	
	26	High		Stop	0,1	
	27	5		Idle	0,1	
LC's: With errors	28	$0.5 U_{max}$	-40	18	0,1	Tip brakes activated
	29	$0.5 U_{max}$	0	18	0,0	Tip brakes activated
	30	$0.5 U_{max}$	+40	18	0,2	Tip brakes activated
	31	25	-40	18	0,4	Large yaw error
	32	25	40	18	1,0	Large yaw error
	33	25	-10	18	2,1	Only one tip brake
	34	25	10	18	2,6	Only one tip brake
	35	25	-10	18	0,0	Only two tip brakes

Table 7-8. Relative contribution to the total fatigue damage from different load combinations (load cases according to DS472, 500 kW turbine, tower subjected to bending).

REFERENCES

Arbejdstilsynet, anvisning nr. 2.2.0.1.

Danish Energy Agency, “Rekommandation for Teknisk Godkendelse af Vindmøller på Havet,” Bilag til *Teknisk Grundlag for Typegodkendelse og Certificering af Vindmøller i Danmark*, Copenhagen, Denmark, 2000.

DS 449, *The Danish Code of Practice for the Design and Construction of Pile Supported Offshore Steel Structures*, Dansk Ingeniørforening, 1983.

DS410, *The Danish Code of Practice for Loads for the Design of Structures*, Dansk Ingeniørforening, 1998.

DS412, *The Danish Code of Practice for Loads for the structural use of steel*, Dansk Ingeniørforening, 1998.

Det Norske Veritas, *Column Stabilized Units (Semisubmersible Platforms)*, Classification Notes No. 31.4, Høvik, Norway, 1987.

Eurocode 1, Basis of design and actions on structures, Section 2-4: *Wind actions on structures*.

Eurocode 3. Design of steel structures-Part 1-1: *General rules and rules for buildings* DS/ENV1993-1-1

Forskningscenter Risø, *Rekommandation til opfyldelse af krav i teknisk grundlag*, Energistyrelsens regeludvalg for godkendelse af vindmøller, Godkendelsessekretariatet, Prøvestationen for Vindmøller, Roskilde, Denmark.

Jørgensen, E., *Notat om undersøgelse af spændingsforhold ved luge på rørtårn*, Prøvestationen for vindmøller, Risø, Denmark, July 1990.

Krohn, S., www.windpower.org, Danish Wind Turbine Manufacturers Association,

Mørk, K., *Vindlast på svingningsfølsomme konstruktioner*, AUC, Aalborg, Denmark.

Thomsen, K., *The Statistical Variation of Wind Turbine Fatigue Loads*, Risø National Laboratory, Risø-R-1063(EN), 1998.

Thomsen, K., P.P. Madsen, E. Jørgensen, *Status og perspektiv for forskning i aeroelastisitet – Lastgrundlag og sikkerhed*, Risø-R-964(DA), Forskningscenter Risø, Roskilde, Denmark, February, 1997.

8. Foundations

Onshore wind turbines are usually supported by either a slab foundation or a pile foundation. Soil conditions at the specific site usually govern whether a slab foundation or a pile foundation is chosen. A slab foundation is normally preferred when the top soil is strong enough to support the loads from the wind turbine, while a pile-supported foundation is attractive when the top soil is of a softer quality and the loads need to be transferred to larger depths where stronger soils are present to absorb the loads. When assessing whether the top soil is strong enough to carry the foundation loads, it is important to consider how far below the foundation base the water table is located.

As regards offshore wind turbines, the foundation is a more comprehensive structure in that it includes a separate structure to transfer loads from the bottom of the wind turbine tower through the water to the supporting soils. In addition to the loads from the wind turbine, such a foundation structure will experience loads from current, waves and ice owing to its placement in a marine environment. Three basically different foundation structure concepts exist for offshore wind turbines:

- monopile
- gravity base
- tripod

The monopile is in principle a vertical pipe, driven or bored into the soil like any other pile, onto which the wind turbine tower is mounted. The gravity base foundation rests on the sea floor or on an excavated bottom by means of its own weight and is usually constructed from reinforced concrete. The wind turbine tower is mounted on top of this concrete structure. The gravity base foundation can also be constructed from steel in which case the necessary weight is achieved by placing a heavy ballast such as crushed

olivine inside the cavities of the steel structure. The tripod foundation is a steel frame structure with three legs. The wind turbine tower is mounted on top of the tripod, while each leg is supported by either a driven pile or a suction bucket for transfer of loads to the supporting soils.

The choice of foundation type is much dependent on the soil conditions prevailing at the planned site of a wind turbine. Once a foundation concept has been selected and a foundation design is to be carried out, the following geotechnical issues need to be addressed:

- bearing capacity, i.e. geotechnical stability, e.g. against sliding and overturning
- degradation of soil strength in cyclic loading
- consolidation settlements
- differential settlements
- scour and erosion

8.1 Soil investigations

8.1.1 General

Soil investigations should provide all necessary soil data for detailed design of a specific foundation structure at a specific location. Soil investigations may be divided into the following parts:

- geological studies
- geophysical surveys
- geotechnical investigations

which are briefly dealt with in the following.

A geological study should be based on information about the geological history of the area where the wind turbine is to be installed. The purpose of the study is to establish a basis for selection of methods and extent of the site investigation.

A geophysical survey can be used to extend the localised information from single

borings and in-situ testing in order to get an understanding of the soil stratification within a given area, and – for offshore locations – of the seabed topography within that area. Such a survey can provide guidelines for selection of a suitable foundation site within the area, if not already decided. Geophysical surveys are carried out by means of seismic methods.

A geotechnical investigation consists of:

- soil sampling for laboratory testing
- in-situ testing of soil

Soil investigations should be tailored to the geotechnical design methods used. The field and laboratory investigations should establish the detailed soil stratigraphy across the site, thus providing the following types of geotechnical data for all important soil layers:

- data for classification and description of the soil, such as
 - unit weight of sample
 - unit weight of solid particle
 - water content
 - liquid and plastic limits
 - grain size distribution
- parameters required for a detailed and complete foundation design, such as
 - permeability tests
 - consolidation tests
- static tests for determination of shear strength parameters such as friction angle ϕ for sand and undrained shear strength c_u for clay (triaxial tests and direct simple shear tests)
- cyclic tests for determination of strength and stiffness parameters (triaxial tests, direct simple shear tests and resonant column tests)

Sampling can be carried out with and without drilling. The cone penetrometer test (CPT) and various vane tests form the most commonly used in-situ testing methods. Results from such in-situ tests can be used to

interpret parameters such as the undrained shear strength of clay. The extent to which the various types of in-situ tests and laboratory tests are required depends much on the foundation type in question, for example, whether it is a piled foundation or a gravity-based foundation.

The recommendations of the Danish Technical Criteria for Type Approval of Wind Turbines (Danish Energy Agency, 1998) specify that a geotechnical report from the geological and geotechnical surveys shall be prepared. This geotechnical report should contain sufficient information about the site and its soils, e.g. in terms of soil strength and deformation properties, to allow for design of the foundation with respect to:

- bearing capacity
- stability against sliding
- settlements
- foundation stiffness
- need for and possibility of drainage
- static and dynamic coefficients of compressibility
- sensitivity to dynamic loading

The geotechnical report is further required to contain identification of soil type at foundation level, classification of environment, and estimation of highest possible water table. For further details, reference is made to Danish Energy Agency (1998).

8.1.2 Recommendations for gravity based foundations

Insofar as regards a gravity-based foundation, an extensive investigation of the shallow soil deposits should be undertaken. This investigation should cover soil deposits to a depth, which is deeper than the depth of any possible critical shear surface. Further, all soil layers influenced by the structure from a settlement point of view should be thoroughly investigated. This also holds for all soil layers contributing to the foundation

stiffness. The foundation stiffness is of importance for the design of the structure supported by the foundation. The depth to be covered by the thorough investigation should at least equal the largest base dimension of the structure.

The extent of shallow borings with sampling should be determined on the basis of the type and size of structure as well as on general knowledge about the soil conditions in the area considered for installation. Emphasis should be given to the upper layers and potentially weaker layers further down. It is recommended that the sampling interval is not in excess of 1.0-1.5 m. A number of seabed samples (gravity cores or the equivalent) evenly distributed over the area should be taken for evaluation of the scour potential.

Shallow CPTs distributed across the installation area should be carried out in addition to the borings. The number of CPTs depend on the soil conditions and on the type and size of structure. If the soil conditions are very irregular across the foundation site, the number of CPTs will have to be increased. The shallow CPTs should provide continuous graphs from the soil surface to the maximum depth of interest.

Special tests such as plate loading tests, pressuremeter tests and shear wave velocity measurements should be considered where relevant.

8.1.3 Recommendations for pile foundations

For lateral pile analysis, shallow cone penetration tests should be carried out from the surface to 20-30m depth. In addition, shallow borings with sampling should be considered for better determination of characteristics of the individual layers identified by the cone penetration tests. It is

recommended that the sampling interval is not in excess of 1.0-1.5m.

As regards axial pile analysis, at least one down-the-hole CPT boring should be carried out to give a continuous CPT profile. Moreover, one nearby boring with sampling should be carried out for the axial pile capacity analysis. The minimum depth should be the anticipated penetration of the pile plus a zone of influence sufficient for evaluation of the risk of punch-through failure. The sampling interval should be determined from the CPT results, but is recommended not to exceed 3 m.

For offshore installations, a number of seabed samples (gravity cores or equivalent) evenly distributed over the area considered for installation of the foundation should be taken for evaluation of the scour potential.

Special attention should be paid when potential end bearing layers or other dense layers are found. Here, additional CPTs and sampling should be carried out in order to determine the thickness and lateral extension of such layers within the area considered for the foundation.

8.2 Gravity-based foundations

Requirements for foundation stability often constitute the most decisive factors as regards determination of foundation area, foundation embedment and necessary weight for a structure with a gravity-based foundation. It is therefore essential in an optimal design process to give high emphasis to foundation stability calculations.

The question of foundation stability is most commonly solved by limiting equilibrium methods, i.e. by ensuring equilibrium between driving and resisting forces. When using limiting equilibrium methods, several

trial failure surfaces will have to be analysed in order to find the most critical one with respect to stability.

However, as foundations of wind turbines usually have relatively small areas, bearing capacity formulas for idealised conditions will normally suffice and be acceptable for design. Bearing capacity formulas are given in the following.

8.2.1 Bearing capacity formulas

Forces

All forces acting on the foundation, including forces transferred from the wind turbine, are transferred to the foundation base and combined into resultant forces H and V in the horizontal and vertical direction, respectively, at the foundation-soil interface.

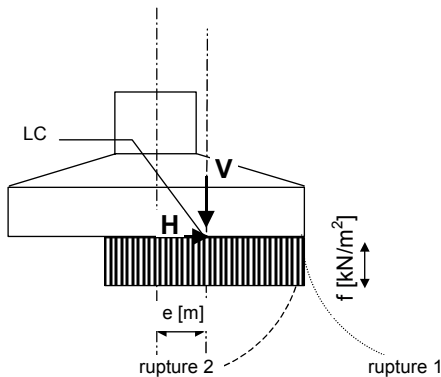


Figure 8-1. Loading under idealised conditions.

In the following, it is assumed that H and V are design forces, i.e. they are characteristic forces that have been multiplied by their relevant partial load factor γ_f . This is indicated by index d in the bearing capacity formulas, hence H_d and V_d . The load centre, denoted LC, is the point where the resultant of H and V intersects the foundation-soil interface, and implies an eccentricity e of the

vertical force V relative to the centre line of the foundation. Reference is made to Figure 8-1, and the eccentricity is calculated as

$$e = \frac{M_d}{V_d}$$

where M_d denotes the resulting design overturning moment about the foundation-soil interface.

Correction for torque

When a torque M_z is applied to the foundation in addition to the forces H and V , the interaction between the torque and these forces can be accounted for by replacing H and M_z with an equivalent horizontal force H' . The bearing capacity of the foundation is then to be evaluated for the force set (H', V) instead of the force set (H, V) . According to a method by Hansen (1978), the equivalent horizontal force can be calculated as

$$H' = \frac{2 \cdot M_z}{l_{eff}} + \sqrt{H^2 + \left(\frac{2 \cdot M_z}{l_{eff}} \right)^2}$$

in which l_{eff} is the length of the effective area as determined in the following.

Effective foundation area

For use in bearing capacity analysis an effective foundation area A_{eff} is needed. The effective foundation area is constructed such that its geometrical centre coincides with the load centre, and such that it follows as closely as possible the nearest contour of the true area of the foundation base. For a quadratic area of width b , the effective area A_{eff} can be defined as

$$A_{eff} = b_{eff} \cdot l_{eff}$$

in which the effective dimensions b_{eff} and l_{eff} depend on which of two idealised loading

scenarios leads to the most critical bearing capacity for the actual foundation.

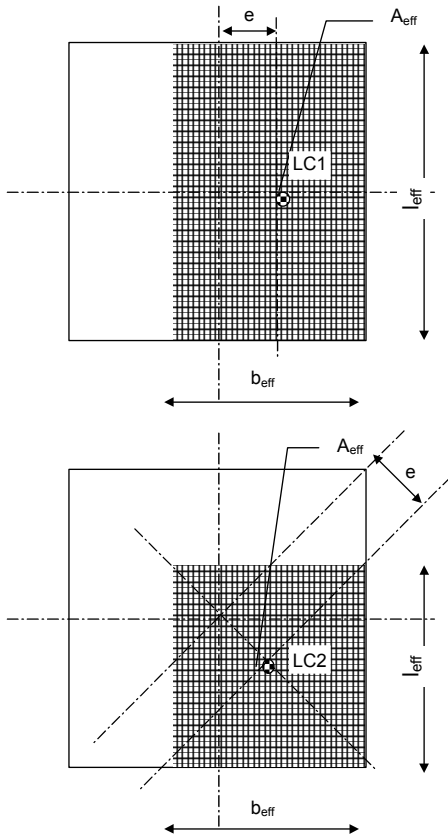


Figure 8-2. Quadratic footing with two approaches to how to make up the effective foundation area.

Scenario 1 corresponds to load eccentricity with respect to one of the two symmetry axes of the foundation. By this scenario, the following effective dimensions are used:

$$b_{eff} = b - 2 \cdot e, \quad l_{eff} = b$$

Scenario 2 corresponds to load eccentricity with respect to both symmetry axes of the foundation. By this scenario, the following effective dimensions are used:

$$b_{eff} = l_{eff} = b - e\sqrt{2}$$

Reference is made to Figure 8-2. The effective area representation that leads to the poorest or most critical result for the bearing capacity of the foundation is the effective area representation to be chosen.

For a circular foundation area with radius R , an elliptical effective foundation area A_{eff} can be defined as

$$A_{eff} = 2 \left[R^2 \arccos\left(\frac{e}{R}\right) - e\sqrt{R^2 - e^2} \right]$$

with major axes

$$b_e = 2(R - e)$$

and

$$l_e = 2R \sqrt{1 - \left(1 - \frac{b}{2R}\right)^2}$$

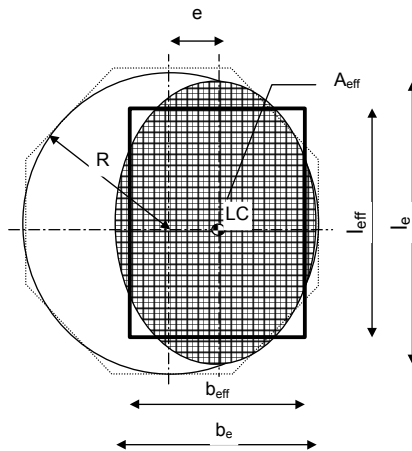


Figure 8-3. Circular and octangular footings with effective foundation area marked out.

The effective foundation area A_{eff} can now be represented by a rectangle with the following dimensions

$$l_{eff} = \sqrt{A_{eff} \frac{l_c}{b_c}} \text{ and } b_{eff} = \frac{l_{eff}}{l_c} b_c$$

For an area shaped as a double symmetrical polygon (octagonal or more), the above formulas for the circular foundation area can be used provided that a radius equal to the radius of the inscribed circle of the polygon is used for the calculations.

Bearing capacity

For fully drained conditions and failure according to Rupture 1 as indicated in Figure 8-1, the following general formula can be applied for the bearing capacity of a foundation with a horizontal base, resting on the soil surface

$$q_d = \frac{1}{2} \gamma' b_{eff} N_\gamma s_\gamma i_\gamma + p'_0 N_q s_q i_q + c_d N_c s_c i_c$$

For undrained conditions, which imply $\phi = 0$, the following formula for the bearing capacity applies

$$q_d = c_{ud} \cdot N_c^0 \cdot s_c^0 \cdot i_c^0 + p_0$$

q_d	design bearing capacity [kN/m ²]
γ'	effective (submerged) unit weight of soil [kN/m ³]
p'_0	effective overburden pressure at the level of the foundation-soil interface [kN/m ²]
c_d	design cohesion or design undrained shear strength assessed on the basis of the actual shear strength profile, load configuration and estimated depth of potential failure surface [kN/m ²]
N_γ N_q	bearing capacity factors, dimensionless
N_c	
$s_\gamma s_q s_c$	shape factors, dimensionless
$i_\gamma i_q i_c$	inclination factors, dimensionless

Reference is made to DS415 (DS 415, 1998).

In principle, the quoted formulas apply to foundations, which are not embedded. However, the formulas may also be applied to embedded foundations, for which they will lead to results, which will be on the conservative side. Alternatively, depth effects associated with embedded foundations can be calculated according to formulas given in DNV (1992).

The calculations are to be based on design shear strength parameters:

$$c_{ud} = \frac{c}{\gamma_c} \text{ and } \phi_d = \arctan\left(\frac{\tan(\phi)}{\gamma_\phi}\right)$$

The material factors γ_c and γ_ϕ must be those associated with the actual design code and the type of analysis, i.e. whether drained or undrained conditions apply.

The dimensionless factors N , s and i can be determined by means of formulas given in the following.

Drained conditions:

Bearing capacity factors N :

$$N_q = e^{\sigma \tan \phi_d} \cdot \frac{1 + \sin \phi_d}{1 - \sin \phi_d}$$

$$N_c = (N_q - 1) \cdot \cot \phi_d$$

$$N_\gamma = \frac{1}{4} \cdot ((N_q - 1) \cdot \cos \phi_d)^{\frac{3}{2}}$$

According to Hansen (1970), N_γ may alternatively be calculated according to

$$N_\gamma = \frac{3}{2} \cdot (N_q - 1) \cdot \tan \phi_d$$

Shape factors s :

$$s_\gamma = 1 - 0.4 \cdot \frac{b_{eff}}{l_{eff}}$$

$$s_q = s_c = 1 + 0.2 \cdot \frac{b_{eff}}{l_{eff}}$$

Inclination factors i :

$$i_q = i_c = \left(1 - \frac{H_d}{V_d + A_{eff} \cdot c_d \cdot \cot \phi_d} \right)^2$$

$$i_\gamma = i_q^2$$

Undrained conditions, $\phi = 0$:

$$N_c^0 = \pi + 2$$

$$s_c^0 = s_c$$

$$i_c^0 = 0.5 + 0.5 \cdot \sqrt{1 - \frac{H}{A_{eff} \cdot c_{ud}}}$$

Extremely eccentric loading

In the case of extremely eccentric loading, i.e. an eccentricity in excess of 0.3 times the foundation width, $e > 0.3b$, an additional bearing capacity calculation needs to be carried out, corresponding to the possibility of a failure according to Rupture 2 in Figure 8-1. This failure mode involves failure of the soil also under the unloaded part of the foundation area, i.e. under the heel of the foundation. For this failure mode, the following formula for the bearing capacity applies

$$q_d = \gamma^l b_{eff} N_\gamma s_\gamma i_\gamma + c_d N_c s_c i_c (1.05 + \tan^3 \phi)$$

with inclination factors

$$i_q = i_c = 1 + \frac{H}{V + A_{eff} \cdot c \cdot \cot \phi}$$

$$i_\gamma = i_q^2$$

$$i_c^0 = \sqrt{0.5 + 0.5 \cdot \sqrt{1 + \frac{H}{A_{eff} \cdot c_{ud}}}}$$

The bearing capacity is to be taken as the smallest of the values for q_d resulting from the calculations for Rupture 1 and Rupture 2.

Sliding resistance of soil

Foundations subjected to horizontal loading must also be investigated for sufficient sliding resistance. The following criterion applies in the case of drained conditions:

$$H < A_{eff} \cdot c + V \cdot \tan \phi$$

For undrained conditions in clay, $\phi = 0$, the following criterion applies:

$$H < A_{eff} \cdot c_{ud}$$

and it must in addition be verified that

$$\frac{H}{V} < 0.4$$

8.3 Pile-supported foundations

A pile foundation consists of one or more piles that transfer loads from a superstructure, such as a wind turbine tower or a distinctive structure supporting the tower, to the supporting soils. The loads applied to a pile at its head are transferred down the pile and absorbed by the soil through axial and lateral pile resistance. The axial and lateral pile resistance arises from soil resistance mobilised against the pile

when the pile, subjected to its loading, is displaced relative to the soil.

For design of piles, it is common to disregard a possible interaction between the axial pile resistance and the lateral pile resistance locally at any point along the pile and to treat these two forms of resistance as being independent of each other. The argument for this is that the soil near the soil surface principally determines the lateral resistance without contributing much to the axial resistance, while the soil further down along the pile toward the pile tip principally determines the axial resistance without contributing much to the lateral capacity. The axial and lateral resistance models presented in the following conform to this assumption of independence between local axial resistance and local lateral resistance.

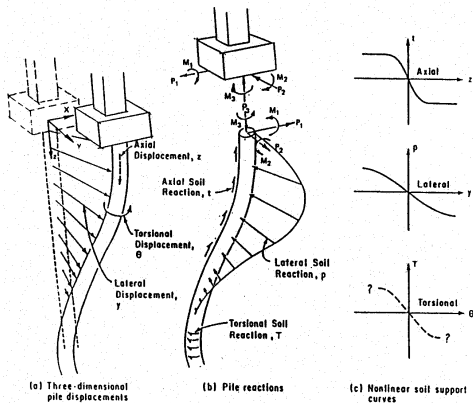


Figure 8-4. Single loaded pile with displacements and reactions, from Reese et al. (1996)

Note, however, that on a global level the lateral pile capacity and the axial pile capacity, resulting from local resistance integrated along the length of the pile, may interact, because second-order effects may cause the axial loading to influence the lateral behaviour of the pile. When the pile is subjected to torque, torsional resistance will be set up in addition to axial and lateral

resistance. Note that the local axial resistance and the torsional resistance, respectively, are interdependent, since they both arise from the skin friction against the pile surface. The axial, lateral and torsional pile displacements and corresponding soil reactions for a single pile subjected to external loading at its head are illustrated in Figure 8-4.

Note that for design of piles, it is important to consider effects of the installation procedure. For example, the stress history during pile driving contributes significantly to fatigue loading and needs to be considered for design against fatigue failure in the pile wall.

8.3.1 Pile groups

For foundations consisting of pile groups, i.e. clusters of two or more piles spaced closely together, pile group effects need to be considered when the axial and lateral resistance of the piles is to be evaluated. There are two types of group effects:

- the total capacity of the pile group is less than the sum of the capacities of the individual piles in the group, because of overlap between plastified soil zones around the individual piles. A lower limit for the axial pile group capacity is the axial capacity of the envelope “pier” that encloses all the piles in the group and the soil between them.
- larger pile displacements of a given load result for an individual pile when it is located in a pile group than when it is an only pile, because its supporting soils will have displacements caused by loads transferred to the soil from adjacent piles in the group. This type of group effect is also known as pile-soil-pile interaction. For practical purposes, such pile-soil-pile interaction can often be reasonably well represented by means of Mindlin’s point force solutions for an elastic halfspace.

The knowledge of the behaviour of a pile group relative to the behaviour of individual piles in the same group is limited, and conservative assumptions are therefore recommended for the prediction of pile group resistance. Note, when dealing with pile groups, that in addition to the above pile group effects there is also an effect of the presence of the superstructure and the way in which it is connected to the pile heads. The interconnection of the piles through their attachment to the common superstructure influences the distribution of the loads between the piles in the group. The piles can often be assumed to be fixed to the superstructure, and the superstructure can often be assumed as a rigid structure or a rigid cap when the responses in the piles are to be determined.

8.3.2 Axial pile resistance

Axial pile resistance is composed of two parts

- accumulated skin resistance
- tip resistance

For a pile in a stratified soil deposit of N soil layers, the pile resistance R can be expressed as

$$R = R_s + R_T = \sum_{i=1}^N f_{si} A_{si} + q_T A_T$$

f_{si} average unit skin friction along the pile shaft in layer i

A_{si} shaft area of the pile in layer i

q_T unit end resistance

A_T gross tip area of the pile

Clay. For piles in mainly cohesive soils, the average unit skin friction f_s may be calculated according to

(1) total stress methods, e.g. the α method, which yields

$$f_{si} = \alpha c_u$$

in which

$$\alpha = \begin{cases} \frac{1}{2\sqrt{c_u/p_0'}} & \text{for } c_u/p_0' \leq 1.0 \\ \frac{1}{2^4\sqrt{c_u/p_0'}} & \text{for } c_u/p_0' > 1.0 \end{cases}$$

where c_u is the undrained shear strength of the soil, and p_0' is the effective overburden pressure at the point in question.

(2) effective stress methods, e.g. the β method, which yields

$$f_{si} = \beta p_0'$$

in which β values in the range 0.1-0.25 are suggested for pile lengths exceeding 15 m.

(3) semi-empirical λ method, by which the soil deposit is taken as one single layer, for which the average skin friction is calculated as

$$f_s = \lambda(p_{0m}' + 2c_{um})$$

p_{0m}' average effective overburden pressure between the pile head and the pile tip

c_{um} average undrained shear strength along the pile shaft

λ dimensionless coefficient, which depends on the pile length as shown in Figure 8-5

Hence, by this method, the total shaft resistance becomes $R_s = f_s A_s$, where A_s is the pile shaft area.

For long flexible piles, failure between pile and soil may occur close to the seabed even before the soil resistance near the pile tip has been mobilized at all. This is a result of the flexibility of the pile and the associated

differences in relative pile-soil displacement along the length of the pile. This is a length effect, which for a strain-softening soil will imply that the static capacity of the pile will be less than that of a rigid pile.

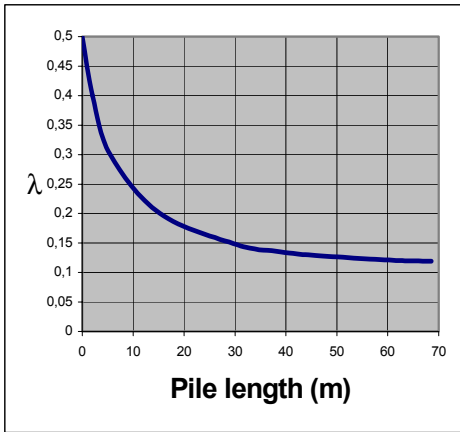


Figure 8-5. Coefficient λ vs. pile length

For deformation and stress analysis of an axially loaded flexible pile, the pile can be modelled as a number of consecutive column elements supported by nonlinear springs applied at the nodal points between the elements. The nonlinear springs are denoted *t-z* curves and represent the axial load-displacement relationship between the pile and the soil. The stress *t* is the integrated axial skin friction per unit area of pile surface and *z* is the relative axial pile-soil displacement necessary to mobilize this skin friction.

Sand. For piles in mainly cohesionless soils (sand), the average unit skin friction may be calculated according to

$$f_s = K p_0' \tan \delta \leq f_l$$

$$K \begin{cases} = 0.8 \text{ for open - ended piles} \\ = 1.0 \text{ for closed - ended piles} \end{cases}$$

p_0' effective overburden pressure

δ angle of soil friction on the pile wall as

given in Table 8-1

f_l limiting unit skin friction, see Table 8-1 for guidance

Tip resistance

The unit tip resistance of plugged piles in cohesionless soils can be calculated as

$$q_p = N_q p_0' \leq q_l$$

N_q can be taken from Table 8-1

q_l limiting tip resistance, see Table 8-1 for guidance

The unit tip resistance of piles in cohesive soils can be calculated as

$$q_p = N_c c_u$$

$N_c = 9$

c_u undrained shear strength of the soil at the pile tip

Density	Soil description	δ (degrees)	f_l (kPa)	N_q (-)	q_l (MPa)
Very loose Loose Medium	Silt Sand-silt ²⁾ Silt	15	48	8	1.9
Loose Medium Dense	Sand Sand-silt ²⁾ Silt	20	67	12	2.9
Medium Dense	Sand Sand-silt ²⁾	25	81	20	4.8
Dense Very dense	Sand Sand-silt ²⁾	30	96	40	9.6
Dense Very dense	Gravel Sand	35	115	50	12.0

1) The parameters listed in this table are intended as guidelines only. Where detailed information such as in-situ cone penetrometer tests, strength tests on high quality soil samples, model tests or pile driving performance is available, other values may be justified.

2) Sand-silt includes those soils with significant fractions of both sand and silt. Strength values generally increase with increasing sand fractions and decrease with increasing silt fractions.

Table 8-1. Design parameters for axial resistance of driven piles in cohesionless siliceous soil (extracted from API (1987)).

***t-z* curves**

The *t-z* curves can be generated according to a method by Kraft et al. (1981). By this

method, a nonlinear relation exists between the point of origin and the point where the maximum skin resistance t_{\max} is reached,

$$z = t \frac{R}{G_0} \ln \frac{z_{IF} - r_f \frac{t}{t_{\max}}}{1 - r_f \frac{t}{t_{\max}}} \text{ for } 0 \leq t \leq t_{\max}$$

- R radius of the pile
- G_0 initial shear modulus of the soil
- Z_{IF} dimensionless zone of influence, defined as the radius of the zone of influence around the pile divided by R
- r_f curve fitting factor

For displacements z beyond the displacement where t_{\max} is reached, the skin resistance t decreases in linear manner with z until a residual skin resistance t_{res} is reached. For further displacements beyond this point, the skin resistance t stays constant. An example of t - z curves generated according to this method is given in Figure 8-6. The maximum skin resistance can be calculated according to one of the methods for prediction of unit skin friction given above.

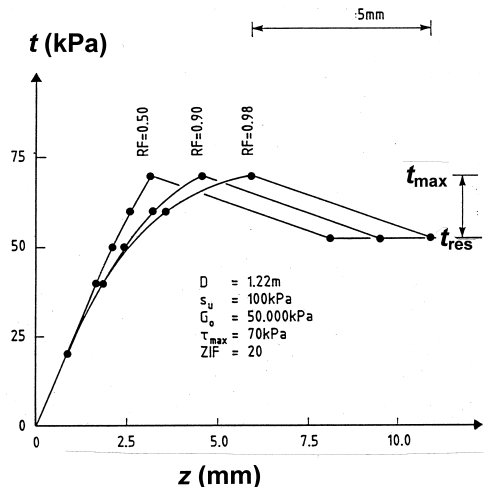


Figure 8-6. Example of t - z curves generated by model.

For clay, the initial shear modulus of the soil to be used for generation of t - z curves can be taken as

$$G_0 = 2600 c_u$$

However, Eide and Andersen (1984) suggest a somewhat softer value according to the formula

$$G_0 = 600c_u - 170c_u \sqrt{OCR-1}$$

- c_u undrained shear strength of the clay
- OCR overconsolidation ratio

For sand, the initial shear modulus of the soil to be used for generation of t - z curves is to be taken as

$$G_0 = \frac{m\sqrt{\sigma_a\sigma_v}}{2(1+\nu)} \text{ with } m = 1000 \cdot \tan\phi$$

- $\sigma_a = 100 \text{ kPa}$, atmospheric pressure
- σ_v vertical effective stress
- ν Poisson's ratio of the soil
- ϕ friction angle of the soil

8.3.3 Laterally loaded piles

The most common method for analysis of laterally loaded piles is based on the use of so-called p - y curves. The p - y curves give the relation between the integral value p of the mobilized resistance from the surrounding soil when the pile deflects a distance y laterally. The pile is modelled as a number of consecutive beam-column elements, supported by nonlinear springs applied at the nodal points between the elements. The nonlinear support springs are characterized by one p - y curve at each nodal point, see Figure 8-7.

The solution of pile displacements and pile stresses in any point along the pile for any applied load at the pile head results from the

solution to the differential equation of the pile

$$EI \frac{d^4 y}{dx^4} + Q_A \frac{d^2 y}{dx^2} - p(y) + q = 0$$

with

$$EI \frac{d^3 y}{dx^3} + Q_A \frac{dy}{dx} = Q_L \text{ and } EI \frac{d^2 y}{dx^2} = M$$

- x position along the pile axis
- y lateral displacement of the pile
- EI flexural rigidity of the pile
- Q_A axial force in the pile
- Q_L lateral force in the pile
- $p(y)$ lateral soil reaction
- q distributed load along the pile
- M bending moment in the pile, all at the position x .

Reference is made to Figure 8-8.

A finite difference method usually forms the most feasible approach to achieve the sought-after solution of the differential equation of the pile. A number of commercial computer programs are available for this purpose. These programs usually provide full solutions of pile stresses and displacements for a combination of axial force, lateral force and bending moment at the pile head, i.e. also the gradual transfer of axial load to the soil along the pile according to the t - z curve approach presented above is included. Some of the available programs can be used to analyse not only single piles but also pile groups, including possible pile-soil-pile interaction and allowing for proper representation of a superstructure attached at the pile heads, either as a rigid cap or as a structure of finite stiffness.

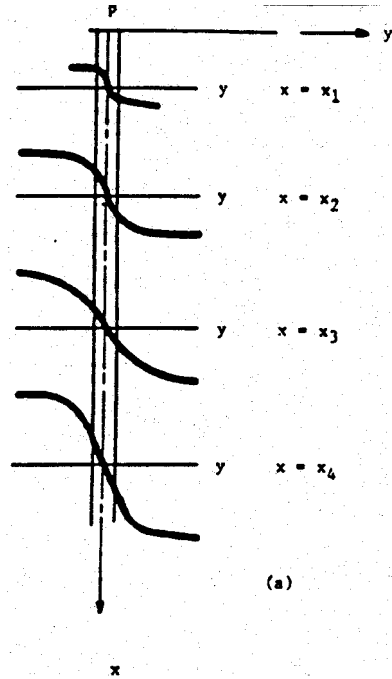


Figure 8-7. p-y curves applied at nodal points in beam column representation of pile, from Reese et al. (1996).

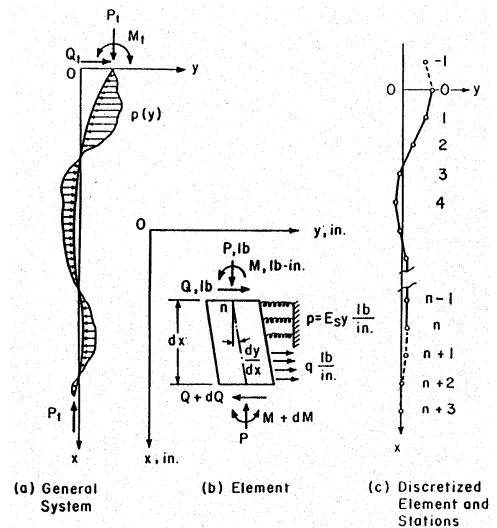


Figure 8-8. Beam column model with details, from Reese et al. (1996).

Several methods are available for representation of the p - y curves that are essential in solving the differential equation for a laterally loaded pile. For construction of p - y curves, the type of soil, the type of loading, the remoulding due to pile installation and the effect of scour should be considered. The most commonly applied procedures for construction of p - y curves are those given by DNV (1992) and API (1987). For piles in clay, the procedure according to DNV is presented below. For sand, the procedures according to DNV and API are identical and are presented below.

The lateral resistance per unit length of pile for a lateral pile deflection y is denoted p . The static ultimate lateral resistance per unit length is denoted p_u . This is the maximum value that p can take on when the pile is deflected laterally.

Clay. For piles in cohesive soils, the static ultimate lateral resistance is recommended to be calculated as

$$p_u = \begin{cases} (3c_u + \gamma' X)D + Jc_u X & \text{for } 0 < X \leq X_R \\ 9c_u D & \text{for } X > X_R \end{cases}$$

where X is the depth below soil surface and X_R is a transition depth, below which the value of $(3c_u + \gamma' X)D + Jc_u X$ exceeds $9c_u D$. Further, D is the pile diameter, c_u is the undrained shear strength of the soil, γ' is the effective unit weight of soil, and J is a dimensionless empirical constant whose value is in the range 0.25-0.50 with 0.50 recommended for soft normally consolidated clay.

For static loading, the p - y curve can be generated according to

$$p = \begin{cases} \frac{p_u}{2} \left(\frac{y}{y_c}\right)^{1/3} & \text{for } y \leq 8y_c \\ p_u & \text{for } y > 8y_c \end{cases}$$

For cyclic loading and $X > X_R$, the p - y curve can be generated according to

$$p = \begin{cases} \frac{p_u}{2} \left(\frac{y}{y_c}\right)^{1/3} & \text{for } y \leq 3y_c \\ 0.72 p_u & \text{for } y > 3y_c \end{cases}$$

For cyclic loading and $X \leq X_R$, the p - y curve can be generated according to

$$p = \begin{cases} \frac{p_u}{2} \left(\frac{y}{y_c}\right)^{1/3} & \text{for } y \leq 3y_c \\ 0.72 p_u \left(1 - \left(1 - \frac{X}{X_R}\right) \frac{y - 3y_c}{12y_c}\right) & \text{for } 3y_c < y \leq 15y_c \\ 0.72 p_u \frac{X}{X_R} & \text{for } y > 15y_c \end{cases}$$

Here, $y_c = 2.5\varepsilon_c D$, in which D is the pile diameter and ε_c is the strain which occurs at one-half the maximum stress in laboratory undrained compression tests of undisturbed soil samples. For further details, reference is made to DNV (1992).

Sand. For piles in cohesionless soils, the static ultimate lateral resistance is recommended to be calculated as

$$p_u = \begin{cases} (C_1 X + C_2 D)\gamma' X & \text{for } 0 < X \leq X_R \\ C_3 D\gamma' X & \text{for } X > X_R \end{cases}$$

where the coefficients C_1 , C_2 and C_3 depend on the friction angle ϕ as shown in Figure 8-9, where X is the depth below soil surface and X_R is a transition depth, below which the value of $(C_1 X + C_2 D)\gamma' X$ exceeds $C_3 D\gamma' X$. Further, D is the pile diameter, and γ' is the submerged unit weight of soil.

The p - y curve can be generated according to

$$p = A p_u \tanh\left(\frac{kX}{A p_u} y\right)$$

in which k is the initial modulus of subgrade reaction and depends on the friction angle ϕ as given in Figure 8-10, and A is a factor to account for static or cyclic loading conditions as follows

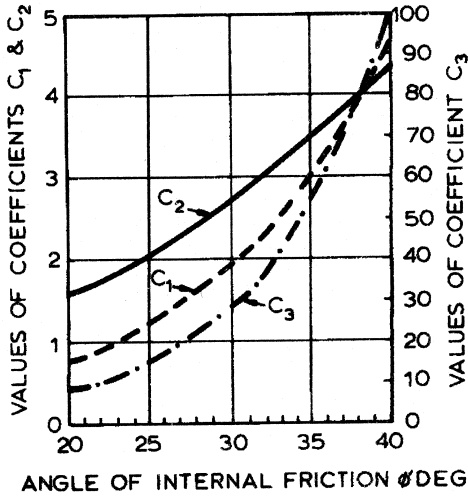


Figure 8-9. Coefficients as functions of friction angle, from DNV Class. Notes 30.4.

$$A = \begin{cases} 0.9 & \text{for cyclic loading} \\ (3 - 0.8 \frac{H}{D}) \geq 0.9 & \text{for static loading} \end{cases}$$

For further details, reference is made to DNV (1992).

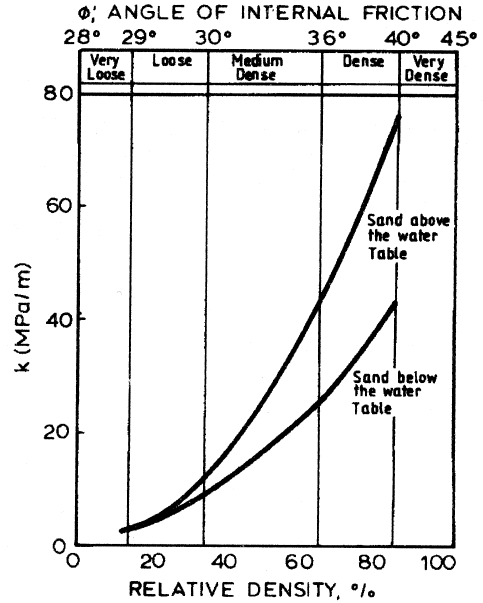


Figure 8-10. Initial modulus of subgrade reaction k as function of friction angle ϕ , from DNV Class. Notes 30.4.

8.3.4 Soil resistance for embedded pile caps

Some piled foundations include an embedded pile cap as indicated in Figure 8-11. Whereas the rotational capacity and stiffness of a pile cap is primarily governed by the axial capacity and stiffness of the piles, it is important to consider the effect on the lateral capacity and stiffness of the soil acting against the embedded part of the cap. This effect is similar to the soil resistance, represented by p - y curves, on piles under lateral loading. When assessing such an effect of soil in front of the pile cap, it is important also to assess the possibility that this soil may be removed due to erosion or other natural actions.

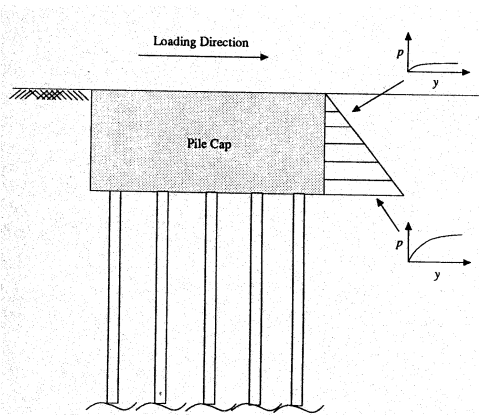


Figure 8-11. Distribution of soil resistance on the front side of pile cap, from Reese et al (1996).

The pile cap as dealt with here is essentially considered and modelled as a rigid structure. Sometimes, however, the pile heads are not interconnected by such a rigid superstructure, but are connected to a superstructure with some finite stiffness, such as a frame or a lattice tower. This will influence the distribution of forces between the piles relative to that of the rigid cap structure and will in turn have an impact on the overall resulting foundation stiffness.

8.4 Foundation stiffness

The overall foundation stiffness is dependent on the strength and stiffness of the soil as well as on the structural foundation elements. The foundation stiffness needs to be determined as a basis for predicting the dynamic structural response to wind, wave and earthquake loading. The foundation stiffness is in general frequency dependent. This is particularly important when predicting dynamic response to earthquake.

The soil that supports a foundation structure usually has finite stiffness. It can therefore usually not be justified to model the soil as a rigid mass. In other words, the foundation

structure cannot be assumed to have a fixed support. In any analysis of a foundation structure and of the wind turbine structure that it supports, it is therefore important to model the actual boundary conditions formed by the supporting soils properly.

To represent the finite stiffness of the supporting soils in such analyses, it is common to model a set of so-called foundation springs to be applied in one or more modelled support points on the structure to be analysed. The set of foundation springs may include the following springs associated with various modes of motion:

- vertical spring stiffness
- horizontal spring stiffness
- rocking spring stiffness
- torsional spring stiffness

Soil behaves in nonlinear manner. Foundation springs are therefore nonlinear. It is common to apply linear spring stiffnesses, in which case the stiffness values are chosen dependent on the strain level that the soil will experience for the load case under consideration. It is common to deal with the shear modulus of the soil, G . This equivalent shear modulus relates to the initial shear modulus G_0 as a function of the shear strain γ , as indicated in Figure 8-12. Figure 8-12 also gives damping ratios ξ for the soil as a function of the shear strain γ .

The following shear strain levels can be expected for the three most important sources of dynamic loading of soils:

- earthquakes: large strains up to 10^{-2} to 10^{-1}
- rotating machines: small strains usually less than 10^{-5}
- wind and ocean waves: moderate strains up to 10^{-2} , typically 10^{-3}

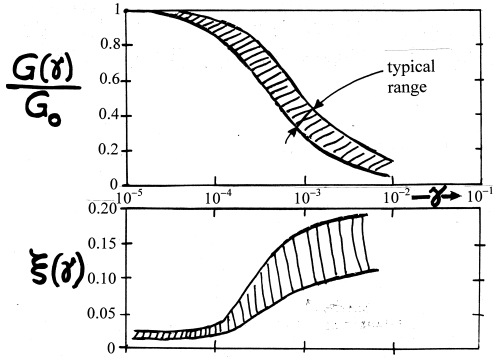


Figure 8-12. Shear modulus and damping ratio vs. strain level.

The following empirical relation can be used to establish the initial shear modulus G_0 in a soil

$$G_0 = A \frac{(3-e)^2}{1+e} \sqrt{\sigma_0'} (OCR)^k$$

in which σ_0' and G_0 are both to be given in units of kPa and $A = 3000 \pm 1000$ depending on material (size, angularity of grains, etc.). OCR denotes the overconsolidation ratio for clay and has to be set equal to 1.0 for sand, the exponent k is a function of the plasticity index I_p as given in Table 8-2, and e is the void ratio.

Plasticity index I_p	k
0	0
20	0.18
40	0.30
60	0.41
80	0.48
>100	0.50

The confining effective stress σ_0' is defined as the average of the three principal effective stresses

$$\sigma_0' = \frac{1}{3} (\sigma_1' + \sigma_2' + \sigma_3')$$

Note that in geotechnics, the effective stress is defined as the total stress minus the pore pressure.

Alternatively, the following relation for sand can be applied

$$G_0 = 1000K \sqrt{\sigma_0'}$$

in which σ_0' and G_0 are both to be given in units of kPa, and K takes on values according to Table 8-3. For clay, one can use the following relation as an alternative to the above formula

$$G_0 = 2600s_u$$

in which s_u is the undrained shear strength of the soil.

Soil type	K
Loose sand	8
Dense sand	12
Very dense sand	16
Very dense sand and gravel	30-40

The steps in establishing the shear modulus and the damping ratio can be listed as follows:

1. determine source of dynamic loading (earthquake, wind, waves and machine vibrations)
2. find expected strain level γ for loading from list below Figure 8-12
3. Find damping ratio ξ from Figure 8-12
4. Find shear modulus ratio G/G_0 from Figure 8-12
5. calculate G_0 from one of the formulas given above, chosen dependent on soil type
6. calculate G as the product of G_0 and G/G_0

Example: wind loading on a foundation in clay with undrained shear strength $s_u = 200$ kPa:

1. the source of loading is wind
2. the expected strain level is typically $\gamma = 10^{-3}$
3. the damping ratio is about $\xi = 0.10-0.15$
4. the shear modulus ratio is $G/G_0 = 0.35$.
5. the initial shear modulus is $G_0 = 2600s_u = 520$ MPa
6. the shear modulus becomes $G = 0.35 \cdot 520 = 180$ MPa

Table 8-4 provides guidance for assessment of Poisson's ratio.

Table 8-4. Poisson's ratio ν .	
Soil type	ν
Dense sands	0.25-0.30
Loose sands, stiff clays	0.35-0.45
Saturated clays	≈ 0.50

Once the equivalent shear modulus G has been established from G_0 and Figure 8-12, and the Poisson's ratio ν has been assessed, the foundation stiffnesses can be derived. The following four stiffnesses are considered:

- vertical stiffness, $K_V = V/\delta_V$, which expresses the ratio between the vertical force V and the vertical displacement δ_V
- horizontal stiffness, $K_H = H/\delta_H$, which expresses the ratio between the horizontal force H and the horizontal displacement δ_H
- rotational stiffness, $K_R = M/\theta$, which expresses the ratio between the overturning moment M and the rotation angle θ in rocking
- torsional stiffness, $K_T = M_T/\theta_T$, which expresses the ratio between the torque M_T and the twist θ_T

Formulas for spring stiffnesses are given in Table 8-5 to Table 8-7 for various types of foundations which cover:

- circular footing on stratum over bedrock
- circular footing on stratum over halfspace
- circular footing embedded in stratum over bedrock
- piled foundations

For the footings it is assumed that they are rigid relative to the soil and always in full contact with the soil. The piled foundations are assumed to be flexible as dealt with below.

The spring stiffnesses given in Table 8-5 to Table 8-7 are all static stiffnesses, i.e. they are stiffnesses for frequencies approaching zero. The dynamic stiffnesses may deviate from the static stiffnesses in particular in case of high-frequent vibrations. However, for wind and wave loading of wind turbine foundations, onshore as well as offshore, the induced vibrations will be of such a nature that the static stiffnesses will be representative for the dynamic stiffnesses that are required in structural analyses. For earthquake loading, however, frequency-dependent reductions of the static stiffnesses to get appropriate dynamic stiffness values may be necessary and should be considered.

The slenderness ratio for a pile is defined as L/D where L is the length and D is the diameter of the pile. For $L/D > 10$, most piles are flexible, i.e. the active length of the pile is less than L , and the pile head response is independent of the length of the pile. Spring stiffnesses at the pile head of flexible piles are given in Table 8-7 for three idealised soil profiles and the following modes of motion:

- horizontal
- rocking
- coupled horizontal-rocking

Reference is made to the Young's modulus of the soil E , which relates to the shear modulus G through

$$E = 2G(1 + \nu)$$

E_S is the value of E at a depth z equal to the pile diameter D , and E_p is the Young's modulus of the pile material.

The formulas given for foundation stiffnesses in the tables in this section can be used to calculate spring stiffnesses to support the tower in aeroelastic wind turbine

analyses. As a rule of thumb, the natural frequency of the tower will be reduced by 0% to 5%, when the assumption of a rigid foundation (fixed-ended tower) is replaced by a realistic finite foundation stiffness. Under special conditions this error may however be up to 20%.

Table 8-5. Circular footing on stratum over bedrock or on stratum over half-space.

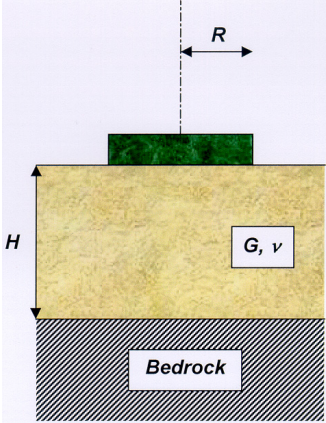
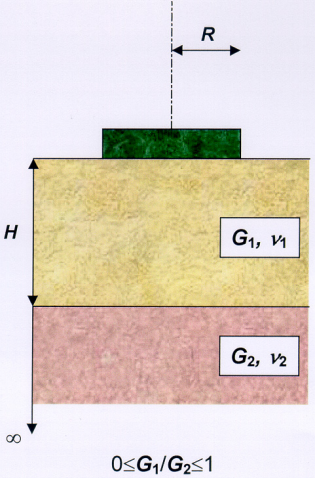
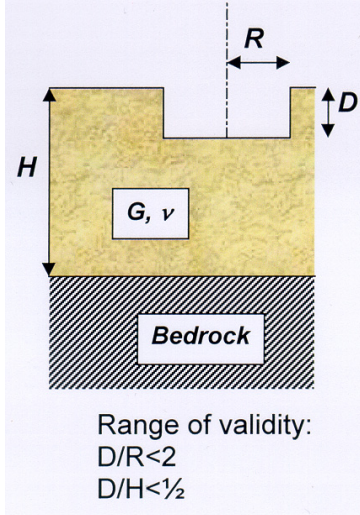
	On stratum over bedrock	On stratum over half-space
		 <p style="text-align: center;">$0 \leq G_1/G_2 \leq 1$</p>
Mode of motion	Foundation stiffness	Foundation stiffness
Vertical	$K_v = \frac{4GR}{1-\nu} \left(1 + 1.28 \frac{R}{H}\right)$	$K_v = \frac{4G_1R}{1-\nu_1} \frac{1 + 1.28 \frac{R}{H}}{1 + 1.28 \frac{R}{H} \frac{G_1}{G_2}}; 1 \leq H/R \leq 5$
Horizontal	$K_H = \frac{4GR}{1-\nu} \left(1 + 1.28 \frac{R}{H}\right)$	$K_H = \frac{8G_1R}{1-\nu_1} \frac{1 + \frac{R}{2H}}{1 + \frac{R}{2H} \frac{G_1}{G_2}}; 1 \leq H/R \leq 4$
Rocking	$K_R = \frac{8GR^3}{3(1-\nu)} \left(1 + \frac{R}{6H}\right)$	$K_R = \frac{8G_1R^3}{3(1-\nu_1)} \frac{1 + \frac{R}{6H}}{1 + \frac{R}{6H} \frac{G_1}{G_2}}; 0.75 \leq H/R \leq 2$
Torsion	$K_T = \frac{16GR^3}{3}$	Not given

Table 8-6. Circular footing embedded in stratum over bedrock



Mode of motion	Foundation stiffness
Vertical	$K_v = \frac{4GR}{1-\nu} \left(1 + 1.28 \frac{R}{H}\right) \left(1 + \frac{D}{2R}\right) \left(1 + (0.85 - 0.28 \frac{D}{R}) \frac{D/H}{1 - D/H}\right)$
Horizontal	$K_H = \frac{8GR}{1-\nu} \left(1 + \frac{R}{2H}\right) \left(1 + \frac{2}{3} \frac{D}{R}\right) \left(1 + \frac{5}{4} \frac{D}{H}\right)$
Rocking	$K_r = \frac{8GR^3}{3(1-\nu)} \left(1 + \frac{R}{6H}\right) \left(1 + 2 \frac{D}{R}\right) \left(1 + 0.7 \frac{D}{H}\right)$
Torsion	$K_t = \frac{16GR^3}{3} \left(1 + \frac{8D}{3R}\right)$

Table 8-7. Flexible pile.

Soil profile	Standardised springs at pile head		
	Horizontal $\frac{K_H}{DE_s}$	Rocking $\frac{K_R}{D^3 E_s}$	Coupled $\frac{K_{H,R}}{D^2 E_s}$
Linear increase with depth $E = E_s z/D$	$0.6 \left(\frac{E_p}{E_s}\right)^{0.35}$	$0.14 \left(\frac{E_p}{E_s}\right)^{0.80}$	$-0.17 \left(\frac{E_p}{E_s}\right)^{0.60}$
Increase with square-root of depth $E = E_s \sqrt{z/D}$	$0.8 \left(\frac{E_p}{E_s}\right)^{0.28}$	$0.15 \left(\frac{E_p}{E_s}\right)^{0.77}$	$-0.24 \left(\frac{E_p}{E_s}\right)^{0.53}$
Homogeneous $E = E_s$	$1.08 \left(\frac{E_p}{E_s}\right)^{0.21}$	$0.16 \left(\frac{E_p}{E_s}\right)^{0.75}$	$-0.22 \left(\frac{E_p}{E_s}\right)^{0.50}$

8.5 Properties of Reinforced Concrete

In the following attention will be paid to concrete with reinforcing steel (RFC). Furthermore, emphasis is given to conditions, which are of importance to the durability. Or, as expressed in the CEB-FIP Model Code 1990 (MC 90): “Concrete structures shall be designed, constructed and operated in such a way that, under the expected environmental influences, they maintain their safety, serviceability and acceptable appearance during an explicit or implicit period of time without requiring unforeseen high costs for maintenance and repair.”

Durability of RFC strongly depends on the exposure, which usually is expressed in terms of environmental classes. As an example the basis for both material and structural specifications in DS411 (DS 411, 1999) distinguishes between different environmental classes, namely passive (P), moderate (M), aggressive (A) and extra aggressive (E). Class P is rarely used in this context, class M is used for onshore foundations when covered by earth, class A is used offshore where class E is also used in the splash zone.

8.5.1 Fatigue

Fatigue analysis of concrete structures for wind turbines is important and must not be omitted. Verification must be performed both for the concrete and for the reinforcement in separate analyses. For verification of the fatigue-life of the foundation only the largest of the base load components M_{tt} (tower tilt moment) or F_m (normal shear force) may be taken into consideration. As regards concrete, adequate fatigue may be assumed according to Eurocode 2, Part 2-2. Otherwise, more refined fatigue verification may be necessary. Under compression, the following expression shall be satisfied

$$\frac{\sigma_{c,\max}}{f_{cd}} \leq 0.5 + 0.45 \cdot \frac{\sigma_{c,\min}}{f_{cd}} \leq 0.9$$

If $\sigma_{c,\min} < 0$ (tension) then: $\frac{\sigma_{c,\max}}{f_{cd}} \leq 0.5$

$\sigma_{c,\max}$ maximum compressive stress at a fibre under the frequent combination of actions

$\sigma_{c,\min}$ minimum compressive stress at the same fibre where $\sigma_{c,\max}$ occurs

f_{cd} design compression strength of the concrete, see Appendix E

In structures without shear reinforcement, adequate fatigue resistance of concrete under shear may be assumed if either of the two equations are satisfied

$$\frac{\tau_{\min}}{\tau_{\max}} \geq 0 : \left| \frac{\tau_{\max}}{\tau_{Rd1}} \right| \leq 0.5 + 0.45 \cdot \left| \frac{\tau_{\min}}{\tau_{Rd1}} \right| \leq 0.9$$

$$\frac{\tau_{\min}}{\tau_{\max}} < 0 : \left| \frac{\tau_{\max}}{\tau_{Rd1}} \right| \leq 0.5 - \left| \frac{\tau_{\min}}{\tau_{Rd1}} \right|$$

τ_{\max} maximum nominal shear stress under the frequent combination of actions

τ_{\min} minimum nominal shear stress at the section where $\sigma_{c,\max}$ occurs

$$\tau_{RD1} = \frac{V_{RD1}}{b \cdot h_{ef}}$$

V_{RD1} design shear resistance, according to Equation (4.18) in EC 2, Part 1-1.

b, h_{ef} see Figure 8-13

For unwelded reinforcement bars subjected to tension, adequate fatigue resistance may be assumed if, under the frequent combination of actions, the stress variation does not exceed

$$\Delta\sigma_s < |70| \text{ N/mm}^2$$

If the stress variation does not fulfil this equation, more refined fatigue verification must be carried out, i.e. using the Palmgren-Miner cumulative damage law. The relationship between the characteristic fatigue strength σ_{fat} and the characteristic fatigue value n_{fat} is given by the expression

$$n_{fat} = \frac{k \cdot 10^{12}}{(\sigma_{fat})^m} \Rightarrow \sigma_{fat} = \left(\frac{k \cdot 10^{12}}{n_{fat}} \right)^{\frac{1}{m}}$$

The Wöhler curves are characteristic values and should be reduced by partial safety factors according to the chosen safety level. The Wöhler constants m and k , according to DEA (1998) can be used.

8.5.2 Crack-width

Crack widths appear in RFC from the influence of the loads and as a result of deformations due to temperature or shrinkage. The size of the crack width w can be found acc. to DS411 (DS 411, 1999) as a function of the reinforcement stress as follows

$$w = 5 \cdot 10^{-5} \cdot \sigma_s \cdot \sqrt{a_w}, \text{ [mm]}$$

The crack parameter a_w [mm] is calculated as the ratio between the active concrete area A_{cef} and the sum of the crack width decisive diameters d_w of the reinforcement bars in the tension zone

$$a_w = \frac{A_{cef}}{\sum d_w}$$

A_{cef} is to be calculated as the maximum concrete area of which the centre of gravity COG is coincident with the COG of the tension reinforcement.

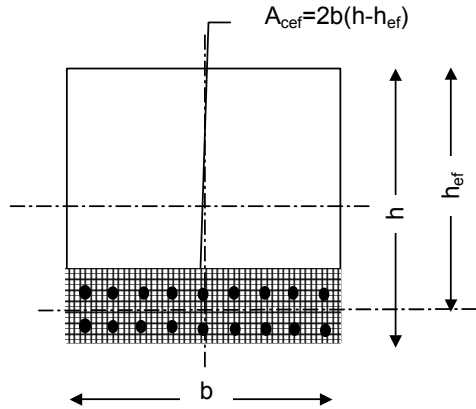


Figure 8-13 Active concrete area in tension zone for calculation of crack-width

The external loads at which the crack widths are determined are usually 60% of the wind turbines maximum operational loads.

The stress in the reinforcement σ_s [N/mm²] due to external load can be found by means of the elasticity theory assuming that the surrounding concrete stress (in tension) is 0. The external force is the sectional moment M only:

Concrete stress
$$\sigma_{c,max} = \frac{M}{\varphi_b \cdot b \cdot h_{ef}^2}$$

Reinforcement stress
$$\sigma_{s,max} = \alpha \cdot \gamma \cdot \sigma_{c,max}$$

M sectional bending moment
 A_s reinforcement area
 b and h_{ef} see Figure 8-13

Parameters α , φ_b and γ to be extracted by iteration from formulas below:

$$\alpha \cdot \varphi = \alpha \cdot \frac{A_s}{b \cdot h_{ef}}$$

$$\beta = \alpha \cdot \varphi \cdot \left(\sqrt{\frac{2}{\alpha \cdot \varphi} + 1} - 1 \right)$$

$$\varphi_b = \frac{1}{6} \cdot \beta \cdot (3 - \beta)$$

$$\gamma = \frac{1 - \beta}{\beta}$$

Adding the contribution from temperature differences shrinkage (and creep) one can do more accurate evaluation of the size of the crack widths. E.g. by determination of the corresponding reinforcement stress expressed by strains as found in FEM-analyses.

Maximum calculated crack-width must in general be within the interval 0.2-0.3 mm. More specific for offshore wind turbine in the splash zone the interval is 0.1-0.2 mm.

Cracks from shrinkage of the concrete are distributed through the reinforcement. In order to minimise the development of these cracks the reinforcement degree

$$\varphi = \frac{A_s}{A_b} \text{ , where } A_s: \text{ Reinforcement area}$$

A_b : Concrete area

is therefore normally set to 0.25-0.50%

In order to minimise the risk of crack formation the temperature must not exceed 70 °C during curing, see DS 482 (1999). Furthermore differences in temperature should be minimised; normally temperature differences ΔT greater than 12-15 °C measured over the cross section is not allowed.

8.5.3 Execution

It must be ensured that the following minimum requirements are fulfilled:

- Water/cement ratio for the concrete is determined in consideration of the environmental class, typically $w/c < 0.55$ at all times.

- maximum aggregate size, $d_{\max} < 32\text{mm}$ or minimum distance between reinforcement bars
- maximum distance between non-prestressed reinforcement bars is 150-200 mm
- application of reinforcement with relatively insignificant reinforcement diameters ($D = 12\text{-}20\text{ mm}$) to the extent possible

When choosing materials for parts of the structure, reinforcement and adhesion for the structure, it shall be ensured that alloys are not applied which will function as cathodes for the additional structure. A distinct risk of corrosion will be present for the metals zinc aluminium and lead in uncured concrete. During corrosion hydrogen develops and as the corrosion products are more voluminous, spalling might happen. The corrosion attack will decrease when the concrete dries out. However, if the concrete remains wet even in hardened condition the attack will persist.

8.6 Selected foundation structure concepts for offshore applications

8.6.1 Introduction to concepts

Three basically different foundation structure concepts exist for offshore wind turbines:

- monopile
- gravity base
- tripod

These three foundation concepts are different in the manner by which they transfer the loads to the supporting soils. The monopile and the tripod both transfer vertical forces as axial shear forces at the pile-soil interfaces. The gravity base foundation transfers such forces as a vertical contact pressure at the foundation-soil interface. Both the monopile and the tripod primarily transfer horizontal forces by way

of horizontal earth pressures against the piles at some depth. The gravity base foundation primarily transfers such forces directly to horizontal shear forces in the soil at the foundation-soil interface. The monopile also transfers bending moments about the seabed as horizontal earth pressures against the pile. The tripod primarily decomposes such overturning moments into axial forces in the three legs, and these forces are then transferred to the soil as axial shear forces at the pile-soil interfaces. The gravity base foundation transfers overturning moments about the seabed by a varying vertical contact pressure over the foundation-soil interface. During design, it is important to make sure that this contact pressure in extreme load situations never takes on negative values. Any significant, negative contact pressure would correspond to a tension, which can hardly be transferred unless purely undrained conditions with development of a suction can be counted on, and which may lead to an undesirable separation between foundation and soil. However, a limited “lift” of the foundation of limited duration during extreme loading is allowable.

Each of the three offshore foundation concepts have their pros and cons. The monopile is usually an attractive foundation solution for wind turbines to be placed in shallow waters and smooth seas. This concept is attractive also because it offers a fast installation. The tripod is preferred over the monopile in harsher climates and less shallow waters, however, the solution with suction buckets under the three legs is only feasible for foundations in clay and will not work in sand or other permeable soils. The tripod concept is a light-weight structure, which is usually cost-efficient. It is an attractive feature of gravity-based foundations that they can be equipped with more or less shallow skirts under their bottoms. This will move the depth of load transfer

deeper below the sea floor, and it will contribute to prevent scour from occurring around and in particular underneath the foundation, especially in sand. Gravity-based foundations may often be feasible from a technical point of view, but may not always come out economically feasible. They form a well-tested concept, which is, however, also a time and resource demanding concept. With these pros and cons of the various foundation types in mind, it should be noted that the type of foundation to be chosen also depends heavily on the actual soil profile and soil properties on the site.

Two of the three distinct foundation structures for offshore wind turbine installations are dealt with in the following sections, viz. the monopile and the tripod structures.

8.6.2 Monopile

General Description

Monopiles have traditionally been used as the preferred foundation solution for some types of marine structures. Piles with diameters up to about 1 m have been used to support lighthouses and moorings. Equipment to install piles of diameters up to 3-4 m to large penetration depths is available and makes monopiles a feasible foundation alternative for offshore wind turbines. An example of a monopile foundation is depicted in Figure 8-14.

Advantages of a monopile foundation include:

- a fast and highly automated installation with no prior preparation of the seabed
- simple fabrication

The monopile foundation of a wind turbine consists of three basic parts: the bare pile, a conical transition to the tower that it supports, and a boat landing. By alteration of the conical transition, the foundation can easily be adjusted to fit different tower diameters.



Figure 8-14. Monopile Foundation, from LIC Engineering (1997)

The boat landing is clamped to the pile and provides a basis for the J-tube that carries the power cable from the seabed to the wind turbine. The conical transition is welded to the pile after completion of the pile driving.

Ice loads have a very large impact on the necessary dimensions of a monopile foundation. If only small variations in the water level are expected, it is possible to design an ice cone, which will reduce the ice load significantly and contribute to eliminate large oscillations of the wind turbine tower. When large variations in water level are present, such an ice cone will not be feasible. This may leave a very large dynamic ice load acting on the monopile, and large oscillations of the wind turbine tower may result.

Determination of monopile dimensions (design approach)

Three basic dimensions characterise a monopile:

- length of pile in soil, L
- outer diameter of pile, D
- wall thickness of pile, t

The values of these geometrical parameters are partly interdependent and have to be selected in an iterative process, because some of the loads, in particular the ice loads and the wave loads, will increase with increasing pile diameter. At the same time, however, the bending stress ranges causing fatigue will decrease with increasing diameter.

The pile diameter D and the wall thickness t are determined from requirements expressed in terms of design rules for the pile as a steel structure. The design rules to be fulfilled consist of four criteria:

- ultimate limit state criterion
- fatigue limit state criterion
- local buckling criterion
- hard driving criteria

Once the pile diameter and the wall thickness have been determined by making sure that these criteria are fulfilled, geotechnical bearing capacity considerations for the supporting soil are used to determine the necessary length L of the pile. The axial load is typically a compressive load. Usually the axial bearing capacity of the pile will be much larger than required, and the requirements for the lateral capacity, needed to counteract the horizontal shear force and the overturning moment set up by wind, wave and ice loads, will govern the design. The most economical design comprises a combination of D , t and L which will minimise the total pile mass. Once D , t and L have been determined, a final step in the design of the monopile consists of a dynamic analysis of the pile subjected to ice loading, and t is adjusted if necessary. The design rules for determination of D and t are listed in the following for the respective limit states considered:

Ultimate Limit State Criterion

In the ULS situation, the maximum design von Mises stress in the pile wall shall be smaller than or equal to the design yield stress. The design von Mises stress is the characteristic von Mises stress multiplied by a load factor. The design yield stress is the characteristic yield stress divided by a material factor.

Fatigue Limit State Criterion

The fatigue damage is calculated as a Miner's sum. For this purpose, a design long-term distribution of stress ranges shall be applied together with a design *S-N* curve. The design stress range distribution is derived from the characteristic stress range distribution by multiplication of all stress range values according to this distribution by a load factor. At wall thickness transitions and at the offshore on-site weld between the pile and the conical transition, stress concentration factors are to be included. The design *S-N* curve is derived from the characteristic *S-N* curve by division of all characteristic stress range values according to this curve by a material factor. The total fatigue damage from wind and wave load and from pile driving shall be below the acceptable level according to the Palmgren-Miner's rule.

Local Buckling Criterion

When a cylinder with a large diameter-to-wall-thickness ratio is exposed to bending or axial loading, a risk of local buckling is present. Local buckling can be checked according to DS 449 (DS 449, 1983).

Hard Driving Criterion

During driving, the pile is exposed to very large axial stresses, which may cause local buckling of the pile during so-called hard driving. Hard driving is defined as more than 820 blows per meter penetration into the soil. Hard driving shall be avoided. The

criterion is taken according to API (API, 1993).

The loads to be considered are:

- loads due to wind acting on the wind turbine.
- loads due to waves and current acting on the foundation. These loads are included in the Ultimate Limit State (ULS) as well as in the Fatigue Limit State (FLS) and may amount to 30-40% of the wind load acting on the wind turbine.
- ice loads are very important. The result of the analysis is a Dynamic Amplification Factor (DAF factor), by which the stresses found from a quasi-static analysis shall be multiplied.

For load calculations, reference is made to Chapter 4.

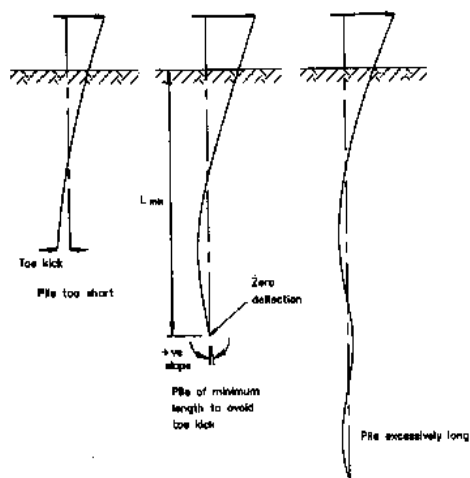


Figure 8-15. Lateral deflections of a pile exposed to horizontal loading. (Bartrop, 1991).

Analysis of laterally loaded piles

The minimum length of the pile is the smallest length for which there will be no toe-kick when the pile head is subjected to a lateral displacement at mudline. This is the length, at which no further reduction of the lateral deflection at mudline can be obtained

when the length of the pile is increased. Reference is made to Figure 8-15 and Barltrop (1991). For details about methods for analysis of laterally loaded piles, reference is made to Section 8.3.

Connection between monopile and tower

The monopile foundation concept includes a conical connection piece between the monopile and the wind turbine tower. The connection piece comprises the access platform as an integral part. At the top of the conical connection piece, a flange for connection of the wind turbine tower is located. At the bottom of the conical connection piece, an in-situ connection to the monopile foundation is to be established.

The connection between the pile and the conical connection piece is an essential part of the monopile foundation concept. The basic requirements to this connection are:

- sufficient strength against extreme and fatigue loading
- easy installation
- low cost

Two alternative concepts are considered feasible:

- flange connection (fast installation)
- welded connection (strong connection)

Reference is made to Lyngesen and Brendstrup (1997) for more details.

Corrosion protection

As the surface of the pile is exposed to a harsh environment due to waves, abrasion from suspended sediments and a high salinity, a large corrosion rate is expected. For unprotected steel, the extreme surface corrosion of an exposed steel pile in ocean water can be estimated to (DS 464/R, 1988):

0 years after installation	0 mm
10 years after installation	8 mm
20 years after installation	11 mm
30 years after installation	14 mm

The design life of a wind turbine foundation usually varies between 30 and 50 years. The maximum corrosion is located in the splash zone. The maximum bending stresses in the pile during extreme loading are found below this zone. Thus extreme stability will be maintained even if a rather large corrosion depth is found in the splash zone.

However, a corroded surface generates areas with very large stress concentrations and cracks will propagate faster in corroded steel than in uncorroded steel. Therefore, it is recommended to use corrosion protection in corrosive environments, even if the structure is capable of accommodating the stresses over the extent of the corroded cross-section (DS 412, 1998).

With a view to the above numbers, this calls for implementation of a corrosion protection system.

Three primary options exist for corrosion protection of a monopile:

- coating (vulnerable to damage during installation)
- cathodic protection by sacrificial anodes (a large number of anodes are required for a 50-year design life)
- impressed current (facilitated by the presence of electrical power supply)

For a design life in excess of 30 years, the preferred option for monopile foundations is protection by use of impressed current.

The pile has a large surface, but normally only a part of this requires protection. The surface exposed to wave action, including the splash zone, shall be protected. Depending on the type of sediment, the potential for scour, etc., also a part of the pile below mudline may need protection. Typically, the area to be protected extends down to a level 2 to 10 m below mudline. Below this limiting level, protection of the pile surface is usually not required.

Inside the hollow pile water will be present, but there will only be little exchange of water. Therefore, corrosion on the inside of the pile is expected to be limited. However, it is recommended that internal zones are protected either with coating or with cathodic protection (DNV, 1998). If the pile is filled with sand, corrosion will be minimised or even prevented (DS 464/R, 1988).

Installation

Driving of large diameter piles is well-known from the offshore industry. Generally, at least three different pile-driving methods are available. These methods are described briefly in the following.

Driving using piling hammer

Pile driving by means of a hammer is the oldest technique. In its simplest version, it consists of a ram dropped on the top of the pile from a certain height. Today, hydraulic fluid is widely used for lifting the ram and further accelerating it during the downward stroke. Hydraulic piling hammers are the most efficient compared to diesel and steam hammers. The technique capitalises on the shock wave which is generated in the pile by the impact from the hammer. The transfer of the shock wave to the soil generates plastic deformations of the soil and thereby moves the pile downwards.

So-called pile refusal occurs when the shock wave amplitude is not large enough to create plastic soil deformations. The penetration of the pile then ceases. Damping of the shock waves caused by soil adhesion along the pile surface may contribute to pile refusal, in particular, in cohesive soils. In this context, it is important to be aware that the smaller the ratio between the cross-sectional pile area and ram area is, the longer is the shock wave transmission time, the smaller is the

shock wave amplitude, and the larger is the possibility for pile refusal.

Driving using vibrators

In frictional soils, the pile may be vibrated into the soil. Vibration is a very fast installation method even compared to driving by hammer. Furthermore, it does not generate very large shock waves in the soil that could otherwise have caused damage of adjacent structures. However, only a few very large vibration hammers are available world-wide. The vibrations generate a liquefaction of the soil locally around the pile, thus reducing the side adhesion to a minimum. Then the pile penetrates into the soil mainly due to its own weight.

Driving using drilling or excavation

For installation of hollow piles, drilling or excavation may be applied. The soil in the core and below the pile is excavated, generating a hole with a diameter usually slightly larger than that of the pile. Then the pile penetrates into the soil due to the mass of the pile. If side adhesion or lateral resistance is required, grout may be injected in the annulus between the pile surface and the soil.

Notes on pile refusal

The pile has to be driven to a particular penetration depth, which is required to enable the pile to carry its design lateral load. However, pile refusal may be encountered before the final penetration depth is reached. This may happen if the piling hammer does not have sufficient excess capacity compared to the theoretically calculated driving resistance.

In case of pile refusal, a decrease of up to 50% in the driving resistance can be obtained by removing the soil plug inside the pile. In sandy and silty soils, this can be achieved by jetting. In clay and tills, this can be achieved by using an auger. The driving

resistance can also be reduced by installation of an external “driving shoe” on the pile tip, however, this may also lead to a reduced lateral capacity and may therefore not always be recommended.

Maintenance

Inspection and maintenance are to be carried out to ensure a sufficient structural strength.

Crack Inspection

Cracks may be initiated at the weld between the monopile and the conical transition section. Therefore, the weld is to be inspected for fatigue cracks. The inspection will consist of:

visual inspection and/or non-destructive testing (NDT):

- magnetic powder inspection (MPI)
- eddy current
- ultrasonic examination

Depending on the fabrication method of the monopile, welds may also be located in the submerged zone above mudline. These welds also need to be inspected. The extent of each inspection will be determined as part of the inspection planning. The interval between each inspection is to be determined on the basis of requirements to the lifetime and on the predicted accumulated fatigue damage.

Inspection of Cathodic Protection

The monopile foundation is protected against corrosion by means of an impressed current system. A reference control point (the point with minimum potential) on the monopile is selected. The electrical potential of this point is measured and is reported through the wind turbine monitoring system. In case the anode disappears or the area of the anode becomes too small, the potential at the control point will increase, and the anode needs to be replaced. Further, it is recommended to perform a visual check of the cathodic protection system whenever an

inspection on the wind turbine tower is carried out.

Inspection of Scour Protection

Scour will occur around the monopile. To provide protection against local scour around the pile, scour protection is installed. Throughout the lifetime of the wind turbine the scour holes around the pile are to be measured from time to time. The holes can be measured by means of a 3-D echo sounder. The scour protection is **not** absolutely stable and needs to be maintained. When an unacceptable degree of scour occurs, additional scour protection is to be installed.

Spring Inspection

When the foundation is located in an environment where ice loading may occur, it is recommended to perform an annual inspection every spring to verify whether ice loading has caused damage to any structural members or coating during the past winter. In case of damage, repair is to be carried out.

Dismantling

In the following, two different methods are outlined for removing the monopile foundation from the seabed after termination of its service life.

1. Cutting off the piles is a method that can be used in general. By this method, the monopile is cut below the mudline. The method is based on the use of a cutting tool lowered down inside the pile. The subsea cutting is performed by a high pressure jet, consisting of water mixed with a non-pollute grinding compound (sand).

The procedure consists of the following steps:

- the soil core inside the tubular is removed to the elevation of the cut line
- the cutting tool is lowered to the elevation of the cut line, inside the pile

- the pile is cut at elevation of cut line
- the upper part of the pile is lifted off and transported to the shore on a barge

The remaining part of the pile will be left below the seabed, and will not cause any damage to the environment.

2. Complete removal of the pile is another method of dismantling. A vibration hammer can be used for this purpose. The vibration hammer is typically used for removal of piles in non-cohesive soils. The hammer is placed on top of the pile, and the induced vibrations in the pile will cause local liquefaction in the soil around the outer surface of the pile. When the soil is liquefied, no skin friction between soil and pile will be present, and the pile can then be pulled up by means of using a crane vessel.

The advantage of this method is that the entire pile is removed. The disadvantage is that the method is not likely to work for removal of piles in cohesive soils.

8.6.3 Tripod

General description

The tripod foundation concept consists of a steel frame that transfers the sectional forces from the tower to primarily tensile and compressive loads in three hollow steel piles that are driven into the seabed. From below the tie-in flange, a large diameter tubular, referred to as the centre column, extends downwards. On the upper section immediately below the flange, the dimension of the centre column is identical to that of the tower. Below this section, a transition section reduces the diameter and increases the wall thickness. Reference is made to Figure 8-16. As the tripod concept is still under development, the presentation given here is relatively brief.

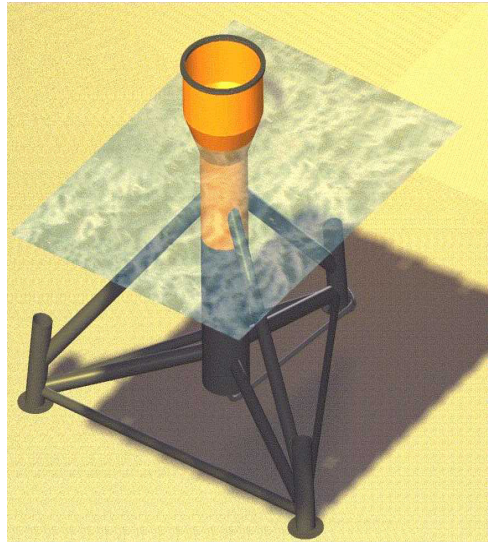


Figure 8-16. Tripod with piles, from Rambøll (1997).

This concept is advantageous for several reasons:

- the steel volume applied as corrosion appliance is reduced since the diameter is reduced.
- the layout of the joints connecting upper leg bracing to centre column is improved with less difference in diameters. The punching shear capacity of the connections between the upper braces and the centre column are increased, and the stiffness of the joint is improved. This is of paramount importance for achieving the desired fatigue life.
- The conical section will decrease the design governing ice loading somewhat, although the cone would have to be higher to provide full reduction for all sea levels depending on the environmental conditions.
- The hydrodynamic loading is reduced.

Each leg frame consists of a pile, a pile sleeve and two braces. At the bottom of each pile sleeve, a mudmat is located to support the structure on the seabed prior to the pile driving. After completion of the pile driving,

the annulus between the pile and the sleeve is filled with grout to form a rigid connection. It is recommended to batter the pile from the vertical, such that the extension of the centre line of the pile intersects with the point of impact of the dominating load on the tripod structure. Note that excessive batter requires the hammer to be supported laterally during pile driving and should therefore be avoided.

As an alternative to using three piles to support the tripod structure and transfer the loads to the soil, so-called skirt foundations may be applied, e.g. in the form of suction buckets. One suction bucket would then have to support each of the three tripod legs. When suction buckets are used for the foundation, a variant of the tripod structure is feasible, in which the central column supporting the tower is extended down to the seabed and further supported by a suction bucket. With this configuration of the central column with a bucket support, only two more supports with suction buckets are needed. These are placed such that their respective frames are perpendicular to each other. This implies that access of service vessels is possible within a 270 degrees angle. By this design, the centre column will participate more actively in the transfer of forces from the tower to the seabed. All supporting elements, including the centre column, are designed as circular tubes acting as strut members, i.e. transferring compressive and tensile forces only. Reference is made to Figure 8-17.

The tripod concept makes use of the conical transition between the tower and the supporting column in the tripod structure as an ice cone. When solid ice is forced against the structure, the conical transition causes the ice to be pressed downwards, and crushing takes place at a level with a smaller



Figure 8-17. Tripod with suction buckets, from Rambøll (1998).

diameter than that of the tower, and the ice load on the structure is correspondingly smaller. A complete elimination of ice crushing is not feasible, since this would pose requirements to the inclination of the conical transition far beyond what would be feasible considering the diameters of the involved tubulars. The disadvantage associated with the use of the conical transition as an ice cone is that it implies that an upwards vertical ice load will be acting on the centre column. However, as the vertical capacity is usually quite large, this disadvantage is usually not critical, yet it needs to be duly accounted for in the design.

The tripod structure is not compatible with too shallow water depths. This is due to the fact that:

- a sufficient water depth above all parts of the structure is required to allow service vessels to approach the structure.

- at very low water depths, the distance between the upper and lower braces becomes too short for the forces to be transferred in any reasonably sized cross-section.
- a solution with the braces protruding the water surface is not desirable due to the possible interlocking or packing of ice and the possibility of collision with service vessels.

The tripod causes relatively little blocking for wave action and for current flows which is of importance for environmentally sensitive areas. This even applies when a large number of foundations are installed as is the case in an offshore wind farm.

Geotechnical analysis – piles

In the ultimate limit state, the foundation analysis shall consist of an elastic and a plastic analysis. The two analysis checks can be described as follows:

In the elastic analysis, a check is carried out of the stresses in the piles and the structure with design loads (ULS) and design material properties. One pile only is allowed to reach its design maximum allowable stress. The allowable design value of the von Mises' stress is the yield stress f_y divided by the partial safety factor for steel strength. The result of the analysis must as a minimum contain the utilisation ratio of the pile steel. In the plastic analysis, the entire tripod structure is checked using design loads (ULS) and design material properties. All the piles are permitted to yield or fail completely, provided that the tripod as a whole can absorb the design loads.

The plastic design moment shall be calculated by

$$M_p(N) = \sigma_\gamma \cdot W_p \cdot \cos\left[\frac{\pi}{2} \cdot \frac{N}{\sigma_\gamma \cdot A}\right],$$

$$W_p = \frac{D^3 - (D-2t)^3}{6}$$

$M_p(N)$	Design plastic moment capacity as a function of the axial force
N	Axial force in pile
σ_γ	Nominal steel yield stress
W_p	Plastic section modulus
D	Pile diameter
t	Pile wall thickness
A	Steel area of pile

As a minimum, the result of the analysis must contain the pile utilization ratio and a verification that the penetration depth is sufficient. All piles are allowed to reach the design plastic moment. The forces and moments at the pile heads shall be in equilibrium with the design loading acting upon the structure and shall be smaller or equal to the allowable design values.

In both elastic and plastic analyses, the following features must be taken into account:

- linear-elastic superstructure that interconnects the piles
- non-linear behaviour of the piles laterally and axially
- pile group effects
- second-order moments in the piles
- soil plug length taken as 0.9 times length of pile embedded in soil

The procedures for development of t - z and q - w curves for the axial bearing capacity and p - y for the lateral bearing capacity can be done by using the API approach (API, 1993).

When characteristic values for the skin friction and tip resistance are given, the t - z curves for axial pile-soil interaction can be established by means of any relevant recognised computer program. The shape of the curves is fully described by

$$t = \frac{2}{\pi} \cdot t_{\max} \cdot \arctan\left[\frac{z}{3} \cdot \frac{\pi}{D} \cdot \frac{G}{t_{\max}}\right]$$

G	Shear modulus
z	Deflection pile/soil
D	Diameter of pile
t_{\max}	Maximum skin friction, calculated in accordance with API procedure
E	Young's Modulus
ν	Poisson's ratio

Reference is made to Clausen et al. (1982).

The shape of the q - w curves for the tip load-displacement relationship can be assumed to be bilinear with a required relative displacement between pile and soil of 5% of the pile diameter to cause yield.

The lateral bearing capacity can be based on p - y data developed by the API-RP2A-WSD procedures using cycling soil strength. Soil parameters needed in the modelling of the curves are:

Clay:	c_u	Undrained shear strength
	γ	Submerged unit weight
	J	Empirical constant
	ϵ_{50}	Strain at one-half the max. stress in laboratory undrained compression test
Sand:	γ	Submerged unit weight
	ϕ	Angle of internal friction (plane)

The curves and the pile group effects can be modeled by means of a relevant recognised computer program.

In a natural frequency and fatigue analysis linear behaviour of the piles laterally and axially can be assumed and modeled as spring constants. The true pile-soil interaction relationship is usually a smooth non-linear curve. The applied spring constants can be taken as the initial slope of the smooth curve.

Geotechnical analysis – Suction Buckets

The buckets work by principle of restricting flow of water from outside the bucket to

inside the bucket. A sudden application of loading yields a remarkable resistance towards pull-out, gradually tapering off if the loading is sustained. This resistance is formed by suction in the porewater inside the bucket, mobilised as the immediate reaction to the suddenly applied load. The bucket foundation is thus primarily designed to absorb load peaks. A static load in excess of a certain limit and acting over some length of time will gradually pull out the bucket as water is allowed to flow from the outside to the inside of the bucket and thereby neutralises and eventually eliminates the suction condition inside the bucket.

The concept is new only in relation to the application of suction technology to the design of offshore wind turbine foundations. The suction (or differential pressure) technology has been suggested and applied as both anchoring device for ships (and tension leg platforms) and as foundation for fixed leg platforms as an alternative to piles. However model testing and analyses are still required in order to obtain a sufficient design basis against hydraulic instability of skirted foundation of offshore wind turbines.

Structural analysis (limit states)

The structure and all structural members shall be verified according to three limit states. Different sets of partial safety factors for load and resistance apply to the different limit states. The normal safety class according to DS449 (DS 449, 1983) can be adopted, as the consequences of failure are limited (loss of investment but no loss of human life).

In the ultimate limit state (ULS), the structure is checked against extreme loads. The structure above seabed should be able to sustain these loads without collapse or permanent deformation. For piles, a fully developed plastic failure mode is accepted. Horizontal ice load is based on static ice

load, multiplied by a dynamic amplification factor (DAF). Vertical ice load may destabilize the structure, because it is applied as an upward load.

In the serviceability limit state (SLS), the maximum deflections are checked with special emphasis on the allowable tilt of the foundation due to differential settlements. In this state, no hydrodynamic loads on the foundation need to be included, since these loads will contribute only marginally to the overall moment on the tripod. All partial load factors are to be set equal to unity, i.e. characteristic loads are to be used in calculations. Loads from the wind turbine shall be taken as the worst damaging load case among all dynamic load cases. The maximum allowable tilt under this characteristic loading is 0.5° from vertical.

In the fatigue limit state (FLS), the structure is checked against failure due to fatigue damage. The cumulative fatigue damage for all load situations during the design life must be taken into account and the integrated effect should be investigated, e.g. by using the rain-flow counting scheme for stress cycles. Fatigue loads from the wind turbine shall be considered in conjunction with wave-induced fatigue loading, and it is to be verified whether it is acceptable to disregard contributions to the fatigue damage from ice crushing.

As fatigue is considered critical for the structure, it is of importance to verify that the fatigue life does not fall short of the design life, based on detailed information of waves from different geographical directions. The areas which are most likely to be dimensioned by fatigue loads are the centre column transition to the ice cone and the upper joint at the centre column where the upper leg framing attaches to the structure. Consider the distribution of stresses due to pure bending of the tower. This will

lead to a maximum stress above the upper joint at two points on a line perpendicular to the axis of the applied moment. The stresses will vary linearly between these points, but as the wind direction changes, also the locations of these points move. Thus, the loading (both in terms of magnitude and in terms of number of stress cycles) shall be applied for a fixed but critical point in the cross-section, i.e. the fatigue loads are to be applied from one particular direction only, and this direction is to be taken as the most critical direction. The conical transition induces an additional stress, which has to be accounted for. The designer may find it feasible to locate internal ringstiffeners, where the cone connects to the tubular, and thereby lower the overall dimensions of the conical section. Several layouts of the stiffener(s) are possible:

- a number of internal ringstiffeners
- bulkheads
- the leg framing may protrude into the interior of the centre column to be joined at the centre line, thereby distributing the loads directly between the leg frames

The most advantageous option may be chosen, taking into consideration the requirements of internal clearance for risers, conductors, power cables, etc.

Natural frequency analysis

A complete natural frequency analysis shall be performed for the combined structure consisting of turbine, tower, tripod and piles. For this purpose, the non-linear soil must be linearised. It is to be verified that the lowest frequencies differ from at least $\pm 10\%$ of the 1P and 3P rotor frequencies at nominal power.

Grouted connections

Axially loaded pile-to-sleeve connections are checked using the formula given by DNV (1977), including a safety factor of 3.0. The connections can be established by a

system widely used within the oil/gas industry. This system consists of flexible grout lines (OD 50 mm) attached to the tubes and connecting a simple manifold above water level to an outlet in the upper part of the pile sleeves.

Corrosion protection

Two options are found advantageous as primary protection. They are both of the cathodic type:

- sacrificial anodes of the ZN-Al-In type, placed as slender anodes in “handles” attached to the structure below sea level
- impressed current system

The disadvantage of the sacrificial anode system is the need for inspection. A sacrificial anode system may have to be renewed during a design life, depending on water salinity. Due to the on-line monitoring system already present for the turbine, measuring potential differences easily monitors an impressed current system. The current requirements may, however, pose a problem for remote and isolated offshore steel structures. Prior to coating, the entire structure must be sandblasted to comply with at least Sa 2½ according to ISO 8501-1n. The areas above the lower limit of the splash zone are to be coated with 2.5 mm of solvent-free epoxy coating. The remaining structure is to be coated with a shop primer to resist the environment at the construction site.

Scour protection

No scour protection is needed for the tripod structure. The small overall dimensions of all members close to the seabed yield rather small increases in velocities, and thus only little local scour. However, the design shall take into account the presence of both local and global scour around the tripod. The centre column must be sealed with a flange in order to avoid resonance between water inside the column and the surrounding sea.

Installation

Besides the geophysical and geotechnical surveys as described in Section 8.1, the only preparation of the seabed necessary before installation can take place is the establishment of the mudmats. The purpose of the mudmats is to secure the on-bottom stability prior to final driving of the three piles. They shall be designed to satisfy the following requirements:

- axial and lateral capacity of the soil
- lateral resistance due to stabbing pile
- horizontal level adjusted installation tolerances

The installation procedure is to a large extent based on the choice made by the contractor and is therefore not taken into consideration here.

Maintenance

The maintenance of the steel structure includes activities that are not specific to the tripod but apply to all steel foundation structures.

Crack monitoring

Crack monitoring of welded joints will have to be performed at regular intervals, at least until general experience with the structure has been established. Crack monitoring consists of ultrasound or X-ray inspection at critical time intervals. For the tripod, the critical details are considered to be the cone sections and the joint between the centre column and the upper leg bracing. To facilitate NDT inspection of the tripod, the centre column can be sealed off at some elevation below the joint and thereby allow for dry testing. The structure may be equipped with attach points for the scanning equipment to facilitate positioning.

By specifying the allowed fatigue utilisation, the designer can allow for a trade-off between initial manufacturing costs and subsequent maintenance costs.

Surface protection system

Maintenance consists of repair of coating in case of damage and monitoring/maintenance of the impressed current system. The impressed current system is believed to have a lifetime of 15 to 25 years after which the anode must be replaced.

Dismantling

The tripod can be moved from the seabed by cutting off the piles at or preferably below mudline. The pile sections thus left behind pose no ecological threat. Total removal of the pile can be accomplished by an inverse driving procedure and/or by vibration equipment.

If suction buckets are used for the foundation, the tripod can be removed completely.

REFERENCES

Aage D. Herholdt et al. *Beton-Bogen* 2.udgave 1986, CtO, Cementfabrikkernes tekniske Oplysningskontor.

API, *Recommended Practice for Planning, Designing and Constructing Fixed Offshore Platforms – Working Stress Design*, API Recommended Practice 2A-WSD(RP2A-WSD) 20th Edition, American Petroleum Institute, July 1, 1993.

API, *Recommended Practice for Planning, Designing and Constructing Fixed Offshore Platforms*, API RP2A, 17th Edition, American Petroleum Institute, 1987.

Bartrop, N.D.P., and A.J. Adams, *Dynamics of Fixed Marine Structures*, The Marine Technology Directorate Limited, Butterworth-Heinemann Ltd., Third Edition, 1991.

CEB-FIP Model Code 1990 (MC 90).

Clausen, C.J.F., P.M. Aas, and I.B. Almeland, “Analysis of the Pile Foundation System for a North Sea Drilling Platform”, *Proceedings*, BOSS, 1982.

DNV, *Rules for the Design, Construction and Inspection of Offshore Structures*, Det Norske Veritas, Høvik, Norway, 1977. (Reprint 1978.)

DNV, *Foundations*, Classification Notes, No. 30.4, Det Norske Veritas, Høvik, Norway, 1992.

DNV, *Rules for Classification of Fixed Offshore Installations*” Det Norske Veritas, Høvik, Norway, 1998.

DS 411, *Code of practice for the structural use of concrete*, 4. edition, Danish standard 1999

DS 412, *Code of Practice for the structural use of steel*, 3. edition, Danish standard 1998.

DS 415, *Code of Practice for foundation engineering*, 4. edition, Danish standard 1998.

DS449 *Dansk Ingeniørforenings Norm for Pælefunderede Offshore Stålkonstruktioner*, (in Danish), Dansk Ingeniørforening, Teknisk Forlag, Normstyrelsens Publikationer, Copenhagen, Denmark, April 1983.

DS 464/R, *Dansk Ingeniørforenings Anvisning for Korrosionsbeskyttelse af Stålkonstruktioner i Marine Omgivelser*, Dansk Ingeniørforening, Teknisk Forlag, Normstyrelsens Publikationer, Copenhagen, Denmark, June 1988.

DS 482, *Execution of Concrete Structures*, 1. edition 1999.

- Eide, O., and K.H. Andersen, *Foundation Engineering for Gravity Structures in the Northern North Sea*, Norwegian Geotechnical Institute, Publication No. 154, Oslo, Norway, 1984.
- Eurocode 2, *Design of concrete structures – Part 1-1: General basis for buildings and civil engineering works*, ENV 1992-1-1:1991
- Part 2-2: Reinforced and Prestressed Concrete Bridges, ENV 1992-2:1996.
- Hansen, B., *Limit Design of Pile Foundations*, Bygningsstatistiske Meddelelser, No. 2, September, 1959.
- Hansen, B., ”Geoteknik og Fundering, Del II Forelæsningsnotater til Kursus 5821 – Geoteknik 2”, Notat nr. 16, Den private ingeniørfond ved Danmarks tekniske Højskole, Lyngby, Denmark, 1978.
- Hansen, J.B., *A Revised and Extended Formula for Bearing Capacity*, Danish Geotechnical Institute, Bulletin No. 28, pp. 5-11, Copenhagen, Denmark, 1970.
- Kraft, L.M., R.P. Ray and T. Kagawa, “Theoretical t-z curves,” *Journal of Geotechnical Engineering*, ASCE, Vol. 107, No. 11, pp. 1543-1561, 1981.
- Lyngesen, S., and C. Brendstrup *Vindmøllefundamenter i Havet*, EFP-96, J.nr. 1363/96-0006, Final Report Mono Pile Foundation, LIC Engineering A/S, February 1997.
- Rambøll, *Vindmøllefundamenter i Havet*, EFP-96, J.nr.1363/96-0006, Tripod Foundation Volume 1 – Report, Rambøll, February 1997.
- Rambøll, *Havmøllefundamenter med sug*, UVE-98 J.nr. 51171/97-0047, Fase 1-rapport, SEAS, Niras, Rambøll, DGI, Risø, September 1998.
- Recommendation to Comply with the Requirements in the Technical Criteria for Danish Approval Scheme for Wind Turbines, Foundations*, Danish Energy Agency, August 1998.
- Reese, L.C. and H. Matlock, “Numerical Analysis of Laterally Loaded Piles”, *Proceedings*, Second Structural Division Conference on Electronic Computation, American Society of Civil Engineers, Pittsburgh, Pennsylvania, pp. 657, 1960.
- Reese, L.C. and S.-T. Wang, *Documentation of Computer Program Group 4.0*, Ensoft, Inc., Austin, Texas, 1996.

9. Electrical System

The electrical system of a grid connected wind turbine includes all components for converting mechanical power into electric power as well as the auxiliary electric aggregates (the yaw system, the cooling system, the ventilation system), the control and supervisory systems. Figure 9-1 illustrates the main components of the electrical system of a grid connected wind turbine.

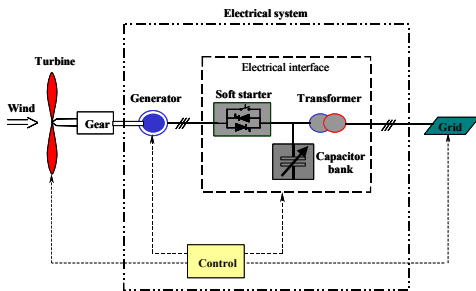


Figure 9-1. Block diagram of wind turbine connected to a grid with an electrical interface.

The scheme comprises the wind turbine rotor, linked via a gearbox to a generator, which through an electrical interface is connected to the grid. A control system is necessary to ensure proper operation of the wind turbine under all conditions. Different configurations of the electrical interface exist. A typical solution contains a softstarter, a capacitor bank and a transformer. The transformer transforms the generator voltage to a higher voltage of the grid. Another popular solution involves a frequency converter instead of the above-mentioned softstarter and capacitor bank.

In the following sections, focus will first be on the most relevant electrical components of a wind turbine: generator, softstarter, capacitorbank and frequency converter. Later on, the most utilised generator configurations and control strategies for wind turbines will be presented. Issues related to power quality, grid connection and

integration of wind turbines are also discussed.

9.1 Electrical components

This section does not seek to provide a general introduction to electrical system technology. Standard literature on the subject is available for this purpose (Heier S., 1998), (Mohan N. et al., 1989). Thus, the following sections will mainly summarise some of the essential properties of the most important types of each electrical component in a wind turbine.

9.1.1 Generators

Insofar as concerns generation of electric power, a wind turbine can, basically, be equipped with any type of generator. However, two specific types of three-phase generators constitute the most frequently used generators in the industry: induction (asynchronous) generators and synchronous generators. Today, the demand for gridcompatible electric current can be met by connecting frequency converters, even if the generator supplies alternating current of variable frequency or direct current.

Induction generator

The most common type of generator used in wind turbines is the induction generator.

In the induction generator, an electric field is induced between the rotor and the rotating stator field by a relative motion (slip), which causes a current in the rotor windings. The interaction of the associated magnetic field of the rotor with the stator field results in the torque acting on the rotor.

The rotor of an induction generator can be designed as a so-called short-circuit rotor (squirrel-cage rotor) or as a wound rotor (Heier S., 1998). The windings of the wound rotor can be externally connected through

slip rings. In this way, the electrical characteristics of the rotor can be controlled from the outside by means of electric equipment.

The induction generator has several advantages such as robustness and mechanical simplicity. Moreover, as it is produced in large series, it can be purchased at a relatively low price.

The major disadvantage is that the stator is dependent on a reactive magnetising current. As the asynchronous generator does not contain any permanent magnets and is not separately excited, it is bound to obtain its exciting current from somewhere else - and thus to consume reactive power. The reactive power may be supplied by the grid or e.g. by the capacitor bank. Its magnetic field is only established when the generator is connected to the grid.

The synchronous speed of the rotating stator field of an induction generator depends on the grid frequency and on the number of pole pairs:

$$n_s = 60 \cdot \frac{f}{p}$$

- f grid frequency in Hz
- p number of pole pairs
- n_s synchronous rotational speed in rpm.

The torque of the induction generator – see Figure 9-2, is a function of the slip s , which is defined as:

$$s = \frac{n_s - n_r}{n_s}$$

n_r rotational speed of the rotor in rpm

The slip is expressed in percentages. It is negative for a generator ($n_r > n_s$) and

positive for a motor ($n_r < n_s$). If the slip is zero (the generator is in synchronism), the generator is running idle (it does not produce torque). If the slip is 1, the rotor is blocked. The torque shows a maximum, the so-called pull-out torque T_p , at the rotational speed n_p , as shown in Figure 9-2.

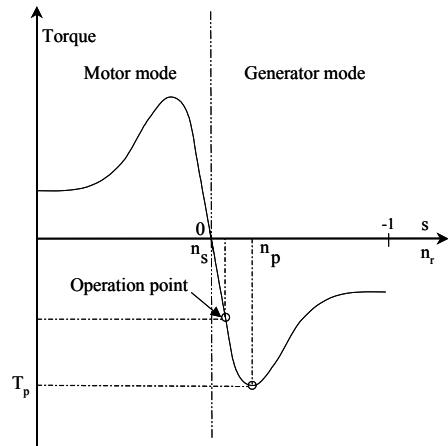


Figure 9-2. Torque characteristics of an induction motor/generator.

Synchronous generator

Another type of generator used in wind turbines is the synchronous generator. It has a wound rotor, which is excited with direct current via slip rings, thus constituting the basic difference between this generator and the above-mentioned induction generator. The rotor winding, through which direct current flows, generates the exciter field, which rotates with synchronous speed. The speed of the synchronous generator is determined by the frequency of the rotating field and of the number of pole pairs of the rotor.

The synchronous generator has one clear advantage compared with the induction generator: it does not need a reactive magnetising current. However, compared to the induction generator it is much more expensive and mechanically more complicated.

9.1.2 Softstarter

The generator should be gradually connected to the grid in order to limit the in-rush current. Without a softstarter, the in-rush current can be up to 7-8 times the rated current, which can cause severe voltage disturbance in the grid. The use of a softstarter, which contains thyristors, can cause a limitation of the in-rush current.

A thyristor is a semiconductor, which has two states: a blocking and a conducting state (Mohan N. et al., 1989). The transition from blocking to conducting state is initiated by supplying the gate with a power impulse. This is called “firing of the thyristor”. The thyristor remains in the conducting state as long as the current flows in the positive direction. As can be seen from Figure 9-3, the function of the softstarter is to slowly “open up” for the voltage and thereby the current by adjusting the firing angle θ .

In this way, the generator is gradually connected to the grid.

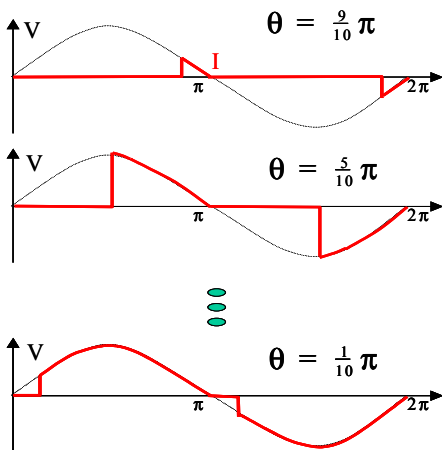


Figure 9-3. Voltage waveforms for a softstarter during start-up.

After in-rush, the thyristors are bypassed in order to avoid conducting losses. The effects of the softstarter are thus:

- reduction of the peak current at in-rush.
- reduction of the voltage dips in the grid at in-rush.
- reduction of the transient torque in the generator and in the gearbox at in-rush.

9.1.3 Capacitor bank

As mentioned, an induction generator is a reactive power consumer while generating active power. The active P and reactive Q electrical power are expressed as:

$$P = \sqrt{3} U_{\text{eff}} I_{\text{eff}} \cos \phi \quad [kW]$$

$$Q = \sqrt{3} U_{\text{eff}} I_{\text{eff}} \sin \phi \quad [kVAr]$$

U_{eff} r.m.s. line-to-line voltage
 I_{eff} line current
 $\cos \phi$ power factor.

Assuming a perfect sinusoidal waveform, the r.m.s. voltage and current can be expressed in terms of the maximum voltage and the maximum current as follows

$$U_{\text{eff}} = \frac{U_{\text{max}}}{\sqrt{2}} \quad \text{and} \quad I_{\text{eff}} = \frac{I_{\text{max}}}{\sqrt{2}}$$

The maximum voltage U_{max} and the maximum current I_{max} are defined as the peak line-to-line voltage and the peak line current, respectively.

The amount of reactive power for the generator varies depending on the wind conditions. This means that if the wind speed is high, the wind turbine can produce more active power, but only if the generator gets more reactive power. Without any electrical components to supply the reactive power, the reactive power for the generator must be taken directly from the grid. Reactive power supplied by the grid causes

additional transmission losses and can, in some situations, make the grid unstable. To avoid this, a capacitor bank can be used between the generator and grid – see Figure 9-4. The capacitor bank is connected to the wind turbine immediately after the generator is coupled to the grid.

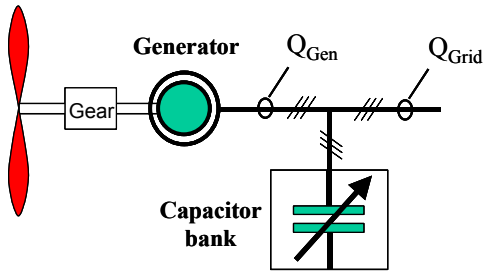


Figure 9-4. Capacitor bank coupled to the wind turbine to compensate the reactive power.

The idea of the capacitor bank is thus to supply locally with reactive power $\sum_i Q_{C_i}$ in such a way that the reactive power taken from the grid Q_{Grid} is minimized. Thus, as the extracted current from the grid decreases, the losses in the grid also decrease. Figure 9-5 illustrates the reactive power consumption Q_{Gen} of the induction generator and how the use of a capacitor bank minimizes the absorbed reactive power from the grid Q_{Grid} .

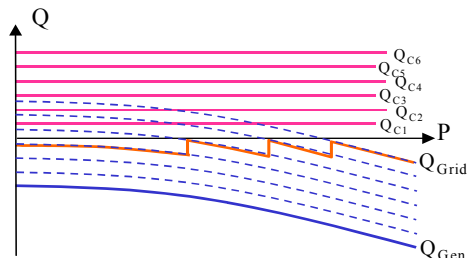


Figure 9-5. Reactive power as a function of active power. Reactive power compensation using a capacitor bank.

There is both a no-load compensation and a full compensation. Whereas, the no-load compensation is only effected when active

power is zero, full compensation is a dynamic compensation, where a certain number of capacitors are connected or disconnected continuously, depending on the varying reactive power demand of the generator.

By ensuring a power factor close to 1, the effects of a capacitor bank are:

- improvement of voltage stability
- reduction of network losses

9.1.4 Frequency converter

The frequency converter, located especially in modern wind turbines, is a power electronic device which facilitates interconnection of two electrical systems with independent frequencies (Mohan N. et al., 1989).

Usually, a modern converter contains IGBT (Insulated Gate Bipolar Transistors) based power devices, which are characterised by a high switching frequency of up to 10 kHz. A switching frequency of 10 kHz is the limit for acceptable switching losses.

Figure 9-6 illustrates two typical basic converter structures: a current source converter and a voltage source converter. The latter is today used in wind turbines (Heier S., 1998).

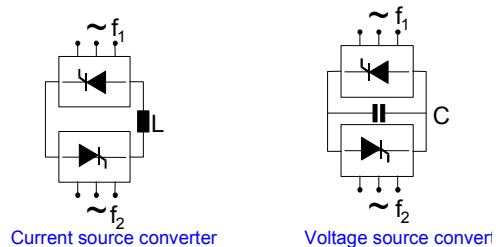


Figure 9-6. Basic power converter structures for frequency converter.

Frequency converters will become more and more significant in future control of wind

turbines. Their most important properties and implications are highlighted in the following:

1. Controllable frequency – is the property of the frequency converter which has the unique possibility to connect a variable speed wind turbine to the grid, thereby allowing the generator frequency to differ from grid frequency. Some of the implications of the *controllable frequency property* are:
 - the rotor behaves as an energy storage (as the variations in wind speeds are absorbed by the rotor speed changes).
 - the loads on the gear and drive train can be reduced.
 - the power capture at low wind speed can be improved.
 - the acoustical noise emission can be reduced (as the wind turbines can have a low rotational speed at low wind speeds).
 - the frequency converter can replace the softstarter and the capacitor bank.
 - the frequency converter is a practical necessity for the gearless wind turbine.
2. Controllable reactive power – is another property of the frequency converter, which makes it possible to improve the power quality. Some of the implications of the *controllable reactive power property* are:
 - the voltage stability is improved.
 - the flicker level is reduced.
 - the frequency converter can replace the capacitor bank.
 - the frequency converter can be used as a local reactive power source.
3. Power plant characteristics – is an important property of the frequency converter because it provides the

possibility for wind farms to behave as active elements in the power system (Sørensen P. et al., 2000). A wind farm with power plant characteristics is able to:

- control the active/reactive power.
- influence positively the stability of the network.
- improve the power quality.

9.2 Wind turbine configurations

In this section the most commonly applied generator and power electronic configurations in wind turbines are presented. Further details can be found in (Hansen L.H. et al., 2001a).

Wind turbines can be divided into two main groups, i.e. fixed speed and variable speed wind turbines.

The fixed speed wind turbine, equipped with a generator connected directly to the grid, a softstarter and a capacitor bank, is the most common type of wind turbine. In order to increase power production, some of the fixed speed wind turbines are equipped with two speed generators instead of with one generator only.

The advantages of the fixed speed wind turbine are:

- simplicity.
- low price of the electrical system.

The disadvantages are:

- limited power quality control.
- mechanical stress on gear and drive train.

The variable speed wind turbine is today not as common as the fixed speed wind turbine. However an increasing number of turbines have variable speed rotors. Two general

configurations of variable speed wind turbines exist:

- 1) one where the generator stator is connected to the grid, while the rotor frequency is controlled. The speed can typically be varied within a limited range only.
- 2) one where the generator stator is connected to the grid through a frequency converter. The speed can be varied to an unlimited extent.

The advantages of variable speed wind turbines are:

- improved power quality.
- reduced mechanical stress.

The disadvantages are:

- losses in power electronics.
- price of frequency converter.

Two possible configurations exist for variable speed wind turbines with controlled rotor frequency (limited variable speed):

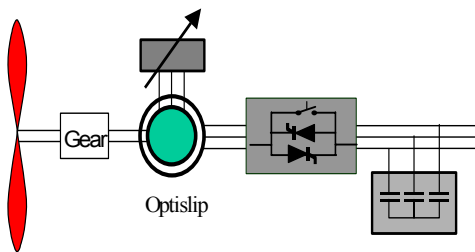


Figure 9-7: Schematics of a wind turbine with controllable rotor resistance.

1. *Induction generator with variable rotor resistance* – see Figure 9-7

A Danish manufacturer produces a wind turbine with an Optislip generator, where the slip can differ with up to 10%, by varying the resistance of the rotor.

2. *Double-fed induction generator with converter connected to the rotor circuit* – see Figure 9-8

This type of variable speed wind turbine is used by several large manufacturers. The rotor is connected to the grid through a frequency converter, which is not a full-scale power converter, since typically only a fraction (up to 70%) of the speed range will be utilised.

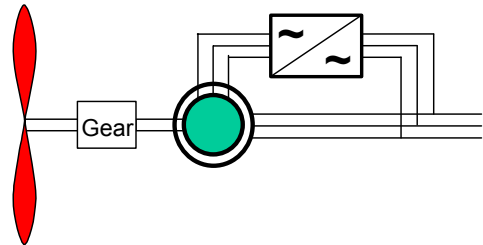


Figure 9-8. Schematics of a wind turbine equipped with a doubly-fed induction generator with a converter connected to the rotor circuit.

Full variable speed systems are equipped with a frequency converter. Two different modes of implementation with full variable speed can be found.

One is the classical configuration, where a cage rotor induction generator is connected to the grid through a full power frequency converter – see Figure 9-9. The range of the variable speed operation is, in principle, from zero to the maximum which can be handled by the wind turbine.

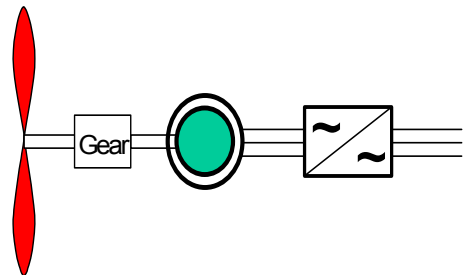


Figure 9-9. Schematics of a wind turbine with frequency control.

Another configuration with full variable speed involves the connection of a multipole synchronous machine to the grid by a

frequency converter. The frequency converter thus converts the variable frequency generator voltage into the grid frequency. A particular feature of this type of configuration is that it avoids the use of a gearbox – see Figure 9-10.

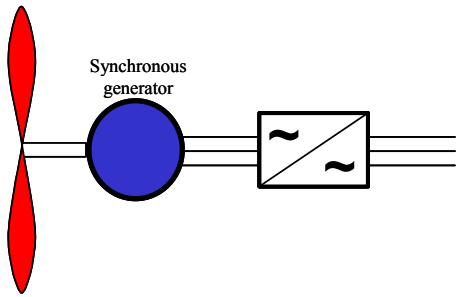


Figure 9-10. Schematics of a variable speed system with a synchronous generator.

9.3 Power quality and grid connection

The term “power quality of a wind turbine” describes the electrical performance of the turbine’s electricity generating system in its interaction with the grid. Methods which can be used to measure and quantify the power quality of wind turbines have earlier on been developed at a national level. However, the need for a common frame of reference across national borders has called for international standardisation work in the field.

A perfect power quality means that the voltage and current are continuous and sinusoidal, implying that they have a constant amplitude and frequency.

Grid connected wind turbines affect the power quality of the grid. The wind turbines and the grid are in continuous interaction, as illustrated in Figure 9-11.

Power quality depends on the interaction between the grid and wind turbines. IEC 61400-21 defines power quality

characteristics of the wind turbine, characteristics which can be used to characterise the influence of the wind turbines on the grid. Grid interference caused by wind turbines can be voltage distortions, frequency distortions and failure – see Figure 9-11.

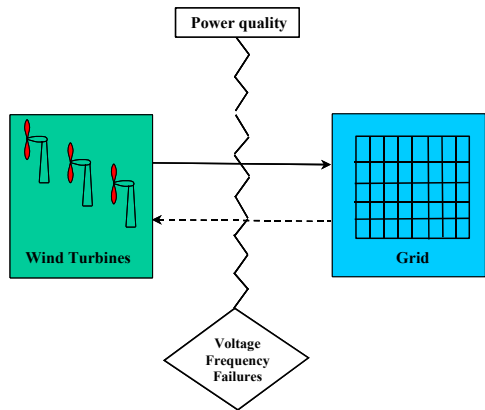


Figure 9-11. Power quality expressed in grid interference of the wind turbines.

The main interference of wind turbines with the grid is caused by voltage distortions. The frequency of large power systems is usually very stable, and therefore wind turbines do not typically influence the frequency. However, this is not the case for small autonomous grids, where wind turbines may cause frequency variations. Wind turbines do not normally cause any interruptions/failures on a high voltage grid. Wind turbines, as they are designed today, are disconnected from the grid by the protection system, if for example grid failures occur. This aspect can generate serious problems in the future. For example in Denmark where it is envisaged to cover 50% of the overall electricity consumption by wind power in 2030. Thus, grid failures can have severe consequences for the stability of the whole power system, if large wind farms are disconnected from the grid simultaneously. As a consequence hereof, research and development are today focused on making

wind farms more robust towards grid faults, for example by using power electronic devices.

Voltage distortions can be described in different time intervals:

- *steady-state voltage variations* are changes in the r.m.s. value of the voltage, occurring with a frequency less than 0.01 Hz.
- *flicker disturbances* are voltage fluctuations between 0.01-35 Hz that can cause visible variations in domestic lighting.
- *harmonics* are voltage fluctuations above 50 Hz, caused by the presence of power electronics (frequency converter).
- *transients* are random voltage fluctuations caused by e.g. connection of capacitor bank.

Power quality analysis is performed both for continuous and switching operation (Risø and DEFU, 1996). Continuous operation means the continuous operation of the wind turbine during permanent grid connection. Switching operation conditions are mainly switching operations, occurring only for short time intervals.

Continuous operation	Switching operation
Steady-state voltage variation	Connection of the generator: - flicker - voltage drop
Flicker	Connection of the capacitor bank: - transients
Harmonics	

Table 9-1. Power quality analysis in different operation modes.

In the case of continuous operation, the analysis is focused on slow voltage variations, on flicker and harmonic

distortions – see Table 9-1. In switching operation focus is on flicker and voltage drop generated at the connection of the generator, and on voltage changes generated at the connection of the capacitor bank.

Depending on the grid configuration and on the specific type of wind turbine used, different power quality problems may arise. For example, in the case of a fixed speed wind turbine, natural variations of the wind and the tower shadow will result in fluctuating power, which may cause flicker disturbances. In the case of a variable speed wind turbine, the presence of the frequency converter will inject harmonic currents into the grid. The frequency of a large power system is normally very stable. However, in the case of a weak or autonomous grid, where diesel engines are used, wind turbines may cause frequency fluctuations.

9.4 Electrical safety

The design of the electrical system for a wind turbine shall ensure minimal hazards to people and livestock as well as minimal potential damage to the wind turbine and the external electrical system during operation and periods of maintenance of the wind turbine under all normal and extreme conditions. It is usually required that the design of the electrical system shall take into account the fluctuating nature of the power generation from the wind turbine. It is usually also required that the electrical system shall include suitable devices that ensure protection against malfunctioning of both the wind turbine and the external electrical system which may lead to an unsafe condition.

A wind turbine should be equipped with an earthing system, both for conducting lightning currents and for earthing the electrical system of the turbine. Connection to the earthing network should be possible at

every location where electrical systems or equipment are located.

It is recommended that disconnection of the electrical system from all electric sources, as required in the case of maintenance or testing, shall be possible. Semiconductor devices should not be used as disconnection devices alone. Where lighting or other electrical systems are necessary for reasons of safety during maintenance, auxiliary circuits should be provided with separate disconnection devices, such that these circuits may remain energised while all other circuits are deenergized. It is recommended that any electrical system operating above 1000 V AC or 1500 V DC shall be able to be earthed for maintenance.

The IEC 61400-1 requires that all electrical components and systems shall meet the requirements set forth in IEC 60204-1, and compliance with the requirements of IEC 60364 for design of the electrical system of a wind turbine is also required.

It is recommended to make provisions to enable the wind turbine to be isolated from the public grid in a safe manner. This applies to normal situations, abnormal and/or faulty conditions as well as during maintenance and repair.

9.5 Wind farm integration

In the last few years the trend has moved from installations with single or small groups of wind turbines, to large wind farms with a capacity of hundreds of MW.

The increasing and concentrated penetration of wind energy makes the power system more and more dependent on and vulnerable to wind energy production. Future wind farms must be able to replace the present power stations, and thus to act as active controllable elements in the power system.

In other words, wind farms must develop power plant characteristics. The two system responsible utilities in Denmark, Eltra (Eltra, 2000) and Elkraft System have laid down requirements for the influence of wind farms on grid stability, power quality and on the control capabilities of wind farms.

Another consequence of the increased size of future wind farms is that large wind farms will be connected directly to the transmission level. Until now, wind turbines and wind farms have been connected to the distribution system, typically on 10/20 kV grid or on 50/60 kV grid. Consequently, main focus has been on the influence of wind farms on the power quality in the distribution system. In Denmark, this has been regulated by the Danish Utilities Research Institute's (DEFU) requirement for grid connection of wind turbines (DEFU KR111, 1998) to the distribution system. However, stricter requirements for large wind farms, connected directly to the transmission system (Eltra, 2000), are now issued by a.o. transmission system operators in Denmark. As mentioned before, national standards for power quality of wind turbines have been supplemented by the new standard IEC 61400-21 (IEC 61400-21, 2001) for measurement and assessment of the power quality of grid connected wind turbines.

An important requirement made by the system responsible is that in future, wind farm owners must provide models that can simulate the dynamic interaction between a given wind farm and a power system during transient grid fault events.

Such developed models will enable both wind farm investors and technical staff at the respective utility grid to undertake the necessary preliminary studies before connecting wind farms to the grid (Hansen A.D. et al., 2001), (Sørensen P. et al.,

2001a). Simulation of the wind farm interaction with the grid may thus provide quite valuable information and may even lower the overall grid connection costs. In addition, these models can be used to study control strategies for wind farms.

Large research projects have been initiated to analyse different control strategies of large wind farms. There are many control topologies, and they all have their particular advantages and disadvantages (Hansen L.H. et al., 2001b). One option is a decentralised control structure with an internal AC grid connected to the main grid, where each wind turbine has its own control system with its own frequency converter. Such a system has the advantage of ensuring that each wind turbine can work optimally with respect to its local wind conditions. Another option is a centralised control structure where, for example, the wind farm is connected to the grid via an HVDC connection. Here, the internal behaviour of wind turbines is separated from the grid behaviour, thus enabling the wind farm to become sufficiently robust to withstand possible failures on the grid. Another way to control wind farms is the combination of wind farms and energy storage systems, which makes it possible to buffer some of the energy.

REFERENCES

- DEFU KR111, *Connection of wind turbines to low and medium voltage networks*, 1998.
- Eltra, *Tilslutningsbetingelser for vindmølleparker tilsluttet transmissions-nettet*, TP98-328b, 2000.
- Hansen A.D., Sørensen P., Janosi L., & Bech J, *Wind farm modelling for power quality*, In_Denver , IECON ' 01, (2001).
- Hansen L.H., Helle L., Blaabjerg F., Ritchie E., Munk-Nielsen S., Bindner H., & Sørensen P, *Conceptual survey of generators and power electronics for wind turbines*, Risø-R-1205 (EN), 2001.
- Hansen L.H., Madsen P.H., Blaabjerg F., Christensen H.C., Lindhard U., & Eskildsen K, *Generators and Power Electronics Technology for Wind Turbines*, In , IECON ' 01, Denver, 2001.
- Heier S, *Grid Integration of Wind Energy Conversion Systems*, 1998.
- IEC 61400-21, Final Draft International Standard - Wind turbine generator systems - Part 21: *Measurement and assessment of power quality characteristics of grid connected wind turbines*, 2001.
- Mohan N., Undeland T.M., & Robbins W.P., *Power Electronics: converters, applications and design*, 1989.
- Risø and DEFU. *Power quality and grid connection of wind turbines - summary report*. Risø-R-853 (Summ.)(EN), 1996.
- Sørensen P., Hansen A.D., Janosi L., Bech J., & Bak-Jensen B., *Simulation of interaction between wind farm and power system*, Risø-R-1281, Risø National Laboratory, 2001.
- Sørensen P., Unnikrishnan A.K., & Sajan A.M. *Wind farms connected to weak grids in India*, Wind Energy, 4. 2001.
- Sørensen P., Bak-Jensen B., Kristiansen? J., Hansen A.D., Janosi L., & Bech J., *Power plant characteristics of wind farms*, In Kassel, 2000.

10. Manuals

10.1 User manual

The user manual and/or operating instructions are issued to assist the wind turbine operator. Normally, the following information will be included:

- general description of the wind turbine
- personal safety instructions
- service/maintenance schedule
- instructions for use of the controller, including settings and list describing alarms
- trouble shooting, incl. instructions for dangerous events like runaway and fire
- description of locking devices for rotor, yaw and pitch system
- list of grease, lubrication oil, hydraulic oil, etc.
- list defining bolt pretension for main connections

In the EU, minimum requirements to the manual are laid down in the Machinery Directive, see European Union (1998).

10.2 Service and maintenance manual

This manual shall assist qualified engineers in their work and will normally include the same information as that which is given in the user manual in addition to specific instructions for the service and maintenance work. The level of detail depends on the education of the service staff. The manual will normally prescribe in detail how to maintain:

- hydraulic systems
- main gear
- yaw system
- blade pitch or tip brake mechanism
- sensors
- lubrication and cooling systems

- inspection for corrosion, wear and cracks, including remedial action
- list of spare parts
- trouble shooting instructions
- relevant drawings, diagrams, specifications and descriptions

10.3 Installation manual

The installation manual will describe the various installation activities as well as the limitation for these with respect to, for example, wind speed. The activities should be described specifying, inter alia:

- general description of the wind turbine
- personal safety instructions
- transportation and handling
- procedures for bolt connections, including pretension procedures
- tests and checks for various parts and systems of the turbine
- commissioning test, normally including start, stop, yawing and test of protection system

REFERENCE

The European Union, *Machinery Directive*, European Directive No. 98/37/EC, 1998.

11. Tests and Measurements

Measurements on wind turbines are made to verify power performance, design loads and function of control and protection systems as well as other types of operational behaviour under field conditions.

In most cases, the wind turbine parameters must be correlated with the wind conditions at the site and for that purpose, a meteorology mast is erected close to the wind turbine. In some cases, measurements can be made without correlation with the wind speed on the site. A meteorology mast, which is to measure the given wind speed on the site, should not be erected too close to the wind turbine. This is due to the fact that the wind speed sensors are influenced by the wind turbine rotor. Neither should the mast be erected too far from the wind turbine, in which case the correlation is decreased substantially. In a flat and non-complex terrain where the topography causes insignificant flow distortion, a good correlation with the wind velocity at the wind turbine position is found. In a complex terrain, the correlation between the wind at the mast and the wind at the wind turbine position is poorer. In such cases, a site calibration must be made. Meanwhile, a

meteorology mast is erected at the position of the wind turbine, and correction factors are found from different directions of the measurement sector.

11.1 Power performance measurements

The purpose of power performance measurements is mostly economic as the performance determines the overall economics of the wind turbine installation. Therefore, power performance measurements are part of contractual matters between wind turbine manufacturers and developers.

When power performance is measured, the smallest uncertainty of the measurement is found in flat and non-complex terrain. In most power performance measurement procedures, IEC, Danish Energy Agency and MEASNET, requirements to the terrain have been set up, so-called “ideal site”, that do not require a site calibration. If these requirements are not met, a site calibration shall be made. A site calibration can be made even in flat terrain to reduce uncertainty of the wind speed measurement, which shall otherwise be stated as 2-3% due

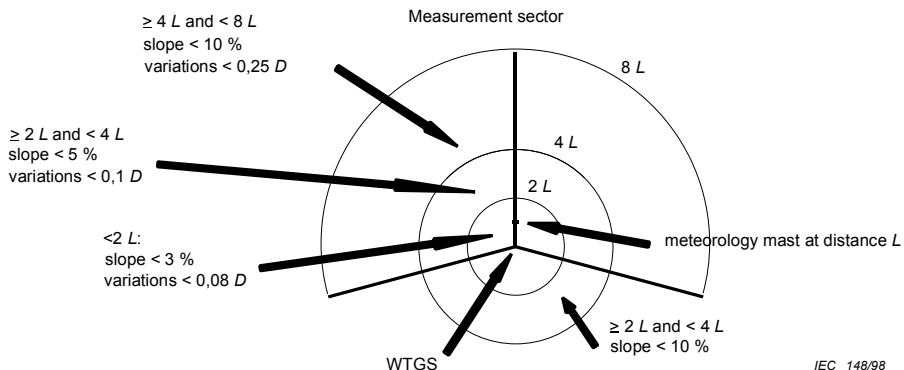


Figure 11-1. Requirements in IEC 61400-12 to topographical variations for an “ideal site”, top view.

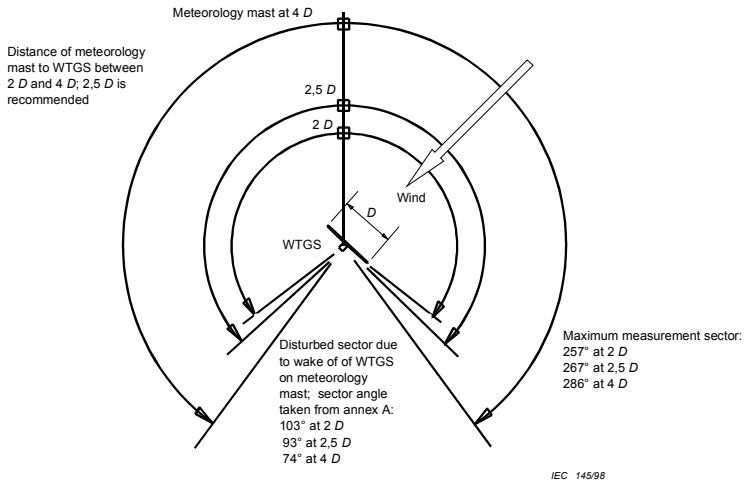


Figure 11-2. Requirements in IEC 61400-12 as to distance of the meteorological mast and maximum allowed measurement sectors.

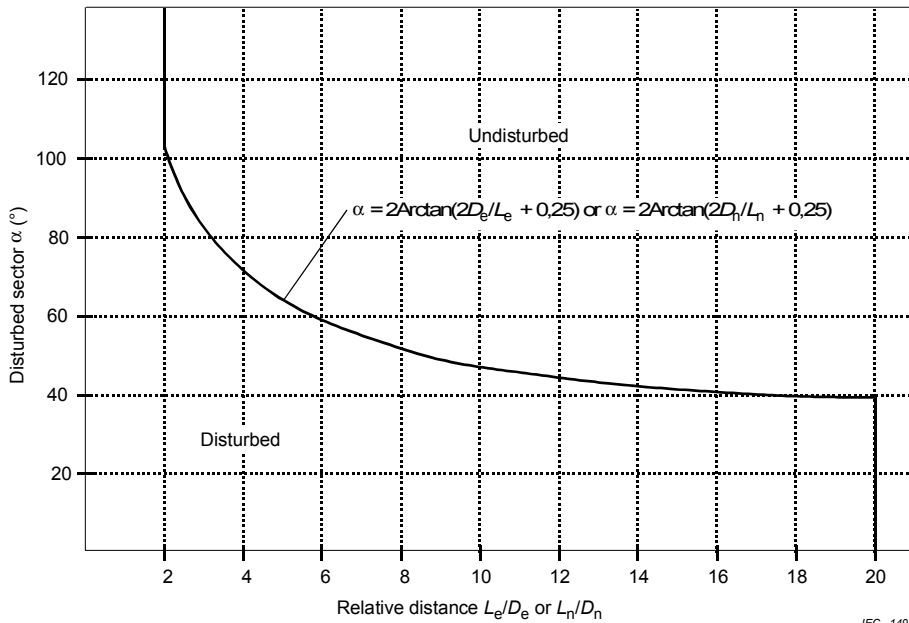


Figure 11-3. Requirements in IEC 61400-12 on the exclusion of particular sectors due to wakes of neighbouring and operating wind turbines and significant obstacles.

to arbitrary site effects, e.g. small topographic variations, wake effects from distant wind turbines, obstacles like trees and houses, roughness changes due to crop changes and climatologic changes over the measurement period.

The measured wind speed in power performance measurements shall be defined as the horizontal wind speed. This means that the vertical turbulence component shall not be taken into account, and when there is inclined flow as in complex terrain, it is only the average horizontal component that is considered. This definition of measured wind speed ensures a reasonable degree of consistency of calculated annual energy production from the power curve measurement in flat and complex terrains. If a vector defined wind speed is used (the vertical wind speed component is included), the measured annual energy production at inclined flow in complex terrain is substantially lower.

Application of a cup anemometer wind speed sensor is required. This constitutes the most accurate wind speed sensor for average wind speed measurements. Some characteristics of the sensors are very important in terms of keeping uncertainties low in measurements: cosine angular characteristics, low distance constant, low maximum overspeeding level and low friction in bearings.

The wind speed, wind direction, air temperature, air pressure, active power of the wind turbine and the status of the wind turbine shall always be measured. The power performance shall be normalised to a specific air density. In Denmark, this air density is 1.225 kg/m^3 . At higher elevation, the specific air density is based on the local average air density.

In addition, for many purposes it is advantageous to measure precipitation, atmospheric stability, wind shear and other wind turbine parameters (rotational speed, pitch angle) to determine more specific behaviour of performance under such parametric variations.

The measurement period should be long enough to include variations of atmospheric conditions like varying stability and front passages.

The power performance measurement procedures should be followed in detail, and specific concern should be paid to the calculations of uncertainty, which should be minimised in all aspects of the measurement, specifically the wind speed measurement.

11.2 Load measurements

Load measurements are made to verify design loads or to investigate loads under specific conditions. Design loads are required to be verified by certification institutes. It is not possible to verify all loads. Certain ranges of external conditions can be covered by field measurements, but extreme conditions cannot be reached. The verification of loads is therefore limited to verification of a number of specific measured load cases. These load cases are used to verify load calculation models, and in this way to extrapolate the verification to extreme design loads.

Loads are measured on blades, shaft, nacelle components, tower and foundation. In principle, the loads being developed in the blade can be followed through the construction. Strain gauges are mostly used in full and half bridges. The loads are measured over 10-minute periods, and equivalent load spectra are generated through rain-flow counting procedures.

Load measurement procedures are found in the recommendations for compliance with the Technical Criteria, July 1992, and in IEC 61400-13.

11.3 Test of control and protection system

The purpose of these tests is to verify that the wind turbine functions as predicted and to verify functionality and efficiency of protection systems. Procedures for function and safety tests are described in recommendations for basic tests by the Danish Energy Agency. The most important part of these tests is the verification of the overspeed protection systems e.g. aerodynamic and mechanical brake systems.

11.4 Power quality measurement

Measurement of power quality i.e. the effects that the wind turbine has on the public electricity network, is standardised in IEC 61400-21. This standard describes measurement procedures for quantifying the power quality of a grid connected wind turbine and the procedures for assessing compliance with power quality requirements. See also section 9.3 of this book.

11.5 Blade testing

Reference is made to IEC 61400-23 and Section 5.1.9 of this book.

11.6 Noise measurements

The objective of noise measurements is to verify that the wind turbine meets the requirements of authorities to noise regulation. Measurement procedures for noise measurements are described in recommendations for basic tests by the Danish Energy Agency. IEC has made a

more detailed measurement procedure, IEC 61400-11.

REFERENCES

Danish Energy Agency, *Recommendation for measuring the power curves of a wind turbine for usage in type approvals of wind turbines in relation to Technical Criteria*, September 18, 1992.

www.vindmoellegodkendelse.dk

Danish Energy Agency, *Requirements to Cup Anemometers Applied for Power Curve Measurements under the Danish Approval Scheme for Wind Turbines*, January 14, 2002, www.vindmoellegodkendelse.dk

Danish Energy Agency, *Recommendation for Basic Tests, According to the Technical Criteria for Type Approval and Certification of Wind Turbines in Denmark*, January 1997.

Danish Energy Agency, *Recommendations for fulfilling requirements in Technical Criteria*, July 1, 1992.

IEC 61400-11, *Wind turbine generator systems, part 11: Acoustic noise measurement techniques*, 1998

IEC 61400-12 *Wind turbine generator systems, part 12: Wind turbine power performance testing*, 1998

IEC 61400-13, *Wind turbine generator systems, part 13: Measurement of mechanical loads*, 1. ed, 2001

IEC 61400-21, *Wind turbine generator systems - Part 21: Measurement and assessment of power quality characteristics of grid connected wind turbines*, Ed. 1.0, 2001

IEC 61400-23, *Wind turbine generator systems - Part 23: Full-scale structural testing of rotor blades*, First edition, 2001-04

MEASNET *Power Performance Measurement Procedure*, version 3, November 2000.

A. Bolt Connections

A.1 Bolt standardization

Bolts and nuts are highly standardized machine elements. The following standards apply:

- ISO 261 ISO general-purpose metric screw threads- General plan
- ISO 262 ISO general-purpose metric screw threads–Selected sizes for screws, bolts and nuts
- ISO 724 ISO general-purpose metric screw threads
- ISO 3506 Corrosion-resistant stainless-steel fasteners-Specifications
- ISO 4762, Allen screws
- ISO 4014; 4017, Cap screws
- ISO 4016; 4018, Bolt with nut
- ISO 4032, 4034, Nuts
- ISO 1896, Tight-fitting bolts
- ISO 7089, 7090, Tempered washers 200 HV
- ISO 7091, Washers 100 HV

A.2 Strength

Bolt strength and mechanical properties are standardised according to ISO898/1-2. The different qualities are characterised, in terms of quality classes, by two numbers separated by a dot. The first number is 1/100 of the minimum ultimate strength measured in MPa. The product of the two numbers is 1/10 of the minimum yield strength, also measured in MPa.

For example, bolt quality 10.9 has a minimum ultimate strength of $100 \cdot 10 = 1000$ MPa and a minimum yield strength of $10 \cdot 10 \cdot 9 = 900$ MPa.

For pre-stressed bolts, only qualities 8.8, 10.9 and 12.9 are relevant. Caution should be exercised when using quality 12.9 because of the risk of brittle failure

associated with this quality, especially at low temperatures.

Stainless steel bolts are standardised according to ISO 3506. Bolts are made from three different types of stainless steel namely:

- austenitic steel
- ferritic steel
- martensitic steel

Normally the austenitic type is used. The quality designation is then A1, A2 and A4 corresponding the strength classes 50, 70 and 80. The numbers are 1/10 of the ultimate strength. The yield strength is correspondingly 210, 450 and 600 MPa.

A.3 Impact strength

In general the elongation at fracture and impact strength are inversely proportional to the strength of the steel. As an example, the impact strength of a grade 12.9 bolt is only the half of that of an 8.8 bolt. For pure static loads this is of no major importance, but in case of dynamic and transient loads this features have to be carefully considered especially at low ambient temperatures. In general the magnitude for impact strength shall at least reach 27 Joule at the lowest temperature for operation.

A.4 Surface treatment

Different surface treatments are available to achieve specific properties such as corrosion protection, and low friction.

The most commonly used bolts are black (no surface treatment) and hot dip galvanized bolts. Hot dip galvanized bolts offers an excellent protection against corrosion in non acidic atmospheres. The bolts are first treated in a grease solvent and then in a pickling agent and finally in a bath

with melted zinc at 540° in few minutes forming a zinc layer of approximate 50-60µm. The actual lifetime for hot dip galvanized bolts are dependent on the environmental conditions (pollution in the atmosphere).

Environment	Average lifetime [years]
Open agricultural areas	45
Small towns	30
Large towns	12
Heavy polluted industrial areas	5
Coast-near areas	30

Table A-1. Average lifetime for hot dip galvanized bolts. (Arvid Nilsson).

For materials with hardness > HV 300, hot dip galvanizing implies a risk of hydrogen embrittlement. Consequently such materials shall be heat treated at approx. 200° for 2-4 hours. In general it is not recommended to hot dip galvanize bolt at higher grade than 8.8. Grade 10.9 may be hot dip galvanized with great caution. It is not possible to hot dip galvanize materials with higher strength because of temper effects and zinc depositions in the grain boundaries causing micro cracks in the structure. The consequences in such cases may be catastrophic.

A.5 S-N curves

For design of bolt connections, the single most important issue is to consider the proper choice of an S-N curve for fatigue predictions. This S-N curve is much dependent on how the bolt is manufactured. Several possibilities exist for this manufacturing, including:

- thread form-rolled and then heat-treated
- material of near nominal diameter fully heat-treated before form-rolling of thread

- for special bolts threads may be cut on a lathe or by hand cutting tools (dies).

A widely used approach for lifetime prediction and strength assessment is the German guideline VDI-2230. VDI distinguishes between thread form-rolled before heat-treated and thread form-rolled after heat-treated.

In the latter case the thread rolling process introduces compression stresses in the surface, causing better fatigue properties but also dependence of the mean-stress in the bolt. For finally heat-treated bolts the following equation will apply

$$\sigma_{ASV} = 0.85 \cdot (150/d + 45)$$

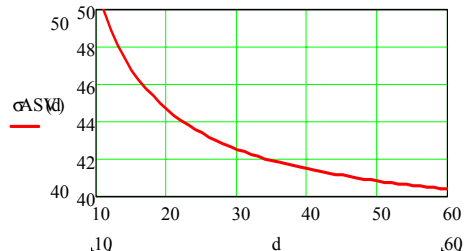


Figure A-1. Fatigue strength as function of bolt diameter for finally heat-treated bolts (VDI 2230) (stress amplitudes).

For finally thread form-rolled bolts the following equation will apply

$$\sigma_{ASG} = (2 - F_{Sm}/F_{0.2}) \cdot \sigma_{ASV}$$

$$F_{Sm} = (F_{Sao} + F_{Sau})/2 + F_{Mzul}$$

Valid for: $0.3 < F_{Sm}/F_{0.2} < 1$

$$F_{Sm}/F_{0.2} = R_b$$

- F_{Sao} higher force from external load
- F_{Sau} lower force from external load
- F_{Mzul} allowable pre-tensional force

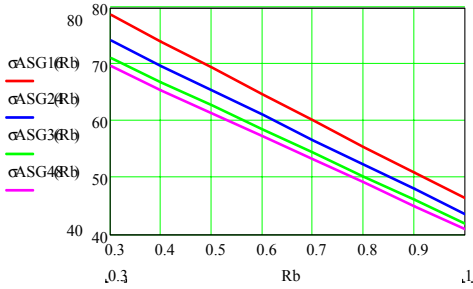


Figure A-2. Fatigue strength of bolts M16 (red), M24 (blue), M36 (green) and M48 (brown) as a function of mean stress ratio F_{Sm}/F_{02} with bolt diameter as parameter for finally form-rolled threads (stress amplitudes).

These values are valid for grade 8.8-12.9 bolts subjected to more than $2 \cdot 10^6$ cycles and correspond to 99% survival probability.

For a number of cycles lower than $2 \cdot 10^6$ the corresponding stress to failure can be found from

$$\sigma_{AZSV} = \sigma_{ASV} \cdot (N_D/N_Z)^{1/3}$$

$$\sigma_{AZSG} = \sigma_{ASV} \cdot (N_D/N_Z)^{1/6}$$

For finally heat-treated and finally thread form-rolled $N_D = 2 \cdot 10^6$ and N_Z is the actual number of load cycles.

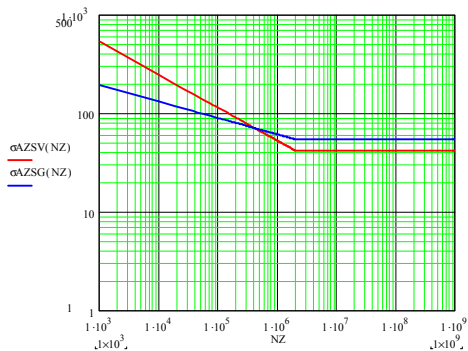


Figure A-3. S-N curve for finally heat-treated (red) and finally thread form-rolled (blue) (VDI 2230) (stress amplitudes).

These $S-N$ curves are intended for use at loads of constant amplitude and are not unconditionally valid for loads with varying amplitudes (defined as a load spectrum) (VDI 2230).

A.5.1 S-N curves in structural steel codes

S-N curves in the structural steel codes DS412 and Eurocode 3 are given for 97.7% survival probability in the following general form

$$\log_{10} N = \log_{10} a - m \cdot \log_{10} \Delta \sigma_f$$

where N is the number of cycles to failure at stress amplitude $\Delta \sigma_f$, and $\log_{10} a$ and m are the parameters of the $S-N$ curve. Depending on the material quality, heat-treatment and pre-stressing different $S-N$ curves can be established.

Standard bolts without controlled pre-stressing

Standard bolt means mass produced bolts according to ISO 898/1-2. For finally heat treated or cut bolts category *36 according to DS 412 / Eurocode 3 will apply (stress amplitudes):

$$N < 10^7: \quad \log_{10} a = 11.101, m = 3$$

$$N > 10^7: \quad \log_{10} a = 13.385, m = 5$$

$$N > 10^8: \quad \sigma_{fat} = 7.5 \text{ MPa}$$

For finally thread form-rolled bolts category *50 will apply (stress amplitude):

$$N < 10^7: \quad \log_{10} a = 11.551, m = 3$$

$$N > 10^7: \quad \log_{10} a = 14.585, m = 5$$

$$N > 10^8: \quad \sigma_{fat} = 11.5 \text{ MPa}$$

Standard bolts with controlled pre-stressing

For class 8.8 and 10.9 standard bolts with controlled pre-stressing category 71 according to DS 412/Eurocode 3 may be

applied based on the S-N curves reported in VDI 2230 (stress amplitudes).

$$N < 5 \cdot 10^6: \log_{10} a = 11.851, m = 3$$

$$N > 5 \cdot 10^6: \log_{10} a = 15.286, m = 5$$

$$N > 10^8: \sigma_{\text{fat}} = 14.5 \text{ MPa}$$

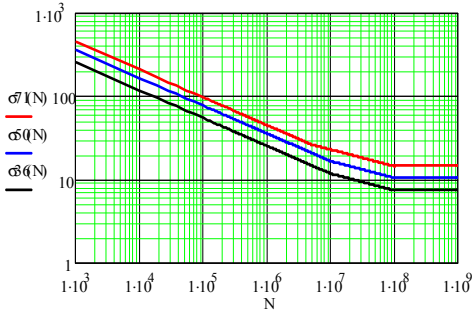


Figure A-4. S-N curve (stress amplitudes) for bolts without pre-stressing *36 (black) and *50 (blue) and with pre-stressing 71 (red) According DS412/Eurocode 3.

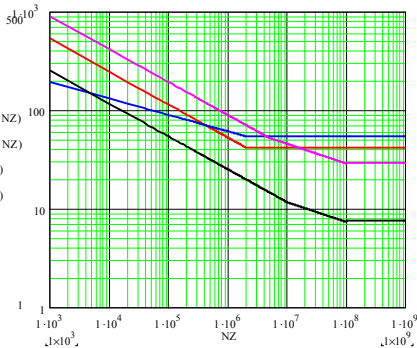


Figure A-5. Comparison of S-N curves (stress amplitudes) from VDI 2230 (red, blue) and category 71 and *36 from DS412/Eurocode 3 (violet, black). VDI curves are valid for M36 with a pre-tension of 0.7 times σ_{02}

These S-N curves will apply for M12 – M36 untreated (black) bolts. For hot dip galvanised bolts the figures will be 12-15% lower.

A.5.2 Allowable surface pressure

The maximum surface pressure between mating surfaces shall be evaluated. Be aware that the allowable surface pressure P_G is not proportional to the ultimate strength of the material. The maximum bolt force shall, of course, always be adjusted to the material with the lower P_G in the actual bolt connection. Figures for some commonly used materials are shown in Table A-2.

Material	Ultimate strength $R_{m,min}$ [MPa]	Allowable surface stress P_G [MPa]
St 37-2	340	490
St 50-2	470	710
St 52-3	510	760
34CrMo4	1000	870
34CrNiMo6	1200	1080
X5 CrNi 18 12	500	630
GG-25	250	900
GGG-40	400	700
GGG-50	500	900
GGG-60	600	1000
AlMgSi 1 F28	260	230

Table A-2. Allowable surface pressure P_G (VDI 2230)

A.6 Pretension

Depending on the bolt diameter and the required accuracy, several types of pre-stressing methods are in use. The most commonly used methods are:

- torque wrench
- turning angel method
- hydraulic tension device
- measurement of bolt extension

In this context only the two first methods will be mentioned since a large majority of bolts are pre-stressed with these methods. For selected bolt diameters, surface treatments and lubrication conditions, suitable pre-tension and pretension torque, can be taken from Table A-3 to A-6.

Bolt dia. [mm]	Area A_s [mm ²]	Bolt force at σ_{02} kN]		
		8.8	10.9	12.9
M12	84.3	54	76	91
M16	157	100	141	170
M20	245	157	220	265
M24	353	226	318	381
M27	459	294	413	496
M30	561	359	505	606
M33	694	444	625	750
M36	817	523	735	882
M42	976	624	878	1054

Table A-3. Bolt forces at σ_{02} . (Arvid Nilsson)

Bolt dia. [mm]	Area A_s [mm ²]	Pre-tension torque M_{V0} [Nm]		
		8.8	10.9	12.9
M12	84.3	81	114	136
M16	157	197	277	333
M20	245	385	541	649
M24	353	665	935	1120
M27	459	961	1350	1620
M30	561	1310	1840	2210
M33	694	1770	2480	2980
M36	817	2280	3210	3850
M42	976	3640	5110	6140

Table A-4. Pre-tension torque for oil lubricated black bolts. (Arvid Nilsson)

Bolt dia. [mm]	Area A_s [mm ²]	Pre-tension torque M_{V0} [Nm]		
		50	70	80
		M12	84.3	27
M16	157	65	140	187
M20	245	127	273	364
M24	353	220	472	629
M27	459	318	682	909
M30	561	434	930	1240
M33	694	585	1250	1670
M36	817	755	1620	2160

Table A-5. Pre-tension torque for stainless steel bolts lubricated with wax. (Arvid Nilsson)

The corresponding average pre-tension force F_{Sm} and pre-tension torque M_v for other

combinations of surface and lubrication can be calculated from:

$$F_{Sm} = F_{s0} \cdot G_F$$

$$M_v = M_{V0} \cdot C$$

Scatter on the average pre-tension:

$$\Delta F_S = F_{Sm} \pm S_F/F_{SM}$$

S_F is the scatter on average pre-tension force
 F_{SM} is the average pre-tension force.

For an M20 8.8 black oiled bolt the with $C = 1.0$ and $G_F = 0.71$ and $M_{V0} = 385\text{Nm}$ it results in a average pre-stress of 0.71 times σ_{02} . For the same bolt lubricated with wax the average pre-stress will arrive at 0.83 times σ_{02} with a corresponding pre-tension torque of 0.63 times M_{V0} .

Surface	Lubri- cation	S_F/F_{SM}	G_F	C
Black	Dry	0.29	0.62	0.96
	Oil	0.16	0.71	1.00
	MoS ₂	0.16	0.75	0.86
Hot dip galva- nised	Dry	0.29	0.55	1.17
	Oil	0.16	0.69	1.07
All	Wax	0.11	0.83	0.63
Stainless steel	Oil	0.29	0.55	0.84
	Wax	0.23	0.65	1.00

Table A-6. Modifying coefficients for pre-tension force G_F and pre-tension torque C as well as scatter at different surface treatments and lubrication conditions. (Arvid Nilsson)

For the turning angel method following guidelines (for grade 8.8) can be given in which d is the bolt diameter:

Total clamping length L_K	Total turning angel after “tight contact” [°]
$L_K < 2d$	120
$2d \leq L_K \leq 4d$	150
$4d \leq L_K \leq 6d$	180
$6d \leq L_K \leq 8d$	210
$8d \leq L_K \leq 10d$	240
$10d > L_K$	By test

Table A-7. Turning angel for mean pretension to 0.7 times the bolt tensile strength (grade 8.8 bolts) (ENV 1090-1).

For torque wrench and turning angle method, the rotating part must be provided with a hardened washer. This to prevent galling and the resulting increase in friction.

The pretension method should be calibrated regularly (ENV 1090-1). For torque wrench and the turning angel method this may be done by means of a bolt connection with the same characteristics as the actual connection, in which the bolt pre-tension force can be monitored. The Accuracy of the torque wrench should be within $\pm 5\%$. (ENV 1090-1). A more detailed method for calculation of pre-tension force and pretension torque can be taken from e.g. VDI 2230 Chapter 5.4.

A.6.1 Safety against loosening

Many damages on machine elements are caused by loose bolt joints. Consequently all essential bolt connections should be carefully evaluated. In principle, two mechanisms are responsible for this effect:

- loss of pre-tension caused by consolidations/deformation of the joint faces etc.
- loose turning of bolt or nut

Main influence factors to consider for loss of pretension:

- plastic deformations between bolt head/nut and contact face
- number of joint faces

- hardness of components
- surface roughness
- geometrical accuracy of joint faces
- accuracy of threads
- liners made from material with low stiffness
- clamping ratio L_K/d
- retightening sequence

Number of joint faces	Internal consolidation For L_K/d [μm]			
	1	2.5	5	10
2 - 3	1	1.5	2	2.5
4 - 5	0.75	1.0	1.25	1.5
6 - 7	0.5	0.7	0.8	1.1

Table A-8. Internal consolidation for each joint face. (Handbuch der Verschraubungstechnik)

Especially bolt connections where more factors are involved e.g. bolt connections with a small clamping ratio, many joint faces and hot dip galvanized surfaces may be critical. In such cases a number of retightening (3-4) after initial assembly are necessary as well as spot-checks at regular intervals.

Main influence factors to consider for loose turning of bolt or nut:

- transverse load
- vibrations
- possibility of transverse movements
- clearance between bolt shaft and hole
- clamping ratio L_K/d

In general pre-stressed bolt are self-locking if the conditions mentioned above are considered. For not pre-stressed bolts it is recommended to use nuts with a locking device or use a sort of locking compound.

A.7 Minimum depth of threaded holes

For standard bolts with nuts in same strength class no further calculation of strength of the

nut is required. For threaded holes in material with lower strength than bolt material it is however required to calculate the min. length of the threaded part of the hole / height of nut. The following equation will apply (VDI 2230)

$$m_{\text{eff,min}} = (R_m \cdot A_S \cdot P) / (C_1 \cdot C_3 \cdot \tau_{\text{BM}} (P/2 + (d - D_2) \tan 30)) \cdot \pi \cdot d + 0.8 \cdot P$$

$m_{\text{eff,min}}$	min. length of the threaded part of the hole / height of nut.
R_m	ultimate strength of bolt material
A_S	stress area of bolt
P	pitch of the threads
τ_{BM}	ultimate shear strength of nut material
d	outer diameter of bolt (nom. diameter)
D_2	flank diameter

$$C_1 = 3.8 \cdot s/d - (s/d)^2 - 2.61$$

$$C_1 = 1 \text{ for threaded holes}$$

$$C_3 = 0.728 + 1.769 \cdot R_S - 2.896 \cdot R_S^2 + 1.296 \cdot R_S^3$$

For $0.4 < R_S < 1$

$$C_3 = 0.897$$

$$\text{For } R_S \geq 1$$

$$R_S = (d \cdot (P/2 + (d - D_2) \cdot \tan 30)) \cdot R_{\text{mM}} / D_1 \cdot (P/2 + (d_2 - D_1) \cdot \tan 30) \cdot R_{\text{mS}}$$

s	width of jaw opening
D_1	core diameter nut
d_2	flank diameter bolt
R_{mM}	ultimate strength nut material
R_{mS}	ultimate strength bolt material

A.8 Bolt force analysis

The internal forces in a bolt connection are unique for this actual detail and dependent of a lot of details such as:

- stiffness of mating components
- stiffness of bolt

- clamping length
- E-modulus of material
- surface properties (roughness, surface treatment, alignment etc.)
- eccentricity
- level of force attack

To deal with every case is beyond the scope of this book. Information can be taken from the literature e.g. VDI 2230 and handbooks of machine elements. However the simple centric case is shown hereafter.

A.8.1 Stiffness of bolts

$$\delta_S = \delta_K + \delta_1 + \delta_2 + \dots + \delta_G + \delta_M$$

δ_S	total stiffness of the bolt
δ_K	stiffness of the bolt head
δ_1	stiffness of the unthreaded part of the bolt
δ_2	stiffness of the threaded part of the bolt
δ_G	stiffness of the threaded part of the bolt in the nut or threaded hole
δ_M	stiffness of the threaded part of the nut

For standardized bolts the following equations will apply

$$\delta_K = 0.4 \cdot d / E_S \cdot A_N$$

d	outer diameter of the bolt
E_S	elastic modulus of the bolt material
A_N	nominal area of the bolt

$$\delta_1 = l_i / E_S \cdot A_N$$

$$\delta_2 = l_i / E_S \cdot A_{d3}$$

l_i length of part with area A_N and A_{d3} respectively

A_{d3} core area

$$\delta_G = 0.5 \cdot d / E_S \cdot A_{d3}$$

$$\delta_M = 0.4 \cdot d / E_S \cdot A_N$$

A.8.2 Stiffness of the mating parts

For the mating parts the effective stiffness of the so called “replacement area” A_{ers} is depending of the amount of material around the bolt hole. The equation for the replacement area is defined for three cases:

For $d_w > D_A$:

$$A_{ers} = \pi / 4 \cdot (D_A^2 - d_h^2)$$

For $d_w \leq D_A \leq d_w + l_K$:

$$A_{ers} = \pi / 4 \cdot (d_w^2 - d_h^2) + \pi / 8 \cdot d_w (D_A - d_w) \cdot [(x + 1)^2 - 1]$$

where

$$x = ((l_K \cdot d_w) / D_A^2)^{1/3}$$

For $D_A \geq d_w + l_K$:

$$A_{ers} = A_{ers} \text{ for } D_A = d_w + l_K$$

- d_w diameter of rest area
- D_A width of the flange
- d_h diameter of the hole
- l_K clamping length

Stiffness of mating parts

$$\delta_p = l_K / A_{ers} \cdot E_p$$

E_p modulus of elasticity for the mating parts

A.8.3 Force triangle

The force ratio is defined as

$$\Phi_K = \delta_p / \delta_p + \delta_s$$

- F_V average pre-stressing force
- F_A applied external force
- F_{SA} additional force from the external applied force experienced by the bolt.
- F_{PA} reduction of the pre-stressing force F_V
- F_{KR} residual pre-stressing force
- δ_p stiffness of mating parts
- δ_s stiffness of bolt

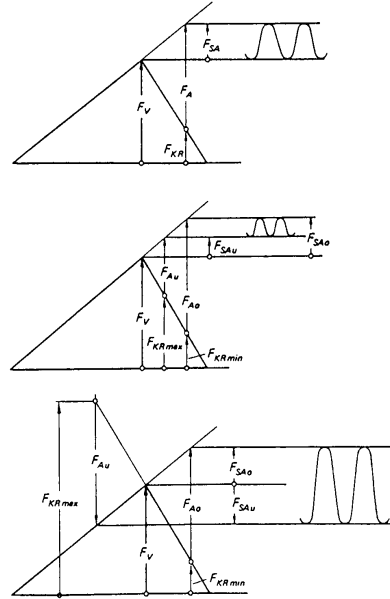


Figure A-6. Typical force-deformation triangles.

The additional bolt force from the external force on the bolt connection:

$$F_{SA} = \Phi_K \cdot F_A$$

Reduction in pre-stressing force:

$$F_{PA} = (1 - \Phi_K) \cdot F_A$$

This magnitude of the force ratio Φ_K is only valid if the force is applied at a level just below the head of the bolt. If the force is applied at another level in the connection the ratio Φ_K will be reduced due to an increased relative flexibility of the bolt as compared to the mating parts. The reduction factor n is defined as the ratio between the distance between force inlets l and the clamping length l_K , see Figure A-7.

$$n = l / l_K$$

$$\Phi_{K, red} = \Phi_K \cdot n$$

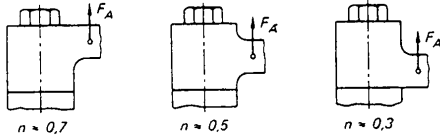


Figure A-7. Illustration of the force inlet ratio n .

Calculation of more complicated bolt connections e.g. eccentric loaded connections is beyond the scope of this book but more information's can be taken from e.g. VDI 2230.

A.9 Connections subjected to shear

Three categories of shear connections in structural steel constructions are defined in DS412/Eurocode 3:

- A. Bearing type
- B. Combination of bearing/friction type
- C. Friction type

Category A:

- it shall be shown that the actual shear force is lower than the shear resistance of the bolt material incl. the relevant partial safety factors
- it shall be shown that the actual shear force is lower than the bearing resistance of the hole inclusive the relevant partial safety factors.

If movements due to clearance in the holes are not allowed in the connection (e.g. caused by change in load direction) tight-fitted bolts should be used. In that case the tolerances for bolt/hole shall be h13/H11.

Pre-stressing of the bolt is not required, but the parts shall be drawn together in “snug-tight” condition. “Snug-tight” condition can generally be identified as that achievable by the effort of a man using a normal size spanner without extension.

For bolts with finally thread form-rolled following equation for shear capacity is defined in Eurocode 3

$$F_{V,R} = c_3 \cdot A \cdot f_{ub} / \gamma_m$$

$F_{V,R}$ design carrying capacity in shear

$c_3 = 0.6$ for quality class 4.6, 5.6, and 8.8 with section through thread.

$c_3 = 0.5$ for quality class 5.8, 6.8 and 10.9 with section through thread.

$c_3 = 0.6$ for all quality classes with section through shaft

A either the stress area of the thread or area of bolt shaft

f_{bu} characteristic ultimate strength for the bolt material

γ_m partial safety factor for material

For bolts with finally cut threads c_3 shall be multiplied by 0.85.

Bearing resistance:

$$F_{b,R} = 2.5 \cdot c_1 \cdot c_2 \cdot d \cdot t \cdot f_u / \gamma_m$$

c_1 and c_2 can be taken from Table A-9

d diameter of the bolt

t thickness of the plate

f_u characteristic ultimate strength for the plate material.

γ_m partial safety factor for material

$1.2d_0 \leq e_1 < 3.0d_0$	$c_1 = e_1 / 3d_0$	Low-est value
$2.2d_0 \leq p_1 < 3.75d_0$	$c_1 = p_1 / 3d_0 - 1/4$	
$1.2d_0 \leq e_2 < 1.5d_0$	$c_2 = e_2 / 0.9d_0 - 2/3$	value
$2.4d_0 \leq p_2 < 3.0d_0$	$c_2 = p_2 / 1.8d_0 - 2/3$	

Table A-9. Magnitude of reduction factors c_1 and c_2 .

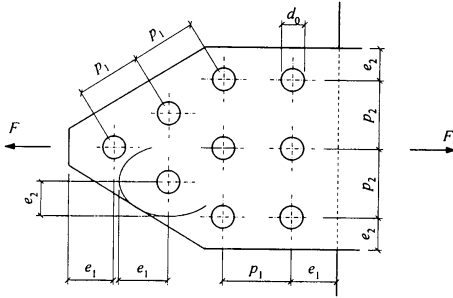


Figure A-8. Definition of hole distances.

	Min. distance	Optimal distance
e_1	$1.2d_0$	$3.0d_0$
p_1	$2.2d_0$	$3.75d_0$
e_2	$1.2d_0$	$1.5d_0$
p_2	$2.4d_0$	$3.0d_0$

Table A-10. Min. bolt distances.

Category B:

For this category the same as for Category A should normally be shown in the ultimate limit state, but also that the friction between the mating surfaces alone can adopt the shear force at serviceability limit state including the relevant partial safety factors.

Category C:

For this category it shall be shown that it is slip-resistant at the ultimate limit state including the relevant partial safety factors. Eurocode 3 defines the capacity as follows:

$$F_{S,R} = c_4 \cdot n \cdot \mu / \gamma_m \cdot F_p$$

$F_{S,R}$ design carrying capacity in friction

- $c_4 = 1$ for normal holes
- $c_4 = 0.85$ for oversize normal holes
- $c_4 = 0.7$ for slotted holes
- n number of friction surfaces
- μ characteristic friction coefficient
- γ_m partial safety factor for material
- F_p mean pre-stressing force, which is maximum $0.7 \cdot f_u$

Bolt diameter d	Normal holes $d_0 - d$	Oversize holes $d_0 - d$	Slotted holes $l - d$
12	1	3	4
14	1	4	4
16	2	4	6
20	2	4	6
22	2	4	6
24	2	6	8
≥ 27	3	8	10

Table A-11. Standard and oversize clearance for bolt holes of diameter d_0 .

Characteristic coefficients of friction for some commonly used surfaces may be taken from Table A-12 and A-13.

Class	Treatment
A	<ul style="list-style-type: none"> • Sand blasted • Sand blasted and sprayed with aluminium /zinc
B	Sand blasted and painted with zinc-silicate painting 50-80 μ
C	<ul style="list-style-type: none"> • Cleaning with steel brush or flame cleaning • Hot dip galvanized and sand stringed
D	Untreated surfaces

Table A-12. Categories of surfaces.

Class	Characteristic friction coefficient
A	0.50
B	0.40
C	0.30, however for hot dip galvanized without sand stringing 0.10
D	0.20

Table A-13. Characteristic friction coefficients of different surfaces.

A.10 Bolts subjected to tensile load

The load carrying capacity of bolts without pre-stressing can according to Eurocode 3 be calculated as

$$F_{t,R} = C \cdot f_{u,b} / \gamma_m \cdot A_S$$

$C = 0.9$ for finally thread form rolled bolts

$C = 0.85$ for finally heat treated bolts

$f_{u,b}$ ultimate strength of bolt material
 A_S stress area of the bolt

A.11 Bolts subjected to tensile load and shear

The following requirement is given in Eurocode 3 for bolts subjected to tensile load and shear:

$$(F_{v,S} / F_{v,R})^2 + (F_{t,S} / F_{t,R})^2 \leq 1$$

$F_{v,S}$ and $F_{t,S}$ actual shear load and tensile load respectively.

$F_{v,R}$ and $F_{t,R}$ load carrying capacity in shear and tension respectively.

A.12 Execution of bolt connections

The following apply, according to ENV 1090-1 and Eurocode 3.

Straightness of mating surfaces in compression

Must be < 0.5mm between an arbitrary located straight edge and the surface.

Washers

For connections in category A washers are not required.

For connections in category B and C with class 8.8 bolts tempered washers are required beneath the turning component.

For connections in category B and C with class 10.9 bolts tempered washers are required beneath both head and nut.

Pretension of bolts

For pre-tensioned bolts the mean pre-tension shall not exceed 0.7 times the characteristic ultimate bolt strength using the stress area of the bolt.

In mechanical engineering higher utilizing of the bolt-material are used commonly 80-100% of the characteristic σ_{02} value depending of the pretension method.

A.13 Codes and Standards

National codes for steel structures might be mandatory to use in some countries. This is often the case for bolt connections in those parts of the wind-turbine, which are defined by the authorities as building structures. The requirements in these national codes may deviate from the methods described above with respect to both design and installation.

REFERENCES

VDI 2230, *Systematische Berechnung hochbeanspruchter Schraubenverbindungen* October 2001

Zeit- und Daurfestigkeit von schwarzen und feurverzinkten hochfesten schrauben, Bauingenieur 61 (1986)

ENV 1090-1, *General rules and rules for buildings*.

ENV, Eurocode 3. *Design of steel structures*, 1993-1-1.

DS 412 *Steel Constructions*, 1998-07-02

RCSC, *Specification for Structural Joints using ASTM A325 or A490 Bolts*, 1985.

Bossard Handbuch der Verschraubungstechnik, Expert Verlag

B. Rules of Thumb

Rules of thumb and laws of similarity, or scaling laws, are of great importance to the designer during the initial phase of the development of a wind turbine. In particular, when adjustments or modifications are to be made on an existing turbine to adapt it to another environment, or eventually to redesign a turbine by means of scaling. It should be emphasized, however, that caution should be exercised when using highly simplified rules as the ones presented in this section. Different turbine designs will to a varying degree be in conformity with these rules.

B.1 Loads

B.1.1 Rotor loads

As an initial estimate of the blade loads it has been common to use static pressure of 300 N/m² over the entire rotor area.

For fatigue loads a pressure of 150 N/m² distributed on the three blades in 10⁷ cycles has commonly been used.

B.1.2 Fatigue loads

For the purpose of comparison it is normal to calculate an equivalent load for an equivalent number of cycles representing the same accumulated damage as the actual load spectre, see section 4.4.1. The equivalent load varies with the equivalent number of cycles

$$S_2 = S_1 \cdot \sqrt[m]{\frac{N_1}{N_2}}$$

in which S_i is the equivalent load corresponding to the equivalent number of cycles N_i .

B.2 Rotor

The following rules apply to stall regulated turbines under the assumption of a constant Reynolds number.

At constant rotational speed the rotor power P is proportional to the power coefficient C_p times the third power of the reciprocal of the tip speed ratio λ^3 as well as to the third power of the tip speed V_{tip} .

$$P = \frac{1}{2} \cdot \rho \cdot A \cdot V_{tip}^3 \cdot (\lambda^3 \cdot C_p)$$

$$\lambda = V/V_{tip}$$

ρ	Air density
A	Rotor area
V_{tip}	Rotor tip speed
V	Wind speed

Now, assuming that the variation of the power coefficient C_p versus the tip speed ratio is independent of the rotational speed for a given set of λ and C_p , the following rule applies:

$$\frac{P_1, (\lambda, C_p)_1}{P_2, (\lambda, C_p)_2} = \left(\frac{\omega_1}{\omega_2}\right)^3 = \left(\frac{n_1}{n_2}\right)^3$$

P	Rotor power
ω	Angular speed
n	Rotational speed

Further, assuming that the C_p curve is valid also for the variation of the rotor radius, the following rule is applicable:

$$\frac{P_1}{P_2} = \left(\frac{R_1}{R_2}\right)^5 \left(\frac{n_1}{n_2}\right)^3$$

P	Rotor power
R	Rotor radius
n	Rotational speed

B.3 Nacelle

B.3.1 Main shaft

A rough estimate of the main shaft diameter signifies that it amounts to 1 % of the rotor diameter.

B.4 Noise

Other things being equal, sound pressure will increase with the fifth power of the speed of the blade relative to the surrounding air.

REFERENCES

Petersen, H., *Simplified Laws of Similarity for Wind Turbine Rotors*, Risø-M-2432, Risø National Laboratory, 1984.

Krohn, S., *www.windpower.org*, Danish Wind Turbine Manufacturers Association, 2001

C. Fatigue Calculations

Fatigue failure takes place by the initiation and propagation of a crack until the crack becomes unstable and propagates fast, if not suddenly, to failure.

To ensure that a structure will fulfil its intended function, fatigue assessment, supported where appropriate by a detailed fatigue analysis, should be carried out for each type of structural detail, which is subjected to extensive dynamic loading. It should be noted that every welded joint and attachment, or other form of stress concentration, is potentially a source of fatigue cracking and should be individually considered. Fatigue design can be carried out by methods based on *S-N* curves from fatigue tests in the laboratory and/or methods based on fracture mechanics.

True fatigue life is a function of workmanship related to fabrication and corrosion protection. Therefore, it is important that the fabrication is performed according to good practice with acceptance criteria fulfilled as assumed for the prediction.

C.1 Stress ranges

Most components in wind turbines are subjected to stress ranges of great variation as illustrated in Figure C-1.

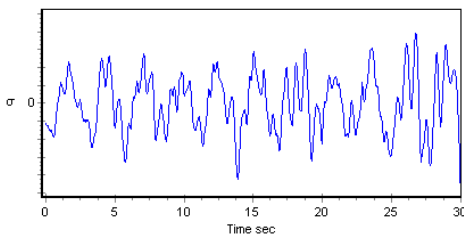


Figure C-1. Simulated time series of bending stress in the main shaft during production at 12 m/s.

This time series is extracted from an aeroelastic computer code as described in Section 4.3.

Through a cycle counting method, as described in Section 4.4.1, a stress range distribution, or design spectrum, illustrated in Figure C-2, is established. From this stress range distribution fatigue analysis is performed.

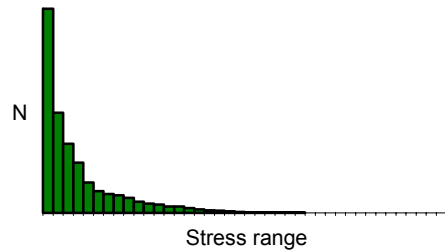


Figure C-2. Stress range distribution.

Great caution shall be exercised in that machine element design most often refers to stress amplitudes, whereas construction design most often refers to stress ranges. Mixing these terms will result in great errors.

C.2 Fracture mechanics

The fatigue life consists of three stages:

- crack initiation
- crack propagation
- final fracture

Since the final fracture happens rapidly, the fatigue life *N* can be expressed as

$$N = N_i + N_p$$

N_i initiation time

N_p propagation time

The initiation and the propagation time for steel components is often expressed by

formulas on the following form, where the latter is known as Paris' power law

$$N_i = B \cdot \left(\frac{\Delta K}{\sqrt{\rho}} \right)^n$$

$$\frac{da}{dN_p} = C \cdot \Delta K^m$$

- n empirical material constant
- B empirical material constant
- ρ dependant on geometry of stress concentration
- a crack length
- C empirical material constant
- m empirical material constant
- ΔK stress intensity range

The stress intensity range ΔK for cracks through a thickness is in its general form written

$$\Delta K = \Delta S \sqrt{\pi a} F$$

- ΔS far-field range of applied stress
- a instantaneous crack length
- F form factor for crack and surrounding geometry

As indicated, a fracture mechanics approach to fatigue requires explicit data of material behaviour and stress conditions that are often difficult to obtain.

A fracture mechanics analysis may be used to predict the number of load cycles in the crack propagation stage of an actual structure. The extent to which a fracture mechanics calculation can provide comparable information on fatigue life with that derived from $S-N$ curves will depend on the number of load cycles in the initiation stage. Frequently, the initiation stage for welded joints is almost negligible, because a fatigue crack will develop from existing

defects, which may often be located in areas with stress concentrations, see Section C.5. Fracture mechanics will mostly apply to calculation of the remaining life of detected cracks.

C.3 S-N curves

Fatigue strength data are usually reported as $S-N$ curves, also known as Wöhler curves. The $S-N$ curve is established through numerous sample tests with different load ranges, resulting in pairs of stress range S and a number of stress cycles N to failure at this stress range. The $S-N$ curve can usually be expressed as

$$N = K \cdot S^{-m}$$

On logarithmic form this results in a linear relationship between $\log S$ and $\log N$

$$\log N = \log K - m \log S$$

- K empirical material constant determining the level of the $S-N$ curve
- m Wöhler exponent, slope of $S-N$ curve

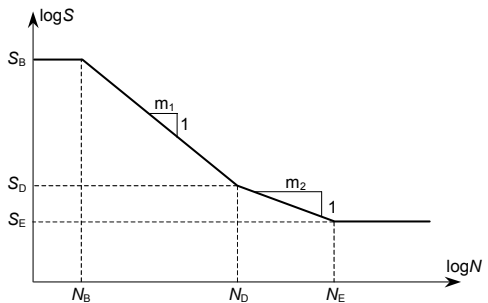


Figure C-3. $S-N$ curve.

- S_E Endurance limit or cut-off limit
- S_D constant amplitude fatigue limit
- S_B often set equal to the ultimate strength

Given a specified stress range S , the $S-N$ curve gives the number of cycles N to failure. The $S-N$ curve shown in Figure C-3

is bilinear which is commonly used for steel. For such a curve two different sets of $\log K$ and m are given depending on whether $N < N_D$ or $N > N_D$. The endurance limit S_E under which failure will not occur, is a property specific for ferrous and titanium alloys.

The material will exhibit a natural variability of $\log N$ about the mean as given by this curve - often expressed in terms of the standard deviation σ . Usually, the mean curve is specified in such a way that in 50% of the cases the true value of $\log N$ will be larger than given by the curve, and in 50% of the cases it will be smaller than given by the curve. For design of wind turbine structures, it is required to use a characteristic $S-N$ curve, which is to be chosen in a conservative manner such that $\log N$ in a large fraction, $1-p$, of the cases exceeds the value given by the characteristic curve. Usually, $1-p$ is taken as 97-98%. When the mean $S-N$ curve is given, the characteristic $S-N$ curve can be found by keeping the values of $\log N$ fixed and changing the corresponding S values according to the following formula

$$S_{1-p} = S_{50\%} \exp\left(-k \frac{\sigma_{\log N}}{m}\right)$$

in which $S_{50\%}$ is the stress range corresponding to the mean $S-N$ curve for given N , S_{1-p} is the corresponding stress range corresponding to the characteristic $S-N$ curve with $1-p$ probability of exceedance, $\sigma_{\log N}$ is the standard deviation of $\log N$ representing the natural variability in $\log N$ for given S , and k depends on p and can be taken from Table C-1.

Fraction p %	20	10	5	2.3	2	1	0.1
K	0.84	1.28	1.65	1.96	2.05	2.33	3.09

When $\sigma_{\log N}$ is not known, it can be set equal to 0.46 for plain steels free from welds, see DNV (1984).

The $S-N$ curve valid for analysis of a structural detail is to be applicable for the material, the structural detail, the state of stress considered and the surrounding environment. The $S-N$ curve should take into account possible material thickness effects.

Recommended characteristic $S-N$ curves for steel are described in Section C.6 and C.7, and recommended characteristic $S-N$ curves for steel bolts are given in Appendix A. For determination of $S-N$ curves for cast iron, reference is made to Hüeck et al.

For design purposes, fatigue analysis based on $S-N$ curves from fatigue tests is normally straightforward and the most suitable method. It is then used in conjunction with Palmgren-Miner's rule for prediction of cumulative damage.

C.4 The Palmgren-Miner rule

The fatigue life – or in other terms the cumulative damage – under varying loads can be predicted based on the $S-N$ curve approach under the assumption of linear cumulative damage by Palmgren-Miner's rule. The total damage that a structure will experience during its design life may be expressed as the cumulative damage from each load cycle at different stress levels, independent of the sequence in which the stress cycles occur, i.e. no sequence-dependency or so-called "load cycle effect" is present.

According to Palmgren-Miner's rule, the accumulated damage D can be predicted as follows

$$D = \sum_{i=1}^k \frac{\Delta n(S_i)}{N(S_i)}$$

in which Δn denotes the number of stress cycles of stress range S in the lifetime of the structure, and N is the number of cycles to failure at this stress range. Δn is determined from the long-term distribution of the stress ranges as the one shown in Figure C-2, and N is determined from the expression for the S - N curve; $\log N = \log K - m \log S$. The sum is over all stress ranges S_i in a sufficiently fine discretisation of the stress range space into k blocks of constant range stress cycles.

It is noted that the expression for the accumulated damage D can be interpreted as a sum of partial damage owing to load cycles at various stress ranges, regardless of the sequence in which the load cycles occur.

When the long-term stress range distribution is a Weibull distribution with scale parameter s_0 and shape parameter h ,

$$F_s(s) = 1 - \exp\left(-\left(\frac{s}{s_0}\right)^h\right),$$

and the total number of stress cycles in the design life is n_{tot} , then the cumulative damage D can be calculated as

$$D = \frac{n_{tot}}{K} \Gamma\left(1 + \frac{m}{h}\right) s_0^m$$

in which $\Gamma()$ denotes the gamma function.

The criterion for design is usually formulated as

$$D \leq 1$$

Caution should be exercised in cases for which load cycle effects are present, and for which the sequence in which the load cycles

arrive is important. In such cases, the expression for D by the Palmgren-Miner's sum may underpredict the true accumulated damage.

Note that the Miner's sum formulation for the cumulative damage used with the quoted S - N curve model disregards a possible dependency on the stress ratio $R = \sigma_{min}/\sigma_{max}$. This is sufficient for most components in wind turbines since they are subjected to fatigue loading with an approximately zero mean stress σ_m , as is the case for the main shaft in Figure C-1. However, in some cases the influence of the mean stress needs to be taken into account. Different S - N curves for different values of σ_m and R can be evaluated or a fatigue life can be assessed through methods that take the mean stress directly into account. See Section C.9.

C.5 Fatigue in welded structures

Welds in structures usually possess defects which may form the basis for crack growth and eventually lead to fatigue failure. For welded joints involving potential fatigue cracking from the weld toe, an improvement in strength by a factor of 2 on the fatigue life can be obtained by controlled local

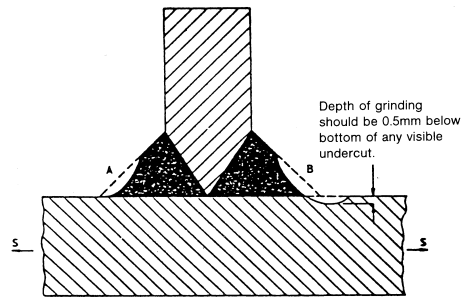


Figure C-4. Grinding a weld toe tangentially to the plate surface (A) will produce little improvement in strength. Grinding must extend below the plate surface (B) in order to remove toe defects, from DNV Class. Notes 30.2.

machining or grinding of the weld toe. This can be carried out by means of a rotary burr. The treatment should produce a small concave profile at the weld toe with the depth of the depression penetrating into the plate surface at least 0.5 mm below the bottom of any visible undercut. The undercut should be small enough to allow the maximum required grinding depth to remain within 2 mm or 5% of the plate thickness, whichever is the smaller. Reference is made to Figure C-4.

By grinding the weld profile such that a circular transition between base material and weld surface is achieved, the stress concentration becomes reduced as the grinding radius is increased. This may lead to additional improvement of the welded joint.

The benefit of grinding may be claimed only for welded joints, which are adequately protected from seawater corrosion. The benefit of grinding should usually not be taken into account during design, as grinding is considered as the only improvement, which can be carried out during fabrication, to increase the fatigue strength.

C.6 Characteristic S-N curves for structural steel

S-N curves for welds and base material of structural steel are classified in DS412 and Eurocode 3. In these standards, guidance is given to selection of S-N curves, on the form $\log N = \log K - m \log S$ for numerous construction and weld details, to be used in conjunction with the Palmgren-Miner rule.

C.7 Characteristic S-N curves for forged or rolled steel

S-N curves for alloyed steel are not standardised in the same manner as in the case of structural steel. Based on empiric relationships between the static material strength and the fatigue strength, so-called synthetic S-N curves are established.

For forged and rolled steel subject to fully reversed stress cycles about a zero-mean stress, i.e. the stress ratio $R = \sigma_{\min}/\sigma_{\max} = -1$, the following applies:

The fatigue strength limit for rotating bending with 50% survival probability at 10^6 cycles can be calculated as

$$\sigma_D = 1.25 \cdot (0.436 \cdot \sigma_y + 77) \cdot f(R_y, \sigma_B) \cdot f(d, r)$$

- σ_y yield strength or 0.2% proof stress for the shaft material, related to the actual dimension. (MPa)
- σ_B ultimate strength for the shaft material, related to the actual dimension. (MPa)

$f(d, r)$ is a size factor, which depends on the shaft diameter d and the fillet radius r . For unnotched parts, the size factor is

$$f(d, r) = 0.8 + \frac{2}{d}$$

and for notched shafts it is

$$f(d, r) = \begin{cases} 0.9 + 1/r & \text{for } r \geq 10 \text{ mm} \\ 1.0 & \text{for } r < 10 \text{ mm} \end{cases}$$

These expressions for the size factor require d and r to be given in units of mm.

$f(R_y, \sigma_B)$ is a surface roughness factor, which is calculated as

$$f(R_y, \sigma_B) = 1 - \frac{\sigma_B}{4000} \log_{10} \left(\frac{R_y}{10} \right)$$

R_y peak-to-peak roughness, $R_y \approx 6R_a$
 R_a mean roughness

The S - N curve slope m is expressed as

$$m = \frac{12}{\beta^2} + 3$$

$$\beta = 1 + \eta(\alpha - 1)$$

$$\eta = 0.62 + 0.2 \log_{10} r + \sigma_y 10^{-4} \log_{10} \left(\frac{400}{r} \right)$$

β notch factor
 α stress concentration factor
 η notch sensitivity
 r fillet radius

The static notch factor is defined as

$$\beta_m = 1 + (\alpha - 1) \left(\frac{\sigma_y}{1000} \right)^2$$

A standard S - N curve, in principle applicable to all non-welded machine steels, can now be constructed, expressed in terms of the above quantities, as shown in Figure C-5. This standard S - N curve, which represents 50% survival probability (i.e. the 50% quantile in the realisation of fatigue tests), is to be considered as a characteristic S - N curve for the material. A materials factor γ_m should be applied to all stress values of this characteristic S - N curve to get a design S - N curve for use in design. For critical components such as the main shaft, $\gamma_m = 1.8$ should be used. Note that the standard S - N curve in Figure C-5 cannot be applied to case-hardened steels.

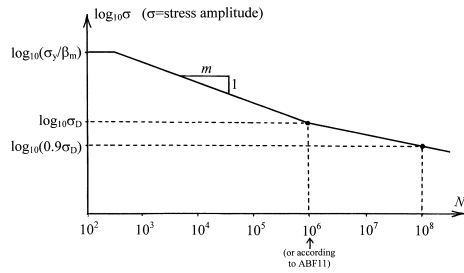


Figure C-5. Characteristic S - N curve for non-welded, forged or rolled machine steel.

Note that the standard S - N curve gives number of cycles to failure N at stress amplitude σ . This is in contrast to structural engineering, where S - N curves give number of cycles to failure N at stress range S , and caution should thus be exercised to avoid confusion and errors. Note also that in structural engineering, the characteristic S - N curve for structural steel is usually defined differently as the S - N curve, which represents 97.7% survival probability (i.e., the 2.3% quantile in the realisation of fatigue tests). Thus, it is usually combined with a smaller requirement to the materials factor γ_m than the 1.8 quoted above for non-welded machine steel.

C.8 S - N curves for composites

S - N curves for composite materials such as fibre reinforced plastics may vary from case to case, depending on the composition of the material. However, many different glass fibre reinforced composites follow the same strain-life curve, denoted ϵ - N curve. Standard ϵ - N curves for design, established from fatigue tests in the laboratory on a number of different materials, can be found in Mayer (1992).

C.9 Other types of fatigue assessment

In order to take the mean stress $\sigma_m \neq 0$ into account, several different approaches have been developed, some of which are described below. These empirical fatigue curves are constructed from static material properties. Each line in Figure C-6 represents different approximations describing the relationship between the mean stress and the stress amplitude above which failure will occur.

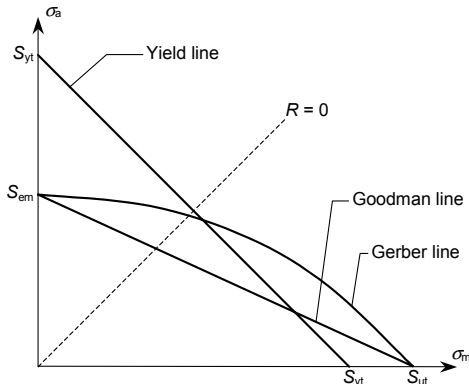


Figure C-6. Different fatigue lines for non-zero mean stress.

- σ_a stress amplitude
- σ_m mean stress
- S_{yt} yield strength in tension
- S_{ut} ultimate strength in tension
- S_{em} modified endurance limit, i.e. reduced for effects of surface, size, reliability etc.
- $R = \sigma_{min} / \sigma_{max}$

The Gerber diagram is a parabola given by

$$\sigma_a = S_{em} \left(1 - \left(\frac{\sigma_m}{S_{ut}} \right)^2 \right)$$

The Goodman line is given by

$$\sigma_a = S_{em} \left(1 - \left(\frac{\sigma_m}{S_{ut}} \right) \right)$$

The Goodman line is combined with the yield line in “the modified Goodman diagram” shown in Figure C-7. This diagram includes compressive stresses. From the diagram can be read the maximum allowed stress amplitude σ_a in order to avoid fatigue failure for a given mean stress σ_m .

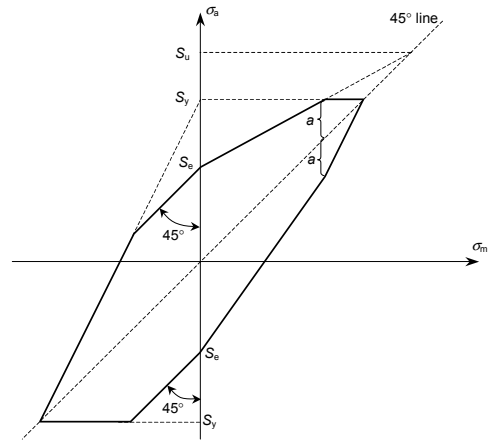


Figure C-7. Modified Goodman diagram.

- S_y yield strength
- S_u ultimate strength
- S_e endurance limit

REFERENCES

DNV, *Fatigue Strength Analysis for Mobile Offshore Units*, Classification Notes No. 30.2, Det Norske Veritas, Høvik, Norway, 1984.

DNV, *Fatigue Assessment of Ship Structures*, Classification Notes No. 30.7, Det Norske Veritas, Høvik, Norway, 1998.

DS 412, *Code of Practice for the structural use of steel*, 3rd edition, 1998-07-02.

Eurocode 3, Design of steel structures – part 1-1: *General rules and rules for buildings*, 2nd edition, September 1993.

Hück, M., Trainer, L., Schütz, W., ABF 11, *Berechnung von Wöhlerlinien für Bauteile aus Stahl, Stahlguss und Grauguss, Synthetische Wöhlerlinien*, Industrieanlagen-Betriebsgesellschaft mbH, 1983.

Mayer, R.M., *Design of Composite Structures against Fatigue, Applications to Wind Turbine Blades*, Mechanical Engineering Publications Ltd., Bury St. Edmunds, Suffolk, U.K., 1996.

Osgood, C. C., *Fatigue Design*, 2nd edition, Pergamon Press, 1982.

D. FEM Calculations

If simple calculations cannot be performed to document the strength and stiffness of a structural component, a Finite Element analysis should be carried out.

The model to be included in the analysis and the type of analysis should be chosen with due consideration to their interaction with the rest of the structure.

Since a FEM analysis is normally used when simple calculations are insufficient or impossible, care must be taken to ensure that the model and analysis reflect the physical reality. This must be done by means of carrying out an evaluation of the input to as well as the results from the analysis. Guidelines for such an evaluation are given below.

D.1 Types of analysis

Though different types of analyses can be performed by means of FEM analysis, most analyses take the form of static analyses for determination of the strength and stiffness of structures or structural components. FEM analyses are usually computer-based analyses which make use of FEM computer programs.

Static analysis

In a static analysis structural parts are commonly examined with respect to determining which extreme loads govern the extreme stress, strain and deflection responses. As the analysis is linear, unit loads can be applied, and the response caused by single loads can be calculated. The actual extreme load cases can subsequently be examined by means of linear combinations - superposition.

Frequency analysis

Frequency analysis is used to determine the eigenfrequencies and normal modes of a structural part.

The FEM program will normally perform an analysis of the lowest frequencies. However, by specifying a shift value, it is possible to obtain results also for a set of higher frequencies around a user-defined frequency.

Note that the normal modes resulting from such analysis only represent the shape of the deflection profiles, not the actual deflections.

Dynamic analysis

Dynamic FEM analysis can be used to determine the time-dependent response of a structural part, e.g. as a transfer function. The analysis is normally based on modal superposition, as this type of analysis is much less time consuming than a 'real' time dependent analysis.

Stability/buckling analysis

Stability/buckling analysis is relevant for slender structural parts or sub-parts. This is due to the fact that the loads causing local or global buckling may be lower than the loads causing strength problems.

The analysis is normally performed by applying a set of static loads. Hereafter, the factor by which this set of loads has to be multiplied for stability problems to occur, is found by the program.

Thermal analysis

By thermal analysis, the temperature distribution in structural parts is determined, based on the initial temperature, heat input/output, convection, etc. This is normally a time-dependent analysis, however, it is usually not very time-consuming as only one degree of freedom is present at each modelled node. Note that a thermal analysis set-up as mentioned here can be used to

analyse analogous types of problems involving other time-dependent quantities than temperature. This applies to problems governed by the same differential equation as the one which governs heat transfer. An example of such an application can be found in foundation engineering for analysis of the temporal evolution of settlements in foundation soils.

Types of analyses

The analyses mentioned above only encompass some of the types of analyses that can be performed by FEM analysis. Other types of analyses are: plastic analyses and analyses including geometric non-linearities.

Furthermore, combinations of several analyses can be performed. As examples hereof, the results of an initial frequency analysis can be used as a basis for subsequent dynamic analysis. Finally, the result of a thermal analysis may be used to form a load case in a subsequent static analysis.

D.2 Modelling

The results of a FEM analysis is normally documented by plots and printouts of selected extreme response values. However, as the structural FEM model used can be very complex, it is important also to document the model itself. Even minor deviations from the intention may give results that do not reflect reality properly.

D.2.1 Model

The input for a FEM model must be documented thoroughly by relevant printouts and plots. The printed data should preferably be stored or supplied as files on a CD-ROM

Coordinate systems

Different coordinate systems may be used to

define the model and the boundary conditions. Hence the coordinate system valid for the elements and boundary conditions should be checked, e.g. by plots. This is particularly important for beam elements given that it is not always logical which axes are used to define the sectional properties.

Similarly, as a wrong coordinate system for symmetry conditions may seriously corrupt the results, the boundary conditions should be checked.

Insofar as regards laminate elements, the default coordinate system often constitutes an element coordinate system, which may have as a consequence that the fibre directions are distributed randomly across a model.

Material properties

Several different material properties may be used across a model, and plots should be checked to verify that the material is distributed correctly.

Drawings are often made by means of using units of mm to obtain appropriate values. When the model is transferred to the FEM program, the dimensions are maintained. In this case care should be taken in setting the material properties (and loads) correctly, as kg-mm-N-s is not a consistent set of units. It is advisable to use SI-units (kg-m-N-s).

Material models

The material model used is usually a model for isotropic material, i.e. the same properties in all directions. Note, however, that for composite materials an orthotropic material model has to be used to reflect the different material properties in the different directions. For this model, material properties are defined for three orthogonal directions. By definition of this material, the choice of coordinate system for the elements has to be made carefully.

D.2.2 Elements

For a specific structural part, several different element types and element distributions may be relevant depending on the type of analysis to be carried out. Usually, one particular element type is used for the creation of a FEM model.

However, different element types may be combined within the same FEM model. For such a combination special considerations may be necessary.

Element types

1D

Models with beam elements are quite simple to create and provide good results for frame like structures.

One difficulty may be that the sectional properties are not visible. Hence, the input should be checked carefully for the direction of the section and the numerical values of the sectional properties. Some FEM programs can generate 3D views showing the dimensions of the sections. This facility should be used, if present.

Naturally, the stresses in the connections cannot be calculated accurately by the use of beam elements only.

2D

Shell and plate elements should be used for parts consisting of plates or constant thickness sub-parts. As shell elements suitable for thick plates exist, the wall thickness does not need to be very thin to obtain a good representation by such elements. These elements include the desired behaviour through the thickness of the plate. The same problems as for beam elements are present for shell elements as the thickness of the plates is not shown. The thickness can, however, for most FEM programs be shown by means of colour

codes, and for some programs the thickness can be shown by 3D views.

The stresses at connections such as welds cannot be found directly by these elements either.

3D

By the use of solid elements the correct geometry can be modelled to the degree of detail wanted. However, this may imply that the model will include a very large number of nodes and elements, and hence the solution time will be very long. Furthermore, as most solid element types only have three degrees of freedom at each node, the mesh for a solid model may need to be denser than for a beam or shell element model.

Combinations

Combination of the three types of elements is possible, however, as the elements may not have the same number of degrees of freedom (DOF) at each node, care should be taken not to create unintended hinges in the model.

Beam elements have six degrees of freedom in each node – three translations and three rotations, while solid elements normally only have three – the three translations. Shell elements normally have five degrees of freedom – the rotation around the surface normal is missing. However, these elements may have six degrees of freedom, while the stiffness for the last rotation is fictive.

The connection of beam or shell elements to solid elements in a point, respectively a line, introduces a hinge. This problem may be solved by adding additional ‘dummy’ elements to get the correct connection. Alternatively, constraints may be set up between the surrounding nodal displacements and rotations. Some FEM

programs can set up such constraints automatically.

Element size/distribution

The size, number and distribution of elements required in an actual FEM model depend on the type of analysis to be performed and on the type of elements used.

Generally, as beam and shell elements have five or six degrees of freedom in each node, good results can be obtained with a small number of elements. As solid elements only have three degrees of freedom in each node, they tend to be more stiff. Hence, more elements are needed.

Furthermore, the shape and order of the elements influence the required number of elements. Triangular elements are more stiff than quadrilateral elements, and first-order elements are more stiff than second-order elements.

This can be seen from the example below, in which a cantilever is modelled by beam, membrane, shell and solid elements.

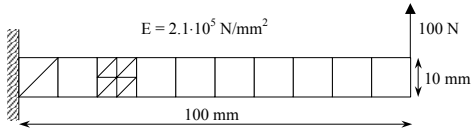


Figure D-1. Cantilever.

Element type	Description	Number of elements	u_y [mm]	$\sigma_{x,node}$ [N/mm ²]	$\sigma_{x,element}$ [N/mm ²]
Analytical result		-	1.9048	600	600
BEAM2D	Beam element, 2 nodes per element, 3 DOF per node, u_x , u_y and θ_z	10	1.9048	600	600
		1	1.9048	600	600
PLANE2D	Membrane element, 4 nodes per element, 2 DOF per node, u_x and u_y	10 x 1	1.9124	570	0
TRIANG	Membrane element, 3 nodes per element, 2 DOF per node, u_x and u_y	10 x 1 x 2	0.4402	141	141
		20 x 2 x 2	1.0316	333	333
		40 x 4 x 2	1.5750	510	510
SHELL3	Shell element, 3 nodes per element, 6 DOF per node	20 x 2 x 2	1.7658	578	405
SOLID	Solid element, 8 nodes per element, 3 DOF per node u_x , u_y and u_z	10 x 1	1.8980	570	570
TETRA4	Solid element, 4 nodes per element, 3 DOF per node u_x , u_y and u_z	10 x 1 x 1	0.0792	26.7	26.7
		20 x 2 x 1	0.6326	239	239
		40 x 4 x 1	1.6011	558	558
TETRA4R	Solid element, 4 nodes per element, 6 DOF per node	20 x 2 x 1	1.7903	653	487

Table D-1. Analysis of cantilever with different types of elements.

Element quality

The results achieved by a certain type and number of elements depend on the quality of the elements.

Several measures for the quality of elements can be used, however, the most commonly used are aspect ratio and element warping.

The aspect ratio is the ratio between the side lengths of the element. This should ideally be equal to 1, but aspect ratios of up to 3-5 do usually not influence the results and are thus acceptable.

Element warping is the term used for non-flatness or twist of the elements. Even a slight warping of the elements may influence the results significantly.

Most available FEM programs can perform checks of the element quality, and they may even try to improve the element quality by redistribution of the nodes.

The quality of the elements should always be checked for an automatically generated mesh, in particular, for the internal nodes and elements. It is usually possible to generate good quality elements for a manually generated mesh.

With regard to automatically generated high-order elements, care should be taken to check that the nodes on the element sides are placed on the surface of the model and not just on the linear connection between the corner nodes. This problem often arises when linear elements are used in the initial calculations, and the elements are then changed into higher-order elements for a final calculation.

Benchmark tests to check the element quality for different element distributions and load cases are given by NAFEMS. These tests include beam, shell and solid elements, as well as static and dynamic loads.

D.2.3 Boundary conditions

Definition of boundary conditions

The boundary conditions applied to the model should as a matter of course be as realistic as possible. This may require that the FEM model becomes extended to

include element models of structural parts other than the particular one to be investigated. One situation where this comes about is when the true supports of a considered structure have stiffness properties which cannot be well-defined unless they are modelled by means of elements that are included in the FEM model.

When such an extended FEM model is adopted, deviations from the true stiffness at the boundary of the structural part in question may then become minor only. As a consequence hereof, the non-realistic effects due to inadequately modelled boundary conditions are transferred further away to the neighbouring structural parts or sub-parts, which are now represented by elements in the extended FEM model.

Types of restraints

The types of restraints normally used are constrained or free displacements/rotations or supporting springs. Other types of restraints may be a fixed non-zero displacement or rotation or a so-called contact, i.e. the displacement is restrained in one direction but not in the opposite direction.

The way that a FEM program handles the fixed boundary condition may vary from one program to another. One approach is to remove the actual degree of freedom from the model, another is to apply a spring with a large stiffness at the actual degree of freedom. The latter approach may lead to singularities if the stiffness of the spring is much larger than the stiffness of the element model. Evidently, the stiffness can also be too small, which may again result in singularities.

An appropriate value for the stiffness of such a stiff spring may be approximately 10^6 times the largest stiffness of the model.

As the program must first identify whether the displacement has to be constrained or free, the contact boundary condition requires a non-linear calculation.

Symmetry/antimetry

Other types of boundary conditions are symmetric and antimetric conditions, which may be applied if the model *and* the loads possess some kind of symmetry. Taking such symmetry into account may reduce the size of the FEM model significantly.

The two types of symmetry that are most frequently used are planar and rotational symmetries. The boundary conditions for these types of symmetry can normally be defined in an easy manner in most FEM programs by using appropriate coordinate systems.

The loads for a symmetric model may be a combination of a symmetric and an antimetric load. This can be considered by calculating the response from the symmetric loads for a model with symmetric boundary conditions, and adding the response from the antimetric loads for a model with antimetric boundary conditions.

If both model and loads have rotational symmetry, a sectional model is sufficient for calculating the response.

Some FEM programs offer the possibility to calculate the response of a model with rotational symmetry by a sectional model, even if the load is not rotational-symmetric, as the program can model the load in terms of Fourier series.

D.2.4 Loads

The loads applied for the FEM calculation are usually structural loads, however, centrifugal and temperature loads are also relevant.

Structural loads consist of nodal forces and moments and of surface pressure. Nodal forces and moments are easily applied, but may result in unrealistic results locally. This is due to the fact that no true loads act in a single point. Thus, application of loads as pressure loads will in most cases form the most realistic way of load application.

Load application

The loading normally consists of several load components, and all of these components may be applied at the same time. As a slightly different load combination in a new analysis will require an entirely new calculation, this is, however, not very rational.

Instead, each of the load components should be applied separately as a single load case, and the results found from each of the corresponding analyses should then be combined. In this way, a large range of load combinations can be considered. To facilitate this procedure, unit loads should be used in the single load cases, and the actual loads should then be used in the linear combinations.

As only one or more parts of the total structure is modelled, care should be taken to apply the loads as they are experienced by the actual part. To facilitate such load application, ‘dummy’ elements may be added, i.e. elements with a stiffness representative of the parts which are not modelled – these are often beam elements. The loads can then be applied at the geometrically correct points and be transferred via the beam elements to the structural part being considered.

D.3 Documentation

D.3.1 Model

The result of a FEM analysis can be documented by a large number of plots and

printouts, which can make it an overwhelming task to find out what has actually been calculated and how the calculations have been carried out.

The documentation for the analysis should clearly document which model is considered, and the relevant results should be documented by plots and printouts.

Geometry control

Control of the geometric model by means of checking the dimensions is an important and often rather simple task. This simple check may reveal if numbers have unintentionally been entered in an incorrect manner.

Mass – volume – centre of gravity

The mass/volume of the model should always be checked. Similarly, the centre of gravity should correspond with the expected value.

Material

Several different materials can be used in the same FEM model of which some may be fictitious. This should be checked on the basis of plots showing which material is assigned to each element, and by listing the material properties. Here, care should be taken to check that the material properties are given according to a consistent set of units.

Element type

Several different element types can be used, and here plots and listing of the element types should also be presented.

Local coordinate system

With regard to beam and composite elements, the local coordinate systems should be checked, preferably, by plotting the element coordinate systems.

Loads – boundary conditions

The loads and boundary conditions should be plotted to check the directions of these, and the actual numbers should be checked from listings. To be able to check the correspondence between plots and listings, documentation of node/element numbers and coordinates may be required.

The above listed aspects can and should be checked prior to performing the analyses. Possibilities of checking the results – besides comparison with hand calculations – also exist in the various available programs.

Reactions

The reaction forces and moments are normally calculated by the FEM programs and should be properly checked. As a minimum, it should be checked that the total reaction corresponds with the applied loads. This is especially relevant when loads are applied to areas and volumes, and not merely as discrete point loads. For some programs it is possible to plot the nodal reactions, which can be very illustrative.

A major reason for choosing a FEM analysis as the analysis tool for a structure or structural part is that no simple calculation can be applied for the purpose. This implies that there is no simple way to check the results. Instead checks can be carried out to make probable that the results from the FEM analysis are correct.

Mesh refinement

The simplest way of establishing whether the present model or mesh is dense enough is to remesh the model with a more dense mesh, and then calculate the differences between analysis results from use of the two meshes. As several meshes may have to be created and tried out, this procedure can, however, be very time-consuming. Moreover, as modelling simplification can induce unrealistic behaviour locally, this

procedure may in some cases also result in too dense meshes. Instead, an indication of whether the model or mesh is sufficient would be preferable.

D.3.2 Results

Unrealistic results

Initially, the results should be checked to see if they appear to be realistic. A simple check is made on the basis of an evaluation of the deflection of the component, which should, naturally, reflect the load and boundary conditions applied as well as the stiffness of the component. Also, the stresses on a free surface should be zero.

Error estimates

Most commercial FEM programs have some means for calculation of error estimates. Such estimates can be defined in several ways. One of the most commonly used estimates is an estimate of the error in the stress. The estimated ‘correct’ stress is found by interpolating the stresses by the same interpolation functions as are used for displacements in defining the element stiffness properties.

Another way of getting an indication of stress errors is given by means of comparison of the nodal stresses calculated at a node for each of the elements that are connected to that node. Large variations indicate that the mesh should be more dense.

Load combinations

If the results are found as linear combinations of the result from single load cases, the load combination factors should of course be clearly stated.

Displacement

The global deflection of the structure should be plotted with appropriately scaled deflections. For further evaluation, deflection components could be plotted as contour plots to see the absolute deflections.

For models with rotational symmetry a plot of the deflection relative to a polar coordinate system may be more relevant for evaluation of the results.

Stress

All components of the stresses are calculated and it is should be possible to plot each component separately to evaluate the calculated stress distribution.

The principle stresses could also be plotted with an indication of the direction of the stress component, and these directions should be evaluated in relation to the expected distribution.

Strain

Similar to the stresses, the components of the strains and the principle strain could be plotted for evaluation of the calculated results.

E. Material Properties

In this appendix, some mechanical properties for the most commonly used materials in wind turbines are given.

The values given for mechanical properties are characteristic values that are to be divided by appropriate material partial coefficients to yield the design values. The values given apply in combination the Danish design codes.

E.1 Steel

E.1.1 Structural steel

Structural steel is commonly used in the tower structure, the base frame and different parts of the transmission system. In Table E-2 and Table E-3 values for yield- and ultimate stress is given for different grades of structural steel. In the table t is the nominal thickness. The values given apply in combination with Eurocode 3 and DS 412.

Modulus of elasticity	E	210 000 MPa
Poisson's ratio	ν	0.3
Shear modulus	G	$E/2(1-\nu)$
Unit mass	ρ	7850 kg/m ³
Coefficient of linear thermal expansion	α	$12 \cdot 10^{-6} \text{ } ^\circ\text{C}^{-1}$

Table E-2. Yield strength for structural steel.

Reference Standard	Grade	Minimum yield strength f_y [MPa]							
		Thickness t [mm]							
		≤ 16	> 16 ≤ 40	> 40 ≤ 63	> 63 ≤ 80	> 80 ≤ 100	> 100 ≤ 150	> 150 ≤ 200	> 200 ≤ 250
EN 10 025	S235	235	225	215	215	215	195	185	175
EN 10 025	S275	275	265	255	245	235	225	215	205
EN 10 025	S355	355	345	335	325	315	295	285	275

Table E-3. Tensile strength for structural steel.

Reference Standard	Grade	Tensile strength f_u [MPa]			
		Thickness t [mm]			
		< 3	≥ 3 < 100	≥ 100 < 150	≥ 150 < 250
EN 10 025	S235	360 – 510	340 – 470	340 – 470	320 – 470
EN 10 025	S275	430 – 560	410 – 560	400 – 540	380 – 540
EN 10 025	S355	510 – 680	490 – 630	470 – 630	450 – 630

E.1.2 Alloy steel

The values given in Table E-4 apply to smooth specimens with diameter d [mm] or thickness t [mm].

Grade	$d \leq 16$ $t \leq 8$		$16 < d \leq 40$ $8 < t \leq 20$		$40 < d \leq 100$ $20 < t \leq 60$		$100 < d \leq 160$ $60 < t \leq 100$		$160 < d \leq 250$ $100 < t \leq 160$	
	f_y	f_u	f_y	f_u	f_y	f_u	f_y	f_u	f_y	f_u
34CrMo4	800	1000 - 1200	650	900 - 1100	550	800 - 950	500	750 - 900	450	700 - 850
42CrMo4	900	1100 - 1300	750	1000 - 1200	650	900 - 1100	550	800 - 950	500	750 - 900
50CrMo4	900	1100 - 1300	780	1000 - 1200	700	900 - 1100	650	850 - 1000	550	800 - 950
36CrNiMo4	900	1100 - 1300	800	1000 - 1200	700	900 - 1100	600	800 - 950	550	750 - 900
34CrNiMo6	1000	1200 - 1400	900	1100 - 1300	800	1000 - 1200	700	900 - 1100	600	800 - 950
30CrNiMo8	1050	1250 - 1450	1050	1250 - 1450	900	1100 - 1300	800	1000 - 1200	700	900 - 1100

f_y yield strength [MPa]

f_u tensile strength [MPa]

E.2 Cast iron

The values given in Table E-5 are valid for a wall thickness below 50 mm. For other dimensions the values must be reduced in accordance with DIN 1693 and proper reduction factors for surface roughness and notches must be included.

Grade	Yield strength f_y [MPa]	Tensile strength f_u [MPa]	Elongation at rupture δ [%]
GGG-35.3	350	220	22
GGG-40	400	250	15
GGG-40.3	400	250	18
GGG-50	500	320	7
GGG-60	600	380	3

E.3 Fibre Reinforced Plastics

E.3.1 Glass fibre reinforced plastics

Table E-6 shows the guiding values given in the Danish design code for the mechanical properties of glass fibre reinforced plastics.

Table E-6. Mechanical properties for GRP.	Mat lamina, 30 weight % glass	Weaved roving lamina, 50 weight % glass ¹
<i>Values to be used in strength calculation</i>		
Tensile strength	80 MPa	170 MPa
Compressive strength	100 MPa	100 MPa
Bending strength	150 MPa	170 MPa
Shear strength		
interlaminar	10 MPa	10 MPa
in plane	20 MPa	20 MPa
Flexural modulus	4 000 MPa	8 000 MPa
<i>Values to be used in deformation calculation</i>		
Modulus of elasticity	6 000 MPa	12 000 MPa
Shear modulus	2 200 MPa	-
Poissons ratio	0.35	-

1. Applies to balanced web, loaded in the main direction.

These values are to be reduced in accordance with DS 456 depending on temperature, load duration, cyclic load and fabrication method.

E.4 Concrete

Reinforced concrete is most often used in the foundation structure but also towers made of prestressed concrete are seen. Here attention will be paid to reinforced concrete (RFC) only.

E.4.1 Mechanical properties

For dimensioning purposes the characteristic strength of concrete and reinforcement respectively are given in Table E-7. In the same table are for overall calculations (in particular FEM-analyses) informative deformation values and density given, acc. to Herholdt et al. (1986). These values are in accordance with Eurocode 2 and DS 411. It shall be noted that concrete itself is not able to absorb tension stress. For this purpose the reinforcement is introduced.

Compression strength of concrete ¹	(M)	f_{ck}	>25 MPa
	(A)		>35 MPa
	(E)		>40 MPa
Yield strength of reinforcement ²	Ks410S	f_{yk}	410 MPa
	Ks550S		550 MPa
	Tentor		550 MPa
Modulus of elasticity		E	$\frac{51000}{1+13/f_{ck}}$
Poisson's ratio		ν	0.1 – 0.25
Shear modulus		G	$E/2(1-\nu)$
Unit mass		ρ	2500 kg/m ³

1. Environmental classes acc. to DS 411, moderate (M), aggressive (A) and extra aggressive (E).
2. Selected steel qualities most often used.

Compression strength of plain concrete should not be chosen less than 5 MPa.

REFERENCES

CEB-FIP Model Code 1990 (MC 90)

Danish Energy Agency, *Recommendation to Comply with the Requirements in the Technical Criteria for Danish Approval Scheme for Wind Turbines, Foundations*, August 1998.

DIN 1693 Blatt 1, *Gusseisen mit Kuglegraphit, Werkstoffsorten unlegiert und niedriglegiert*, Oktober 1973.

DS 411, *Code of practice for the structural use of concrete*, 4. edition, 1999-03-03

DS 412, *Code of Practice for the structural use of steel*, 3. edition, 1998-07-02.

DS 456, *Code of Practice for the structural use of glass fibre reinforced unsaturated polyester*, 1. edition, April 1985

DS 481, *Concrete – materials*, 1. edition 1999

EN 10025, *Hot rolled products of non-alloy structural steels – Technical delivery conditions*, March 1990 + amendment A1, August 1993.

EN 10083, *Quenched and tempered steels – Part 1: technical delivery conditions for special steels*, 1997.

Eurocode 2: Design of concrete structures – Part 1-1: *General basis for buildings and civil engineering works*, ENV 1992-1-1:1991

Eurocode 3: Design of steel structures – Part 1-1: *General rules and rules for buildings*, 2. edition, September 1993.

Herholdt A. D. et al., *Beton-Bogen* 2.udgave 1986, CtO, Cementfabrikkernes tekniske Oplysningskontor

F. Terms and Definitions

This appendix contains terms and definitions that are not explicitly described elsewhere in the book. The list is based on the definitions in the references listed in the end of this appendix.

Actuator: Device that can be controlled to apply a constant or varying force and displacement.

Anemometer distance constant: Quantity related to the response time of an anemometer.

Angle of attack: Angle between the direction of the resulting wind velocity on the blade and the chord line of the blade airfoil section.

Annual average: Mean value of a set of measured data of sufficient size and duration to serve as an estimate of the expected value of the quantity. The averaging time interval shall comprise a whole number of years to average out non-stationary effects such as seasonality.

Augmenter: Device or structure which increases an air flow's speed by reducing the area through which it passes.

Autonomous system: Wind turbine in combination with at least one other source of energy (e.g. diesel generator, solar collector, biogas system, etc.) commonly used to improve the continuity of supply.

Auto-reclosing cycle: Event with a time period, varying from approximately 0.01 second to a few seconds, during which a breaker, released after a grid fault, is automatically reclosed and the line is reconnected to the network.

Availability: Percentage of time that a wind turbine generator is available for production.

Axial: Direction or motion perpendicular to the rotor plane.

Betz limit: Maximum energy conversion efficiency theoretically obtainable from a wind turbine rotor, equal to $16/27 \approx 0.593$ of

the total kinetic energy contained by the wind at a given wind speed within a given capture area. (Established by the German scientist A. Betz).

Bin: Interval for test data grouping.

Blade Angle: Angle between the plane of the rotor and the local chord line of the blade profile

Blade cone angle: Angle between the rotor plane and the blade quarter chord line.

Blade load distribution: Description of the manner in which blade loads are distributed along the quarter chord line.

Blade root: Part of the rotor blade that is closest to the hub.

Buckling: Failure mode characterised by a non-linear increase in deflection with a change in compressive load.

Calibration load: Forces and moments applied during calibration.

Capacity factor: Ratio of the average power produced by a wind turbine to its rated power. (Usually taken over a period of time - daily, weekly, monthly, annually - used as a prefix).

Capacity: Total rated power of a wind turbine or group of wind turbines. In the case of electricity producing turbines, it denotes the rated generator power.

Capture matrix: Organisation of the measured time series according to mean wind speeds and turbulence intensities.

Catastrophic failure: Disintegration or collapse of a component or structure.

Characteristic value (of a material property): Value having a prescribed probability of not being attained in a hypothetical unlimited test series.

Chord line: Straight line connecting an

airfoil's leading and trailing edges.

Complex terrain: Surrounding terrain that features significant variations in topography and terrain obstacles that may cause flow distortion.

Cone angle: See Blade Cone Angle.

Constant amplitude loading: Denotes the application of load cycles with a constant

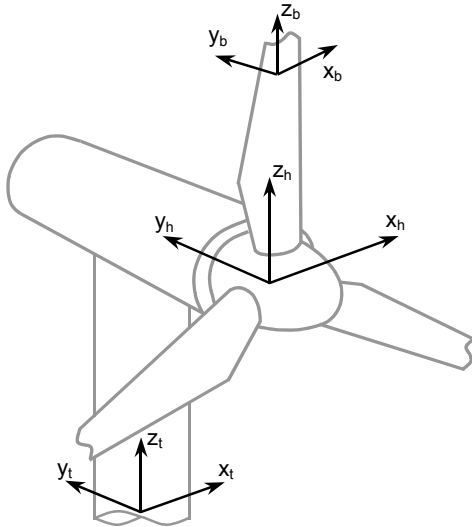


Figure F-1. DS 472 Co-ordinate.

Creep: Time-dependant increase in strain under a sustained load.

Cup anemometer: Rotating device for measuring wind speed, characterised by cups mounted on radial arms which rotate about a vertical axis.

Cut-in wind speed (V_{in}): Lowest mean wind speed at hub height at which the wind turbine starts to produce power.

Cut-out wind speed (V_{out}): Highest mean wind speed at hub height at which the wind turbine is designed to produce power.

Design limits: Maximum or minimum values used in a design.

Design loads: Loads that the turbine is designed to withstand. They are obtained by applying the appropriate partial load factors to the characteristic values.

amplitude and mean value during a fatigue test.

Co-ordinate system: Co-ordinate systems as defined in DS 472 and IEC 61400 are shown in Figure F-1 and Figure F-2, respectively.

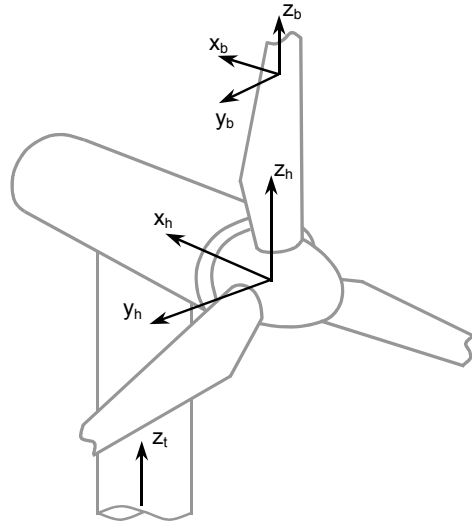


Figure F-2. IEC 61400 Co-ordinate.

Diurnal: Daily. Used to describe meteorological conditions (temperature, atmospheric pressure, wind speed, turbulence, etc.) that normally vary regularly with the time of day.

Dormant failure (also known as latent fault): Failure of a component or system which remains undetected during normal operation.

Downwind: Denotes the main wind direction.

Dump load: A load connected to a wind turbine for the purpose of dissipating or storing excess power. It may be electrical (e.g. resistive heating coils or a battery) or mechanical (e.g. a flywheel).

Edgewise: Direction that is parallel to the local chord of the blade.

Electric power network: Particular installations, substations, lines or cables for the transmission and distribution of electricity.

Electromagnetic interference: Impairment of an electromagnetic signal, either by electrical field interference or by deflection of a radio transmitted signal.

Environmental conditions: Characteristics of the environment (altitude, temperature, humidity, etc.) which may affect the WTGS behaviour.

External conditions: Factors affecting operation of a wind turbine, including wind regime, electrical grid, temperature, snow, ice, etc.

Fatigue strength: Measure of the load-bearing capacity of a material or structural element subjected to repetitive loading.

Fatigue test: Test in which a cyclic load of constant or varying amplitude is applied to the test specimen.

Feathering: To change the blade pitch angle of all or part of a blade to reduce the aerodynamic lift.

Flap: Direction which is perpendicular to the swept surface of the non-deformed rotor blade axis.

Flapping: Blade motion in the out-of-plane of rotation direction.

Flapwise: Direction that is perpendicular to the surface swept by the non-deformed rotor blade axis.

Flatwise: Direction that is perpendicular to the local chord, and spanwise blade axis.

Freewheeling: Free rotation of the wind turbine with the generator disconnected.

Furling: To adjust the wind turbine structure in order to reduce the driving force of the wind, for instance feathering - yawing out of the wind.

Gamma function: The Euler gamma function is given by $\Gamma(x) = \int_0^{\infty} e^{-u} u^{x-1} du$

Grid: Network for transmission and distribution of electricity.

Guy (wire): Cable or wire used as a tension support between the ground and a tower.

Horizontal axis wind turbine (HAWT): Wind turbine whose rotor axis is substantially parallel to the wind flow.

Hub height: Height of the centre of the rotor above the terrain surface.

Idling: Condition of a wind turbine generator that is rotating slowly and not producing power.

Inboard: Towards the blade root.

Inertial sub-range: Frequency interval of the wind turbulence spectrum, where eddies - after attaining isotropy - undergo successive break-up with negligible energy dissipation.

NOTE - at a typical 10 m/s wind speed, the inertial sub-range is roughly from 0.02 Hz to 2 kHz.

Infinite life design: Design where the operating stresses does not result in damage.

In-plane: Direction or motion parallel with the rotor plane.

Kite anemometer: Kite which has been calibrated to give quantitative wind speed data.

Leading edge: Part of a blade at the incidence of the air flow.

Lead-lag: Blade motion in the plane of rotation (HAWT).

Loads: Typical term for the different load components with reference to Figure F-3:

Blade loads

Term refer to directions in and perpendicular to the rotor plane (while the terms in parenthesis refer to directions along and perpendicular to the local blade chord).

M_{be} : Leadwise (edgewise) bending moment

M_{bf} : Flapwise (flatwise) bending moment

M_{bt} : Torsional moment

F_{be} : Leadwise (edgewise) shear force

F_{bf} : Flapwise (flatwise) shear force

F_{bs} : Spanwise (axial) force

Hub loads

M_{hr} : Rotor torque/roll

M_{ht} : Tilt moment

- M_{hy} : Yaw moment
- F_{hg} : Gravitational force
- F_{hs} : Side force
- F_{ht} : Rotor thrust

Tower loads

- M_{tl} : Tower lateral bending moment
- M_{tt} : Tower tilt/normal bending moment
- M_{ty} : Tower yaw/torsion moment
- F_{tg} : Tower gravitational force
- F_{tl} : Tower lateral shear force
- F_{tn} : Tower normal shear force

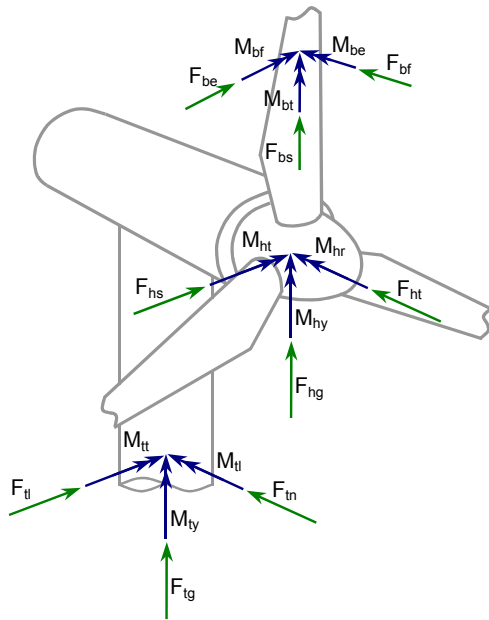


Figure F-3. Loads.

Load envelope: Collection of maximum design loads in all directions and spanwise positions.

Method of bins: Data reduction procedure by which test data are grouped into wind speed intervals (bins). For each bin, the number of samples and sum of parameter samples are recorded. The average parameter value within each wind speed bin can then be evaluated. (This is a general technique applicable to a variety of parameters).

Modal tests: Test carried out to determine

the natural frequencies, damping and mode shapes of a structure.

Natural frequency: Frequency at which a structure will choose to vibrate when perturbed and allowed to vibrate freely.

Net power: The power available from a wind turbine less any power needed for control, monitoring, display or maintaining operation, i.e. power available to the user. Unless otherwise specified, P will be 10-minute average values.

Net reactive power: The reactive power supplied by the power system or absorbed by the power system.

Non-destructive testing (NDT): Inspection methods that do not alter the properties of the structure.

One-seventh power law: Wind speed profile which uses the power law with an exponent $\alpha = 1/7$.

Operating limits: Set of conditions, defined by the WTGS designer, that govern the activation of the control and protection system.

Outboard: Towards the blade tip.

Overspeed control: System that limits rotor speed to a maximum value.

Parking brake: A brake capable of preventing rotor movement at wind speeds up to and including the survival wind speed.

Peak power ratio operation: Variable speed operation when maintaining the tip speed ratio for maximum power output.

Peak value: Maximum value occurring during the time under consideration.

Point loading: Load or series of loads that are applied at discrete spanwise positions.

Power collection system: Electric connection system that collects the power from one or more wind turbines. It includes all electrical equipment connected between the WTGS terminals and the network connection point.

Power conditioning: To change or modify the characteristics of electric power.

Power density: Amount of power in the wind per unit of cross-sectional area of the

wind stream. Usually given in W/m^2 .

Power output: Electrical power delivered by a WTGS.

Prevailing wind: Wind direction occurring most frequently at a site.

Primary (or main) Generator: Generator connected to the mains power grid when the wind turbine is supplying nominal power.

Projected area: Area covered at any instant by the rotor blades, as seen from the direction of wind velocity. (Area solidly covered by the blades as opposed to the swept area).

Radial position: Distance from the rotor centre to a point in the rotor plane.

Rated wind speed: Specified wind speed at which a wind turbine's rated power is achieved.

Reference wind speed (V_{ref}): Basic parameter for wind speed used for defining WTGS classes in the IEC standard.

Resonance: Dynamic condition in which the frequency of an applied force is close to a system's natural frequency resulting in amplified vibration or oscillation.

Rotationally sampled wind velocity: Wind velocity experienced at a fixed point of the rotating wind turbine rotor. The turbulence spectrum of a rotationally sampled wind velocity is distinct from the normal turbulence spectrum. While rotating, the blade cuts through a wind flow, which varies in space. As a consequence hereof, the resulting turbulence spectrum will contain sizeable amounts of variance at the frequency of rotation and harmonics of the same.

Rotor axis: Axis through the rotor centre and the main shaft.

Rotor centre: Point on the centre of the hub in the rotor plane.

Rotor diameter: For a HAWT, diameter of the circular swept area of the rotor and blade assembly.

Rotor plane: For a HAWT, the plane perpendicular to the rotor axis where the quarter chord lines intersect, or pass closest

to the rotor axis.

Rotor speed: Rotational speed of a wind turbine rotor about its axis.

R-ratio: Ratio between minimum and maximum value during a load cycle.

Safe life: A prescribed service life with a declared probability of catastrophic failure.

SCF: Stress Concentration Factor. Factor for increased stress due to geometrical irregularities such as holes, notches, etc.

Scheduled maintenance: Preventive maintenance carried out in accordance with an established time schedule.

Service loads: Load spectrum, including sequence, which is representative of the actual operating conditions.

Site electrical facilities: All electrical, electronic, safety and control sub-systems required to connect the WTG to the main power system.

Solidity: Rotor projected area divided by the swept area of the rotor.

Spanwise: Direction parallel to the longitudinal axis of a rotor blade.

Spar: Primary lengthwise structural member of a wind turbine rotor blade.

SRF: Stress Reserve Factor. Safety factor on top of partial safety factors.

$SRF = L_D / R_D$ in which L_D is the design load, and R_D is the design resistance.

Stand-alone: WTG not part of a large energy network.

Standstill: Condition of a WTG that is stopped.

Start-up wind speed: The lowest wind speed at which a wind turbine will begin rotation but will not necessarily have a net energy output.

Static test: Test in which a specified load of constant magnitude and direction is applied to a test specimen.

Steady-state operation: State of operation during which the turbine and the external conditions remain in a steady state.

Stiffness: Ratio of change of force (or torque) to the corresponding change in displacement of an elastic body.

Strain: Ratio of the elongation (or shear displacement) of a material subjected to stress, to the original length of the material.

Support structure: Part of a wind turbine comprising the tower and foundation.

Survival wind speed: Maximum wind speed (normally a 3-second gust) that a WTG has been designed to sustain without damage to structural components or loss of ability to function normally.

Swept area: Projected area perpendicular to the wind direction that a rotor will describe during one complete rotation.

Tare loads: Forces and moments created by gravity.

Tip-speed: Linear speed of a blade tip.

$V_{tip} = r \cdot \omega$ (rotor radius·angular speed)

Tower shadow: Disturbance of the flow field around, and created by, the tower.

Trailing edge: Aft portion of a blade, normally pointed.

Transient event: Event during which the state of operation of the wind turbine changes, such as during shut-down or gust.

Twist: Spanwise variation in angle of the chord lines of blade cross-sections.

Ultimate strength: Measure of the maximum (static) load-bearing capacity of a material or structural element.

Unscheduled maintenance: Maintenance carried out, not in accordance with an established time schedule, but after reception of an indication regarding the state of an item.

Upwind: Denotes the direction opposite to the main wind direction.

Utility grid: Electrical distribution system for public supply.

Utility interconnection: Electrical connection between a wind turbine generator system and a utility grid in which energy can be transferred from the WTGS to the utility grid and vice versa.

Variable amplitude loading: Application of load cycles of non-constant mean, and/or cyclic range.

Wind turbine generator system (WTGS):

System which converts kinetic energy in the wind into electric power.

Wind turbine heating system (WTHS): Wind turbine where the output energy is in the form of heat.

Wind turbine pump (WTP): Wind turbine directly coupled to a pump.

Wind vane: Device for indicating or recording wind direction.

Wind velocity: Vector describing the speed and the direction of the wind.

Wind-diesel system: See Autonomous System.

Yaw rate: Rate of change nacelle yaw position (usually measured in °/sec.)”

REFERENCES

DS472, *Last og sikkerhed for vindmøllekonstruktioner*, Dansk Ingeniørforening, 1st edition, Copenhagen, Denmark, 1992.

Elliot, George, *Recommended practices for wind turbine testing, 8. Glossary of terms*, National Wind turbine Centre, Dept. of Trade & Industry, National Engineering Laboratory, Glasgow, UK, 2nd edition 1993.

IEC, Wind turbine generator systems – Part 1: *Safety requirements*, International Standard, IEC61400-1, 2nd edition, 1999.

IEC, *Measurement of mechanical loads*, TS 61400-13, 1st edition, 2001-06.

IEC, *Full-scale structural testing of rotor blades*, TS 61400-23, 1st edition 2001-04.

G. Tables and Conversions

G.1 English/metric conversion

Conversion between US units and metric units

Metric units	US units
LENGTH	
0.3048 m	1 foot
1 m	3.281 feet
1 m	39.37 inches
2.540 cm	1 inch
1 km	0.621 mile
1.609 km	1 mile
AREA	
1 km ²	0.3861 square mile
2.590 km ²	1 square mile
1 m ²	10.76 square feet
0.093 m ²	1 square foot
VOLUME	
1 m ³	353 cubic feet
0.0283 m ³	1 cubic foot
CAPACITY	
1 litre	0.0353 cubic feet
28.33 litre	1 cubic foot
1 litre	61.02 cubic inches
0.01639 litre	1 cubic inch
1 litre	0.2642 US gallon
3.7854 litre	1 US gallon
MASS and WEIGHT	
1 metric ton	1.1 tons
1 kg	2.2046 lbs
0.4536 kg	1 lb
1 kN	0.2247 kips
4.45 kN	1 kip
1 kPa	0.000147 ksi
6804 kPa	1 ksi
1 kPa	0.147 psi
6.804 kPa	1 psi

Temperature conversion:

Celsius temperature =
Fahrenheit temperature times 5/9 minus 32.

Fahrenheit temperature =
Celsius temperature times 1.8 plus 32.

G.2 Air density vs. temperature

The density ρ of air in units of kg/m³ can be expressed as

$$\rho = \frac{353.12}{273.15 + T}$$

in which T is the temperature in Celsius.

G.3 Air density vs. height

The change $\Delta\rho$ in air density for an increase Δh in the elevation above sea level can be expressed as

$$\frac{\Delta\rho}{\Delta h} = -1.194 \cdot 10^{-4} \text{ kg/m}^3$$

G.4 Rayleigh wind distribution

The long-term distribution of the 10-minute mean wind speed U_{10} at a given site is usually well represented by a Weibull distribution

$$F_{U_{10}}(u) = 1 - \exp\left(-\left(\frac{u}{u_0}\right)^k\right)$$

in which u_0 and k are distribution parameters. When $k = 2$, which is often a good approximation for wind speed data, the distribution becomes a Rayleigh distribution,

$$F_{U_{10}}(u) = 1 - \exp\left(-\left(\frac{u}{u_0}\right)^2\right)$$

and the following relationship exists between u_0 and the mean value $E[U_{10}]$ in the long-term distribution:

$$u_0 = \frac{2}{\sqrt{\pi}} E[U_{10}]$$

Let the cumulative probability be denoted p .
The corresponding value of the wind speed,
 u , can then be found by

$$u = u_0 \cdot x,$$

where x is tabulated in Table G-1.

Table G-1. Quantiles of standard Rayleigh distribution	
Probability p	Quantile x
0.0001	0.0100
0.001	0.0316
0.002	0.0447
0.005	0.0708
0.01	0.1003
0.1	0.3246
0.2	0.4724
0.3	0.5972
0.4	0.7147
0.5	0.8326
0.6	0.9572
0.7	1.0973
0.8	1.2686
0.9	1.5174
0.99	2.1460
0.995	2.3018
0.998	2.4929
0.999	2.6283
0.9999	3.0349

Index

- Accessibility 2, 29, 149, 153
- Acetal (POM) 165
- Active brakes 146
- Aerodynamic
 - coefficients 60, 65, 70, 71
 - damping 58, 74, 88, 115, 175
 - data extrapolation 71
 - modelling 61, 63
- Aeroelastic calculation 60, 70, 75, 173, 180
- Air
 - density 49, 250, 277
 - kinematic viscosity 174
- Alloyed steel 126, 138, 143, 269
- Amplitude decay ratio 73
- Anemometer 63, 236
- Annual energy production 5, 7, 236
- Aspect ratio *See Blades*
- Asynchronous generator 3, 152, 154, 155, 224
- Atmospheric conditions 32, 40, 236
- Atmospheric pressure 49
- Autocorrelation function 39
- Availability 6
- Beam theory 68, 104, 129, 173, 178, 198, 262
- Bearings
 - alignment 128
 - basic dynamic capacity 136
 - clearance 133
 - friction torque moment 164
 - gear 135
 - lubrication 130, 136, 156, 163, 165
 - main bearing 116, 123, 127
 - rating life 132, 135
 - rolling bearings 132, 136, 163, 166, 167
 - seals 130, 131, 165
 - slide bearings 163, 165, 166
 - spherical roller bearing 127, 130, 135
 - tight fits 122, 123
- Betz' law 6
- Bevel gears 134, 135
- Blades
 - aspect ratio 65, 264
 - buckling 110, 112, 115
 - core 106, 107
 - damping 58, 72, 73, 75, 88, 115
 - element momentum method 63, 66, 70
 - elements 105
 - gelcoat 106
 - geometry 4, 104
 - leading edge 4, 51, 63, 64, 75
 - loads 89, 117, 250
 - material 58, 79, 104, 111
 - mould 108
 - natural frequency 73, 113
 - number 1, 3, 59
 - pitch angle 4, 69, 104
 - pressure side 104, 150
 - principal axes 68, 69, 105
 - profile 58, 67, 68, 104, 105
 - resin 106, 107
 - sizing 106
 - suction side 104
 - tests 26, 110, 113, 114, 116
 - tip angle 117, 118
 - trailing edge 4, 63, 65, 110
 - twist 58, 74, 104
 - web 104, 105, 106, 110
 - wet hand lay-up 108
- Blocking mechanisms 29, 162, 233
- Bolts
 - clamping length 244, 245, 246
 - connections 118, 178, 239
 - fatigue 175, 240
 - impact strength 239
 - pretension 27, 126, 233, 242, 249
 - quality classes 239
- Boundary layer theory 35, 64
- Bowen ratio 41
- Brakes
 - aerodynamic 14, 15, 60, 106, 109, 110
 - callipers 146, 162
 - disc 146, 147, 148, 162
 - electrical 156, 163
 - mechanical .14, 87, 146, 148, 154, 237
 - pads 146, 148

Braking loads	60	Cost	5
Braking systems	12, 14, 146, 150, 156	Couplings ..	120, 122, 123, 126, 141, 145
Brittle fracture .	18, 22, 48, 165, 179, 239	Coupon test	144, 145
Bulk temperature	140	Crack	
		growth	27, 252, 255
Cable twist	3, 12, 13, 159, 166	inspection	145, 214
Capacitor bank	225, 226	monitoring	220
Capacity factor	7	Cumulative damage	24, 25, 76, 77, 117, 207, 254, 255
Cast iron	118, 269	Cut-in wind speed	7, 81
Caughey series	72	Cyclones	32, 46
Centrifugal forces	58, 117, 152		
Ceramic brake pads	148	Damping	
Certification	28, 30, 236	aerodynamic	58, 74, 88, 115, 175
Characteristic chord length	64, 75, 89	negative	60, 74
Characteristic values	11, 20	structural	58, 72, 73, 74, 88
Charnock's formula	33	Danish approval scheme	7, 154, 188
Clay 188, 193, 195, 197, 199, 202, 203, 209, 213, 218		Darrieus	2
Coating 51, 156, 212, 213, 214, 220, 221		Davenport	39, 62, 84, 182
Coefficient of variance	81, 183	Delamination	113, 114, 115
Coherence model	39, 62	Design codes	<i>See Standards</i>
Common-cause failures	14, 16, 17, 18	Design lifetime	11, 112, 157, 176
Computational fluid dynamics	65	Design parameters	21
Concepts		Design situations	10, 11, 55
downwind	2	Detail categories	175, 176, 177
horizontal axis	2, 30, 159, 163	Deterministic method	21, 100
upwind	1, 2	Diffraction theory	98
vertical axis	2	Dismantling	2, 126, 214, 215, 221
Concrete	206, 270	Displacement transducers	115
Conductor cable	114	Drag 51, 58, 60, 64, 65, 71, 74, 75, 76, 87, 95, 96, 97, 98, 182	
Cone penetrometer test (CPT)	188	Drivetrain	<i>See Transmission</i>
Configurations		Ductility	22, 119, 120
clusters	7, 194	Duhamel's integral	52
parks	8	Dynamic amplification factor ...	211, 219
stand-alone	7	Dynamic load rating	28, 132, 136
wind farms	8, 36, 227, 229, 231	Dynamic response	71, 148, 171
Control system	9, 12, 27, 29	Dynamic stall	74, 76
modelling	69		
parameters	12, 69	Earthquake	51, 52, 99, 201, 202, 203
Conversions	277	Eccentric loading	193
Cooling system	149, 155, 223, 233	Economy	5, 8, 10, 21
Coordinate system	129, 160, 261	Edgewise vibrations	60
Coriolis forces	58	Effective foundation area	190
Coriolis parameter	44		
Corrosion protection 51, 130, 131, 166, 179, 208, 212, 213, 214, 220, 239, 252			

Efficiency	2, 4, 6, 7	Flange coupling	145
aerodynamic	1, 6	Flapwise vibrations	74
electrical	6	Flash temperature criterion	140
mechanical	6	Flex4	70
Efficiency factor ... <i>See Power coefficient</i>		Flicker	13, 227, 230
Eigenfrequency ... <i>See Natural frequency</i>		Flutter	69, 75
Electrical safety	230	Foundation	
Embedded foundations	192	bearing capacity factor	192
Emergency stop	29	friction angle	188, 197, 199, 200
Endurance limit	139	gravity base	187, 188, 208
Environmental classes	206	inclination factors	192, 193
Environmental conditions 30, 46, 110,		monopile	98, 187, 208, 209
130		shape factor	193
EP additives	131, 132, 137	shear strength parameters	188, 192
Equivalent loads	81, 163, 164, 250	skin friction 194, 196, 197, 215, 217,	
Euler force	178	218	
External conditions	29, 32, 48, 55	spring stiffness	201, 203, 204
Extreme value analysis	43, 77, 82, 85	stability	189
Extreme value distribution	44, 82, 84	stiffness	172, 188, 189, 201, 203, 204
Extreme winds	43	tripod	187, 209, 215
		Four-point ball bearing	163, 165
Fabrication .. 26, 209, 214, 252, 256, 269		Fracture mechanics	252, 253
Fail-grace	10	Frechet distribution	34, 35
Fail-safe	14, 15, 150, 154, 157	Frequency analysis	16, 219, 260, 261
Failure mode analysis	15, 16, 18, 55	Frequency converter 154, 155, 156, 223,	
Failure probability	10, 18, 19, 26, 136	226, 227, 228, 229, 230, 232	
Fatigue		Fretting corrosion	27
assessment 24, 79, 112, 117, 121, 125,		Friction coefficient	248
132, 185, 206, 211, 219, 252		Frictional velocity	32, 33, 41
design life	11, 27, 80, 136, 252	Full-scale test	26, 114
equivalent loads	81, 136, 164, 183	Functional load	60
load spectrum	81, 89		
loads	76, 80, 125, 170	Galvanization	239, 240
S-N curves 24, 79, 81, 124, 211, 240,		Gamma function	7, 24, 35, 111, 255
252, 253, 256		Gear	
Fault tree analysis	16	design contact stress	138
Feasibility assessment	10, 21	gearless	8, 227
FEM	<i>See Finite element method</i>	gray staining	<i>See Micro pitting</i>
Fibre reinforcements 104, 106, 118, 257,		heat treatment	137, 143
269		helical	134
Filtering	132, 150, 156	hypoid	134
Finite element method	61, 70, 260	installation	142
Fire	16, 149, 233	materials	137, 142
Firing angle	225	micro pitting	27, 137, 140, 141, 143
First-order reliability method	23, 24	scuffing	140, 144
Fixed speed	227	surface durability	137, 138, 146
Flange connections	118, 175, 179	tooth form	134, 139

Generator	
asynchronous	3, 152, 154, 155, 224
induction	223
multiple-poled	157
multipole	228
overload	13, 115, 155, 157
reactive power	224, 225, 226, 227
size	5
slip	152, 224
synchronous	152, 155, 157, 223, 224, 229
variable speed	6, 69, 154, 181, 227, 228, 229, 230
Geological study	187
Geometrical size effect	121, 122
Geophysical survey	187
Geostrophic wind speed	40, 44
Geotechnical analysis	187, 188, 218
Gerber diagram	258
Germanischer Lloyd	30
Glauert's correction	67
Goodman diagram	258
Gravity loads	58, 87, 90, 112, 117
Grid connection	13, 80, 223, 229, 231
Grid loss	148
Grinding	255
Gumbel distribution	23, 44, 83, 85, 86, 89
Gust	43, 55, 57, 87, 152, 174
Gyroscopic effects	3, 58, 59, 161
Hail	51
Harris spectrum	37, 38
HawC	61, 70
High-cycle fatigue	77
Homogeneous terrain	33, 35, 37, 39, 62
Humidity	41, 50, 110, 153
Hurricanes	45
Ice	33, 50, 214
cone	210, 216, 219
loads	50, 60, 99, 210, 214, 216, 218
Ideal site	234
Idling	13, 15, 55, 56, 57, 79, 80, 81, 155
Induction factor	66
Induction generator	223
Inertia	
coefficient	95, 96
loads	58, 96, 98
Inflow angle	64, 65, 66, 71, 76, 166
In-rush current	225
Inspection	11, 13, 176
intervals	26, 176
Installation	28, 29, 55, 142, 175, 194, 199, 209, 212, 213, 220, 233
Insulation	28, 153, 156, 157
Integral temperature criterion	140
Interference factor	..See <i>Induction factor</i>
JONSWAP spectrum	93
Kaimal spectrum	38, 39, 62, 88
Labour safety	28, 29, 180, 233
Labyrinth seals	130, 131
Lift	
coefficients	64, 65, 66, 71, 76, 158
curve	65, 70, 75
forces	60, 63, 64, 104
Light conditions	29
Lightning	28, 53, 106, 113, 114, 230
Limit states	11, 18, 19, 23, 24, 27, 56, 117, 145, 210, 217, 218, 248
Load	
distribution	24, 25, 89
verification	93, 96, 170, 171
Load combination	
extreme	11, 20, 99, 174, 260, 267
fatigue	81, 90, 91, 120, 174
Logarithmic decrement	72, 73
Longuet-Higgins distribution	95
Low-cycle fatigue	77, 126
Lubrication	27, 130, 136, 137, 141, 165, 233
grease	130, 131, 166
oil	132, 137, 141
relubrication interval	131, 132, 165
viscosity ratio	136, 137
Main shaft	87, 120, 130, 133, 251, 257
Mann model	62, 63
Manual operation	56, 159
Manuals	29, 233

Material certificates	11, 143	Palmgren-Miner rule 24, 77, 125, 176, 177, 207, 211, 254, 255, 256
Material properties	268	Parametrised load spectra
Mean stress 78, 79, 81, 110, 112, 117, 123, 124, 241, 255, 256, 258		89
Measurements	49, 234	Parks <i>See Wind farms</i>
damping	72, 73	Partial safety factors 11, 20, 21, 22, 23, 26, 101
full-scale test	26	calibration
load	170, 236	20, 21, 22
model verification	62, 70, 171	Passive brakes
noise	237	148
power performance	7, 234	Peak counting method
power quality	237	77, 78
uncertainty	27, 46, 234	Peak-over-threshold method
wind speed	37, 46, 234	89
Meteorology mast	234	Periodical maximum method
Micro pitting	<i>See Gear</i>	89
Middelgrunden	98	Personal safety
Miner	<i>See Palmgren-Miner</i>	<i>See Labour safety</i>
Minimal cut set analysis	17	Pile foundation 187, 189, 193, 203, 205, 209
Modal analysis	61, 70, 181	Pile refusal
Monin-Obukhov length	41	213
Monitoring 4, 12, 13, 15, 132, 141, 150, 220		Pile-driving 194, 210, 211, 213, 215, 220
Morison's equation	95	Pile-soil-pile interaction
NACA profiles	71	194, 198
Natural frequency 73, 88, 91, 113, 115, 171, 173, 204, 218, 219, 260		Pitch angle
Near-coastal locations	33	4, 69, 104
Network connection .. 12, 13, 55, 57, 226		Pitch control
Nitrided gears	145	<i>See Power regulation</i>
Noise	1, 3, 130, 158, 227, 237, 251	Planetary gears
Nominal power	<i>See Power</i>	134
Non destructive testing	118, 127, 214	Polyamide (PA)
Notch sensitivity factor	122, 123	165
Offshore turbines 8, 33, 50, 51, 179, 187, 208		Polyethylene Terephthalate (PET)
Operation range	13	165
Operation temperature	48, 120	Polyurethane (PUR)
Operational conditions	55, 60, 79	165
Operational load	<i>See Functional load</i>	Potential annual energy
Operational procedures	29, 233	7
Outgassing	108	Power
Overconsolidation ratio	197, 202	coefficient
Overloading	155	6, 250
Overspeed	12, 13, 155, 157, 237	electrical
		6
		iso-power curve
		4
		mechanical
		69
		nominal
		12, 155
		performance
		5, 7, 234
		curve
		6
		quality
		229, 232, 237
		rated
		4, 152
		Power regulation
		3, 6, 69
		active stall
		4
		pitch
		4, 6, 155
		stall
		4, 6, 63, 152
		Power spectral density 38, 39, 40, 75, 93
		Prandtl's tip loss factor
		67
		Probabilistic method 22, 24, 26, 28, 100, 181
		Protection system 10, 11, 15, 149, 150, 153
		P-y curves
		197, 198, 199, 200

Quality	
assurance	30, 109, 120, 127, 144, 145
control	26, 142
Quarter chord point	64, 75
Quasi-static method	87
Quasi-steady analysis	74
Radiation	50
Rain	50, 116, 158
Rain-flow counting	77, 112, 174
Range counting method	77, 78
Rayleigh damping model	72, 73
Rayleigh distribution	80, 94, 95, 277, 278
Recurrence period	11, 43, 48, 88, 170
Redundant design	14, 148, 150, 151, 166
Reinforced concrete	206, 270
crack width	207
Relative humidity	50, 153
Reliability	
analysis	10, 17
index	19, 21, 23, 24
Reynolds number	64
Richardson number	41
RIX number	47, 48
Rødsand	98
Rotating bending	256
Rotor coning	58, 158
Rotor loads	59, 87, 91
Rotor speed	
fixed	1, 86, 170
variable	1, 69, 171
Roughness parameter	33, 34, 38, 44
Safety	
classes	10, 14, 22, 218
electrical	230
philosophy	10
requirements	10, 11, 20, 28, 126
Safety factors	<i>See Partial safety factors</i>
Safety system	<i>See Protection system</i>
Saffir-Simpson	45
Sand	149, 196, 199, 202, 213, 218, 248
Scaling laws	250
Scour protection	214
Scuffing	140
Seals	130, 131, 165
Sensors	9, 14, 152, 159, 166
cable twist	166
direction	159
Service schedule	233
Serviceability limit state	11, 18, 219, 248
Shear modulus	107, 197, 201, 202, 203
Short-circuit	154, 155, 157
Shrink fits	120, 122, 123, 126, 146
Shutdown	14, 15, 29, 56, 57, 80, 141
Site assessment	46
Slab foundation	187
Slewing bearing	163
service life curve	164
Slide bearing	165
Slip rings	3, 224
S-N curve	<i>See Fatigue</i>
Softstarter	225
Soil conditions	51, 93, 187, 189
Poisson's ratio	203
skin friction	195, 196
sliding resistance	193
stratigraphy	188
Solar radiation	46, 50
Specific power performance	5, 7
Specific rotor power	5
Spoilers	14
Spur gears	134
Stall angle	64
Stall regulation	<i>See Power regulation</i>
Stall strips	75, 76
Stall-induced vibrations	73
Standard components	159
Standards	19, 20, 21, 30, 33, 111, 127, 141, 151, 192, 239, 249, 268, 269
DIBt Richtlinien	30
DS 412	48, 175, 177, 179, 247, 256
DS 472	10, 15, 30, 35, 37, 48, 56, 89, 90, 112, 160, 182, 183, 184
IEC 61400-1	15, 30, 35, 37, 38, 55, 57, 130, 172, 231
NVN 11400-0	30
Start-up	56, 79, 80, 112, 132, 154, 172, 225
Stop ring	133
Storms	45, 99
Strain gauges	115

Stress concentration factors	117, 118, 121, 122, 123, 176, 177, 211, 212, 253, 256
Stress range distribution	24, 25, 79, 80, 112, 211, 252, 255
Stress ratio	121, 123, 255, 256
Strouhal number	175
Structural	
damping	58, 72, 73, 74, 88
modelling	68
redundancy	10
reliability analysis	18, 19, 21, 22, 24
safety	11, 18, 19, 20, 21, 27, 28
standards	20, 48, 127, 175, 177, 179
Structural steel	127, 268
Student's t distribution	82, 84
Surface conditions	117, 121
Surface roughness	121
Tail vane	158
Technological size effect	121
Teetering hub	3
Temperatures	11, 48, 49
Terrain	
complex	37, 39, 47, 93, 234, 236
homogeneous	33, 35, 37, 39, 62
roughness parameter	32, 34, 35
types	33
Tests	<i>See Measurements</i>
Thermal analysis	260
Thyristor	225
Tilt angle	113
Tip angle	117, 118
Tip brake	<i>See Brakes</i>
Tip speed ratio	69, 250
Tolerances	27, 113, 118, 123, 126, 133, 158, 162, 163, 172, 179, 180, 220, 247
Topography	41, 47, 53, 188, 234
Tower	
blade clearance	3, 113, 172
buckling	52, 177
connections	178, 187, 212
cost	169, 170
damping	72, 172
door	176
erection	170, 174, 187
guided	170
height	8, 169, 175, 178
imperfection	178, 179
lattice	169, 170, 201
loads	22, 30, 60, 88, 170, 173
natural frequency	171, 172, 204
relative slenderness ratio	177, 178
shadow	2, 56, 60, 170, 230
tubular	169, 173
vortex shedding	60, 174
Transient wind conditions	43, 56
Transmission system	27, 70, 116, 129, 146, 151
Transportation	28, 55, 169, 170, 233
Trends	1, 93, 231
Turbulence	25, 34, 62, 70, 88
intensity	36, 47, 63, 79
length scale	62, 63
model	37, 62
scale parameter	38
simulation	43
wake	36
Turkstra's rule	100
Two-dimensional flow	64
T-z curves	196, 217
US units	277
Vacuum bagging	109
Variable speed	227
Veers model	62, 63
Velocity pressure	44, 45
Viscosity classes	141, 142
Von Karman's constant	32, 33, 35, 44
Vortex generators	75, 76
Vortex-induced vibrations	175
Wake effect	36, 56, 236
Washers	249
Wasp Engineering	47
Wave loads	93, 99, 210
Waves	33, 51, 99, 203, 212
Weak grids	13
Wear	15, 27, 130, 132, 157

- Weibull distribution 7, 32, 46, 80, 255, 277
 - scale parameter 24, 25, 32, 90, 183
 - shape parameter 32, 90
- Welds 175, 177, 214, 254, 255, 256, 262
- Wind
 - climate 7, 32, 37, 99
 - data 43, 47
 - direction 42
 - profile *See Wind shear*
 - resource 13, 169
 - rose 42
 - shear 40, 43, 55, 57, 173
 - synthetic field 62
- Wind farms 36, 42, 56, 93, 229, 231, 232
- Wind speed
 - 10-minute mean 32, 37, 43, 45, 46, 277
 - 50-year 33, 43, 45, 82, 100
 - distribution 7, 182
 - extreme 43, 47, 57
 - gust 43, 57, 87, 152, 174
 - nominal stall 89
 - profile 32, 33, 40, 42, 47, 55, 57, 61, 173
 - standard deviation 34, 46, 63
- Wind tunnel 64, 71, 76
- Wings *See Blades*
- Wöhler curve *See S-N curve*
- Working areas 29
- Worm gears 134

- Yaw
 - active 3, 86, 159, 161
 - brake 29, 146, 162
 - error 12, 56, 71, 81, 112, 158, 159, 160, 161, 162, 166
 - loads 60, 160
 - passive 3, 158, 161
 - system 2, 59, 146, 157, 158, 233
- Yield strength 23, 122, 124, 125, 146, 239, 256, 258, 268, 269
- Young's modulus 138, 165, 203, 204